

# Expansion of AASHTOWare ME Design Inputs for Asphalt Layers

---

Hadi Nabizadeh (ARA)  
Harold L. Von Quintus, P.E. (ARA)  
Ramon Bonaquist, P.E. (AAT)

Applied Research Associates, Inc. (ARA)  
Advanced Asphalt Technologies, Inc. (AAT)

WisDOT ID No. 0092-20-03

March 2022



RESEARCH & LIBRARY UNIT



WISCONSIN HIGHWAY RESEARCH PROGRAM

**WISCONSIN DOT**  
PUTTING RESEARCH TO WORK

## TECHNICAL REPORT DOCUMENTATION PAGE

<b>1. Report No.</b> 0092-20-03	<b>2. Government Accession No.</b>	<b>3. Recipient's Catalog No.</b>	
<b>4. Title and Subtitle</b> Expansion of AASHTOWare ME Design Inputs for Asphalt Layers		<b>5. Report Date</b> March 2022	
		<b>6. Performing Organization Code</b>	
<b>7. Author(s)</b> Hadi Nabizadeh, Harold L. Von Quintus, and Ramon Bonaquist		<b>8. Performing Organization Report No.</b> <b>004000</b>	
<b>9. Performing Organization Name and Address</b> Applied Research Associates, Inc. (ARA) 100 Trade Centre Drive, Suite 200 Champaign, IL 61820-7233		<b>10. Work Unit No.</b>	
		<b>11. Contract or Grant No.</b> WHRP 0092-20-03	
<b>12. Sponsoring Agency Name and Address</b> Wisconsin Department of Transportation Research & Library Unit 4822 Madison Yards Way Room 911 Madison, WI 53705		<b>13. Type of Report and Period Covered</b> Final Report October 2019 to February 2022	
		<b>14. Sponsoring Agency Code</b>	
<b>15. Supplementary Notes</b> No supplementary notes.			
<b>16. Abstract</b> The Wisconsin Department of Transportation (WisDOT) has supported several research studies in the past decades to measure the mechanical or performance properties of asphalt mixtures in support of the AASHTOWare Pavement ME Design (PMED) software to design pavement structures in Wisconsin. The outcome from these studies was to prepare a library or catalog of the asphalt materials inputs that can be integrated into the WisDOT pavement design practice for using the AASHTOWare PMED software. This research study expanded the catalog or material library of asphalt mixtures that are being paved in Wisconsin in support of the PMED software's use. The catalog includes the level 1 material inputs that can be selected by pavement designers in Wisconsin to reflect the mixtures used in day to day practice. The research study also provided an update to the structural layer coefficients required by the AASHTO 1972 Interim Design Guide, for which WisDOT currently uses, to represent the current asphalt mixtures being placed in Wisconsin.			
<b>17. Key Words</b> Pavement ME Design, Mechanistic-Empirical Pavement Design Guide, Dynamic Modulus, Creep Compliance and Strength, Repeated Load Plastic Strain Coefficients, Fatigue Strength Coefficients, IDT Tensile Strain at Failure, AASTHO Structural Layer coefficients.		<b>18. Distribution Statement</b> No restrictions. This document is available through the National Technical Information Service. 5285 Port Royal Road Springfield, VA 22161	
<b>19. Security Classif. (of this report)</b> Unclassified	<b>20. Security Classif. (of this page)</b> Unclassified	<b>21. No. of Pages</b> 180	<b>22. Price</b>

Form DOT F 1700.7 (8-72)

Reproduction of completed page authorize

**DISCLAIMER**

This research was funded through the Wisconsin Highway Research Program (WHRP) by the Wisconsin Department of Transportation and the Federal Highway Administration under Project 0092-20-03. The contents of this report reflect the views of the authors who are responsible for the facts and accuracy of the data presented herein. The contents do not necessarily reflect the official views of the Wisconsin Department of Transportation or the Federal Highway Administration at the time of publication.

This document is disseminated under the sponsorship of the Department of Transportation in the interest of information exchange. The United States Government assumes no liability for its contents or use thereof. This report does not constitute a standard, specification or regulation.

The United States Government does not endorse products or manufacturers. Trade and manufacturers' names appear in this report only because they are considered essential to the object of the document.

**EXECUTIVE SUMMARY**

The Wisconsin Department of Transportation (WisDOT) has supported several research studies in the past decades to measure the mechanical or performance properties of asphalt mixtures in support of the AASHTOWare Pavement ME Design (PMED) software to design pavement structures in Wisconsin. The outcome from these studies was to prepare a library or catalog of the asphalt materials inputs that can be integrated into the WisDOT pavement design practice for using the AASHTOWare PMED.

This research study expanded the catalog or material library of asphalt mixtures that are being paved in Wisconsin in support of the PMED software's use. The materials library catalog includes the level 1 material inputs selected by pavement designers in Wisconsin to reflect the mixtures used in day to day practice.

The research study also provided an update to the structural layer coefficients required by the American Association of State Highway and Transportation Officials (AASHTO) 1972 Interim Design Guide, for which WisDOT currently uses, to represent the current asphalt mixtures placed in Wisconsin.

TABLE OF CONTENTS

LIST OF FIGURES .....	viii
LIST OF TABLES .....	x
CHAPTER 1 INTRODUCTION .....	1
Background.....	1
Research Objectives.....	2
Organization of Report .....	2
CHAPTER 2 LITERATURE REVIEW .....	4
2.1 Major Updates in the WisDOT Specification.....	4
2.2 Review of Wisconsin Research Studies.....	6
2.3 Review Other Agencies Asphalt Material Input Libraries .....	7
2.4 Sensitivity Studies.....	9
2.5 Summary.....	9
CHAPTER 3 ASPHALT BINDER AND MIXTURE TESTS.....	12
3.1 Asphalt Binders.....	12
3.2 Asphalt Mixtures.....	14
3.3 Asphalt Mixture Test Results .....	14
3.3.1 Dynamic Modulus Tests.....	14
3.3.2 Indirect Tensile Creep Compliance Tests.....	21
3.3.3 Indirect Tensile Strength Tests .....	23
3.3.4 Repeated Load Plastic Strain Tests .....	24
3.3.5 Bending Beam Fatigue Strength Tests .....	29
3.3.6 IDT Tensile Strain at Failure Tests.....	32
CHAPTER 4 INTERPRETATION OF TEST RESULTS .....	35
4.1 Asphalt Binder .....	35
4.2 Dynamic Modulus.....	36
4.3 IDT Creep Compliance and Strength.....	39
4.3.1 Creep Compliance .....	39
4.3.2 IDT Tensile Strength .....	45
4.4 Plastic Strain Coefficients.....	46
4.5 Fatigue Strength Coefficients .....	50
4.5.1 Flexural Bending Beam Fatigue Tests.....	51
4.5.2 Tensile Strain at Failure.....	52
4.5.3 Fatigue Strength Coefficients for WisDOT Base Mixtures.....	55

## Expansion of AASHTOWare ME Design Inputs

4.6	Summary – Asphalt Layer Property Libraries .....	56
CHAPTER 5 AASHTO ASPHALT STRUCTURAL LAYER COEFFICIENT .....		58
5.1	Site Specific Inputs and Assumptions for the Simulations.....	58
5.2	Distress Sensitivity to Asphalt Mixtures included in the Asphalt Material Library. 60	
5.2.1	Length of Transverse Cracks .....	60
5.2.2	Rut Depth.....	61
5.2.3	Bottom-up Fatigue Cracking .....	64
5.3	AASHTO Layer Coefficients .....	66
5.3.1	Elastic Modulus Approach .....	66
5.3.2	Distress Prediction/Simulation Approach .....	68
5.3.3	Summary.....	69
CHAPTER 6 CONCLUSIONS AND RECOMMENDATIONS .....		70
6.1	Conclusions and Observations.....	70
6.2	Recommendations: Moving Forward with ME Design Implementation.....	73
REFERENCES .....		77
APPENDIX A—SUMMARY OF WISCONSIN RESEARCH STUDIES FOR ASPHALT MIXTURE PROPERTIES.....		81
A.1	Review of WISDOT Specification Changes .....	81
A.2	Review of Wisconsin Research Studies.....	83
A.2.1	WHRP 0092-04-07 .....	83
A.2.2	WHRP 0092-08-06.....	84
A.2.3	WHRP 0092-10-06.....	85
A.2.4	WHRP 0092-10-07 .....	86
A.2.5	WHRP 0092-09-01 .....	88
A.2.6	WHRP 0092-13-02 .....	88
A.2.7	WHRP 0092-12-02 .....	89
A.2.8	WHRP 0092-14-20 .....	89
A.2.9	WHRP 0092-15-04 .....	89
A.2.10	WHRP 0092-16-06.....	91
A.3	Appendix A References .....	91
APPENDIX B—SUMMARY OF ASPHALT MIXTURE LIBRARIES: OTHER STATE DOTS .....		93
B.1	Agency Libraries for Asphalt Mixtures .....	93
B.1.1	Pennsylvania Department of Transportation (PENNDOT).....	93
B.1.2	Federal Highway Administration (FHWA).....	97

**Expansion of AASHTOWare ME Design Inputs**

B.1.3	Nebraska Department of Roads (NDOR).....	97
B.1.4	Michigan Department of Transportation (MDOT).....	98
B.1.5	Missouri Department of Transportation (MoDOT).....	99
B.1.6	Indiana Department of Transportation (INDOT) .....	100
B.1.7	Ohio Department of Transportation (ODOT).....	100
B.1.8	Virginia Department of Transportation (VDOT) .....	101
B.1.9	Kansas Department of Transportation (KDOT) .....	101
B.1.10	Utah Department of Transportation (UDOT).....	102
B.1.11	Mississippi Department of Transportation (MDOT).....	102
B.2	Summary .....	102
B.3	Appendix B References .....	103
APPENDIX C—ASPHALT BINDER TEST DATA.....		106
C.1	AASHTO T 315 Test Data .....	106
C.2	AASHTO M 332 Data .....	108
C.3	Graphical Presentation and Comparison of Asphalt Binder Test Data .....	108
APPENDIX D—ASPHALT MIXTURE DESIGN DATA.....		112
D.1	Asphalt Base Mixtures with PG58-28 Binders.....	112
D.2	Wearing Surface Mixtures with PG58-28 Binders .....	113
D.3	Wearing Surface Mixtures with PG58-34 Binders .....	115
APPENDIX E—DYNAMIC MODULUS TEST DATA.....		116
E.1	Dynamic Modulus Tabular Summary of Test Data.....	116
E.2	Dynamic Modulus Master Curves .....	121
E.3	Appendix E References .....	129
APPENDIX F—IDT CREEP COMPLIANCE AND STRENGTH TEST DATA .....		130
F.1	Indirect Tensile Creep Compliance Tabular Summary of Test Data.....	130
F.2	Indirect Tensile Creep Compliance Master Curves .....	135
F.3	Appendix F References.....	140
APPENDIX G—REPEATED LOAD PLASTIC STRAIN TEST DATA .....		141
G.1	Graphical Presentation of Repeated Load Plastic Strain Test Data.....	141
G.2	Procedure to Derive the Plastic Strain k-Coefficients .....	147
G.2.1	Definition/Classification of the Accumulated Plastic Strain Responses .....	147
G.2.2	Determine Plastic Strain Coefficients for Individual Test Specimens .....	149
G.2.3	Combine Results to Derive the Plastic Strain k-Coefficients.....	151
G.3	Appendix G References .....	152

**Expansion of AASHTOWare ME Design Inputs**

APPENDIX H—BENDING BEAM FATIGUE STRENGTH TEST DATA..... 153

- H.1 Graphical Presentation of Bending Beam Fatigue Strength Test Data..... 153
- H.2 Procedure to Derive the Fatigue Strength k-Coefficients..... 155
  - H.2.1 Definition of Fatigue Life or Strength..... 155
  - H.2.2 Determine Fatigue Life of Individual Beam Specimens for Same Test Temperature ..... 155
  - H.2.3 Determine Fatigue Strength K-Coefficients for Combined Test Temperatures  
156

APPENDIX I—TENSILE STRAIN AT FAILURE TEST DATA..... 158

- I.1 Graphical Presentation of Indirect Tensile Failure Strain Test Data ..... 158
- I.2 Relationship between Dynamic Modulus and Tensile Failure Strain..... 166
- I.3 Procedure to Estimate the Fatigue Strength k-Values ..... 168
  - I.3.1 Summary of Test Procedure ..... 168
  - I.3.2 Failure Strain Definition for Fatigue Strength Estimate..... 169
  - I.3.3 Analysis of the IDT Failure Strain Data ..... 171
  - I.3.4 Determine the Fatigue Strength k-Coefficients ..... 172
- I.4 Appendix I References..... 174

APPENDIX J—PROCEDURE TO DERIVE THE AASHTO ASPHALT STRUCTURAL LAYER COEFFICIENT..... 175

- J.1 Procedure to Derive Structural Layer Coefficients..... 175
- J.2 Selected Examples ..... 176
  - J.2.1 Example 1 – Madison Climate, High Traffic (HT) ..... 176
  - J.2.2 Example 2 –Green Bay Climate, Moderate Traffic (MT) ..... 177
  - J.2.3 Example 3 –Mercer Climate, Moderate Traffic (LT)..... 178



LIST OF FIGURES

Figure 1. Maximum Allowable Percent Binder Replacement Specified in the 2020 and 2010 WisDOT Standard Specifications. .... 10

Figure 2. Graphical Comparison of  $N_{design}$  Gyration and Dynamic Modulus Measured at 130°F (54.4 °C) and 25 Hz. .... 19

Figure 3. Input Level 1 Measured Dynamic Modulus Compared to Input Level 3 Global Dynamic Modulus for the Wearing Surface Mixtures..... 20

Figure 4. Input Level 1 Measured Dynamic Modulus Compared to Input Level 3 Global Dynamic Modulus for the Asphalt Base Mixtures. .... 20

Figure 5. Graphical Comparison of Input Levels 1 and 3 Creep Compliance for Mixtures with a PG58-28 Asphalt Binder. .... 23

Figure 6. Graphical Comparison of Input Levels 1 and 3 Creep Compliance for Mixtures with a PG58-348 Asphalt Binder..... 23

Figure 7. Graphical Comparison of Input Levels 1 and 3 IDT Strengths..... 24

Figure 8. Typical Plastic Strain Curve for an Asphalt Mixtures for a Single Test Temperature in Logarithmic Scale Exhibiting Three Response Zones..... 25

Figure 9. Impact of  $N_{Design}$  on the Intercept Coefficient from the Repeated Load Plastic Strain Test Data. .... 28

Figure 10. Impact of  $N_{Design}$  on the Slope Coefficient from the Repeated Load Plastic Strain Test Data. .... 28

Figure 11. Impact of  $N_{Design}$  on the Measured Resilient Strain from the Repeated Load Plastic Strain Test Data..... 29

Figure 12. LVDTs Attached to the IDT Test Specimen for Measuring Horizontal and Vertical Displacements in the Center of the Specimen. .... 33

Figure 13. Correspondence between  $N_{Design}$  and IDT Strength from Multiple Data Sources..... 45

Figure 14. Correspondence between  $N_{Design}$  and the Intercept Coefficient,  $k_{1r}$ . .... 49

Figure 15. Correspondence between  $N_{Design}$  and the Load Cycle Exponent or Slope,  $k_{3r}$ . .... 49

Figure 16. Correspondence between  $N_{Design}$  and the Temperature Exponent or Slope,  $k_{2r}$ . .... 50

Figure 17. Correspondence between  $N_{Design}$  and Fine Aggregate Angularity ..... 56

Figure 18. Predicted Lengths of Transverse Cracks for different Climate Locations using Traffic Level MT. .... 61

Figure 19. Predicted Lengths of Transverse Cracks for different Traffic Levels for the Madison Climate Location; PG58-28 Asphalt..... 62

Figure 20. Predicted Lengths of Transverse Cracks for different Traffic Levels for the Mercer Climate Location; PG58-34 Asphalt..... 62

Figure 21. Predicted Lengths of Transverse Cracks for different Amounts of RAP/RAS for the Plover Climate Location and Traffic Level HT; PG58-34 Asphalt..... 63

Figure 22. Predicted Rut Depths for different Climate Locations using the Traffic Level MT. .. 63

Figure 23. Predicted Rut Depths for different Traffic Levels for the Plover Climate Location; PG58-34 Asphalt..... 64

Figure 24. Predicted Rut Depths for different Amounts of RAP/RAS for the Madison Climate Location and Traffic Level MT; PG58-28 Asphalt. .... 64

Figure 25. Predicted Bottom-Up Fatigue Cracks for different Climate Locations using the Traffic Level HT. .... 65

## Expansion of AASHTOWare ME Design Inputs

Figure 26. Predicted Bottom-Up Fatigue Cracks for different Traffic Levels for the Mercer Climate Location; PG58-34 Asphalt.....	65
Figure 27. Predicted Bottom-Up Fatigue Cracks for different Amounts of RAP/RAS for the Mercer Climate Location and Traffic Level HT; PG58-34 Asphalt.....	66
Figure A28. Dynamic modulus master curves for the Christian/Gade mixtures in WHRP 0092-08-06 project.....	85
Figure A29. Cycles to 1 percent permanent strain in the confined Flow Number tests in WHRP 0092-08-06 project.....	85
Figure A30. Averaged creep compliance master curves in WHRP 0092-10-07 project.....	87
Figure A31. Flow Number in comparison with MSCR Jnr at 3.2 kPa in WHRP 0092-14-20 project (Bahia et al., 2016).....	90
Figure A32. Flow Number in comparison with MSCR %R in WHRP 0092-14-20 project (Bahia et al., 2016). ....	90
Figure B33. Clustering of the PENNDOT asphalt mixtures that result in similar rut depth predictions.....	96
Figure B34. Clustering of the PENNDOT asphalt mixtures that result in similar bottom-up alligator cracking predictions.....	96
Figure B35. Clustering of the PENNDOT asphalt mixtures that result in similar transverse cracking predictions.....	96
Figure B36. Comparison of the strain exponent and intercept for the R <sup>2</sup> AMs and neat, virgin asphalt mixtures. ....	98
Figure G37. Pattern A typical plastic strain curve for an asphalt mixture in logarithmic scale.	148
Figure G38. Pattern B typical plastic strain curve for an asphalt mixture in logarithmic scale.	149
Figure G39. Pattern C typical plastic strain curve for an asphalt mixture in logarithmic scale.	149
Figure I40. LVDTs Attached to the IDT Test Specimen for Measuring Horizontal and Vertical Displacements in the Center of the Specimen. ....	169
Figure I41. Test Results from the IDT Strength Test at the Low Test Temperature (40 °F).....	170
Figure I42. Test Results from the IDT Strength Test at the High Test Temperature (80 °F). ....	171

**LIST OF TABLES**

Table 1. Maximum allowable binder replacement – 2010 specification. .... 4

Table 2. Maximum allowable binder replacement – 2011 specification. .... 5

Table 3. Switching from “E” mixtures to “LT”, “MT”, and “HT” mixtures – 2017 specification. 6

Table 4. Updates in SMA mixture design – 2020 specification. .... 6

Table 5. Summary of key findings from the review of WisDOT studies. .... 7

Table 6. Sensitivity of PMED software to asphalt material inputs. .... 9

Table 7. Asphalt binder grades included in the testing plan, defined by AASHTO M 350. .... 12

Table 8. Asphalt binder testing plan. .... 13

Table 9. Asphalt binder test result summary, AASHTO T 315. .... 13

Table 10. Average complex shear modulus values for the different AASHTO T 350 asphalt binder grade designations. .... 13

Table 11. Asphalt mixture testing plan. .... 15

Table 12. Asphalt mixtures included in the test plan. .... 15

Table 13. Job mix formula information for the asphalt mixtures included in test plan. .... 16

Table 14. Gradation of the asphalt mixtures, organized by base and surface layers. .... 17

Table 15. Selected volumetric properties of the asphalt mixtures. .... 18

Table 16. Dynamic modulus measured on selected mixtures (mixtures organized by increasing stiffness). .... 19

Table 17. Creep compliance measured on selected mixtures at 100 second load duration (mixtures organized by increasing creep compliance). .... 22

Table 18. Creep compliance grouped into different categories. .... 22

Table 19. Summary of accumulated percent plastic strain (mixtures organized by increasing resistance to rutting; first mixtures listed are those most susceptible to rutting). .... 26

Table 20. Average intercept coefficient, a, from steady state region. .... 27

Table 21. Average slope coefficient, b, from steady state region. .... 27

Table 22. Average resilient strain. .... 29

Table 23. Fatigue strengths measured on selected asphalt base mixtures (in accordance with the traditional definition of failure or fatigue strength). .... 31

Table 24. Fatigue strength coefficients for reference temperature (traditional definition of failure or fatigue strength). .... 32

Table 25. Average tensile strain at failure from the IDT test. .... 34

Table 26. IDT failure strain test results. .... 34

Table 27. Complex shear modulus and phase angle for PG58-28. .... 35

Table 28. Complex shear modulus and phase angle for PG58-34. .... 36

Table 29. Dynamic moduli for asphalt wearing surface using an  $N_{Design}$  of 100 gyrations (50 percent RAP/RAS included in mixture), psi. .... 37

Table 30. Dynamic moduli for asphalt base layer using an  $N_{Design}$  of 100 gyrations (50 percent RAP/RAS included in mixture), psi. .... 37

Table 31. Average dynamic moduli for selected WisDOT asphalt mixtures without RAP/RAS, psi. .... 38

Table 32. Average dynamic moduli for asphalt mixtures designed using an  $N_{Design}$  of 40 gyrations (lower to moderate amounts of RAP/RAS included in mixture), psi. .... 38

Table 33. Average dynamic moduli for asphalt mixtures designed using an  $N_{Design}$  of 75 gyrations (lower to moderate amounts of RAP/RAS included in mixture), psi. .... 39

**Expansion of AASHTOWare ME Design Inputs**

Table 34. Average dynamic moduli for asphalt mixtures designed using an  $N_{\text{Design}}$  of 100 gyrations (lower to moderate amounts of RAP/RAS included in mixture), psi. .... 39

Table 35. Creep compliance values measured for a WisDOT high recycle surface course mixture (50 percent RAP/RAS added to mixture);  $N_{\text{Design}}$  is 100 gyrations, 1/psi. .... 41

Table 36. Creep compliance values measured for WisDOT mixtures with a PG58-28 binder designed using an  $N_{\text{Design}}$  of 75 gyrations without RAP/RAS, 1/psi..... 41

Table 37. Creep compliance values measured for WisDOT mixtures with a PG58-28 binder designed using an  $N_{\text{Design}}$  of 100 gyrations without RAP/RAS, 1/psi..... 42

Table 38. Creep compliance values measured for WisDOT mixtures with a PG58-34 binder designed using an  $N_{\text{Design}}$  of 75 gyrations without RAP/RAS, 1/psi..... 42

Table 39. Creep compliance values measured for WisDOT mixtures with a PG58-34 binder designed using an  $N_{\text{Design}}$  of 100 gyrations without RAP/RAS, 1/psi..... 42

Table 40. Creep compliance values measured for WisDOT mixtures with a PG58-28 binder designed using an  $N_{\text{Design}}$  of 100 gyrations with low to moderate amounts of RAP/RAS, 1/psi.. 43

Table 41. Creep compliance values measured for WisDOT mixtures with a PG58-28 binder designed using an  $N_{\text{Design}}$  of 75 gyrations with low to moderate amounts of RAP/RAS, 1/psi.... 43

Table 42. Creep compliance values measured for WisDOT mixtures with a PG58-28 binder designed using an  $N_{\text{Design}}$  of 40 gyrations with low to moderate amounts of RAP/RAS, 1/psi.... 43

Table 43. Creep compliance values measured for WisDOT mixtures with a PG58-34 binder designed using an  $N_{\text{Design}}$  of 100 gyrations with low to moderate amounts of RAP/RAS, 1/psi.. 44

Table 44. Creep compliance values measured for WisDOT mixtures with a PG58-34 binder designed using an  $N_{\text{Design}}$  of 75 gyrations with low to moderate amounts of RAP/RAS, 1/psi.... 44

Table 45. Creep compliance values measured for WisDOT mixtures with a PG58-34 binder designed using an  $N_{\text{Design}}$  of 40 gyrations with low to moderate amounts of RAP/RAS, 1/psi.... 44

Table 46. MEPDG rut depth transfer function plastic strain coefficients for WisDOT mixtures. 48

Table 47. MEPDG rut depth transfer function plastic strain coefficients for selected WisDOT high RAP/RAS mixtures (50 percent), FHWA sponsored study (Von Quintus, 2019). .... 48

Table 48. Rut depth transfer function plastic strain coefficients for the WisDOT asphalt materials library. .... 50

Table 49. MEPDG flexural bending beam coefficients (equation 7) for WisDOT base mixtures. .... 52

Table 50. MEPDG flexural bending beam coefficients (equation 7) for selected WisDOT high RAP/RAS mixtures (50 percent), FHWA sponsored study (Von Quintus, 2019)..... 52

Table 51. MEPDG fatigue strength coefficients estimated from the IDT failure strain test for WisDOT base mixtures. .... 54

Table 52. Fatigue strength coefficients for the WisDOT asphalt materials library. .... 56

Table 53. Matrix for selecting a set of asphalt mixture properties for use in design..... 57

Table 54. Site specific inputs: climate or location and subgrade soil. .... 59

Table 55. Traffic inputs; based on asphalt mixture design levels. .... 59

Table 56. Asphalt structural layer coefficients derived from the elastic or dynamic modulus of the mixture (see Chapter 3)..... 67

Table 57. Asphalt structural layer coefficients derived from predicted distresses using the PMED software and asphalt material property catalog (see Chapter 4) ..... 68

Table 58. Wearing surface asphalt mixtures and subgrade soil XML files created for use in design with the PMED software. .... 71

Table 59. Asphalt base mixture XML files created for use in design with the PMED software.. 72

## Expansion of AASHTOWare ME Design Inputs

Table 60. Subgrade soil XML files created for use in design with the PMED software.....	72
Table A61. Maximum allowable binder replacement – 2010 specification. ....	81
Table A62. Maximum allowable binder replacement – 2011 specification. ....	81
Table A63. Switching from “E” mixtures to “LT”, “MT”, and “HT” mixtures – 2017 specification. ....	82
Table A64. Updates in SMA mixture design – 2020 specification. ....	83
Table A65. Experimental matrix in WHRP 0092-04-07 project. ....	84
Table A66. Experimental matrix in WHRP 0092-08-06 project. ....	84
Table A67. Recommended binder replacement criteria in WHRP 0092-10-06. ....	86
Table A68. Experimental matrix in WHRP 0092-10-07 project. ....	87
Table A69. Recommended criteria for the Flow Number test in WHRP 0092-09-01 project. ....	88
Table A70. Suggested translation from PG to MSCR Binder grade in WisDOT Facilities Development Manual – 2019.....	90
Table B71. PENNDOT’s Asphalt Mixture Library.....	94

## CHAPTER 1 INTRODUCTION

### Background

The Mechanistic Empirical Pavement Design Guide (MEPDG) was adopted by the American Association of State Highway and Transportation Officials (AASHTO) in 2015 to replace the empirical 1993 AASHTO Design Guide. The AASHTOWare Pavement ME Design® (PMED) software includes the computational methodology described and explained in the MEPDG Manual of Practice.

The MEPDG uses a mechanistic-empirical (ME) approach for the design of pavement structures. In other words, traffic and climatic-induced mechanistic pavement responses (stresses, strains, and deflections) are calculated and used to compute incremental “damage” over time. Empirical relationships (i.e., transfer function) between the cumulative damage and the observed pavement distresses are then used to determine pavement performance over its design life.

The transfer functions were calibrated using pavement performance data stored in the Long Term Pavement Performance (LTPP) database. Site specific soils, traffic, climate, and structural inputs were used in the global calibration of the asphalt pavement transfer functions. Few asphalt pavement properties, however, are included in the LTPP database. As such, the transfer functions should be verified and locally calibrated, if needed, to account for differences in terms of material properties, asphalt specifications, and construction practice.

The material properties required for the AASHTOWare PMED software are tied to a hierarchical input approach: level 1 inputs represent project specific mixture properties derived from comprehensive laboratory and/or field testing; level 2 inputs are calculated from volumetric properties or other variables using regression equations embedded in the PMED software; and level 3 inputs represent “best-guessed” material properties.

The Wisconsin Department of Transportation (WisDOT) has supported several research studies in the past decades to measure the mechanical or performance properties of asphalt mixtures in support of the PMED software to design pavement structures. The outcome from these studies was to prepare a library or catalog of the asphalt materials inputs that can be integrated into the WisDOT pavement design practice for using the AASHTOWare PMED.

Sections 450 through 475 of the WisDOT *Standard Specifications for Highway and Structure Construction* have gone through several revisions in recent years to include more sustainable and innovative asphalt materials and technologies (e.g., Reclaimed Asphalt Pavement (RAP), Reclaimed Asphalt Shingles (RAS), warm mix asphalt (WMA), etc.). The databases developed from the previous studies may or may not represent the mechanical behavior of asphalt mixtures currently being produced and placed in Wisconsin. As such, there is a need to confirm previous measured asphalt properties and expand the library to include some of the sustainable and innovative asphalt mixtures.

## **Research Objectives**

The objective of this research study was to expand the catalog or material library of asphalt mixtures that are being paved in Wisconsin in support of the PMED software's use. The catalog includes the level 1 material inputs that can be selected by pavement designers in Wisconsin to reflect the mixtures used in day to day practice using the PMED software. A couple of other secondary objectives included:

- Estimate the empirical asphalt structural layer coefficient needed by the AASHTO 1972 Interim Design Guide to represent the current asphalt mixtures being placed in Wisconsin.
- Understand how the material/construction specification changes influence the PMED inputs for input levels 1, 2, and 3. In summary, the outcomes of this study will help WisDOT understand how frequently the PMED inputs library needs to be updated and expanded.

## **Organization of Report**

The report is organized into six chapters, including the Introduction (Chapter 1). The following is a brief discussion on the contents within each chapter.

- Chapter 2 is a summary of the literature review of information that was documented within two interim reports that were prepared and submitted for review. Specifically, Chapter 2 includes a review of major revisions made to the WisDOT asphalt specifications, an overview of the WisDOT research studies focused on the MEPDG and its implementation in Wisconsin, a review of other agencies studies related to the asphalt mixtures and the MEDPG, an overview of the PMED sensitivity studies to identify the more important asphalt input variables, and a summary of these studies.
- Chapter 3 lists the asphalt binder and mixtures included in this study and an overview of the asphalt binder and mixture test results. The asphalt mixture tests included: dynamic modulus, IDT creep compliance and strength, repeated load plastic strain, bending beam fatigue strength, and IDT strain at failure. Each mixture property includes a brief background on the mixture property and its use in the PMED software and how it is measured.
- Chapter 4 is an interpretation of the asphalt binder and mixture test results in terms of how they are to be applied in the PMED software. This interpretation includes the derived mixture properties to predict the distress and performance of typical flexible pavement structures using version 2.6 of the PMED software.
- Chapter 5 illustrates and compares the predicted distresses based on the asphalt catalog of mixtures included in the expanded materials library. Chapter 5 also explains and derives the AASHTO 1993 Structural Layer Coefficients for the current asphalt mixtures being placed in Wisconsin based on the test results presented in Chapters 3 and 4.

**Expansion of AASHTOWare ME Design Inputs  
Final Report WHRP 0092-20-03**

- The final chapter or Chapter 6 provides an overall summary and conclusions focused on the test results discussed in Chapter 2 to Chapter 4. Chapter 6 also includes recommendations for the future implementation of the PMED software in Wisconsin and the default input variables recommended for use.

Ten appendices are included in the report. The ten appendices include more detailed information and present all of the asphalt binder and mixture test data generated within the study. The ten appendices are listed below:

- Appendix A is a summary of the major updates made to the WisDOT asphalt specifications and other studies related to the implementation of the MEDPG in Wisconsin.
- Appendix B is a summary of the asphalt mixture libraries generated and used by other state DOTs as part of the adoption and use of the PMED software.
- Appendix C includes the asphalt binder test data.
- Appendix D is a summary of the asphalt mixture design properties for each of the mixtures tested within this study.
- Appendix E includes the dynamic modulus test data.
- Appendix F includes the IDT creep compliance and strength data.
- Appendix G includes the repeated load plastic strain test data, as well as the interpretation of the test data for estimating the coefficients of the rut depth transfer function in the PMED software.
- Appendix H includes the bending beam fatigue strength test data, as well as the interpretation of the test data for estimating the coefficients of the bottom-up fatigue cracking transfer function in the PMED software.
- Appendix I includes the IDT strain at failure test data as a surrogate for the bending beam fatigue strength test. Appendix I also includes the interpretation of the test data for estimating the coefficient for the bottom-up fatigue cracking transfer function in the PMED software.
- Appendix J describes the procedure used to derive the AASHTO asphalt structural layer coefficients from the predicted performance of flexible pavements across Wisconsin. In addition, a few examples illustrating the procedure are included in Appendix J.



## CHAPTER 2 LITERATURE REVIEW

This chapter includes a review of information and data pertinent to the objectives of this research study which is grouped into the four topics or areas listed below:

- The chronological updates to the WisDOT *Standard Specifications for Highway and Structure Construction* of WisDOT with respect to the objective of this study.
- WisDOT research studies delivering information related to the characterizing the asphalt materials used in WisDOT’s projects, including WisDOT’s pavement design methods, implementation and adoption of AASHTOWare PMED software by WisDOT, and the studies resulted in changes to WisDOT’s specification.
- Activities completed by other State Highway Agencies (SHAs) to develop catalogs or libraries of asphalt material inputs for use in the PMED software.
- A summary relative to the sensitivity of predicted distresses to asphalt material properties using the PMED software.

### 2.1 Major Updates in the WisDOT Specification

The following provides a list of the changes made in the WisDOT asphalt materials specifications since the first local calibration of the PMED software in Wisconsin in 2010.

#### 2010 Specifications

- Starting 2010, the use of RAP, RAS, and Fractioned Reclaimed Asphaltic Pavement (FRAP), or their combination as well as the maximum allowable percent binder replacement without changing the asphalt binder grade was specified (see Table 1). It should be noted that the use of up to 35 percent RAP material in lower layers and up to 20 percent in upper layer were allowed in earlier specifications. Changes in the portions of RAP and RAS and how they are included in the mixture design process will have an impact on the asphalt performance properties.

**Table 1. Maximum allowable binder replacement – 2010 specification.**

Recycled Materials	Lower Layers	Upper Layer
RAS only	20%	15%
RAP only	35%	20%
FRAP only	35%	25%
RAS and RAP	30%	20%
RAS and FRAP	30%	25%
RAS, RAP, and FRAP	30%	25%

#### 2011 Specifications

- The maximum allowable binder replacement from the use of recycled materials (RAS/RAP/FRAP) without changing the asphalt binder grade was increased (see Table 2). Changes in the binder replacement will have an impact on the fracture properties of the asphalt mixtures.

**Table 2. Maximum allowable binder replacement – 2011 specification.**

Recycled Materials	Lower Layers	Upper Layer
RAS only	25%	20%
RAP and FRAP	40%	25%
RAS, RAP, and FRAP	35%	25%

*2013 Specifications*

- WMA additives or processes was allowed to be used. The change allowing the use of WMA will have a minimal impact on the asphalt mixture properties. In addition, most WMA mixtures are still produced at the higher production temperatures, The WMA additives or technology is used from a compaction aide standpoint.
- As part of the quality control (QC) management, the voids in the mineral aggregate (VMA) control and warning limits for the job mix formula (JMF) were tightened from -1.5 and -1.2 to -0.5 and -0.2, respectively. This change to the specifications has been found to have a minimal impact on the asphalt performance properties.

*2015 Specifications*

- The minimum VMA for E-3 mixtures (i.e.,  $1 \times 10^6 < \text{equivalent single axle loads (ESALs)} < 3 \times 10^6$  [20 year design life]) with 9.5 mm and 12.5 mm nominal maximum aggregate size (NMAS) was increased by 0.5 percent to 14.5 and 15.5, respectively. For such mixtures and nominal size of aggregate, the specified voids filled with asphalt (VFA) range was also increased to 70 and 76 percent from 65 and 75 percent.
- As part of the QC management, the asphalt content control and warning limits for JMF were tightened from +/-0.4 and +/-0.3 to -0.3 and -0.2, respectively. This change also had a minimal impact on the asphalt performance properties.

*2017 Specifications*

- The Multiple Stress Creep Recovery (MSCR) grading specification in accordance with AASHTO M332, “Standard Specification for Performance-Graded Asphalt Binder Using Multiple Stress Creep Recovery (MSCR) Test” was implemented. As such, the Standard (S), Heavy (H), Very Heavy (V), and Extremely Heavy (E) designation was added to quantify the polymer modification being made and replace the older grade bumping system.
- The mixture design requirement was restructured to account for switching from “E” mixtures to “LT”, “MT”, and “HT” mixtures. Table 3 shows the ESAL range for these mixtures. It should be noted that the mixture requirements (e.g., air voids, VFA, etc.) for the “LT”, “MT”, and “HT” mixtures correspond to “E – 0.3”, “E – 3”, and “E – 10”, respectively.
- The Tensile Strength Ratio (TSR) requirement was increased by 5 percent.

*2018 Specifications*

- The regressed design, i.e., regress air voids from 4 percent design to 3 percent target in JMF, was implemented. Accordingly, the target JMF asphalt binder content first needs to be determined based on the mixture design data at 4.0 percent air voids and the specified design number of gyration ( $N_{des}$ ). Additional asphalt binder is then added to achieve the regressed air void (i.e., 3 percent).
- As part of the QC management, the air voids control and warning limits for JMF were tightened from +/-1.3 and +/-1.0 to +1.3/-1.0 and +1.0/-0.7, respectively.

**Expansion of AASHTOWare ME Design Inputs  
Final Report WHRP 0092-20-03**

- As part of the QC management, the minimum required density was increased by 0.5 percent to 93 percent for upper and lower layers at all traffic levels.

*2020 Specifications*

- The ESAL range for “LT”, “MT”, and “HT” mixtures, shown in Table 3, was removed. However, Chapter 14 of the WisDOT Facilities Development Manual – 2019 specifies the traffic level for these mixtures as follows. The only difference is the maximum number of ESALs for “LT” mixtures which is specified as 1 million (it was 2 million in 2019 specification).
  - LT:  $ESAL \leq 1$  million
  - MT:  $1 \text{ million} < ESAL \leq 8$  million
  - HT:  $> 8$  million
- Table 4 shows the summary of pertinent updates were applied to 2020 specification with regard to stone matrix asphalt (SMA) mixtures.

**Table 3. Switching from “E” mixtures to “LT”, “MT”, and “HT” mixtures – 2017 specification.**

E Mixtures		LT, MT, and HT Mixtures		
Mixtures	ESALs $\times 10^6$ (20 years Design Life)	Mixtures	ESALs $\times 10^6$ (20 years Design Life)	Mixture Requirements
E – 0.3	ESAL < 0.3	LT	ESAL < 2	Similar to E – 0.3
E – 1	$0.3 < ESAL < 1$			
E – 3	$1 < ESAL < 3$	MT	$2 < ESAL < 8$	Similar to E – 3
E – 10	$3 < ESAL < 10$			
E – 30	$10 < ESAL < 30$	HT	ESAL > 8	Similar to E – 10
E – 30x	ESAL > 30			

**Table 4. Updates in SMA mixture design – 2020 specification.**

Requirement	Updates
Percent air voids at $N_{des}$	Increased by 0.5% to 4.5%
Maximum allowable percent binder replacement	Limited to 15%
Maximum percent passing sieve #200 in aggregate gradation	Dropped by 1% to 11% for SMA No. 4 and by 2% to 12% for SMA No. 5
SMA stabilizer	Required to add a cellulose fiber stabilizing additive
Number of gyration for $N_{ini}$ and $N_{max}$	Dropped from 8 and 160, respectively, to 7 and 100

**2.2 Review of Wisconsin Research Studies**

WisDOT has supported several research studies to measure the mechanical properties of asphalt mixtures and/or develop a library or catalog of the asphalt materials inputs that can be integrated into the WisDOT pavement design practice for using the AASHTOWare PMED software. A brief overview of these studies is presented in Table 5 while more details on each study can be found in Appendix A.

**Expansion of AASHTOWare ME Design Inputs  
Final Report WHRP 0092-20-03**

The outcome of the Wisconsin Highway Research Program (WHRP) 0092-08-06 and WHRP 0092-10-07 projects are being used in WisDOT practice for pavement structural design using the AASHTOWare PMED software (see Table 5). These two studies provide the mechanical or performance properties for representative WisDOT asphalt mixtures with a complete level 1 library of asphalt mixtures.

**Table 5. Summary of key findings from the review of WisDOT studies.**

<b>Project</b>	<b>Summary</b>
WHRP 0092-04-07 (Williams et al., 2007)	Dynamic modulus ( $E^*$ ) and flow number ( $Fn$ ) tests were performed to characterize the stiffness and rutting resistance of 21 field-sampled hot mix asphalt (HMA) mixtures.
WHRP 0092-08-06 (Bonaquist, 2010)	Dynamic modulus ( $E^*$ ) and flow number ( $Fn$ ) tests were performed for 12 laboratory-produced asphalt mixtures representing typical and good performing WisDOT mixtures.
WHRP 0092-10-07 (Bonaquist, 2011b)	Low temperature creep compliance and tensile strength properties of 16 WisDOT mixtures, including the mixtures examined in WHRP 0092-08-06, were measured.
WHRP 0092-10-06 (Bonaquist, 2011a)	The practices for using RAP/RAS in asphalt mixtures and the properties of recycled asphalt binders from Wisconsin sources were evaluated.
WHRP 0092-09-01 (Bonaquist, 2012)	The use of the unconfined flow number test in mixture design and acceptance was evaluated and the effect of changes in mixture composition on the flow number was investigated.
WHRP 0092-13-02 (Delgadillo et al., 2007) WHRP 0092-13-02 (Bahia et al., 2013)	In this two-phase study, specification criteria applicable to modified binder being used in the production of Wisconsin asphalt mixtures were established.
WHRP 0092-14-20 (Bahia et al., 2013)	Laboratory test results and field performance data were collected and analyzed to validate the findings and recommendations of the previous research works on the proposed asphalt binder specification.
WHRP 0092-12-02 (Bonaquist et al., 2014)	Two draft specifications for asphalt concrete that cover all types of mixtures (i.e., hot mix asphalt (HMA), WMA, SMA, mixtures with high RAP/RAS content) were developed and recommended. The draft specifications developed in this study have been yet implemented in WisDOT Standard Specifications.
WHRP 0092-15-04 (Bahia et al., 2016)	The use of performance-related properties of asphalt mixtures as a supplement to the Superpave volumetric mixture design and the implementation of asphalt pavement performance-based specifications was evaluated.
WHRP 0092-16-06 (West et al., 2018)	The impact of the air voids regression approach (regressed mixture design) on cracking, rutting, and moisture damage resistance of asphalt mixtures for a total of six mixes designed for low, medium, and high traffic levels was evaluated.

### 2.3 Review Other Agencies Asphalt Material Input Libraries

Many SHAs have developed material libraries or catalogs for the implementation of the PMED software in the past decade. The asphalt material properties measured by several State Department of Transportation (DOT) (Pennsylvania, Nebraska, Michigan, Missouri, Indiana, Ohio, Virginia, Kansas, Utah, and Mississippi) in setting up their asphalt materials library are summarized in

**Expansion of AASHTOWare ME Design Inputs  
Final Report WHRP 0092-20-03**

Appendix B. Some key finding from other DOTs relative to implementing the PMED software are summarized in the following paragraphs.

The asphalt material libraries consist of laboratory-derived properties for agency-specific asphalt mixtures. The asphalt mixture tests being used by most agencies are listed below:

- Dynamic modulus in accordance with AASHTO T 342, “Standard Method of Test for Determining Dynamic Modulus of Hot-Mix Asphalt Concrete Mixtures” and AASHTO T 378, “Standard Method of Test for Determining the Dynamic Modulus and Flow Number for Asphalt Mixtures Using the Asphalt Mixture Performance Tester (AMPT)”.
- Repeated load plastic deformation in accordance with a modified version of AASHTO T 378 or the NCHRP Report 719 procedure (Von Quintus et al., 2012).
- Fatigue strength in accordance with AASHTO T 321, “Standard Method of Test for Determining the Fatigue Life of Compacted Asphalt Mixtures Subjected to Repeated Flexural Bending”. This test method is time-consuming and expensive. As such, some agencies are using the indirect tensile (IDT) strength/failure tensile strain in accordance with a modified version of ASTM D6931, “Standard Test Method for Indirect Tensile (IDT) Strength of Asphalt Mixtures” for estimating the fatigue strength.
- IDT creep compliance and strength in accordance with AASHTO T 322, “Standard Method of Test for Determining the Creep Compliance and Strength of Hot-Mix Asphalt (HMA) Using the Indirect Tensile Test Device”.

Dynamic modulus was considered the cornerstone for developing the asphalt material libraries by some agencies when the first production version of the software was released. Creep compliance and IDT strength tests were the next common tests among the reviewed material libraries. The reason why SHAs focused more on using the dynamic modulus test is related to the hypothesis/assumption included in the NCHRP 1-37A project report (ARA, 2004). The hypothesis used in writing the PMED rudimentary software was the dynamic modulus measured on different asphalt mixtures adequately accounted for differences between the plastic deformation and fatigue strength differences between asphalt mixtures. Thus, one set of plastic strain and fatigue strength coefficients was assumed to be applicable for all asphalt mixtures which was used in the global calibration.

That hypothesis, however, has been found to be incorrect or false. As such, many agencies are now moving towards actually measuring the fatigue strength and plastic strain coefficients in the laboratory, as well as dynamic modulus. Most, if not all, of the reviewed research studies are now sponsoring projects to determine the laboratory-derived mixture k-values measured for the rutting and fatigue cracking using repeated load plastic strain test and flexural bending beam test or the IDT strength/failure strain test, respectively.

The laboratory-derived properties that are mixture-specific have explained some of the residual error between the predicted and measured distresses. Another important finding from the review of previous calibration and material studies is the importance of field investigations for the test sections to derive the local calibration values.

## 2.4 Sensitivity Studies

Since the release of the research-grade or rudimentary version of the PMED software (version 0.7) in 2004, the sensitivity of the predicted distresses or performance indicators to the asphalt mixture properties has been evaluated by many researchers including: Lee (2004), El-Basyouny and Witczak (2005), El-Basyouny et al. (2005), Carvalho and Schwartz (2006), Chehab and Daniel (2006), Graves and Mahboub (2006), Kim et al. (2007), Mallela, et al. (2008), Aguiar-Moya et al. (2009), Ayyala et al. (2010), Yin et al. (2010), Thyagarajan et al. (2010), Cooper et al. (2012), Schwartz et al. (2013), Tarefder et al. (2014), and Tran et al. (2017).

Most of these studies have investigated the degree of sensitivity of the PMED distress prediction to changes in the asphalt mixture and binder input parameters. A summary of the sensitivity evaluation of the PMED predicted distresses to asphalt material properties is summarized in Table 6. [Note: Table 6 represents the overall results from multiple sensitivity analysis referenced in the above paragraph.]

**Table 6. Sensitivity of PMED software to asphalt material inputs.**

Asphalt Material Inputs	Distress			
	Bottom-Up Fatigue Cracking	Longitudinal Cracking <sup>1</sup>	Thermal Cracking	Asphalt Rutting
Dynamic modulus	S*	S	NS	S
Binder grade/stiffness	S	S	S	VS
Creep compliance	NS*	NS	VS	NS
Indirect tensile strength at 14°F	NS	NS	VS	NS
Air voids	VS*	VS	VS	VS
Effective binder content	VS	VS	VS	VS
Heat capacity	NS	NS	S	NS
Thermal conductivity	NS	NS	S	NS
Aggregate coefficient of thermal contraction	NS	NS	VS	NS
Poisson's ratio	S	S	S	S
Unit weight	NS	NS	NS	NS

\* NS: Not sensitive; S: Sensitive; VS: Very sensitive.

NOTE 1 – Longitudinal cracking represented top-down cracking in the PMED versions prior to 2.6. The original top-down cracking transfer function was replaced in version 2.6. All of the sensitivity studies reviewed were completed on older versions of the top-down cracking transfer function.

## 2.5 Summary

The review of the chronological updates in the WisDOT Standard Specifications regarding the objective of this study found the 2020 WisDOT Standard Specifications allows for higher usage of recycled materials without changing the asphalt binder grade as compared to the 2010 specifications (see Figure 1). WisDOT has implemented a 3.0 percent air void regression (regressed mixture design) approach in 2018. It is anticipated that regressed mixture design results in a substantial improvement in asphalt mixtures flexibility (i.e., fatigue cracking resistance) without significantly jeopardizing the rutting resistance. Another major update implemented in 2017 is the switch from “E” mixes to “Low Traffic (LT)”, “Medium Traffic (MT)”, and “High Traffic (HT)” mixes, and subsequent changes in the mixture requirements with respect to the 20-

year design ESALs. AASHTO M 332 (MSCR specification) was implemented in the 2017 specification.

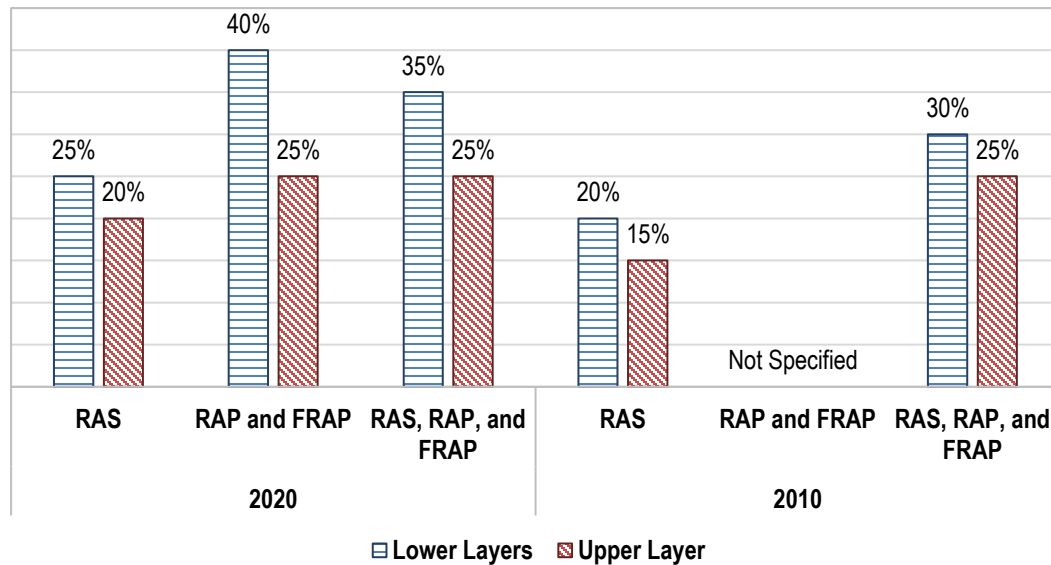


**Figure 1. Maximum Allowable Percent Binder Replacement Specified in the 2020 and 2010 WisDOT Standard Specifications.**

Four points related to the literature and specification review for asphalt mixtures in Wisconsin are listed and discussed below.

1. The volumetric properties applied in this study were determined from the average values reported in the asphalt mixture design reports (see Appendix D) and measured on the test specimens prepared for testing within this study. With all of the changes made to the WisDOT asphalt specifications, it is important to identify or determine if the asphalt mixture default volumetric properties have changed so that different input values should be used for mixtures designed and placed in accordance with the specification at different times. It is suggested that the annual construction data be reviewed over the past couple of years to determine if the default volumetric values should be changed than were determined when the PMED software was first implemented and used in Wisconsin.
2. Dynamic modulus and IDT creep compliance and strengths were measured on selected WisDOT wearing surface mixtures from other research projects. The data measured from these other studies were combined with the test results from this study.
3. Most, if not all, of the earlier research studies measured and reported the flow number. The flow number, however, is not an input for the asphalt mixtures in the PMED software. The laboratory-derived mixture inputs are the k-values measured from a repeated load plastic strain test and represent confined testing conditions. It is our understanding that the earlier flow number tests used in the WHRP projects represent unconfined testing conditions. The unconfined tests should not be used in comparison to the confined test conditions because the effect of the aggregate is typically not captured by unconfined tests. The raw data for

confined flow number tests can be used as a comparison to the confined repeated load plastic strain test, as long as conditioning cycles are included or considered in the flow number test results.

The regression equations used in NCHRP project 1-40B (Von Quintus, et al., 2009) can be used to estimate the  $k_r$ -coefficients of the rut depth transfer function based on the volumetric and component properties of the mixture. These regression equations to calculate the  $k_r$ -coefficients, however, were excluded from the MEPDG Manual of Practice. Thus, repeated load plastic strain tests were included in this study to measure the rut depth  $k_r$ -coefficients to predict the rut depth in the asphalt base layers and wearing surfaces.

4. None of the research studies reviewed included flexural bending beam fatigue tests for measuring the fatigue strength of asphalt base mixtures in Wisconsin. The regression equations used in NCHRP project 1-40B (Von Quintus, et al., 2009) can be used to estimate the fatigue strength  $k_f$ -coefficients of WisDOT asphalt base mixtures. The regression equations to calculate the  $k_f$ -coefficients, however, were excluded from the MEPDG Manual of Practice. Thus, flexural bending beam fatigue and IDT failure strain tests were included in this study to measure the fatigue strength  $k_f$ -coefficients to predict bottom-up fatigue cracks of flexible pavements.



## CHAPTER 3 ASPHALT BINDER AND MIXTURE TESTS

The binders and mixtures procured and used in this study were approved by WisDOT and obtained from different local suppliers and producers, which were used in actual construction projects.

### 3.1 Asphalt Binders

Only six binder grades (shown in Table 7) have been used in the Wisconsin construction projects since the start of this project in 2019. All six binder grades were included in the testing plan for this study, because they represent the greatest usage of asphalt binders in Wisconsin. The finalized test plan included each of the six asphalt binder grades from two sources (i.e., a total of twelve asphalt binder samples) that were anticipated to have differences in binder properties with the same grade.

**Table 7. Asphalt binder grades included in the testing plan, defined by AASHTO M 350.**

PMED Binder Grade; AASHTO T 315	MSCR Binder Grade; AASHTO M 350
PG58-28	PG58-28S
	PG58-28H
	PG58-28V
PG58-34	PG58-34S
	PG58-34H
	PG58-34V

The level 1 inputs required by the PMED software includes the asphalt binder complex shear modulus ( $G^*$ ) and phase angle ( $\delta$ ) measured on Rolling Thin Film Oven (RTFO) aged binders at multiple test temperatures. The MSCR test is not required as an input to the PMED software, but is recommended for better evaluation of binder modification. The MSCR test likely will be included in the MEPDG Manual of Practice, as an enhancement in the future. Thus, the asphalt binder test plan summarized in Table 8 included both  $G^*$  and  $\delta$  measurements for multiple temperatures, as well as the MSCR testing at the high temperature grade (i.e., 58°C [136.4°F]).

The asphalt binder data is used to determine the dynamic modulus and creep compliance master curves for predicting the load and non-load related distresses. The RTFO aged asphalt binder data is also used to harden or age the asphalt mixture with time for calculating the dynamic modulus with pavement depth over the design life of the pavement.

The 6 asphalt binder samples from source 1 and the 6 samples from source 2 are listed in Table 8. Appendix C includes the test results from all of the 12 asphalt binders, while Table 9 includes a summary of the test results for comparing the different binders. The asphalt binders in Table 9 are listed in order of increasing binder stiffness as defined by  $G^*$  measured at 22°C (71.6°F). The PG58-28 asphalt binders have a significantly higher  $G^*$  than the PG58-34 asphalt binders. Table 10 lists the average  $G^*$  values measured at 58°C (136.4°F) for AASHTO T 350, but segregated by the primary asphalt binder grades of PG58-28 and PG58-34. As shown,  $G^*$  decreases from the “V” grade binders to the “S” grade binders. In addition, there is a greater difference between the PG58-28 and PG58-34 binders in values for the grade “V” binders compared to the grade “S” binders measured at 58°C (136.4°F).

**Table 8. Asphalt binder testing plan.**

Asphalt Binder Sources and Grades		Test Procedure; All Binders	Comment
Source 1	Source 2		
AC2111; PG 58-28 S AC2113; PG 58-28 H AC2128; PG 58-28 V AC2115; PG 58-34 S AC2116; PG 58-34 H AC2117; PG 58-34 V	AC2112; PG 58-28 S AC2118; PG 58-28 H AC2119; PG 58-28 V AC2121; PG 58-34 S AC2122; PG 58-34 H AC2125; PG 58-34 V	AASHTO T 315 “Standard Method of Test for Determining the Rheological Properties of Asphalt Binder Using a Dynamic Shear Rheometer (DSR)”	$G^*$ and $\delta$ on RTFO aged binder at multiple test temperatures.
		AASHTO T 350 “Standard Method of Test for Multiple Stress Creep Recovery (MSCR) Test of Asphalt Binder Using a Dynamic Shear Rheometer (DSR)”	$J_{nr}$ and $J_{nr,diff}$ on RTFO aged binder at the high PG temperature.

**Table 9. Asphalt binder test result summary, AASHTO T 315.**

Binder Identification	Binder Grade	Test Temp. 22 °C (71.6 °F)		Test Temp. 58 °C (136.4 °F)	
		Complex Shear Modulus, Pa	Phase Angle, degrees	Complex Shear Modulus, Pa	Phase Angle, degrees
AC2119	PG58-28V	1,330,000	58.9	11,200	62.8
AC2128	PG58-28V	1,295,000	60.6	8,110	64.1
AC2111	PG58-28S	1,262,000	64.0	3,450	83.7
AC2118	PG58-28H	1,192,000	61.0	8,870	68.8
AC2113	PG58-28H	1,074,000	62.5	6,350	76.6
AC2112	PG58-28S	1,013,000	66.5	2,910	84.4
AC2125	PG58-34V	530,000	62.2	6,450	62.9
AC2122	PG58-34H	449,800	63.4	5,850	64.7
AC2121	PG58-34S	434,200	65.1	3,920	76.6
AC2117	PG58-34V	430,300	63.4	4,900	60.0
AC2116	PG58-34H	416,500	64.2	3,740	65.8
AC2115	PG58-34S	394,200	65.1	2,840	73.6

**Table 10. Average complex shear modulus values for the different AASHTO T 350 asphalt binder grade designations.**

Asphalt Binder Grades, AASHTO T 315	AASHTO Binder Grade Designations, AASHTO T 350	Average Complex Shear Modulus at 58°C (136.4°F), Pa
PG58-28	V	9,655
	H	7,610
	S	3,180
PG58-34	V	5,675
	H	4,795
	S	3,380

## 3.2 Asphalt Mixtures

The asphalt mixtures for expanding WisDOT's asphalt mixture library were grouped into two types of mixtures: surface and base mixtures, as noted in Table 11 and Table 12 – the asphalt mixture test plan. The mixtures selected for this study were those that represent the higher tonnage of surface and base mixtures placed in Wisconsin over the past 3 years. The mixtures were tested to derive the asphalt mixture or layer properties that are inputs to the PMED software and compare the input level 1 laboratory test results to the input level 3 global default values that are in the AASHTOWare PMED software.

The specific asphalt mixtures sampled and included in the test plan are listed in Table 12, while Table 13 includes a summary of the mixture design information. A summary of the WisDOT mixture design reports provided are included in Appendix D. Table 14 and Table 15 summarize the volumetric and component properties extracted from the JMF, and used to prepare and test the asphalt mixtures in accordance with the MEPDG Manual of Practice.

## 3.3 Asphalt Mixture Test Results

This section of Chapter 3 summarizes the results from the asphalt mixtures included in the test plan and provides a brief comparison of the test results.

### 3.3.1 Dynamic Modulus Tests

Dynamic modulus is the material property used in the MEPDG to characterize the stiffness of all asphalt layers throughout different seasons and under different truck loading configurations. The dynamic modulus is measured in accordance with AASHTO T 342, *Standard Method of Test for Determining Dynamic Modulus of Hot-Mix Asphalt Concrete Mixtures*.

The result or outcome from the test procedure is the dynamic modulus values for different temperatures and load frequencies. The PMED software requires at least 5 test temperatures and 4 frequencies. The test temperatures included in the test plan were 14, 40, 70, 100, and 130 °F (-10, 4.4, 21.1, and 54.4 °C), and the loading frequencies were 0.1, 0.5, 1, 5, 10, and 25 Hz which are the values normally used to generate the dynamic modulus master curve. The dynamic modulus values measured for the asphalt mixtures identified in Table 12 are included in Appendix E.

The temperature-time dependent dynamic modulus is used to predict bottom-up and top-down fatigue or alligator cracking and rut depth in the asphalt layers. The higher the dynamic modulus values, the greater the resistance to load-related cracking and rutting. The MEPDG assumes the dynamic modulus regression equation included in the software to calculate dynamic modulus (input level 3) is applicable to all dense-graded asphalt mixtures.

Table 16 lists the average dynamic modulus measured for some selected temperatures and frequencies. The mixtures are organized by increasing stiffness measured at a test temperature of 130°F (54.4°C) and load frequency of 25 Hz. Figure 2 is a graphical comparison of the dynamic modulus and number of design gyrations used in mixture design ( $N_{\text{Design}}$ ). As shown, the dynamic modulus at the higher test temperatures increases with  $N_{\text{Design}}$ . Asphalt mixture #0057 is identified

**Expansion of AASHTOWare ME Design Inputs  
Final Report WHRP 0092-20-03**

as an outlier in Table 16, because it has a much higher dynamic modulus than the other asphalt mixtures for  $N_{Design}$  of 40 gyrations. Mixture #0057, however, contains a higher percent of RAP and RAS, and higher fine aggregate angularity (FAA) with a value of 44.0 than the other mixtures designed with an  $N_{Design}$  of 40 gyrations. Mixtures #0208 and #8357 with  $N_{Design}$  of 40 gyrations contain no RAS and the FAA is less than 43 exhibited the lower dynamic modulus of all the asphalt mixtures.

**Table 11. Asphalt mixture testing plan.**

Test Procedure	Number of Mixture	Comment
<i>AASHTO T 378-17</i> ; Dynamic Modulus and <i>AASHTO R 84-17</i> ; Dynamic Modulus Master Curve Development	17 Mixtures	Dynamic modulus test performed on the asphalt surface and base mixtures.
<i>AASHTO T 322-07</i> ; Indirect Tensile Creep Compliance and Strength	10 Mixtures	Creep compliance test performed only on mixtures placed on the surface
<i>NCHRP 9-30A</i> ; Repeated Load Plastic Deformation	11 Mixtures	RLPD test performed on the representative number of asphalt surface and base mixtures.
<i>AASHTO T 321-17</i> ; Repeated Flexural Bending Beam for Fatigue	4 Mixtures	Fatigue test performed on the representative number of base mixtures.
<i>NCHRP 9-06</i> ; Indirect Tensile Strength and Failure Strain	5 Mixtures	IDT test performed on the representative number of base mixtures.

**Table 12. Asphalt mixtures included in the test plan.**

Mixture Identification			Dynamic Modulus	Repeated Load Plastic Deformation	Creep Compliance	Tensile Strain at Failure	Bending Beam Fatigue
003	Base	PG58-28S; 3MT	√			√	
057	Base	PG58-28S; 3LT	√	√		√	√
093	Surface	PG58-28H; 4HT	√		√		
119	Base	PG58-28S; 3HT	√			√	√
121	Surface	PG58-28V; 4SMA	√	√	√		
127	Surface	PG58-34S; 4MT	√		√		
165	Surface	PG58-28S; 4HT	√		√		
208	Surface	PG58-28S; 4LT	√	√	√		
236	Surface	PG58-28S; 4MT	√	√	√		
251	Surface	PG58-28V; 4HT	√	√			
258	Surface	PG58-28S; 4MT	√	√	√		
319	Surface	PG58-28H; 4MT	√	√	√		
1020	Surface	PG58-34V; 4SMA	√	√	√		
1060	Base	PG58-28H; 3HT	√	√		√	√
1166	Base	PG58-28S; 2HT	√			√	√
7130	Surface	PG58-34V; 5MT	√	√			
8357	Surface	PG58-34S; 4LT	√		√		

**Table 13. Job mix formula information for the asphalt mixtures included in test plan.**

Mixture Identification			Percent RAP/RAS	N <sub>Design</sub> Gyration	Specific Gravities		Additive	
					G <sub>se</sub> *	G <sub>mm</sub> **	Type	Amount
003	Base	PG58-28S; 3MT	32 (RAP)	75	2.705	2.513	---	---
057	Base	PG58-28S; 3LT	24 (RAP/RAS)	40	2.761	2.567	---	---
119	Base	PG58-28S; 3HT	20 (RAP)	100	2.753	2.561	---	---
1060	Base	PG58-28H; 3HT	14 (RAP/RAS)	100	2.784	2.553	---	---
1166	Base	PG58-28S; 2HT	12 (RAP/RAS)	100	2.694	2.483	Evotherm	0.35
093	Surface	PG58-28H; 4HT	25 (RAP)	100	2.769	2.538	---	---
127	Surface	PG58-34S; 4MT	18 (RAP)	75	2.657	2.453	---	---
165	Surface	PG58-28S; 4HT	13 (RAP/RAS)	100	2.709	2.505	Evotherm	0.40
208	Surface	PG58-28S; 4LT	20 (RAP)	40	2.722	2.517	Evotherm	0.35
236	Surface	PG58-28S; 4MT	20 (RAP)	75	2.782	2.557	---	---
251	Surface	PG58-28V; 4HT	12.4 (RAP/RAS)	100	2.754	2.534	---	---
258	Surface	PG58-28S; 4MT	20 (RAP)	75	2.707	2.488	---	---
319	Surface	PG58-28H; 4MT	23 (RAP)	75	2.731	2.517	---	---
7130	Surface	PG58-34V; 5MT	22 (RAP)	75	2.701	2.455	---	---
8357	Surface	PG58-34S; 4LT	20 (RAP)	40	2.659	2.451	---	---
121	Surface	PG58-28V; 4SMA***	3 (RAS)	100	2.666	2.432	Lime	10
1020	Surface	PG58-34V; 4SMA***	3 (RAS)	100	2.666	2.432	Lime	10

\* G<sub>se</sub> is the effective specific gravity of the aggregate blend.

\*\* G<sub>mm</sub> is the maximum or Rice specific gravity of the asphalt mixture.

\*\*\* SMA – Stone Matrix Asphalt.

Similarly, asphalt mixture #0003 for N<sub>Design</sub> of 75 gyrations was found to have a slightly higher dynamic modulus than mixture #0165 at 100 N<sub>Design</sub> gyrations. Asphalt mixture #0003, however, is the mixture with the highest amount of RAP (32 percent) and significantly exceeds the amount of RAP/RAS in mixture #0165 (13 percent).

**Table 14. Gradation of the asphalt mixtures, organized by base and surface layers.**

Mixture Identification			Mix Size Designation	Gradation, percent passing sieve size			
				¾-inch	3/8-inch	#4	#200
003	Base	PG58-28S; 3MT	12.5 mm	99.1	80.6	63.2	4.2
057	Base	PG58-28S; 3LT	19 mm	99.0	82.0	59.5	4.1
119	Base	PG58-28S; 3HT	19 mm	97.9	70.5	57.4	3.1
1060	Base	PG58-28H; 3HT	19 mm	96.7	83.9	68.0	3.9
1166	Base	PG58-28S; 2HT	25 mm	88.7	73.2	53.8	3.0
093	Surface	PG58-28H; 4HT	12.5 mm	100	89.1	78.0	3.4
127	Surface	PG58-34S; 4MT	12.5 mm	100	77.2	63.6	3.3
165	Surface	PG58-28S; 4HT	12.5 mm	100	87.8	65.9	4.4
208	Surface	PG58-28S; 4LT	12.5 mm	100	82.3	63.1	4.7
236	Surface	PG58-28S; 4MT	12.5 mm	100	82.8	66.8	4.1
251	Surface	PG58-28V; 4HT	12.5 mm	100	89.6	66.5	5.1
258	Surface	PG58-28S; 4MT	12.5 mm	99.6	88.4	74.5	4.7
319	Surface	PG58-28H; 4MT	12.5 mm	100	89.0	67.1	4.5
7130	Surface	PG58-34V; 5MT	9.5 mm	100	95.9	73.2	3.1
8357	Surface	PG58-34S; 4LT	12.5 mm	100	84.4	64.8	4.7
121	Surface	PG58-28V; 4SMA	12.5 mm	100	78.2	34.7	8.3
1020	Surface	PG58-34V; 4SMA	12.5 mm	100	78.2	34.7	8.3

**Table 15. Selected volumetric properties of the asphalt mixtures.**

Mixture Identification			Percent RAP/RAS	G <sub>se</sub> *	Asphalt Content		VMA, design	Air Voids
					Total by weight	Effective by Volume		
003	Base	PG58-28S; 3MT	32 (RAP)	2.705	5.2	10.5	13.4	6.9
057	Base	PG58-28S; 3LT	24 (RAP/RAS)	2.761	4.8	10.7	14.2	7.0
119	Base	PG58-28S; 3HT	20 (RAP)	2.753	5.0	10.6	13.8	7.0
1060	Base	PG58-28H; 3HT	14 (RAP/RAS)	2.784	5.2	10.2	14.0	7.0
1166	Base	PG58-28S; 2HT	12 (RAP/RAS)	2.694	5.3	11.6	15.5	6.9
093	Surface	PG58-28H; 4HT	25 (RAP)	2.769	5.7	11.6	15.5	6.7
127	Surface	PG58-34S; 4MT	18 (RAP)	2.657	5.7	12.2	15.3	7.1
165	Surface	PG58-28S; 4HT	13 (RAP/RAS)	2.709	5.7	12.1	14.6	6.9
208	Surface	PG58-28S; 4LT	20 (RAP)	2.722	5.4	11.7	14.8	6.7
236	Surface	PG58-28S; 4MT	20 (RAP)	2.782	5.5	11.7	15.8	7.4
251	Surface	PG58-28V; 4HT	12.4 (RAP/RAS)	2.754	5.7	11.0	14.6	7.1
258	Surface	PG58-28S; 4MT	20 (RAP)	2.707	5.6	11.5	14.8	6.8
319	Surface	PG58-28H; 4MT	23 (RAP)	2.731	5.6	11.3	14.8	7.3
7130	Surface	PG58-34V; 5MT	22 (RAP)	2.701	6.1	12.0	15.9	6.9
8357	Surface	PG58-34S; 4LT	20 (RAP)	2.659	5.3	11.9	15.2	6.9
121	Surface	PG58-28V; 4SMA***	3 (RAS)	2.666	5.95	12.8	17.8	6.9
1020	Surface	PG58-34V; 4SMA***	3 (RAS)	2.666	5.9	12.9	17.8	6.9

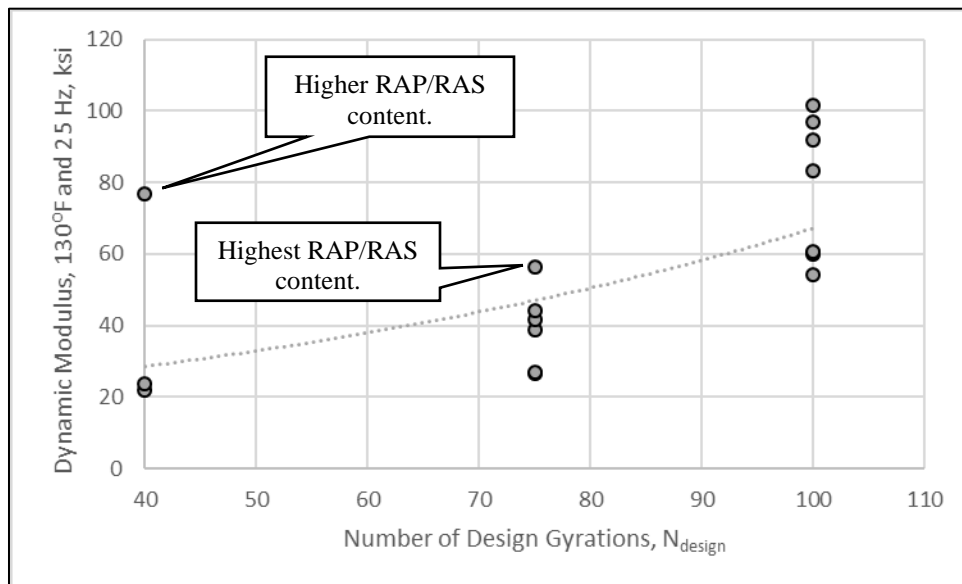
\* Effective specific gravity of the aggregate blend from the job mix formula.

\*\* 10 percent lime includes in all of the SMA mixtures.

**Table 16. Dynamic modulus measured on selected mixtures (mixtures organized by increasing stiffness).**

Mixture Identification					Mix Size Designation	N <sub>Design</sub> Gyration	Dynamic Modulus, ksi		
							Temperature, °F (°C)		
							14 (-10)	70 (21.1)	130 (54.4)
							Load Frequency, Hz.		
			0.1	5	25				
208	Surface	PG58-28S	4 LT	12.5 mm	40	1,684	344	22.1	
8357	Surface	PG58-34S	4 LT	12.5 mm	40	1,310	289	23.8	
236	Surface	PG58-28S	4 MT	12.5 mm	75	1,530	289	26.7	
127	Surface	PG58-34S	4 MT	12.5 mm	75	1,427	267	27.1	
7130	Surface	PG58-34V	5 MT	9.5 mm	75	1,533	356	38.7	
258	Surface	PG58-28S	4 MT	12.5 mm	75	1,319	330	41.6	
319	Surface	PG58-28H	4 MT	12.5 mm	75	1,737	476	44.1	
165	Surface	PG58-28S	4 HT	12.5 mm	100	1,822	603	54.2	
003	Base	PG58-28S	3 MT	12.5 mm	75	2,152	680	56.5	
1020	Surface	PG58-34V	4 SMA	12.5 mm	100	2,069	687	59.9	
121	Surface	PG58-28V	4 SMA	12.5 mm	100	1,772	535	60.4	
1166	Base	PG58-28S	2 HT	25 mm	100	1,821	559	60.6	
057	Base	PG58-28S	3 LT	19 mm	40	2,336	874	76.9	
093	Surface	PG58-28H	4 HT	12.5 mm	100	2,151	788	83.2	
119	Base	PG58-28S	3 HT	19 mm	100	2,267	862	92.0	
1060	Base	PG58-28H	3 HT	19 mm	100	2,104	816	97.0	
251	Surface	PG58-28V	4 HT	12.5 mm	100	2,110	846	101.4	

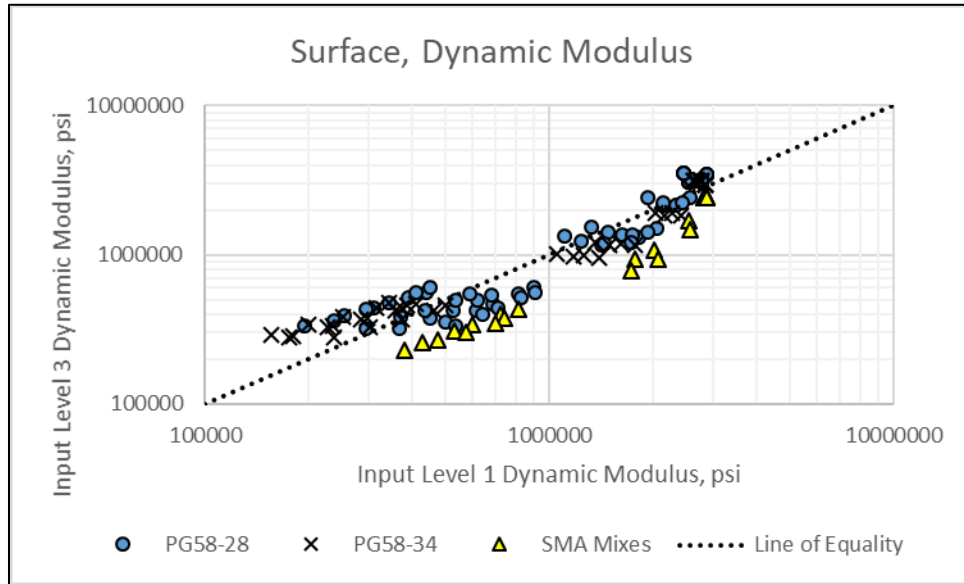
Note: Highlighted cells are believed to be an outlier or an anomaly.



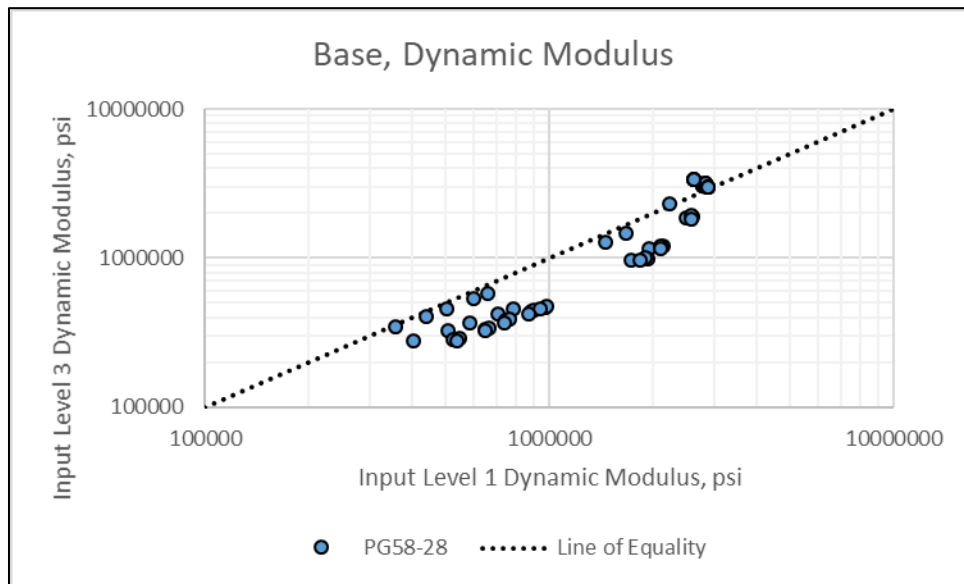
**Figure 2. Graphical Comparison of N<sub>design</sub> Gyration and Dynamic Modulus Measured at 130°F (54.4 °C) and 25 Hz.**



Figure 3 displays a comparison of the input level 3 dynamic modulus calculated by the PMED software and the measured values for the wearing surface mixtures (see Table 12). Similarly, Figure 4 compares input level 1 and input level 3 dynamic moduli for the asphalt base mixtures. As shown, the input level 3 calculated dynamic moduli are different for the wearing surface mixtures and the difference is dependent on the mixture type and binder grade.



**Figure 3. Input Level 1 Measured Dynamic Modulus Compared to Input Level 3 Global Dynamic Modulus for the Wearing Surface Mixtures.**



**Figure 4. Input Level 1 Measured Dynamic Modulus Compared to Input Level 3 Global Dynamic Modulus for the Asphalt Base Mixtures.**

The input level 1 measured dynamic moduli are consistently higher than the input level 3 calculated dynamic moduli for the asphalt base mixtures (see Figure 4). The difference is greater for the higher temperatures or less stiff mixtures, so it is stiffness dependent. The difference is

sufficient to result in a significant bias between the distresses predicted by the PMED software. Some of the potential reasons or explanations for these differences are listed below.

1. One load frequency (25 Hz) of the laboratory measured values for input level 1 was used in the comparison to input level 3 calculated values from the PMED software. The frequency used in the PMED software is asphalt depth and truck speed dependent. The frequency decreases with depth in the asphalt layer. Lower load frequencies are used in the asphalt base layers in comparison to the wearing surfaces.
2. The laboratory measured dynamic moduli (input level 1) are dependent on the asphalt binder properties (grade designations “V,” “H,” and “S.” One default set of binder properties are used for PG58-28 and one set of properties are used for PG58-34 to calculate the dynamic moduli (input level 3).
3. The majority of the asphalt mixtures used to develop the dynamic modulus regression equation included in the PMED software did not include substantial amounts of RAP and/or RAS in the mixtures.

### ***3.3.2 Indirect Tensile Creep Compliance Tests***

Creep compliance is the material property used in the MEPDG to characterize the low temperature properties of asphalt wearing surface throughout different seasons. Creep compliance is measured in accordance with AASHTO T 322, *Standard Method of Test for Determining the Creep Compliance and Strength of Hot Mix Asphalt (HMA) Using the Indirect Tensile Test Device*.

The result or outcome from the test is the creep compliance values for different temperatures measured over long term load durations. The PMED software requires 3 test temperatures and 100 second loading time or duration. The test temperatures included in the test plan were -4, 14, and 32 °F (-20, -10, 0 °C), and the creep compliance is measured over a load duration of 100 seconds. The creep compliance values are entered into the PMED software are load durations of 1, 2, 5, 10, 20, 50, and 100 seconds. The creep compliance values measured for the asphalt mixtures identified in Table 12 are included in Appendix F.

The temperature-load duration dependent creep compliance values are used to predict the length of transverse cracks. The higher the creep compliance or the more compliant the mixture, the greater the resistance to the occurrence of transverse cracks. The MEPDG assumes the creep compliance regression equation included in the software to calculate creep compliance (input level 3) is applicable to all dense-graded asphalt mixtures.

Table 17 lists the average creep compliance measured for the 3 test temperatures at a load duration of 100 seconds. The mixtures are organized by increasing creep compliance measured at 14°F (-10°C) for 100 loading seconds. Higher creep compliance values results in lower predicted lengths of transverse cracks. Table 18 is a reordering of the creep compliance values from the least to most compliant mixtures illustrating that the IDT creep compliance values are dependent on the asphalt binder grade and  $N_{\text{design}}$  gyrations.

**Table 17. Creep compliance measured on selected mixtures at 100 second load duration (mixtures organized by increasing creep compliance).**

Mixture Identification			VMA *	V <sub>be</sub> ,** %	N <sub>design</sub> Gyrations	Creep Compliance, 10 <sup>-7</sup> in./psi (100 seconds)			IDT Strength, psi
						Temperature, °F (°C)			
						-4 (-20)	14 (-10)	32 (0)	
093	PG58-28H	4 HT	15.5	11.6	100	4.41	8.39	22.8	512
121	PG58-28V	4 SMA	17.8	12.8	100	4.63	10.5	28.0	448
165	PG58-28S	4 HT	14.6	12.1	100	5.23	11.9	31.5	430
319	PG58-28H	4 MT	14.8	11.3	75	5.17	11.1	37.2	465
208	PG58-28S	4 LT	14.8	11.7	40	5.96	16.5	73.2	358
1020	PG58-34V	4 SMA	17.8	12.9	100	6.33	18.4	64.4	378
258	PG58-28S	4 MT	14.8	11.5	75	6.85	20.2	74.9	457
236	PG58-28S	4 MT	15.8	11.7	75	6.57	23.1	101.0	481
127	PG58-34S	4 MT	15.3	12.2	75	8.30	22.4	106.0	417
8357	PG58-34S	4 LT	15.2	11.9	40	8.51	29.8	138.0	398

\* VMA – Voids in mineral aggregate.

\*\* V<sub>be</sub> – Effective asphalt content by volume.

**Table 18. Creep compliance grouped into different categories.**

Mix #	Asphalt Grade Designation		N <sub>Design</sub> Gyrations	Creep Compliance, 10 <sup>-7</sup> in./psi (100 seconds)			IDT Strength, psi
				Temperature, °F (°C)			
				-4 (-20)	14 (-10)	32 (0)	
093	PG58-28	H	100	4.41	8.39	22.8	512
121		V		4.63	10.5	28.0	448
165		S		5.23	11.9	31.5	430
319		H	75	5.17	11.1	37.2	465
258		S		6.85	20.2	74.9	457
236		S		6.57	23.1	101.0	481
208		S		40	5.96	16.5	73.2
1020	PG58-34	V	100	6.33	18.4	64.4	378
127		S	75	8.30	22.4	106.0	417
8357		S	40	8.51	29.8	138.0	398

Figure 5 and Figure 6 display a comparison of the input level 3 creep compliance values calculated by the PMED software and the measured values. The input level 3 calculated creep compliance values are statistically higher than input level 1 measured creep compliance. The difference is greater for the lower test temperature for the PG58-34 asphalt binder, while the difference is greater for the higher test temperature for the PG58-28 asphalt binder, so the difference is stiffness dependent. The difference is sufficient to result in a significant bias between the lengths of transverse cracks predicted by the PMED software.

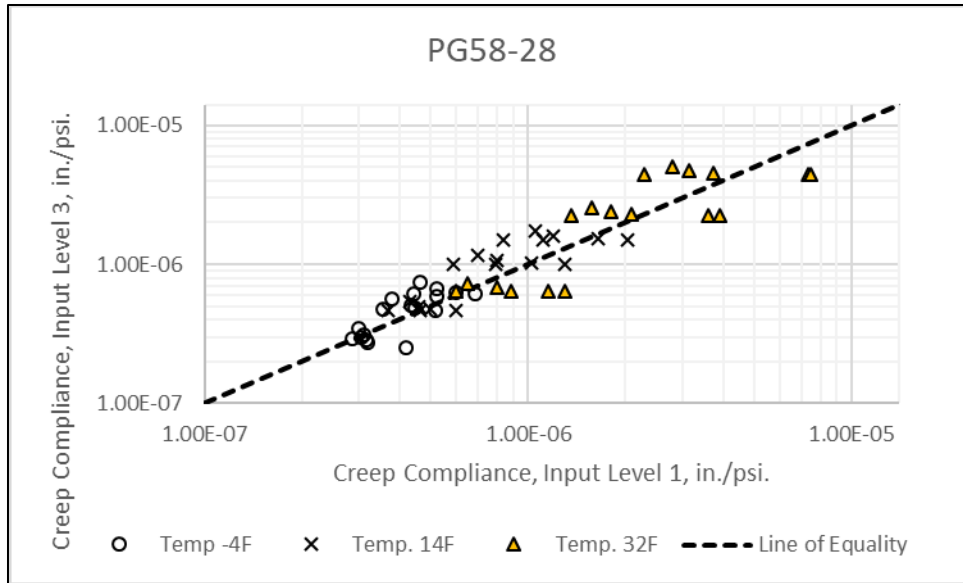


**Figure 5. Graphical Comparison of Input Levels 1 and 3 Creep Compliance for Mixtures with a PG58-28 Asphalt Binder.**

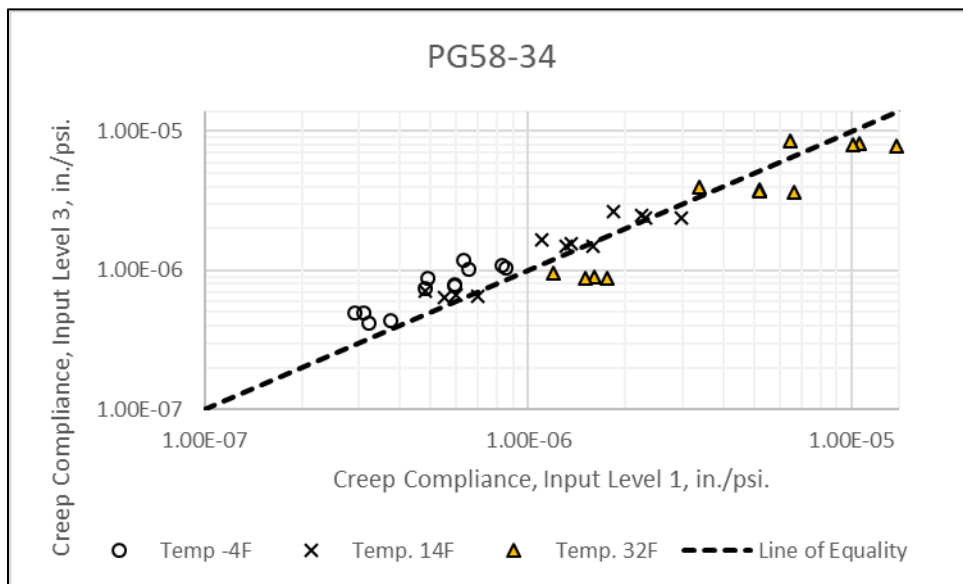


**Figure 6. Graphical Comparison of Input Levels 1 and 3 Creep Compliance for Mixtures with a PG58-348 Asphalt Binder.**

### 3.3.3 Indirect Tensile Strength Tests

The AASHTOWare PMED software predicts the length of transverse cracks using the average IDT tensile strength of the mixture measured at -10 °C (14 °F) for input level 2. The software interface and definition of the input levels were revised in 2017. Input level 1 includes measuring the IDT strength at three or more test temperatures, while input level 2 includes measuring the IDT strength at -10 °C (14 °F) and the software calculates the IDT strengths at higher temperatures.

Input level 3 is the same as in previous versions of the software, the strength at -10 °C (14 °F) is calculated from regression equations derived from data measured on virgin, neat asphalt mixtures.

The IDT strength is measured in accordance with AASHTO T 322, and analysis of the AASHTO strength test data is straightforward; the average of the tensile strengths measured on three test specimens is reported as the asphalt mixture's IDT strength. The IDT strengths from the test are entered directly into the PMED software for specific temperatures from the laboratory test data. Table 18 lists the IDT strengths for the mixtures identified in Table 12.

Figure 7 includes a graphical comparison of input levels 1 and 3 IDT strengths. The difference between the measured (input level 1) and calculated (input level 3) IDT strengths are asphalt grade dependent.

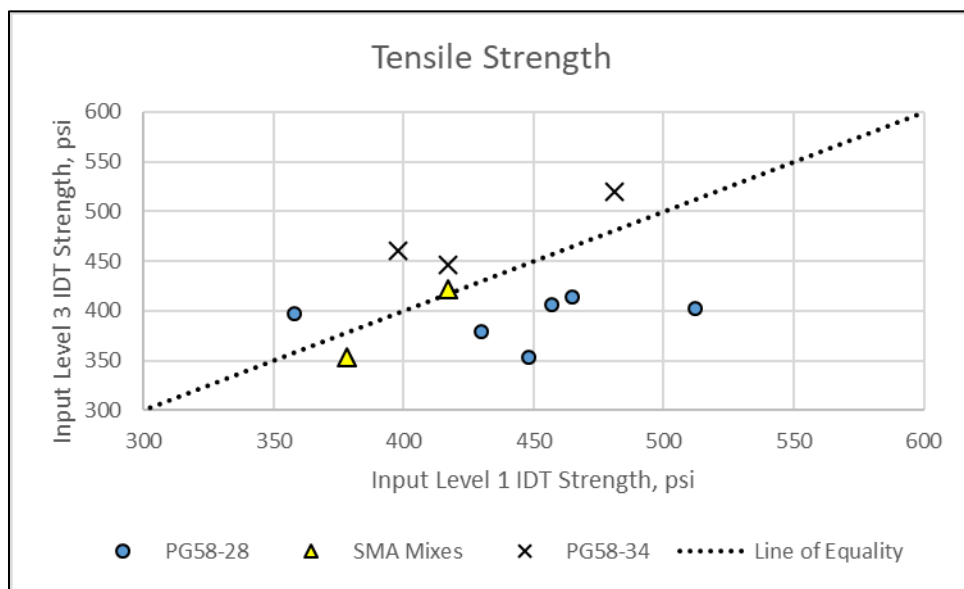


Figure 7. Graphical Comparison of Input Levels 1 and 3 IDT Strengths.

### 3.3.4 Repeated Load Plastic Strain Tests

NCHRP 9-30A, *Calibration of Rutting Models for HMA Structural and Mix Design*, recommended revisions to the original MEPDG rutting model (Von Quintus, et. al., 2012). These revisions are incorporated in the current version of AASHTOWare PMED, to allow pavement designers to enter asphalt mixture specific plastic strain coefficients ( $k_{1r}$ ,  $k_{2r}$ ,  $k_{3r}$ ) for the asphalt layers. The plastic strain coefficients are derived from a laboratory repeated load plastic strain test, and are used to predict rutting in the asphalt layers.

Figure 8 shows a typical log-log plot from a repeated load plastic strain test and identifies the slope and intercept used in AASHTOWare PMED software. The repeated load plastic strain curve can exhibit three zones, as defined below.

1. The first part of the curve is termed the “primary” zone. The primary zone is where the plastic strain increases at a decreasing rate with increasing load cycles.
2. The second part of the curve is termed the “secondary” or steady state zone, and is where the slope of the plastic strain curve is nearly constant. The rut depth prediction model in AASHTOWare PMED software uses the slope and intercept from the secondary zone of the plastic strain curve, as shown in Figure 8.
3. The third part of the curve is termed the “tertiary” zone, and is where the slope of the plastic strain curve increases at an increasing rate with increasing load cycles. Asphalt mixtures resistant to plastic strain do not exhibit the tertiary zone. Mixtures that exhibit the tertiary response under confined testing conditions are susceptible to excessive rutting.

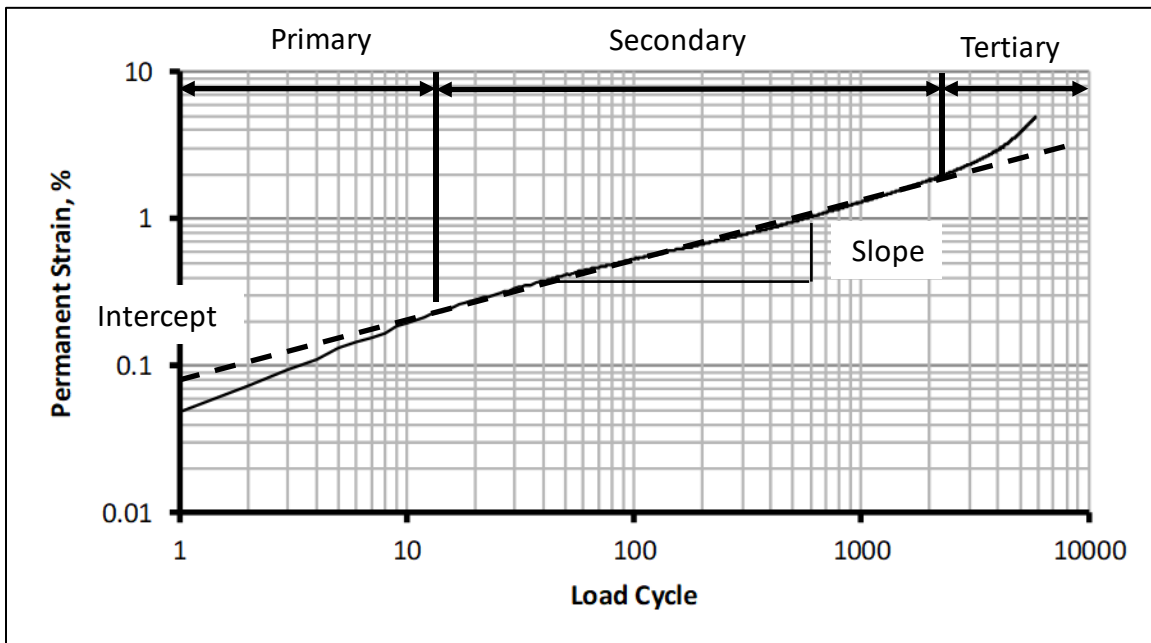


**Figure 8. Typical Plastic Strain Curve for an Asphalt Mixture for a Single Test Temperature in Logarithmic Scale Exhibiting Three Response Zones.**

The MEPDG uses the secondary or steady state zone to predict the rut depth throughout the pavement design period. The primary and tertiary zones of the plastic strain curve are excluded from the analyses to derive the plastic strain coefficients. The lower the intercept and slope, the more resistant the asphalt mixture is to rutting.

A graphical display of the repeated load plastic strain test results are included in Appendix G for the asphalt mixtures identified in Table 12. Table 19 summarizes the test results relative to the different zones of a repeated load plastic strain test and variables used in the PMED software for predicting rut depth. The results in Table 19 are organized and presented in order of increasing resistance to rutting from the top to the bottom of the table. The resistance to rutting or excessive plastic strain is related to  $N_{\text{Design}}$  gyrations. The asphalt mixtures designed at  $N_{\text{Design}}$  of 40 gyrations with a FAA less than 43 are highly susceptible to distortion for intermediate and high temperatures.

**Table 19. Summary of accumulated percent plastic strain (mixtures organized by increasing resistance to rutting; first mixtures listed are those most susceptible to rutting).**

Mixture Identification				Mix Size Designation	N <sub>Design</sub> Gyration	Percent Plastic Strain		
						Temperature, °C (°F)		
						20 (68.0)	34 (93.2)	48 (118.4)
8357	Surface	PG58-34S	4 LT	12.5 mm	40	1.384	4.870 (4017)*	4.588 (369)
208	Surface	PG58-28S	4 LT	12.5 mm	40	0.794	4.837 (7312)	4.578 (725)
236	Surface	PG58-28S	4 MT	12.5 mm	75	0.627	2.209	4.742 (5411)
319	Surface	PG58-28H	4 MT	12.5 mm	75	0.463	1.475	4.727 (5411)
258	Surface	PG58-28S	4 MT	12.5 mm	75	0.625	1.641	4.085
1020	Surface	PG58-34V	4 SMA	12.5 mm	100	0.612	1.558	2.523
7130	Surface	PG58-34V	5 MT	9.5 mm	75	0.603	1.315	2.058
057	Base	PG58-28S	3 LT	19 mm	40	0.465	1.079	2.372
121	Surface	PG58-28V	4 SMA	12.5 mm	100	0.501	1.106	1.939
1060	Base	PG58-28H	3 HT	19 mm	100	0.362	0.908	1.532
251	Surface	PG58-28V	4 HT	12.5 mm	100	0.280	0.876	1.523

\* Number in the parentheses is the number of load cycles that the test was stopped because of the high percent plastic strain values.

Note: The highlighted cells identify mixtures that are believed to be an outlier or an anomaly.

The repeated load plastic strain data were analyzed using the procedure in Appendix G to determine the slope and intercept of the individual test specimens in accordance with equation 1.

$\log(\epsilon_p) = \log(a[T]) + b * \log(N)$ <p>Where:  <math>\epsilon_p</math> = Plastic axial strain                  N = Number of load cycles                  a[T] = Intercept from the secondary or steady state zone at temperature T (see Figure 8).                  b = Slope for the secondary or steady state zone (see Figure 8)</p>	Equation 1
--	------------

The average intercept (a) and slope (b) for the test temperatures are included in Table 20 and Table 21 using the same order of mixtures included in Table 19, respectively. Figure 9 displays the impact of N<sub>Design</sub> gyrations on the intercept coefficient a (see equation 1), while Figure 10 displays the impact of N<sub>Design</sub> on the slope coefficient, b. N<sub>Design</sub> has a significant impact on the slope for the higher test temperatures, but a lower impact on the intercept from the steady state zone of the repeated load plastic strain test. More importantly, the impact of temperature on the intercept coefficient changes from the lower to the higher test temperature.

**Table 20. Average intercept coefficient, a, from steady state region.**

Mixture Identification		N <sub>Design</sub> Gyrations	Intercept, Log a(T)		
			Temperature, °C (°F)		
			20 (68.0)	34 (93.2)	48 (118.4)
8357	PG58-34S	40	-2.614	-2.730	-2.486
208	PG58-28S	40	-2.683	-2.775	-2.563
236	PG58-28S	75	-2.513	-2.391	-2.417
319	PG58-28H	75	-3.078	-2.554	-2.603
258	PG58-28S	75	-2.732	-2.463	-2.504
1020	PG58-34V	100	-2.766	-2.245	-2.081
7130	PG58-34V	75	-2.678	-2.329	-2.374
057	PG58-28S	40	-3.040	-2.604	-2.455
121	PG58-28V	100	-2.885	-2.381	-2.169
1060	PG58-28H	100	-3.050	-2.722	-2.342
251	PG58-28V	100	-3.435	-2.890	-2.306

Note: The highlighted cells identify mixtures that are believed to be an outlier or an anomaly.

**Table 21. Average slope coefficient, b, from steady state region.**

Mixture Identification		N <sub>Design</sub> Gyrations	Slope, b		
			Temperature, °C (°F)		
			20 (68.0)	34 (93.2)	48 (118.4)
8357	PG58-34S	40	0.189	0.396	0.456
208	PG58-28S	40	0.149	0.368	0.427
236	PG58-28S	75	0.097	0.184	0.299
319	PG58-28H	75	0.198	0.193	0.379
258	PG58-28S	75	0.133	0.167	0.279
1020	PG58-34V	100	0.161	0.110	0.121
7130	PG58-34V	75	0.115	0.112	0.172
057	PG58-28S	40	0.177	0.159	0.208
121	PG58-28V	100	0.145	0.107	0.115
1060	PG58-28H	100	0.148	0.171	0.132
251	PG58-28V	100	0.219	0.209	0.122

Note: The highlighted cells identify mixtures that are believed to be an outlier or an anomaly.

Another observation from the test data considered important, the asphalt mixtures that exhibited tertiary flow (accelerated deformation with increasing load cycles, see Table 19) have a FAA less than about 44, while all of the asphalt mixtures that did not exhibit tertiary flow have a FAA greater than about 44. Other mixture variables that have an impact on the plastic strain values include the amount of RAP/RAS, asphalt content, and gradation.

Table 22 lists the average resilient strain measured for each test temperatures. The resilient strain is used in estimating the  $k_r$ -coefficients for the rut depth transfer function (see Appendix G). Figure 11 displays the impact of N<sub>Design</sub> on the average resilient strain measured during the repeated load



plastic strain test.  $N_{Design}$  has little impact of the resilient strain at lower test temperature of 20°C (68°F), and a much larger impact at the higher test temperature.

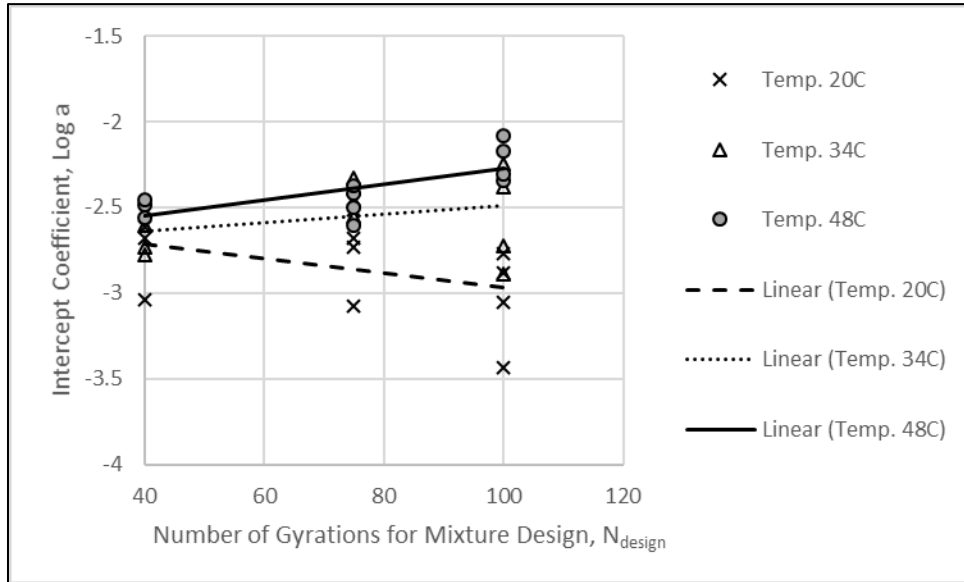


**Figure 9. Impact of  $N_{Design}$  on the Intercept Coefficient from the Repeated Load Plastic Strain Test Data.**

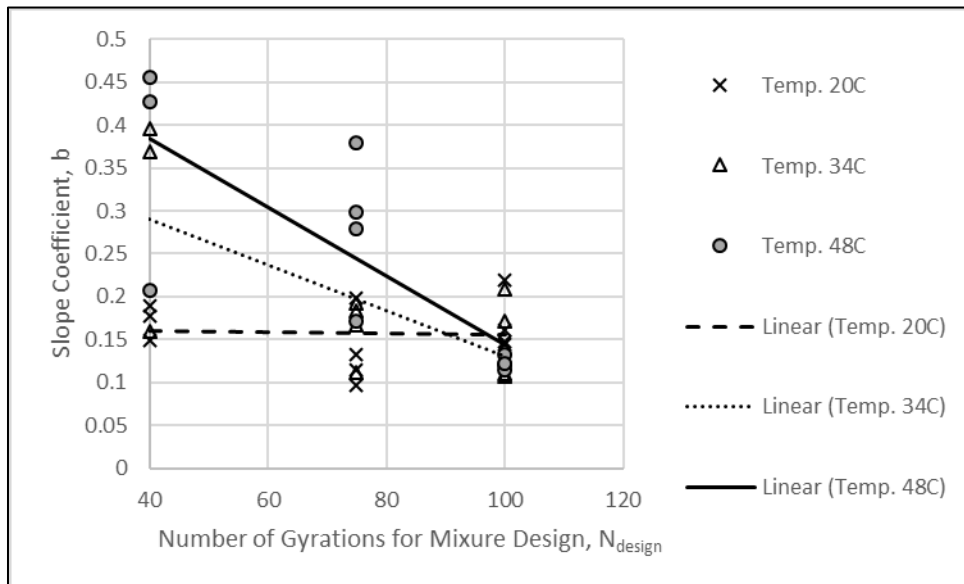


**Figure 10. Impact of  $N_{Design}$  on the Slope Coefficient from the Repeated Load Plastic Strain Test Data.**

**Table 22. Average resilient strain.**

Mixture Identification		N <sub>Design</sub> Gyrations	Resilient Strain, in./in.		
			Temperature, °C (°F)		
			20 (68.0)	34 (93.2)	48 (118.4)
8357	PG58-34S	40	9.625E-04	1.646E-03	2.297E-03
208	PG58-28S	40	7.542E-04	1.37E-03	1.935E-03
236	PG58-28S	75	7.057E-04	1.420E-03	1.960E-03
319	PG58-28H	75	7.367E-04	1.144E-03	1.870E-03
258	PG58-28S	75	7.737E-04	1.224E-03	1.807E-03
1020	PG58-34V	100	8.637E-04	1.340E-03	1.884E-03
7130	PG58-34V	75	7.387E-04	1.180E-03	1.755E-03
057	PG58-28S	40	7.700E-04	1.183E-03	1.775E-03
121	PG58-28V	100	6.473E-04	8.96E-04	1.387E-03
1060	PG58-28H	100	6.346E-04	8.210E-04	1.206E-03
251	PG58-28V	100	5.930E-04	7.457E-04	1.050E-03

Note: The highlighted cells identify mixtures that are believed to be an outlier or an anomaly.

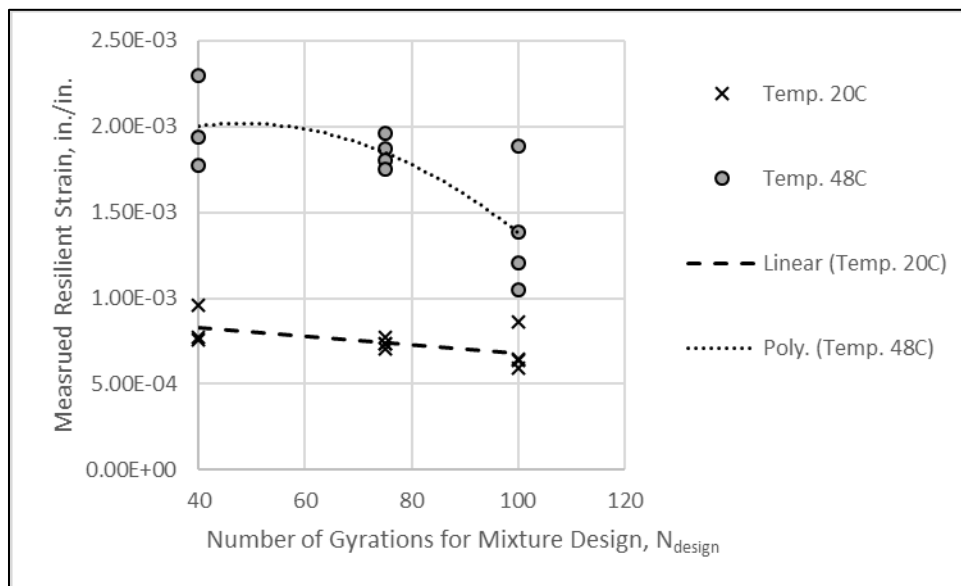


**Figure 11. Impact of N<sub>Design</sub> on the Measured Resilient Strain from the Repeated Load Plastic Strain Test Data.**

### 3.3.5 Bending Beam Fatigue Strength Tests

The AASHTOWare PMED software predicts two types of load related cracks: (1) cracks which are assumed to initiate at the bottom of the asphalt layer; and (2) cracks which are assumed to initiate at the surface. The bending beam fatigue strength data provide information and properties for predicting bottom-up fatigue cracks. The fatigue cracking model embedded in the PMED software, version 2.6 predicts the area of alligator cracks using the tensile strain at the bottom of the lower asphalt layer and the average dynamic moduli calculated for the truck loading condition

and layer temperatures. The asphalt content (effective by volume) and air voids also have a significant impact on the predicted area of bottom-up fatigue cracks.

The dynamic modulus is measured in accordance with AASHTO T 342, as discussed earlier in this chapter. The fatigue strength is determined from AASHTO T 321, *Standard Method of Test for Determining the Fatigue Life of Compacted Asphalt Mixtures Subjected to Repeated Flexural Bending*. In recent changes to AASHTO T 321, the current definition of fatigue life is the number of cycles where the product of the specimen stiffness and load cycles is a maximum. The previous definition of fatigue strength has been commonly used and is referred to now as the traditional fatigue strength. The traditional definition of the fatigue life for a strain or stress controlled flexural fatigue test is the number of cycles required to decrease the flexural stiffness to 50 percent of the initial stiffness value.

The analysis of flexural or bending beam fatigue data includes determining the fatigue life of multiple test specimens. Beam test specimens are tested over a range of three to four tensile strains for three different temperatures. Appendix H includes a summary of the fatigue strengths measured for individual beam specimens based on the traditional definition of fatigue strength, which has been used in all earlier versions of the PMED software.

Table 23 includes a listing of the fatigue strengths measured at different test temperatures and strain levels. The results from the bending beam fatigue tests are evaluated in accordance with equation 2 for each test temperature.

$$N_f = k_1 \left( \frac{1}{\varepsilon_t} \right)^{k_2}$$

Equation 2

Where:

$N_f$  = Number of load cycles to failure

$\varepsilon_t$  = Tensile strain,  $\mu$ strain

$k_1, k_2$  = Regression fitting coefficients

Equation 2 is the relationship between the tensile strain and fatigue strength or number of load cycles to failure. Table 24 summarizes the coefficients of the fatigue relationship between tensile strain and fatigue strength (number of load cycles to a 50 percent reduction in the flexural beam stiffness) at the reference test temperature (20 °C [68°F]). As shown, the results from the fatigue strength tests are highly variable. More importantly, asphalt mixture #1060 is considered an outlier because the intercept or  $k_1$  value is extremely high and the slope or  $k_2$  value has a very high negative value. The  $k_1$  and  $k_2$  coefficients are related because of the mathematical derivation from the test data.

**Table 23. Fatigue strengths measured on selected asphalt base mixtures (in accordance with the traditional definition of failure or fatigue strength).**

Mix #	Number of Gyration, $N_{Design}$	Temperature, °C	Micro-Strain	Flexural Modulus or Stiffness, MPa	Fatigue Strength, Cycles to Failure, $N_f$
0057	40	10	201	9,941	1,513,560
		10	300	8,958	332,400
		10	399	8,734	39,600
		10	499	9,052	11,040
		20	252	6,513	3,260,860
		20	350	6,134	206,530
		20	450	5,837	50,110
		20	553	5,138	20,050
		30	299	2,301	2,015,780
		30	401	2,359	618,960
		30	501	2,088	270,180
		30	597	2,176	57,690
0003	75		NA	NA	NA
0119	100	10	199	8,085	1,096,470
		10	248	9,089	665,780
		10	322	7,400	195,730
		10	398	7,319	25,240
		20	186	3,821	4,276,720
		20	250	4,860	166,590
		20	327	3,407	101,930
		20	375	4,118	139,630
		30	199	1,940	4,986,290
		30	300	1,690	560,180
		30	398	1,798	363,070
		30	497	1,541	84,240
1166	100	10	200	6,037	Did Not Fail
		10	299	6,198	228,200
		10	399	6,870	79,830
		10	495	5,642	14,710
		20	250	3,212	2,165,480
		20	350	2,912	676,080
		20	450	2,693	156,070
		20	545	2,630	54,810
		30	299	1,256	996,160
		30	399	1,023	393,540
		30	497	8,02	370,110
		30	595	1,121	371,530
1060	100	5	201	11,919	Did Not Fail
		5	302	13,240	299,680
		5	402	9,974	184,780
		5	502	11,151	35,660
		15	301	6,978	9,797,400

		15	402	6,816	398,100
		15	503	7,056	111,340
		15	606	5,878	11,560
		25	401	3,583	3,345,370
		25	505	3,064	82,2240
		25	606	2,882	681,290
		25	703	2,724	54,670

**Table 24. Fatigue strength coefficients for reference temperature (traditional definition of failure or fatigue strength).**

Mixture Identification			Mix Size Designation	N <sub>design</sub> Gyration Level	Fatigue Coefficients, at 70°F (see Appendix H)		Dynamic Modulus, ksi (10 Hz)
					k <sub>1</sub> , Intercept	k <sub>2</sub> , Slope	
0057	PG58-28S	3 LT	19 mm	40	3E+11	-2.699	1,036
0003	PG58-28S	3 MT	12.5 mm	75	NA	NA	681
1166	PG58-28S	2 HT	25 mm	100	6E+17	-4.75	678
0119	PG58-28S	3 HT	19 mm	100	3E+17	-4.88	1,022
1060	PG58-28H	3 HT	19 mm	100	9E+29	-9.292	954

Note: Units of the intercept term,  $k_1$ , are micro-strains ( $\mu$ strains).

### 3.3.6 IDT Tensile Strain at Failure Tests

A test procedure that has been used as a surrogate to estimate the fatigue strength coefficients is the IDT strength test, and is a modification of ASTM D6931 and AASHTO T 322 (Von Quintus, et al., 1991). The following summarizes the testing to estimate the coefficients, which is input level 2 in the MEPDG.

An IDT strength is performed in accordance with ASTM D6931, except that the horizontal and vertical deformations near the center of the specimen are measured during the test as described in AASHTO T 322. Figure 12 shows the horizontal and vertical linear voltage displacement transducers (LVDTs) attached to the center of the test specimens on one face. LVDTs are placed on both cut faces of the test specimen.

The load is applied at a ram rate of 2 inches per minute, as described in ASTM D6931. A minimum of three test specimens are tested at each test temperature because the indirect tensile strain can be highly variable. The three test temperatures are: 4.4, 15.6, and 26.7 °C (40, 60, and 80 °F). These three temperatures are applicable to most dense-graded asphalt mixtures. The higher temperature depends on the asphalt grade. A higher test temperature range (40, 70 and 100 °F) can be used for stiff mixtures, while a lower temperature range (40, 55, and 70 °F) can be used for soft mixtures.

The failure strain is determined when the IDT specimen starts to exhibit cracks along the edge of the loading platens, which is difficult to identify by the data acquisition system. The failure tensile strain has been defined as the tensile strain at peak load, which is easy to determine from a data acquisition standpoint, but the IDT specimen is in a damaged condition at peak load. In other words, the IDT specimen can still sustain higher loads, but the test specimen is exhibiting damage

outside the measurement zone. The damage area has an impact on the test outcome, which can be highly dependent on localized surface conditions.

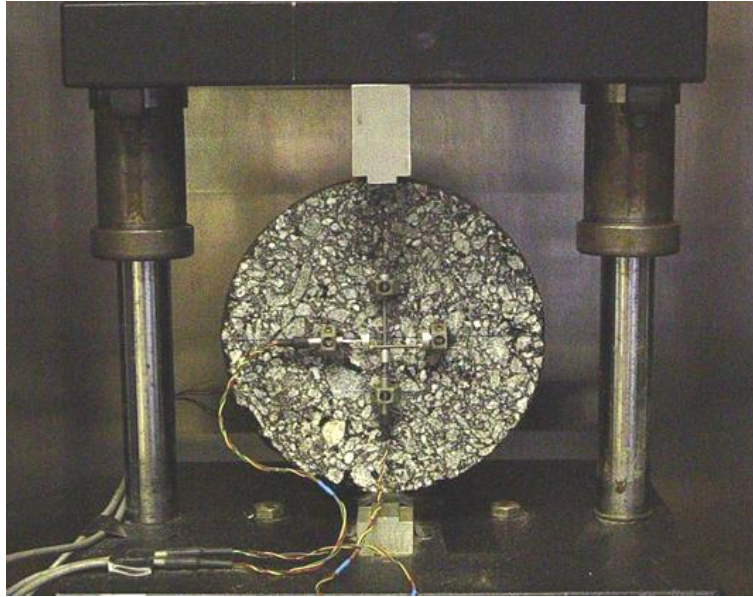


**Figure 12. LVDTs Attached to the IDT Test Specimen for Measuring Horizontal and Vertical Displacements in the Center of the Specimen.**

This physical condition to define the failure tensile strain is difficult to determine, especially at the higher test temperatures. To minimize the end effects caused by localized cracking around the loading platens, 99 percent of the peak load or stress is determined to define the tensile strain at failure in mils per inch, as explained in Appendix I. Table 25 lists the average tensile strain at failure for each test temperature. A relationship between the tensile strain at failure and dynamic modulus (see equation 3) is used to evaluate the test results. Table 26 lists the intercept coefficient ( $b_f$ ) and slope ( $m_f$ ) for each of the asphalt base mixtures.

$$\text{Log} \epsilon_f = b_f - m_f (\text{Log} E_{Uniaxial}^*) \quad \text{Equation 3}$$

Where:

$\epsilon_f$  = Tensile failure strain, mils/inch.

$E_{Uniaxial}^*$  = Dynamic modulus at 10 Hz from uniaxial cylindrical specimen, psi.

$b_f, m_f$  = Regression fitting coefficients;  $m_f$  is the slope and  $b_f$  is the intercept.

**Table 25. Average tensile strain at failure from the IDT test.**

Mixture Identification		Mix Size Designation	N <sub>Design</sub> Gyration Level	Temp., °F*	Tensile Strain at Failure, mils/in.	Dynamic Modulus, ksi (10 Hz)
0057	PG58-28S	19 mm	40	40	1.547	2,260
				60	4.115	1,420
				80	7.371	710
0003	PG58-28S	12.5 mm	75	40	3.233	2,075
				60	8.067	1,210
				80	11.133	540
1166	PG58-28S	25 mm	100	40	5.067	1,775
				60	9.000	1,020
				80	14.233	450
0119	PG58-28S	19 mm	100	40	2.167	2,340
				60	5.433	1,410
				80	8.900	720
1060	PG58-28H	19 mm	100	40	2.106	2,040
				60	3.724	1,290
				80	7.986	680

\* Note: 40 °F (4.4 °C), 60 °F (15.6 °C), 80 °F (26.7 °C)

**Table 26. IDT failure strain test results.**

Mixture Identification			Mix Size Designation	N <sub>Design</sub> Gyration Level	Fatigue Coefficients, at 70°F (see Appendix H)		Dynamic Modulus, ksi (10 Hz)
					b <sub>f</sub> , Intercept	m <sub>f</sub> , Slope	
0057	PG58-28S	3 LT	19 mm	40	8.604	-1.316	1,036
0003	PG58-28S	3 MT	12.5 mm	75	7.574	-1.119	681
1166	PG58-28S	2 HT	25 mm	100	5.421	-0.755	678
0119	PG58-28S	3 HT	19 mm	100	9.422	-1.434	1,022
1060	PG58-28H	3 HT	19 mm	100	7.978	-1.213	954

Note: The units for the intercept coefficient, b<sub>f</sub>, are mils per inch.

## CHAPTER 4 INTERPRETATION OF TEST RESULTS

Chapter 4 describes the interpretation of the laboratory test data to determine the asphalt layer inputs to the PMED software. Chapter 4 is organized similar to Chapter 3 in discussing the results from the asphalt binder and mixture tests in support of the MEPDG.

### 4.1 Asphalt Binder

The input level 1 asphalt binder properties required by the PMED software consists of complex shear modulus and phase angle. The asphalt binder complex shear modulus and phase angle are measured in the laboratory in accordance with AASHTO T 315 and no data manipulation is required, other than checking for anomalies or outliers in the data. Appendix C listed the measured values and included a graphical comparison on the asphalt binder properties measured within this study.

Asphalt binders sampled from two sources were tested, as discussed in Chapter 3. The difference between the two binder sources was minimal with the exception of one sample (AC2113, PG58-28H). Thus, the average binder properties were determined for each binder grade in accordance with AASHTO T 350. Table 27 lists the asphalt binder properties for the PG58-28 binders, while Table 28 lists the properties for the PG58-34 binders.

**Table 27. Complex shear modulus and phase angle for PG58-28.**

Asphalt Binder Grade	Test Temperature (°C [°F])	Complex Shear Modulus, G* (Pa)	Phase Angle, $\delta$ (°)
58-28S	10 [50]	8,760,500	56.1
58-28S	22 [71.6]	1,137,500	65.3
58-28S	34 [93.2]	133,450	72.9
58-28S	46 [114.8]	17,800	79.1
58-28S	58 [136.4]	3,180	84.1
58-28H	10 [50]	10,280,000	53.4
58-28H	22 [71.6]	1,192,000	61.0
58-28H	34 [93.2]	192,800	64.6
58-28H	46 [114.8]	37,300	65.8
58-28H	58 [136.4]	8,870	68.8
58-28V	10 [50]	10,098,000	53.5
58-28V	22 [71.6]	1,312,500	59.7
58-28V	34 [93.2]	197,350	63.2
58-28V	46 [114.8]	37,050	63.4
58-28V	58 [136.4]	9,655	63.5



**Table 28. Complex shear modulus and phase angle for PG58-34.**

Asphalt Binder Grade	Test Temperature (°C [°F])	Complex Shear Modulus, G* (Pa)	Phase Angle, $\delta$ (°)
58-34S	10 [50]	3,642,000	56.9
58-34S	22 [71.6]	414,200	65.1
58-34S	34 [93.2]	75,050	67.7
58-34S	46 [114.8]	14,500	71.1
58-34S	58 [136.4]	3,380	75.1
58-34H	10 [50]	3,633,500	56.5
58-34H	22 [71.6]	433,150	63.8
58-34H	34 [93.2]	81,710	64.3
58-34H	46 [114.8]	17,210	64.3
58-34H	58 [136.4]	4,795	65.3
58-34V	10 [50]	2,983,000	60.7
58-34V	22 [71.6]	480,150	62.8
58-34V	34 [93.2]	90,595	62.5
58-34V	46 [114.8]	19,500	61.4
58-34V	58 [136.4]	5,675	61.5

## 4.2 Dynamic Modulus

For pavement structural design in accordance with the MEPDG, constructing a dynamic modulus master curve is the primary analysis performed on the dynamic modulus data, which is completed within the PMED software. The analysis is the same for all asphalt mixtures or layers.

Dynamic moduli are measured in accordance with AASHTO T 342 and entered into the PMED software for specific temperatures and loading frequencies. No additional manipulation of the data is required. Appendix E provides a tabular listing of the dynamic modulus values measured for all of the asphalt mixtures included in the study. The dynamic moduli measured on the asphalt mixtures were found to be dependent on the number of gyrations for  $N_{\text{Design}}$  that was used for mixture design (see Chapter 3).

Dynamic moduli were also measured on other asphalt mixtures in studies sponsored by the FHWA and WisDOT (Von Quintus, et al., 2019; Williams et al., 2007; Bonaquist, 2010). The following provides a brief discussion on the applicability and comparison of the dynamic moduli measured and reported between different studies.

- The FHWA sponsored a study to measure the asphalt properties required by the MEPDG. One of those properties was dynamic moduli. Table 29 and Table 30 summarize the dynamic moduli measured on two asphalt mixtures in the study sponsored by FHWA: a wearing surface and an asphalt base mixture. Both mixtures were designed using an  $N_{\text{Design}}$  of 100 gyrations. For these two asphalt mixtures, however, 50 percent RAP/RAS was included in the JMF. Another difference between these two mixtures and the mixtures included in this study was the asphalt binder. The closest binder grade for the 50 percent

RAP/RAS was PG76-22. These asphalt mixtures are different than the mixtures currently being produced and placed in Wisconsin. In summary, the measured dynamic moduli for the high RAP/RAS mixtures are significantly greater than the dynamic moduli reported in this study with the lower amounts of RAP/RAS. One reason for the higher dynamic moduli is the higher amount of RAP/RAS and different binder grade. Dynamic moduli from the FHWA sponsored study were included as a separate set of dynamic moduli for high RAP/RAS mixtures for creating dynamic moduli input files to be used with the PMED software.

**Table 29. Dynamic moduli for asphalt wearing surface using an  $N_{\text{Design}}$  of 100 gyrations (50 percent RAP/RAS included in mixture), psi.**

Test Temperature, °F	Loading Frequency, Hz					
	0.1	0.5	1.0	5.0	10.0	25.0
14	2,072,501	2,416,819	2,557,524	2,860,660	2,979,845	3,126,250
40	996,458	1,316,403	1,464,110	1,818,802	1,972,761	2,173,788
70	304,197	457,342	539,790	771,436	888,045	1,056,269
100	89,575	138,361	167,195	258,415	310,285	392,480
130	34,834	50,504	59,929	90,974	109,579	140,579

**Table 30. Dynamic moduli for asphalt base layer using an  $N_{\text{Design}}$  of 100 gyrations (50 percent RAP/RAS included in mixture), psi.**

Test Temperature, °F	Loading Frequency, Hz					
	0.1	0.5	1.0	5.0	10.0	25.0
14	1,737,918	2,012,713	2,122,806	2,355,163	2,444,563	2,552,736
40	790,066	1,055,206	1,177,831	1,471,465	1,598,151	1,762,510
70	231,303	351,498	417,307	605,063	700,706	839,520
100	76,816	117,294	141,400	218,380	262,524	332,857
130	37,492	53,811	63,652	96,134	115,610	148,028

- WisDOT sponsored an earlier laboratory study to evaluate the impact of volumetric properties on dynamic modulus and flow number (Williams, 2007). The results from the flow number tests are discussed under the repeated load plastic strain section of this chapter. The primary volumetric properties in the dynamic modulus comparison included: air voids, gradation (NMAS), type of aggregate, and asphalt content. A limited number of test temperatures were used to statistically compare the dynamic moduli from 19 projects and defining what material properties were important or had an impact on the measured dynamic moduli at selected temperatures. Sufficient temperatures to generate a dynamic modulus master curve were not reported. The dynamic moduli reported in the 2007 study were compared to the values measured in this study and they were found to be in the same range. The amount of RAP/RAS and  $N_{\text{Design}}$  gyrations found to be important within this study, however, were not reported in the 2007 report. In summary, the dynamic moduli reported and used in the 2007 William’s study were not mixed or included with the results from this study for creating dynamic moduli input files to be used with the PMED software.

- WisDOT sponsored another laboratory study to measure the dynamic modulus and flow number on different asphalt mixtures regarding asphalt mixture design (Bonaquist, 2010). The results from the flow number tests are discussed under the repeated load plastic strain section of this chapter. Within the WisDOT 2010 study for measuring the dynamic moduli two asphalt binder grades were used (PG58-28 and PG70-28) and two levels of  $N_{Design}$  gyrations were used for preparing the test specimens (75 and 100 gyrations). The important difference between the WisDOT 2010 laboratory study and this study is no RAP/RAS was included in the asphalt mixtures tested in the 2010 study. Table 31 includes the average dynamic moduli for the test temperatures and load frequencies in accordance with the MEPDG. Although  $N_{Design}$  was provided, Bonaquist reported the two  $N_{Design}$  levels had minimal impact on the dynamic moduli. In summary, the dynamic moduli reported by Bonaquist are lower than the dynamic moduli measured within this study. Dynamic moduli from the Bonaquist study were included as a separate set of dynamic moduli for no RAP/RAS mixtures for creating dynamic moduli input files to be used with the PMED software.

**Table 31. Average dynamic moduli for selected WisDOT asphalt mixtures without RAP/RAS, psi.**

Test Temperature, °F	Loading Frequency, Hz					
	0.1	0.5	1	5	10	25
14	1,680,725	2,022,100	2,154,525	2,421,313	2,518,200	2,630,325
40	660,875	976,750	1,129,075	1,498,575	1,656,650	1,857,850
70	148,900	248,950	310,413	506,313	61,5250	781,063
100	46,350	67,589	81,300	130,325	161,888	216,875
130	25,263	30,988	34,500	46,638	54,388	68,063

Table 32, Table 33, and Table 34 list the average dynamic moduli measured for the different  $N_{Design}$  levels, regardless the asphalt mixture type (asphalt base layers or wearing surfaces). The average dynamic moduli included in Tables 29 to Table 34 represent the sets of clustered dynamic moduli measured from the other research studies cited above and in Chapter 2. The clustered sets of dynamic moduli are defined by  $N_{Design}$  and the amount of RAP/RAS in the mixture.

**Table 32. Average dynamic moduli for asphalt mixtures designed using an  $N_{Design}$  of 40 gyrations (lower to moderate amounts of RAP/RAS included in mixture), psi.**

Test Temperature, °F	Loading Frequency, Hz					
	0.1	0.5	1	5	10	25
14	1,497,460	1,878,714	2,028,415	2,330,571	2,439,902	2,565,664
40	437,272	725,390	875,159	1,260,629	1,433,269	1,658,013
70	62,231	117,341	155,142	291,586	376,259	515,200
100	15,958	23,757	29,118	50,085	64,887	92,849
130	8,767	10,514	11,617	15,562	18,175	22,977

**Table 33. Average dynamic moduli for asphalt mixtures designed using an  $N_{\text{Design}}$  of 75 gyrations (lower to moderate amounts of RAP/RAS included in mixture), psi.**

Test Temperature, °F	Loading Frequency, Hz					
	0.1	0.5	1	5	10	25
14	1,616,310	1,982,968	2,124,855	2,407,642	2,508,731	2,624,144
40	554,696	866,186	1,022,185	1,411,308	1,580,966	1,798,197
70	98,702	177,078	227,879	399,615	500,275	659,159
100	26,551	39,714	486,095	82,274	105,140	146,779
130	14,334	17,390	19,324	26,235	30,792	39,100

**Table 34. Average dynamic moduli for asphalt mixtures designed using an  $N_{\text{Design}}$  of 100 gyrations (lower to moderate amounts of RAP/RAS included in mixture), psi.**

Test Temperature, °F	Loading Frequency, Hz					
	0.1	0.5	1	5	10	25
14	2,042,147	2,331,819	2,437,525	2,639,997	2,710,226	2,789,358
40	952,976	1,320,427	1,483,892	1,850,627	1,996,463	2,173,622
70	217,777	370,222	459,757	727,423	866,485	1,067,201
100	51,677	82,967	103,577	177,665	224,946	306,050
130	21,941	28,962	33,447	49,548	60,128	79,216

### 4.3 IDT Creep Compliance and Strength

The asphalt properties needed for the transverse cracking model are: (1) the coefficient of thermal contraction, (2) a creep compliance master curve, (3) the tensile strength measured at -10 °C (14 °F), and (4) Poisson’s ratio. The coefficient of thermal contraction is estimated from the volumetric composition of the asphalt mixture and not measured in the laboratory. Bonaquist (2010), however, suggested WisDOT use a representative linear coefficient of thermal contraction of  $1.4 \times 10^{-5}/^{\circ}\text{F}$  ( $2.5 \times 10^{-5}/^{\circ}\text{C}$ ). This linear coefficient of thermal contraction is also suggested for use in Wisconsin.

For input level 1, the IDT creep compliance master curve, tensile strength, and Poisson’s ratio are measured in accordance with AASHTO T 322. The MEPDG Manual of Practice suggests that Poisson’s ratio be calculated by the PMED software as a function of temperature. The temperature dependent Poisson’s ratio has been used in all global calibrations. Thus, the IDT creep compliance and strength are the two low temperature asphalt properties needed for input level 1 to predict the length of transverse cracks.

#### 4.3.1 Creep Compliance

The AASHTOWare PMED software predicts the length of transverse cracks using the IDT creep compliance values measured for 21 combinations of temperature and loading time (input level 1). The temperatures are 0, -10, and -20 °C (32, 14, and -4 °F). Creep compliance values are required for loading times of 1, 2, 5, 10, 20, 50, and 100 seconds. The creep compliance values are entered

**Expansion of AASHTOWare ME Design Inputs  
Final Report WHRP 0092-20-03**

directly into the software for combinations of temperature and loading time. No additional manipulation of the test data is required.

For pavement structural design in accordance with the MEPDG, constructing a creep compliance master curve is the primary analysis performed on the creep compliance data. The creep compliance master curve, however, is completed within the PMED software. Constructing a creep compliance master curve outside of the PMED software is not required, other than to review the creep compliance data to identify outliers and/or anomalies. The analysis is the same for all asphalt mixtures.

Appendix F provides a tabular listing of the creep compliance and strengths measured for all of the asphalt wearing surface mixtures included in the study. The creep compliance measured on the asphalt mixtures were found to be dependent on the asphalt binder grade and number of gyrations for  $N_{\text{Design}}$  that was used for mixture design (see Chapter 3).

Creep compliance was also measured on other asphalt mixtures in studies sponsored by the FHWA and WisDOT (Von Quintus, et al., 2019; Williams et al., 2007; Bonaquist, 2010). The following provides a brief discussion on the applicability and comparison of the creep compliance measured and reported between the different studies.

- FHWA sponsored a study to measure the asphalt properties required by the MEPDG. Two of the properties included in the FHWA study were creep compliance and strength. Some WisDOT asphalt mixtures were included in the FHWA study (Von Quintus, et al., 2019). Table 35 summarizes the creep compliance measured on the WisDOT asphalt wearing surface mixture included in the FHWA study. The IDT strengths will be discussed in the next section. The WisDOT mixture was designed using an  $N_{\text{Design}}$  of 100 gyrations. For the asphalt mixture, however, 50 percent RAP/RAS was included in the job mix formula. Another difference between the WisDOT mixture included in the FHWA study and the mixtures included in this study was the asphalt binder. The closest binder grade for the 50 percent RAP/RAS was PG76-22. The asphalt mixture is different than the wearing surface mixtures currently being produced and placed in Wisconsin. In summary, the measured creep compliance values for the high RAP/RAS mixture are significantly lower than the creep compliance reported in this study with the lower amounts of RAP/RAS. One reason for the lower creep compliance is the higher amount of RAP/RAS and different binder grade. In summary, creep compliance from the FHWA sponsored study were included as a separate set of creep compliance values for high RAP/RAS mixtures for creating creep compliance input files to be used with the PMED software.
- WisDOT sponsored a laboratory study to measure the creep compliance and strength on different asphalt mixtures regarding asphalt mixture design (Bonaquist, 2010). Within the WisDOT 2010 study for measuring the creep compliance and strength two asphalt binder grades (PG58-28 and PG58-34), two levels of  $N_{\text{Design}}$  gyrations (75 and 100 gyrations), and two RAP amounts (0 and 25 percent) were used in preparing the test specimens. Although  $N_{\text{Design}}$  was provided, Bonaquist reported the two  $N_{\text{Design}}$  levels had minimal impact on the dynamic moduli. The IDT strengths will be discussed in the section that follows. In summary, the creep compliance reported by Bonaquist for the mixtures with 25 percent

RAP are within the same range of values measured within this study. Creep compliance for the mixtures without RAP from the Bonaquist study were higher and are included as a separate set of creep compliance data for creating creep compliance input files to be used with the PMED software. Table 36 and Table 37 lists the creep compliance values for the PG58-28 mixtures without RAP for  $N_{Design}$  values of 75 and 100 gyrations, respectively. Table 38 and Table 39 includes the creep compliance values for the PG58-34 mixtures without RAP for  $N_{Design}$  values of 75 and 100, respectively. In summary, creep compliance from the Bonaquist study were included as a separate set of creep compliance values for mixtures containing no RAP/RAS for creating creep compliance input files to be used with the PMED software.

**Table 35. Creep compliance values measured for a WisDOT high recycle surface course mixture (50 percent RAP/RAS added to mixture);  $N_{Design}$  is 100 gyrations, 1/psi.**

Loading Time, seconds	Test Temperature, °F		
	-4	14	32
1	3.04E-07	4.40E-07	8.90E-07
2	3.19E-07	5.1E-07	1.08E-06
5	3.51E-07	6.06E-07	1.44E-06
10	3.74E-07	7.03E-07	1.70E-06
20	4.01E-07	7.93E-07	2.04E-06
50	4.46E-07	9.72E-07	2.62E-06
100	4.96E-07	1.11E-06	3.21E-06

**Table 36. Creep compliance values measured for WisDOT mixtures with a PG58-28 binder designed using an  $N_{Design}$  of 75 gyrations without RAP/RAS, 1/psi.**

Loading Time, seconds	Test Temperature, °F		
	-4	14	32
1	4.08E-07	5.36E-07	1.012E-06
2	4.27E-07	6.055E-07	1.265E-06
5	4.63E-07	7.39E-07	1.76E-06
10	5.04E-07	8.875E-07	2.315E-06
20	5.6E-07	1.095E-06	3.075E-06
50	6.69E-07	1.49E-06	4.575E-06
100	7.89E-07	1.94E-06	6.25E-06

**Table 37. Creep compliance values measured for WisDOT mixtures with a PG58-28 binder designed using an  $N_{Design}$  of 100 gyrations without RAP/RAS, 1/psi.**

Loading Time, seconds	Test Temperature, °F		
	-4	14	32
1	4.03E-07	4.945E-07	8.36E-07
2	4.18E-07	5.49E-07	1.037E-06
5	4.48E-07	6.58E-07	1.445E-06
10	4.82E-07	7.825E-07	1.91E-06
20	5.3E-07	9.61E-07	2.575E-06
50	6.28E-07	1.32E-06	3.915E-06
100	7.39E-07	1.73E-06	5.45E-06

**Table 38. Creep compliance values measured for WisDOT mixtures with a PG58-34 binder designed using an  $N_{Design}$  of 75 gyrations without RAP/RAS, 1/psi.**

Loading Time, seconds	Test Temperature, °F		
	-4	14	32
1	4.445E-07	6.8E-07	1.605E-06
2	4.745E-07	7.975E-07	2.060E-06
5	5.325E-07	1.02E-06	2.935E-06
10	5.955E-07	1.27E-06	3.880E-06
20	6.815E-07	1.6E-06	5.180E-06
50	8.465E-07	2.24E-06	7.655E-06
100	1.0265E-06	2.93E-06	1.0325E-05

**Table 39. Creep compliance values measured for WisDOT mixtures with a PG58-34 binder designed using an  $N_{Design}$  of 100 gyrations without RAP/RAS, 1/psi.**

Loading Time, seconds	Test Temperature, °F		
	-4	14	32
1	4.02E-07	6.57E-07	1.555E-06
2	4.365E-07	7.77E-07	1.980E-06
5	5.01E-07	9.975E-07	2.765E-06
10	5.685E-07	1.235E-06	3.590E-06
20	6.59E-07	1.55E-06	4.700E-06
50	8.255E-07	2.125E-06	6.750E-06
100	1.001E-06	2.735E-06	8.945E-06

Table 40, Table 41, and Table 42 includes the average creep compliance values measured for the different  $N_{Design}$  levels of 40, 75, and 100 gyrations, respectively. Similarly, Table 43, Table 44, and Table 45 includes the average creep compliance values measured for wearing surfaces with a PG58-34 asphalt binder for different  $N_{Design}$  levels of 40, 75, and 100 gyration, respectively. The average creep compliance values included in Table 35 to Table 45 represent the sets of clustered creep compliance values measured from the other research studies cited above and in Chapter 2.

The clustered sets of creep compliance values are defined by the asphalt binder grade, levels of percent RAP/RAS, and  $N_{Design}$ .

**Table 40. Creep compliance values measured for WisDOT mixtures with a PG58-28 binder designed using an  $N_{Design}$  of 100 gyrations with low to moderate amounts of RAP/RAS, 1/psi.**

Loading Time, seconds	Test Temperature, °F		
	-4	14	32
1	2.98E-07	4.20E-07	6.83E-07
2	3.17E-07	4.68E-07	8.00E-07
5	3.41E-07	5.52E-07	1.05E-06
10	3.66E-07	6.13E-07	1.31E-06
20	3.90E-07	6.94E-07	1.58E-06
50	4.35E-07	8.61E-07	2.15E-06
100	4.75E-07	1.02E-06	2.74E-06

**Table 41. Creep compliance values measured for WisDOT mixtures with a PG58-28 binder designed using an  $N_{Design}$  of 75 gyrations with low to moderate amounts of RAP/RAS, 1/psi.**

Loading Time, seconds	Test Temperature, °F		
	-4	14	32
1	3.15E-07	5.38E-07	1.23E-06
2	3.46E-07	6.33E-07	1.57E-06
5	3.89E-07	8.02E-07	2.24E-06
10	4.29E-07	9.57E-07	2.92E-06
20	4.72E-07	1.13E-06	3.74E-06
50	5.51E-07	1.47E-06	5.36E-06
100	6.20E-07	1.81E-06	7.10E-06

**Table 42. Creep compliance values measured for WisDOT mixtures with a PG58-28 binder designed using an  $N_{Design}$  of 40 gyrations with low to moderate amounts of RAP/RAS, 1/psi.**

Loading Time, seconds	Test Temperature, °F		
	-4	14	32
1	3.05E-07	5.00E-07	1.15E-06
2	3.35E-07	6.00E-07	1.50E-06
5	3.75E-07	7.30E-07	2.15E-06
10	4.05E-07	8.65E-07	2.83E-06
20	4.45E-07	1.02E-06	3.61E-06
50	5.2E-07	1.31E-06	5.25E-06
100	5.96E-07	1.65E-06	7.32E-06



**Table 43. Creep compliance values measured for WisDOT mixtures with a PG58-34 binder designed using an  $N_{Design}$  of 100 gyrations with low to moderate amounts of RAP/RAS, 1/psi.**

Loading Time, seconds	Test Temperature, °F		
	-4	14	32
1	3.10E-07	4.80E-07	1.20E-06
2	3.40E-07	5.80E-07	1.52E-06
5	4.00E-07	7.50E-07	2.08E-06
10	4.46E-07	9.19E-07	2.68E-06
20	4.9E-07	1.1E-06	3.38E-06
50	5.75E-07	1.45E-06	4.95E-06
100	6.33E-07	1.84E-06	6.44E-06

**Table 44. Creep compliance values measured for WisDOT mixtures with a PG58-34 binder designed using an  $N_{Design}$  of 75 gyrations with low to moderate amounts of RAP/RAS, 1/psi.**

Loading Time, seconds	Test Temperature, °F		
	-4	14	32
1	2.90E-07	6.00E-07	1.60E-06
2	3.30E-07	7.20E-07	2.05E-06
5	4.10E-07	9.50E-07	3.00E-06
10	5.33E-07	1.14E-06	4.06E-06
20	5.93E-07	1.36E-06	5.2E-06
50	7.13E-07	1.78E-06	7.63E-06
100	8.3E-07	2.24E-06	1.06E-05

**Table 45. Creep compliance values measured for WisDOT mixtures with a PG58-34 binder designed using an  $N_{Design}$  of 40 gyrations with low to moderate amounts of RAP/RAS, 1/psi.**

Loading Time, seconds	Test Temperature, °F		
	-4	14	32
1	3.75E-07	7.00E-07	1.75E-06
2	4.15E-07	8.30E-07	2.40E-06
5	4.78E-07	1.10E-06	3.60E-06
10	5.28E-07	1.3E-06	4.89E-06
20	5.92E-07	1.59E-06	6.64E-06
50	7.11E-07	2.19E-06	9.76E-06
100	8.51E-07	2.98E-06	1.38E-05

### 4.3.2 IDT Tensile Strength

The AASHTOWare PMED software predicts the length of transverse cracks using the average IDT tensile strength of the mixture measured at -10 °C (14 °F) for input level 2. The software interface and definition of the input levels were revised in 2017. Input level 1 includes measuring the IDT strength at three or more test temperatures, while input level 2 includes measuring the IDT strength at -10 °C (14 °F). For input level 2, the software calculates the IDT strengths at higher temperatures. Input level 3 is the same as in previous versions of the software, the strength at -10 °C (14 °F) is calculated from regression equations derived from data measured on virgin, neat asphalt mixtures.

Analysis of the AASHTO T 322 strength test data is straightforward; the average of the tensile strengths measured on three test specimens is reported as the asphalt mixture’s IDT strength. The average IDT strength is entered directly into the PMED software. No other manipulation of the data is required.

IDT strengths were measured in the FHWA and WisDOT studies mentioned above. Figure 13 displays a comparison between  $N_{\text{Design}}$  used for mixture design and the IDT strength measured on a range of asphalt mixtures from the different data sources. There is no statistical difference in the measured IDT strength between  $N_{\text{Design}}$  levels of 75 and 100 gyrations. No statistical difference was also found between the different asphalt grades or mixtures with different amounts of RAP/RAS. In summary, the following IDT strengths represent the sets of clustered IDT strength measured from the other research studies cited above and in Chapter 3 and are suggested for use in predicting the length of transverse cracks.

- $N_{\text{Design}}$  of 75 and 100 gyrations (all combination of mixes): IDT strength – 451 psi.
- $N_{\text{Design}}$  of 40 gyrations (all combination of mixes): average IDT strength – 378 psi,

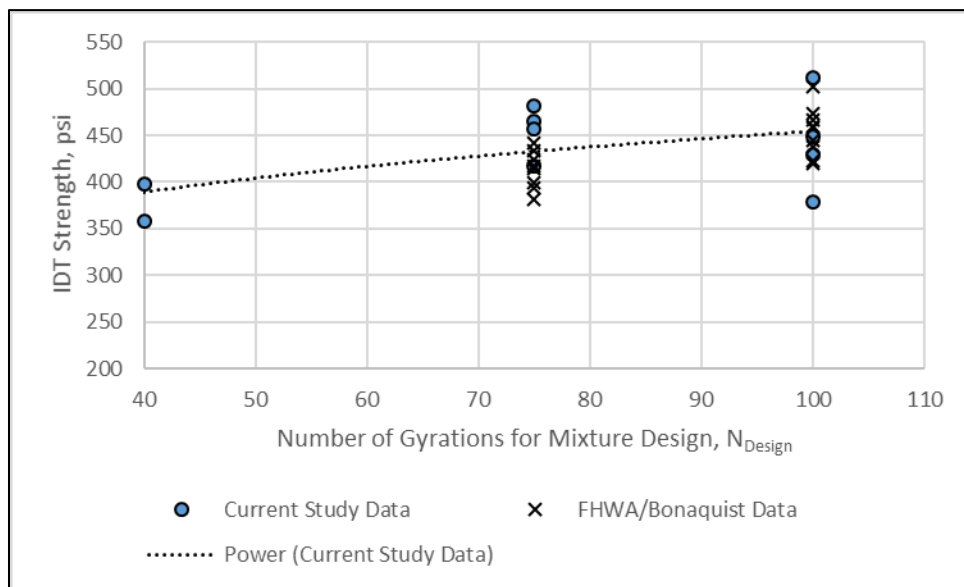


Figure 13. Correspondence between  $N_{\text{Design}}$  and IDT Strength from Multiple Data Sources.

[Note: Only three of the 17 asphalt mixtures were designed at an  $N_{\text{Design}}$  of 40 gyrations. This is too few mixtures to statistically say the IDT strength at 40 gyrations are lower than the IDT strengths at 75 and 100 gyrations.]

#### 4.4 Plastic Strain Coefficients

This section of Chapter 4 presents the data analysis and interpretation of the repeated plastic strain test results for deriving the coefficients of the rut depth transfer function (see equation 4). The accumulated plastic strain data are included in Appendix G which were measured in accordance with the procedure outlined in the NCHRP 9-30A procedure (Von Quintus, et al., 2012). The NCHRP 9-30A procedure has two options for testing the asphalt mixtures: option A includes three test temperatures, while option B uses one test temperature. Option A with three test temperatures represents input level 1 for deriving the plastic strain coefficients and was used in this study. The three temperatures were: 20 °C (68 °F), 34 °C (93 °F), and 48 °C (118 °F).

$\varepsilon_p = \varepsilon_r 10^{k_{1r}\beta_{1r} N^{k_{3r}\beta_{3r}} T^{k_{2r}\beta_{2r}}}$ <p>Where:</p> <p><math>\varepsilon_p</math> = Accumulated axial plastic strain in the test specimen, in/in.</p> <p><math>\varepsilon_r</math> = Resilient or elastic strain in the test specimen, in/in.</p> <p>N = Number of load cycles.</p> <p>T = Test temperature, °F.</p> <p><math>k_{1r}, k_{2r}, k_{3r}</math> = Laboratory-derived, plastic strain coefficients using linear regression techniques.</p> <p><math>\beta_{1r}, \beta_{2r}, \beta_{3r}</math> = Calibration coefficients; the <math>\beta</math>-values are not a part of the measured or laboratory-derived analyses. They are the parameters to remove any bias between the measured and predicted rut depths.</p>	Equation 4
--	------------

The coefficients of the MEPDG rut depth transfer function are defined below, as derived from the repeated load plastic strain test:

- $k_{1r}$  is the intercept (N=1). The lower the intercept, the lower the predicted rut depth. Equation 5 is used to estimate the intercept of the rut depth transfer function from the repeated load plastic strain data.
- $k_{3r}$  is the number of load cycles exponent or slope within the secondary zone, and assumed to be independent of temperature. The lower the slope, the lower the growth rate of the predicted rut depth and the lower the predicted rut depth. Coefficient  $k_{3r}$  is proportional to coefficient b derived from the simplified plastic strain accumulation equation included in Chapter 3 (equation 1);  $k_{3r}$  is equal to coefficient b times 1.36 (the field adjustment factor), as described in Appendix G.
- $k_{2r}$  is the temperature exponent and assumed to be independent of time. The lower the temperature exponent, the less sensitive plastic strains are to temperature and the lower the

predicted rut depth. Coefficient  $k_{2r}$  is derived from an analysis of the intercepts measured for three test temperatures of the same mixture. Equation 6 is used to estimate the temperature exponent of the rut depth transfer function; in that  $c$  in equation 6 is proportional to  $k_{2r}$ .

$$k_{1r} = \text{Log}(a_0) - \text{Log}(\epsilon_r[T]) \quad \text{Equation 5}$$

Where:

$a_0$  = Intercept regression constant as included in equation 6 when combining all three test temperatures on a logarithmic scale.

$\epsilon_r$  = Resilient strain as a function of temperature T, in./in.

$$\text{Log}(a[T]) = \text{Log}(a_0) + c\text{Log}(T) \quad \text{Equation 6}$$

Where:

$a[T]$  = Intercept from the secondary or steady state zone of the plastic strain versus load cycles relationship on a logarithmic scale for a specific temperature, T.

The procedure for deriving the plastic strain coefficients ( $k_{1r}$ ,  $k_{2r}$ , and  $k_{3r}$ ) in the rut depth transfer function (equation 4) is discussed in Appendix G. The primary analysis of repeated load plastic strain test data for pavement design is the determination of the log intercept and slope of the secondary zone of the plastic strain curve. Figure 8 in Chapter 3 illustrated the slope and intercept used to determine the plastic strain characteristics or coefficients of asphalt mixtures in the AASHTOWare PMED software. The intercept and slope from the test data are obtained by fitting the data within the secondary zone of the plastic strain curve to the simplified equation 1 in Chapter 3. The intercept ( $a$ ) and slope ( $b$ ) were derived for each test specimen and test temperature, as tabulated in Chapter 3.

The PMED software calculates the resilient strain as a function of temperature in equation 4. The dynamic modulus is measured using an unconfined test condition (see Chapter 3), while the repeated load plastic strain test is confined. The difference in testing conditions will result in an error in the predicted rut depth. This error, however, is believed to be small and is accounted for within the calibration process for the rut depth transfer function (AASHTO, 2010). In addition, the field adjustment factor mentioned in Appendix G takes this difference into account.

Table 46 summarizes the three rut depth transfer function coefficients derived from the repeated load plastic strain test. The organization of the mixtures is the same as included in Chapter 3, going from mixtures susceptible to rutting to those resistant to rutting or accumulation of plastic strain. An observation from the plastic strain coefficients included in Table 46 is all of the asphalt mixtures susceptible to rutting were designed using an  $N_{\text{Design}}$  of 40 gyrations, while all of the mixtures resistant to rutting were designed using  $N_{\text{Design}}$  of 100 gyrations. Figure 14 displays the relationship between  $N_{\text{Design}}$  and the intercept coefficient ( $k_{1r}$ ), while Figure 15 and Figure 16 display relationships between  $N_{\text{Design}}$  and the load cycle exponent ( $k_{3r}$ ) and temperature exponent ( $k_{2r}$ ), respectively. As shown, the rut depth transfer function coefficients are related to  $N_{\text{Design}}$ , which should be considered in setting up the asphalt materials library.

**Table 46. MEPDG rut depth transfer function plastic strain coefficients for WisDOT mixtures.**

Mixture Identification					Mix Size Designation	N <sub>design</sub> Gyration	Plastic Strain k-Coefficients		
							k <sub>1r</sub>	k <sub>2r</sub>	k <sub>3r</sub> **
Global Default Values						-2.45	3.010	0.220	
8357*	Surface	PG58-34S	4 LT	12.5 mm	40	-0.30	0.266	0.579	
208*	Surface	PG58-28S	4 LT	12.5 mm	40	-0.316	0.284	0.540	
319*	Surface	PG58-28H	4 MT	12.5 mm	75	-2.025	1.336	0.515	
236*	Surface	PG58-28S	4 MT	12.5 mm	75	-0.150	0.277	0.407	
258	Surface	PG58-28S	4 MT	12.5 mm	75	-0.798	0.648	0.379	
7130	Surface	PG58-34V	5 MT	9.5 mm	75	-1.000	0.86	0.234	
1020	Surface	PG58-34V	4 SMA	12.5 mm	100	-2.335	1.814	0.218	
057	Base	PG58-28S	3 LT	19 mm	40	-2.027	1.568	0.246	
121	Surface	PG58-28V	4 SMA	12.5 mm	100	-2.511	1.909	0.220	
1060	Base	PG58-28H	3 HT	19 mm	100	-2.448	1.825	0.220	
251	Surface	PG58-28V	4 HT	12.5 mm	100	-4.140	2.919	0.282	

\* Designates mixtures that exhibited tertiary flow for one or more test temperatures and are susceptible to rutting.

\*\* From previous test results, slopes with values greater the 0.55 suggest mixtures being susceptible to moisture damage.

Note: The highlighted cells identify mixtures that are believed to be anomalous.

Repeated load plastic strain tests were also performed on asphalt mixtures in a study sponsored by the FHWA that included a couple of other WisDOT mixtures (Von Quintus, et al., 2019). For these two asphalt mixtures, however, 50 percent RAP/RAS was included in the JMF. Another difference between these two mixtures and the mixtures included in this study was the asphalt binder. The closest binder grade for the 50 percent RAP/RAS was PG76-22. These asphalt mixtures are different than the mixtures currently being produced and placed in Wisconsin. In summary, the plastic strain coefficient derived from the FHWA study for the high RAP/RAS mixtures are similar and within the range of values derived within this study. The results from this testing are summarized in Table 47 and included in Figure 14, Figure 15, and Figure 16.

**Table 47. MEPDG rut depth transfer function plastic strain coefficients for selected WisDOT high RAP/RAS mixtures (50 percent), FHWA sponsored study (Von Quintus, 2019).**

Mixture Identification					Mix Size Designation	N <sub>Design</sub> Gyration	Plastic Strain k-Coefficients		
							k <sub>1r</sub>	k <sub>2r</sub>	k <sub>3r</sub> **
Global Default Values						-2.45	3.010	0.220	
FHWA	Base	PG70-22	NA	19 mm	100	-3.300	2.404	0.343	
FHWA	Surface	PG70-22	NA	12.5 mm	100	-4.327	3.499	0.227	

WisDOT also sponsored studies for measuring the flow number on multiple asphalt mixtures to evaluate their rutting resistance (Williams et al., 2007; Bonaquist, 2010). As noted in Chapter 3, the flow number is not an input to the PMED software. AASHTO T 378, *Standard Method of Test for Determining the Dynamic Modulus and Flow Number for Asphalt Mixtures Using the Asphalt*

*Mixture Performance Tester (AMPT)*, does not require conditioning cycles. Conditioning cycles are not required because the flow number is determined through changes in the plastic strain and not the absolute values. The repeated load plastic strain test to derive the inputs required by the MEPDG is based on the absolute values or magnitudes of the plastic strain accumulations. Without conditioning cycles, the results can be biased and result in substantial errors. Thus, the flow number tests were excluded and not used within this study to create or expand the WisDOT asphalt material libraries for the rut depth transfer function coefficients.

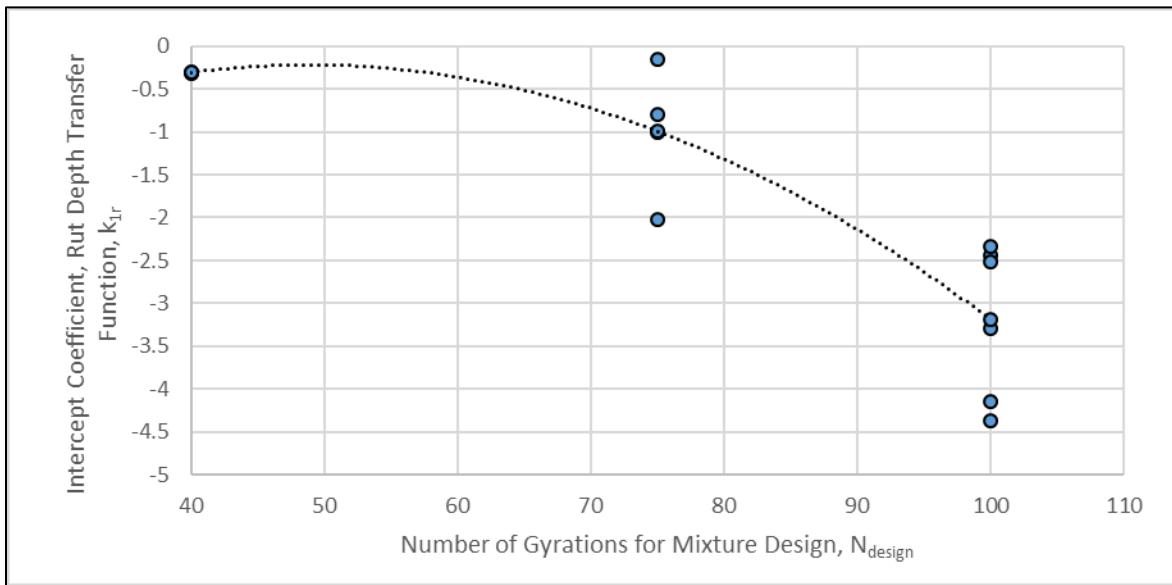


**Figure 14. Correspondence between  $N_{Design}$  and the Intercept Coefficient,  $k_{1r}$ .**

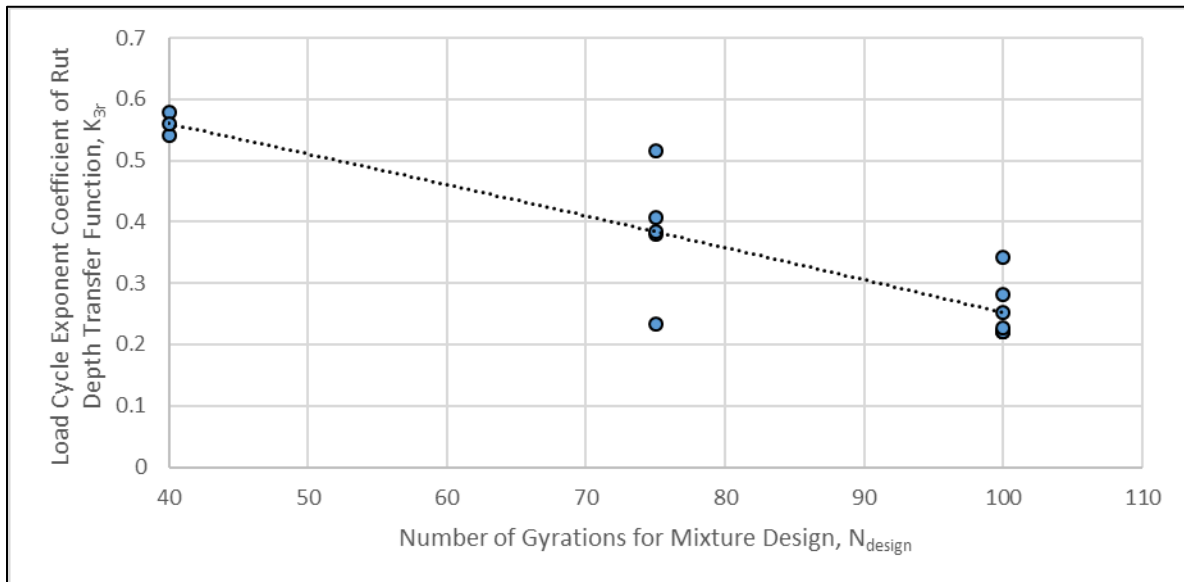


**Figure 15. Correspondence between  $N_{Design}$  and the Load Cycle Exponent or Slope,  $k_{3r}$ .**

Table 48 includes the average plastic strain coefficients of the rut depth transfer function derived for the different  $N_{Design}$  levels of 40, 75, and 100 gyrations. The average plastic strain coefficients

listed in Table 48 represent the sets of clustered plastic strain coefficients from the other research studies cited above and in Chapter 3. The clustered sets of plastic strain coefficients are defined by  $N_{Design}$ .

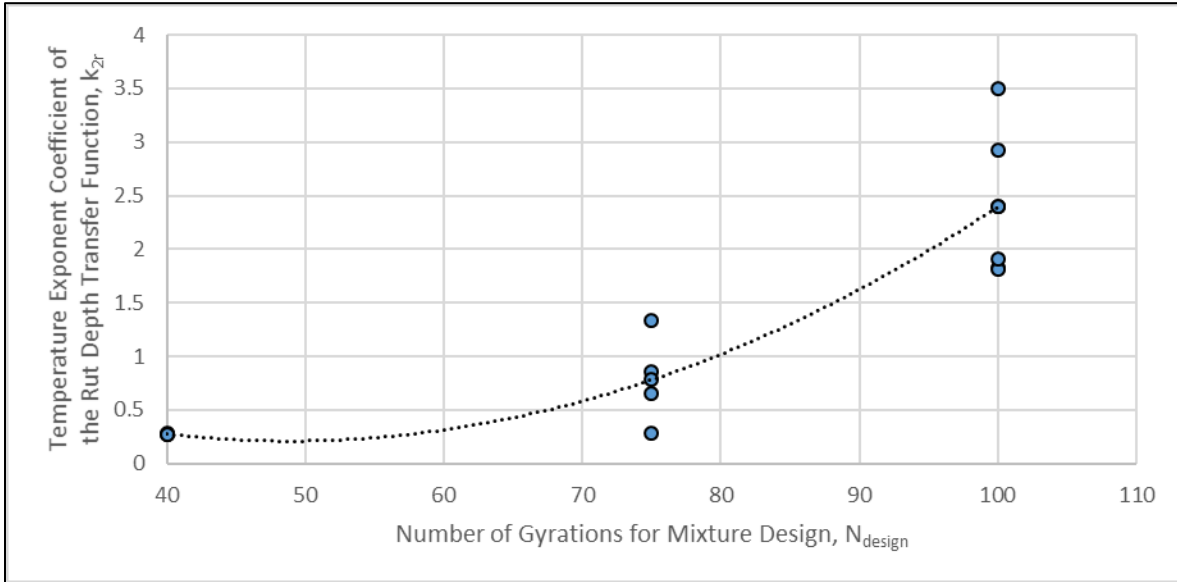


Figure 16. Correspondence between  $N_{Design}$  and the Temperature Exponent or Slope,  $k_{2r}$ .

Table 48. Rut depth transfer function plastic strain coefficients for the WisDOT asphalt materials library.

Asphalt Layer or Mixture	Fine Aggregate Angularity	$N_{design}$ Gyration	Plastic Strain k-Coefficients		
			Intercept, $k_{1r}$	Temperature Exponent, $k_{2r}$	Load Cycle Exponent, $k_{3r}$
Wearing Surface	<43	40	-1.00*	0.275	0.56
	43 to 45	75	-1.27	1.10	0.38
	>45	100	-2.43	1.85	0.25
Base Layer	>43	All	-2.24	1.70	0.23

\* Note: The maximum value or boundary value was -1.00 from NCHRP 9-30A project. Values higher than -1.0 result in extremely high rut depths. Thus, the intercept value was set at -1.0 from a practical standpoint.

#### 4.5 Fatigue Strength Coefficients

This section of Chapter 4 presents the data analysis and interpretation of the fatigue strength tests for deriving the coefficients of the bottom-up fatigue strength model (see equation 7). Two tests were used to estimate the fatigue strength of the WisDOT asphalt base mixtures: flexural, bending beam fatigue and the IDT failure strain tests. The flexural, bending beam test results are included in Appendix H, while the IDT failure strain test results are included in Appendix I.

#### 4.5.1 Flexural Bending Beam Fatigue Tests

Analysis of the flexural fatigue data collected in accordance with AASHTO T 321 to determine the fatigue life of individual beam test specimen is straightforward and summarized in Chapter 3 and Appendix H.

$$N_f = k_{1f} C \left( \frac{1}{\varepsilon_t} \right)^{k_{2f}} \left( \frac{1}{E_{flexural}} \right)^{k_{3f}} \quad \text{Equation 7}$$

Where:

$N_f$  = Allowable number of load cycles to failure.

$\varepsilon_t$  = Tensile strain, in/in.

$E_{flexural}$  = Asphalt flexural modulus, psi.

$C$  = Mixture volumetric property factor; defined by equation 8.

$k_{1f}, k_{2f}, k_{3f}$  = Laboratory-derived fatigue strength coefficients.

$$C = 10^{(VFA-0.69)} \quad \text{Equation 8}$$

Where:

$VFA$  = Voids filled with asphalt expressed as a decimal.

Multiple beam specimens are tested in accordance with AASHTO T 321 at different tensile strains for two or three test temperatures, as discussed in Chapter 3 and in Appendix H. The outcome from the flexural beam tests is a tabulation of tensile strain, temperature, and fatigue life or number of load cycles to the specific definition of failure (see Table 23 in Chapter 3).

The analysis of flexural fatigue data from multiple beam specimens is to develop a relationship (see equation 2 in Chapter 3) by performing a regression of the logarithm of the fatigue life versus the logarithm of the flexural strain. The fitting is performed using the regression function in Excel, as explained in Appendix H. The fatigue strength data for each test temperature is reviewed to identify any anomalies or outliers. A regression is then performed on all of the fatigue strength data (combining the data from all test temperatures) for a mixture to determine the fatigue strength coefficients in equation 7 without using the mixture volumetric property factor,  $C$ .

An important point to recognize is flexural bending beam fatigue testing between specimens can be highly variable, even taking into consideration the difference in volumetric properties between specimens (the  $C$  volumetric adjustment factor in equation 8). Table 49 lists the fatigue strength coefficients derived from the bending beam test data for the WisDOT base mixtures included in the test program. The fatigue strength coefficients included in Table 49 include the volumetric adjustment factor. As noted in Chapter 3, mixture #1060 is considered an outlier, because of the extremely high strain and modulus exponents.

Flexural bending beam fatigue were also performed on asphalt mixtures in a study sponsored by the FHWA that included a couple of WisDOT mixtures (Von Quintus, et al., 2019). For the two asphalt mixtures, however, 50 percent RAP/RAS was included in the job mix formula. Another difference between these two mixtures and the mixtures included in this study was the asphalt binder. The closest binder grade for the 50 percent RAP/RAS was PG76-22. These asphalt mixtures are different than the mixtures currently being produced and placed in Wisconsin. In



summary, the fatigue strength coefficient derived from the FHWA study for the high RAP/RAS mixtures are summarized in Table 50 in comparison to the global default values for neat asphalt mixtures without RAP/RAS.

**Table 49. MEPDG flexural bending beam coefficients (equation 7) for WisDOT base mixtures.**

Mixture Identification			N <sub>MAS</sub>	Gyrations, N <sub>Design</sub>	Fatigue Coefficients		
					Intercept, k <sub>1f</sub>	Strain Exponent, k <sub>2f</sub>	Temperature Exponent, k <sub>3f</sub>
0057	PG58-28S	3 LT	19 mm	40	2.590E-05	5.938	1.881
0003	PG58-28S	3 MT	12.5 mm	75	NA	NA	NA
1166	PG58-28S	2 HT	25 mm	100	1.809E-05	4.078	1.277
0119	PG58-28S	3 HT	19 mm	100	1.994E-05	4.722	1.027
1060	PG58-28H	3 HT	19 mm	100	3.735E-05	8.315	3.180

NOTE: The units for the intercept,  $k_{1f}$ , in the PMED software is mils/inch, while the units for the intercept parameter in Table 49 are in./in.

**Table 50. MEPDG flexural bending beam coefficients (equation 7) for selected WisDOT high RAP/RAS mixtures (50 percent), FHWA sponsored study (Von Quintus, 2019).**

Mixture Identification			N <sub>MAS</sub>	N <sub>Design</sub> Gyrations	Fatigue Strength k-Coefficients		
					Intercept, k <sub>1f</sub>	Strain Exponent, k <sub>2f</sub>	Temperature Exponent, k <sub>3f</sub>
Global Default Values					3.75E-03	2.870	1.460
FHWA	Base	PG70-22	19 mm	100	1.78E-01	4.895	1.799
FHWA	Surface	PG70-22	12.5 mm	100	3.57E-07	4.496	0.553

NOTE: The units for the intercept,  $k_{1f}$ , in the PMED software is mils/inch, while the units for the intercept parameter in Table 50 are in./in.

#### 4.5.2 Tensile Strain at Failure

The outcome from the IDT strength-failure strain test is the dynamic modulus at the test temperature for 10 Hz (AASHTO T 342) and tensile strain at failure. The dynamic modulus – tensile failure strain relationship represented by equation 9 is similar to the flexural bending beam and IDT fatigue strength relationship for the tensile strain value for one load cycle to cause failure (the intercept value) on a log-log basis (see equation 10). The IDT repeated load fatigue test exhibits the same relationship to the bending beam fatigue test, except the magnitudes of the coefficients are different (Rauhut, et al., 1984).

$$\text{Log}\epsilon_f = b - m(\text{Log}E_{Uniaxial}^*) \quad (9)$$

Where:

$\epsilon_f$  = Tensile failure strain, mils/inch.

$E_{Uniaxial}^*$  = Dynamic modulus at 10 Hz from uniaxial cylindrical specimen, psi.

$m, b$  = Regression fitting coefficients;  $m$  is the slope and  $b$  is the intercept.

$$\text{Log}\epsilon_t = \frac{\text{Log}(k_{1f})}{k_{2f}} - \frac{k_{3f}}{k_{2f}} (\text{Log}E_{Flexural}) \quad (10)$$

The intercept “ $b$ ” and slope exponent “ $m$ ” are an estimate of the fatigue strength coefficients from the bending beam flexural fatigue test outcomes.

The fatigue strength model coefficients are determined from the flexural beam fatigue test, AASHTO T 321. Equation 7 is the mathematical relationship resulting from the beam fatigue tests using 3 to 4 strain levels and 3 temperatures. Chapter 3 overviewed the IDT strength test as a surrogate for estimating the fatigue strength of dense-graded asphalt mixtures. Appendix I describes the procedure for determining the fatigue strength coefficients or laboratory-derived  $k$ -values from IDT strength-failure strain test. Use of the IDT strength test to estimate the fatigue strength parameters dates back to the Asphalt-Aggregate Mixture Analysis (AAMAS) procedure (Von Quintus, et al., 1991).

Equation 9 is the mathematical relationship between the dynamic modulus ( $E_{Uniaxial}^*$ ) and tensile strain at failure from the IDT strength test. The equation fits the data well in most cases (see Appendix I. Equation 10 defines the intercept term for different modulus values from the beam fatigue test ( $N=1$ ). The mathematical parameters in equation 10 are proportional to the parameters in equation 8, regarding the flexural beam fatigue strength test and the IDT strength test outcomes, excluding the volumetric property factor in equation 7.

The assumption that the failure strains from the flexural beam and IDT test are directly proportional for all mixtures is questionable but believed to be reasonable for a surrogate test. Equations 8 and 9 relate the coefficients from each equation.

$$k_{2f} = \left( \frac{-k_{3f}}{m} \right) \left( \frac{\text{Log}(E_{Flexural})}{\text{Log}(E_{Uniaxial}^*)} \right) \quad \text{Equation 8}$$

$$k_{2f} = \frac{\text{Log}(k_{1f})}{\text{Log}\left(\frac{b}{1000}\right)} \quad \text{Equation 9}$$

The term  $\text{Log}(E_{Flexural})/\text{Log}(E_{Uniaxial}^*)$  is temperature dependent, but the MEPDG assumes it, as well as the  $k_{2f}$  coefficient, to be temperature independent. The flexural modulus is not measured during IDT strength testing, while  $E_{Uniaxial}^*$  is measured on different test specimens. From different studies regarding a comparison of the flexural and dynamic uniaxial-based modulus values and other test methods, a default logarithmic modulus ratio of 1.08 is applied to all test temperatures

and dense-graded mixtures. Equation 10 is the relationship or correspondence between the intercept,  $k_{1f}$ , and the modulus exponent,  $k_{3f}$ , derived for many dense-graded asphalt mixtures.

$$\text{Log}(k_{1f}) = 7.218(k_{3f}) - 15.693 \quad \text{Equation 10}$$

Equation 11 estimates the modulus exponent, while equation 12 estimates the tensile strain exponent from the IDT strength-failure strain test.

$$k_{3f} = \frac{15.693}{1.08\left(\frac{\text{Log}(b/1000)}{m}\right)+7.218} \quad \text{Equation 11}$$

$$k_{2f} = \frac{k_{3f}}{m} (1.08)F_{IDT-Flex} \quad \text{Equation 12}$$

Where:  
 $F_{IDT-Flex}$  = Factor translating the IDT response to the flexural beam response.  
 The default value for dense-graded neat asphalt mixtures is 1.86.

The  $k_{1f}$  ( $Specimen_{IDT}$ ) intercept in mils per inch represents the average VFA for the test specimens included for a specific mixture or set of cores. Equation 13 is used to adjust the intercept to a standard volumetric property with the volumetric factor,  $C$  (see equation 8). The intercept is directly related to the “b” coefficient from the IDT strength test. Equation 13 estimates the intercept based on IDT tests. For simplicity, the  $k_{1f}$  intercept in mils per inch is equal to the “b” value from the IDT strength-failure strain data in mils per inch.

$$k_{1f}\left(\frac{\text{mils}}{\text{inch}}\right) = \frac{k_{1f}(Specimen_{IDT})}{c} = \frac{b}{c} \quad \text{Equation 13}$$

Table 51 lists the derived fatigue strength coefficients from the IDT failure strain and dynamic modulus tests. The  $k_{1f}$  values included in Table 51 include the adjustment to a standard volumetric property with the volumetric factor,  $C$ .

**Table 51. MEPDG fatigue strength coefficients estimated from the IDT failure strain test for WisDOT base mixtures.**

Mixture Identification			NMAAS	Gyrations, N <sub>Design</sub>	Fatigue Strength Coefficients		
					Intercept, k <sub>1f</sub>	Strain Exponent, k <sub>2f</sub>	Temperature Exponent, k <sub>3f</sub>
0057	PG58-28S	3 LT	19 mm	40	1.222 E-02	2.724	1.786
0003	PG58-28S	3 MT	12.5 mm	75	3.465E-03	2.850	1.694
1166	PG58-28S	2 HT	25 mm	100	4.866E-03	3.979	1.500
0119	PG58-28S	3 HT	19 mm	100	2.737E-03	2.506	1.795
1060	PG58-28H	3 HT	19 mm	100	3.228E-03	2.851	1.727

NOTE: The units for the intercept,  $k_{1f}$ , in the PMED software is mils/inch, while the units for the intercept parameter in Table 51 are in./in.

### 4.5.3 Fatigue Strength Coefficients for WisDOT Base Mixtures

Fatigue strength coefficients were derived for the two fracture test: flexural bending beam and IDT failure strain tests. Only one set of fatigue strength coefficients should be used with the PMED software. The following summarizes a comparison of the results from both tests.

- The derived strength coefficients from the flexural bending beam test are highly variable, while the derived coefficients from the IDT failure strain test are much less variable. This observation was not unexpected based on testing from many different asphalt mixtures on other projects. Variability of the flexural bending beam test was one reason for using the IDT failure strain as a surrogate test to estimate the fatigue strength coefficients.
- The derived  $k_{3f}$  coefficient from both tests are within the same range with the exception of the flexural bending beam results for mixture #1060. These results can be combined for determining the  $k_{3f}$  coefficient suggested to be included in the asphalt material library for use in design.
- As in the above bullet and in Chapter 3, mixture #1060 is considered an outlier, because of the extremely high strain and modulus exponents. The fatigue strength data in Appendix H were reanalyzed by setting the modulus exponent to the average of the other values from the flexural bending beam and IDT failure strain tests. This reanalysis changed the intercept term but did not have a significant impact on the strain exponent, because the data show a steep slope for the strain exponent; a small change in the applied tensile strain results in a very large change in the number of load cycles to failure. The reason for this outcome is unknown. Thus, this base mixture was excluded from determining the fatigue strength coefficients included in the asphalt mixture library.
- The strain exponent has an impact on the intercept coefficient. As the strain exponent increases, the intercept decreases because of the linear regression and form of the transfer function.
- Grouping the test data by various other parameters ( $N_{\text{Design}}$ , FAA, asphalt content by weight, effective asphalt content by volume, VMA, etc) did not result in a logical change in the fatigue strength coefficients between the mixtures. Within each of the groups, the individual fatigue strength coefficients were found to be statistically the same because of the variability in the data. However, the fatigue strength coefficients were grouped into different levels of FAA for the available data.

Table 52 lists the fatigue strength coefficients suggested for use in flexible pavement design. The values in Table 52 were determined from the IDT failure strain-dynamic modulus tests and flexural bending beam fatigue test (see Table 49, Table 50, and Table 51), only including the asphalt base mixtures and excluding the outlier. There is a consistent difference between the derived  $k_{1f}$  intercept and  $k_{2f}$  strain exponent from the flexural bending beam and IDT failure strain tests. The values included in the asphalt mixture library were based on the results from the IDT failure strain tests.

**Table 52. Fatigue strength coefficients for the WisDOT asphalt materials library.**

FAA	$N_{Design}$ Gyrations	Fatigue Strength Coefficients		
		Intercept, $k_{1f}$ *	Strain Exponent, $k_{2f}$	Temperature Exponent, $k_{3f}$ **
43 to 45	75	7.843E-03	2.95	1.61
>45	100	3.610E-03		

\* The units for the intercept,  $k_{1f}$ , in the PMED software is mils/inch, while the units for the intercept parameter in Table 52 are in./in.

\*\* The temperature exponent is significantly lower than the global default value derived for neat asphalt mixtures under NCHRP project 1-37A. The lower value may be characteristics of higher RAP mixtures.

#### 4.6 Summary – Asphalt Layer Property Libraries

Many of the asphalt properties that are inputs to the PMED software were found to be related to  $N_{Design}$ . Multiple volumetric properties and mixture component properties were evaluated to explain why  $N_{Design}$  was found to a key variable in establishing the asphalt mixture libraries. The volumetric properties available in the mixture design reports (see Appendix D) that were compared to  $N_{Design}$  included: asphalt content by weight, effective asphalt content by volume, effective aggregate specific gravity, maximum specific gravity, and FAA. The parameter found to be related to  $N_{Design}$  was the FAA. Figure 17 displays the relationship or correspondence between  $N_{Design}$  and FAA.

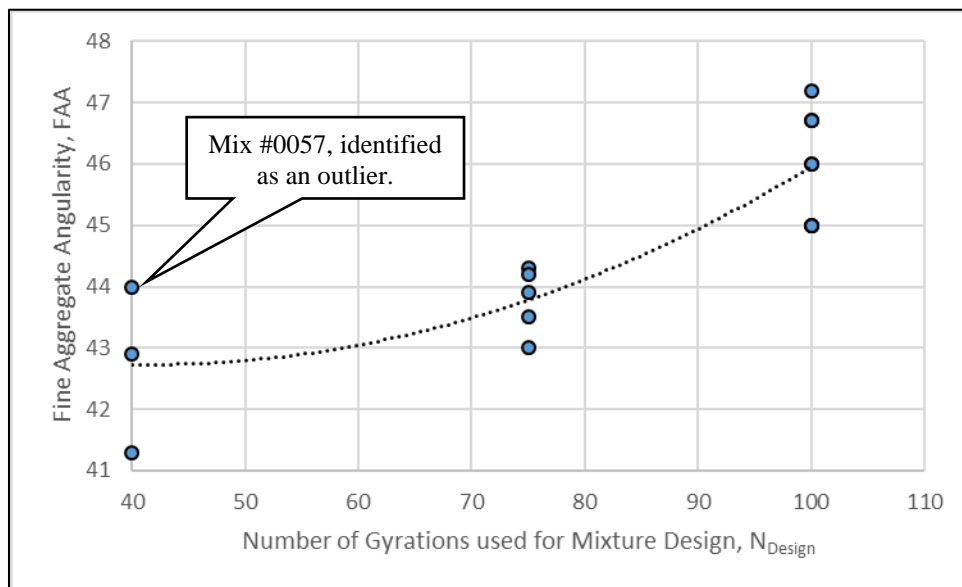


**Figure 17. Correspondence between  $N_{Design}$  and Fine Aggregate Angularity**

Asphalt mixture #0057 was originally believed to be an outlier or anomaly in comparison to the other mixtures designed using an  $N_{Design}$  of 40 gyrations. However, the FAA for mixture #0057 was much higher and explains the reason for the higher dynamic modulus and better rutting resistance. This observation and outcome supports the specification that aggregate particles with more angularity will be stiffer and more resistant to rutting and exhibit better performance, so asphalt mixture #0057 is not considered an outlier relative to the FAA value. Thus, FAA was

**Expansion of AASHTOWare ME Design Inputs  
Final Report WHRP 0092-20-03**

included in the materials matrix for selecting a set of asphalt material properties to be used in design.

Table 53 is the suggested decision tree or matrix for selecting a set of asphalt mixture properties from the XML files created for use in flexible pavement design using the PMED software.

**Table 53. Matrix for selecting a set of asphalt mixture properties for use in design.**

Asphalt Layer Property	Selection Variable							
Asphalt Binder, $G^*$ and $\delta$	AASHTO T 350	PG58-28	Grade "S"				Table 27	
			Grade "H"				Table 27	
			Grade "V"				Table 27	
		PG58-34	Grade "S"					Table 28
			Grade "H"					Table 28
			Grade "V"					Table 28
Dynamic Modulus, $E^*$	RAP/RAS Content	None					Table 31	
		Low to Moderate Amounts	FAA	<43	$N_{Design}$	40	Table 32	
				43 to 45	$N_{Design}$	75	Table 33	
				>45	$N_{Design}$	100	Table 34	
		High Amount	FAA	>45	$N_{Design} - 100$	Surface		Table 29
				>45	$N_{Design} - 100$	Base		Table 30
IDT Creep Compliance; $D(t)$ , Only Wearing Surface	RAP/RAS Content	None	PG58-28	FAA	43 to 45	$N_{Design} - 75$	Table 36	
				FAA	>45	$N_{Design} - 100$	Table 37	
			PG58-34	FAA	43 to 45	$N_{Design} - 75$	Table 38	
				FAA	>45	$N_{Design} - 100$	Table 39	
		Low to Moderate Amounts	PG58-28	FAA	<43	$N_{Design} - 40$	Table 42	
				FAA	43 to 45	$N_{Design} - 75$	Table 41	
				FAA	>45	$N_{Design} - 100$	Table 40	
			PG58-34	FAA	<43	$N_{Design} - 40$	Table 45	
				FAA	43 to 45	$N_{Design} - 75$	Table 44	
				FAA	>45	$N_{Design} - 100$	Table 43	
		High Amount	PG58-28 & PG58-34	FAA	>45	$N_{Design} - 100$	Table 35	
		IDT Strength, $S_t$ , Only Wearing Surface	FAA	>43	$N_{Design}$	75 & 100		451 psi
<43	$N_{Design}$			40		378 psi		
Plastic Strain Coefficients, $k_r$	FAA	<43	$N_{Design}$	40	$k_{1r}, k_{2r}, k_{3r}$	Table 48		
		43 to 45	$N_{Design}$	75	$k_{1r}, k_{2r}, k_{3r}$	Table 48		
		>45	$N_{Design}$	100	$k_{1r}, k_{2r}, k_{3r}$	Table 48		
Fatigue Strength Coefficients, $k_f$ , Only Base Mixes	FAA	43 to 45	$N_{Design}$	75	$k_{1f}, k_{2f}, k_{3f}$	Table 52		
		>45	$N_{Design}$	100	$k_{1f}, k_{2f}, k_{3f}$	Table 52		

## CHAPTER 5 AASHTO ASPHALT STRUCTURAL LAYER COEFFICIENT

Chapter 5 uses the different sets of asphalt mixture properties presented in Chapter 4 to predict total rut depth, bottom-up and top-down fatigue cracking, transverse cracking, and roughness (represented by the International Roughness Index [IRI]). The predicted distress with AASHTOWare PMED version 2.6 are used for the following two purposes:

1. Illustrate the differences in the predicted values between the different sets of asphalt layer properties included in the asphalt material library for different climate locations, traffic volumes, and pavement structures.
2. Estimate the 1993 AASHTO asphalt structural layer coefficients from the asphalt material library so they are representative of current practice.

Chapter 5 is divided into three parts including: the flexible pavement simulations and a brief review of the site specific input parameters, the outcome from the simulations in terms of the predicted distresses, and estimating the AASHTO asphalt structural layer coefficients based on the asphalt materials library.

### 5.1 Site Specific Inputs and Assumptions for the Simulations

A common set of inputs was used for the runs made with the AASHTOWare PMED software version 2.6 for comparing the predicted distresses between the different input level 1 laboratory-derived asphalt layer properties measured within this study and used to estimate the structural layer coefficients. The following summarizes the inputs and assumptions.

- General Design Information:
  - Design Life – a 20-year design period was assumed for all simulations. [Note: The specific pavement age when a distress threshold value was exceeded defines the ESALs used to estimate the structural layer coefficient (see section 5.3.2 and Appendix J).]
  - Two reliability levels were used: 50 percent and 90 percent.
  - The distress threshold values included in the simulations were the values included in WisDOT's earlier User Manual for the MEPDG.
- Climate: the MERRA2 climate grid points. Five climate locations were selected and used to show the impact of varying climates on the predicted distresses. For estimating the AASHTO asphalt structural coefficients, the climates selected were grouped into the southern and norther portions of Wisconsin. Table 54 lists the climate sites via the closest city. Many of the simulation runs were based on the sites defined as the northern and southern locations because the asphalt binder used is climate dependent. The depth to the water table was set at 15 feet (4.6 meters) for all simulations.
- Subgrade Inputs: the subgrade soil for the pavement simulations was defined by the soils commonly exhibited near the MERRA2 grid points for the climate simulations. The subgrade soil properties were extracted from WHRP project WisDOT ID No. 0092-03-11

(Titi, et al., 2006) and the LTPP database for similar types of soils. Table 54 includes the subgrade soil type used for each location. None of the simulations included a rigid layer.

**Table 54. Site specific inputs: climate or location and subgrade soil.**

Site #	Location, Climate	Grid Point	Subgrade Soil	
1-South	Madison	147602	Dodgeville	A-6
2-Central	Plover	149330	Chetek	A-2-4
3-North	Mercer	151057	Pence	A-2-4
4-West	Eau Claire	149903	Eleva	A-2-4
5-East	Green Bay	149332	Shiocton	A-4

- **Crushed Aggregate Base Inputs:** A typical crushed aggregate base was used in all of the simulations. The properties of the aggregate base included in WHRP project WisDOT ID No. 0092-11-02 (Titi, et al., 2012) and the LTPP database were reviewed. The Port Washington crushed aggregate base reported in WHRP project WisDOT ID No. 0092-11-02 was selected as a representative material for these simulations for all climate locations.
- **Traffic Inputs:** most of the traffic inputs were assumed to be the same between all simulations, regardless of location. The following summarizes some of the truck traffic inputs, while Table 55 lists the truck traffic inputs that were varied between the simulations:
  - The total number of trucks for the 20-year design period is listed in Table 55.
  - One lane was simulated with 100 percent trucks in the design lane and direction. The AADTT included in Table 55 represents one-way truck traffic.
  - A 3 percent linear growth rate was used in all simulations.
  - Unity was assumed for the monthly adjustment factors.
  - The global default values for the number of axles per axle type and truck classification was assumed.

**Table 55. Traffic inputs; based on asphalt mixture design levels.**

Traffic Category Description		18-kip ESALs, millions	AADTT; One-Way Traffic	TTC*	NALS**	Total 18-Kip ESALs, millions
1	LT, low traffic	<1	200	TTC-12	Light	0.97
2	MT, moderate traffic	1 to 8	800	TTC-8	Typical	8.51
3	HT, high traffic	> 8	4,000	TTC-1	Heavy	43.74

\* TTC – Truck Traffic Classification group as included in the MEPDG.

\*\* NALS – Normalized Axle Load Spectra.



- **Structural Inputs:**
  - A conventional flexible pavement was simulated for all runs and consisted for two asphalt layers (a wearing surface and asphalt base layer), a crushed aggregate base and a prepared subgrade layer.
    - The thickness of the asphalt wearing surface was 1.5 inches for traffic level LT and 2 inches (50.8 mm) for traffic levels MT and HT, while the thickness of the asphalt base layer varied with traffic level. The thickness of the asphalt base was selected to result in higher levels of distress for comparing the amount of distress between the simulations. A total asphalt layer thickness of 5.5 inches (140 mm) was simulated for the LT category, 8 inches (203 mm) for the MT category, and 12 inches (305 mm) for the HT category. The asphalt base thickness was varied so the life of the pavement was generally between 15 to 20 years.
    - The thickness of the crushed aggregate base was 8 inches (203 mm) for the LT category, 10 inches (254 mm) for the MT category, and 12 inches (305 mm) for the HT category. The design resilient modulus was determined based on the resilient modulus testing of the aggregate base layers included in WisDOT ID No. 0092-11-02 (Port Washington base material). The design resilient modulus varied with the total thickness of the asphalt layer.

## **5.2 Distress Sensitivity to Asphalt Mixtures included in the Asphalt Material Library**

Selected runs were made with the PMED software to illustrate the difference in the predicted distress and performance measures for the asphalt properties included in the asphalt material library (see Chapter 4). The distresses included in the comparison are transverse cracks, rut depth, and bottom-up alligator cracks. The simulations were also used to estimate the AASHTO asphalt structural layer coefficient, but only using the asphalt mixtures tested within this study.

This section graphically displays some of the runs made for the comparisons for the five locations listed in Table 54 and the three truck traffic levels included in Table 55. The results from the simulation using the global calibration factors can be used to judge the application of the global calibration factors to Wisconsin.

### **5.2.1 Length of Transverse Cracks**

Figure 18 displays the length of transverse cracks predicted for the asphalt mixture included in the asphalt materials catalog for the five designated locations (see Table 54) for the MT truck traffic level ( $N_{\text{Design}}$  of 75 gyrations and FAA between 43 and 45). Figure 19 displays the length of predicted transverse cracks for mixtures designed for the three truck traffic levels for the south Wisconsin site (Madison), while Figure 20 displays the length of predicted transverse cracks for the north Wisconsin site (Mercer). Figure 21 displays the length of predicted transverse cracks for different amounts of RAP/RAS for the central Wisconsin location (Plover climate location) and traffic level HT ( $N_{\text{Design}}$  of 100 gyrations and FAA greater than 45). As shown, binder type and the amount of RAP/RAS have a significant impact on the predicted lengths of transverse cracks. The

traffic mixture design level (LT, MT, HT) has a lower impact on the predicted lengths of transverse cracks.

### 5.2.2 Rut Depth

Table 48 listed the plastic strain coefficients determined for the asphalt mixtures that were clustered by FAA or  $N_{Design}$ . To demonstrate the difference between the different mixtures and which mixtures are susceptible to rutting, the plastic strain coefficients for a specific mixture were assumed to apply to all of the layers in the layer simulations. (Note: The rut depths displayed in the figures and discussed in the following paragraphs, represent higher values than will be measured along the roadway because the coefficients derived in the laboratory were applied to both the wearing surface and asphalt base layer for a flexible pavement simulation.)

Figure 22 displays the rut depths predicted for the asphalt mixture included in the asphalt materials catalog for the five designated locations (see Table 54) for the MT truck traffic level ( $N_{Design}$  of 75 gyrations and FAA between 43 and 45). Figure 23 displays the rut depths for mixtures designed for the three truck traffic levels for the central Wisconsin site (Plover). Figure 24 displays the rut depths for different amounts of RAP/RAS for the south Wisconsin location (Madison climate) and traffic level MT ( $N_{Design}$  of 75 gyrations and FAA between 43 and 45). The traffic level or  $N_{Design}$  and FAA has a significant impact on the predicted rut depths. The predicted rut depths for traffic level LT is very high and suggests mixtures susceptible to high distortion, while the predicted rut depths for traffic level HT are low. The FAA for asphalt mixtures designed for traffic level LT is lower than for mixtures designed for traffic level HT.

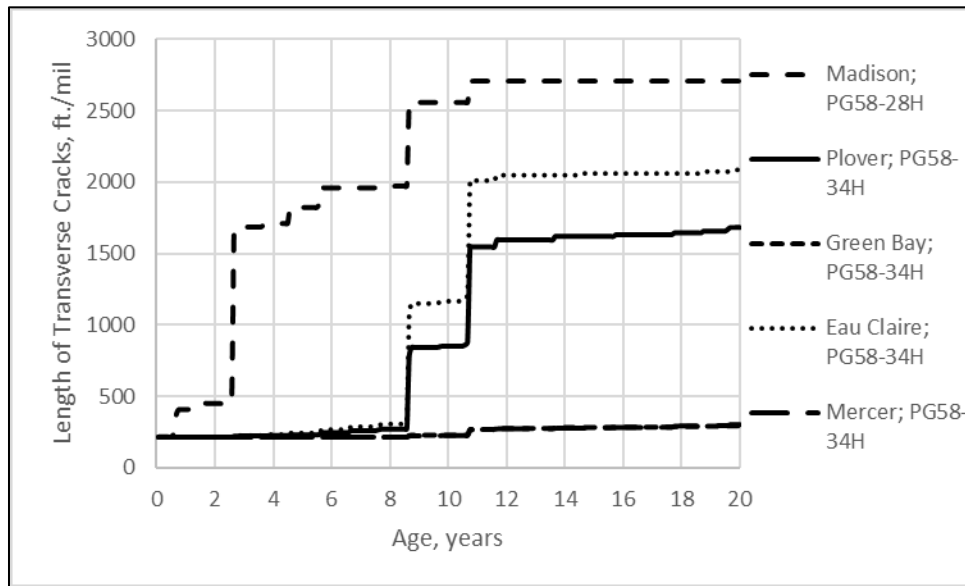
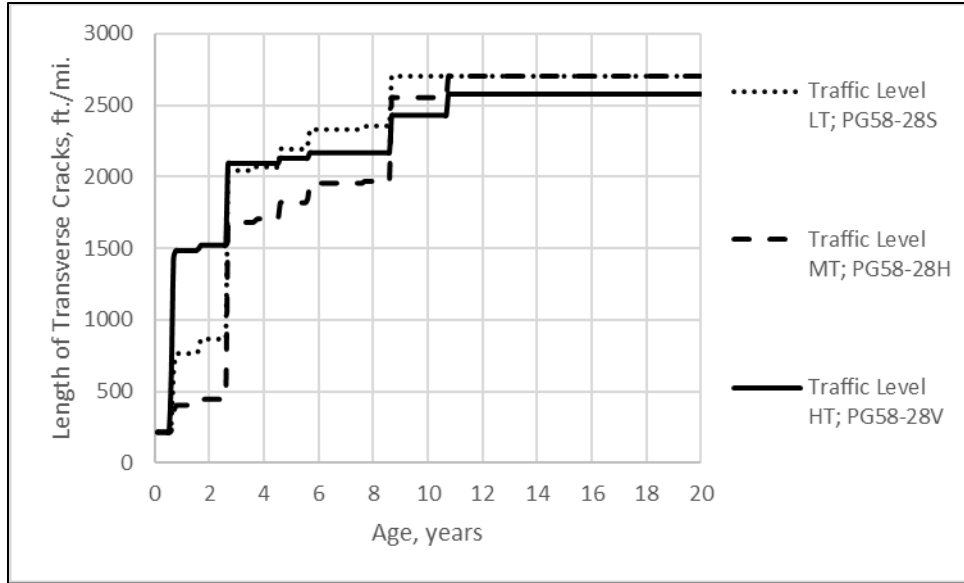
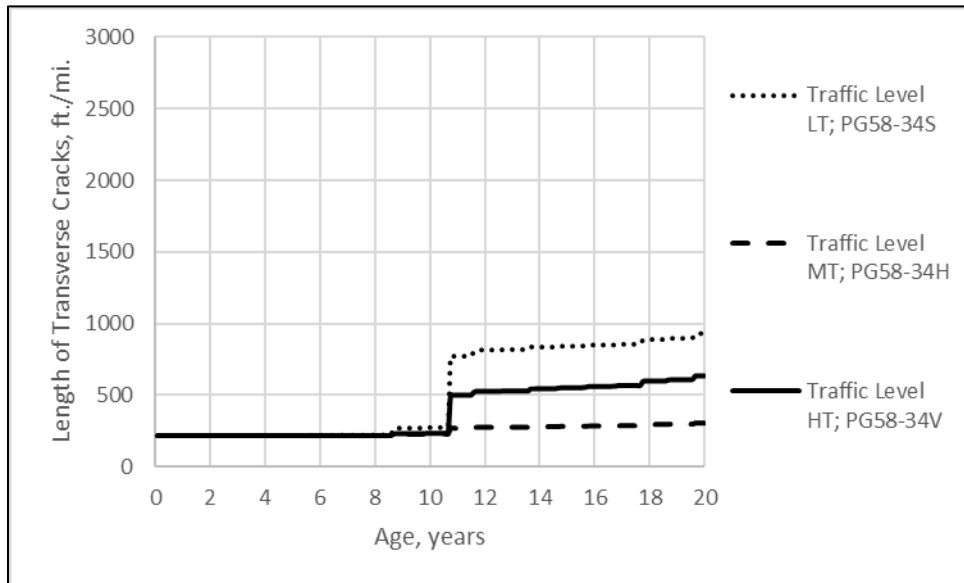


Figure 18. Predicted Lengths of Transverse Cracks for different Climate Locations using Traffic Level MT.



**Figure 19. Predicted Lengths of Transverse Cracks for different Traffic Levels for the Madison Climate Location; PG58-28 Asphalt.**



**Figure 20. Predicted Lengths of Transverse Cracks for different Traffic Levels for the Mercer Climate Location; PG58-34 Asphalt.**

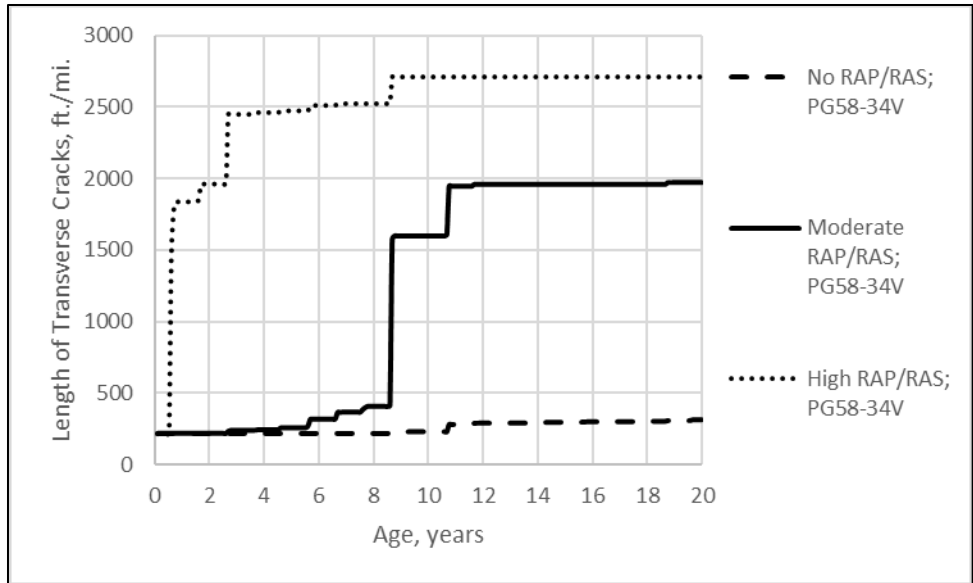


Figure 21. Predicted Lengths of Transverse Cracks for different Amounts of RAP/RAS for the Plover Climate Location and Traffic Level HT; PG58-34 Asphalt.

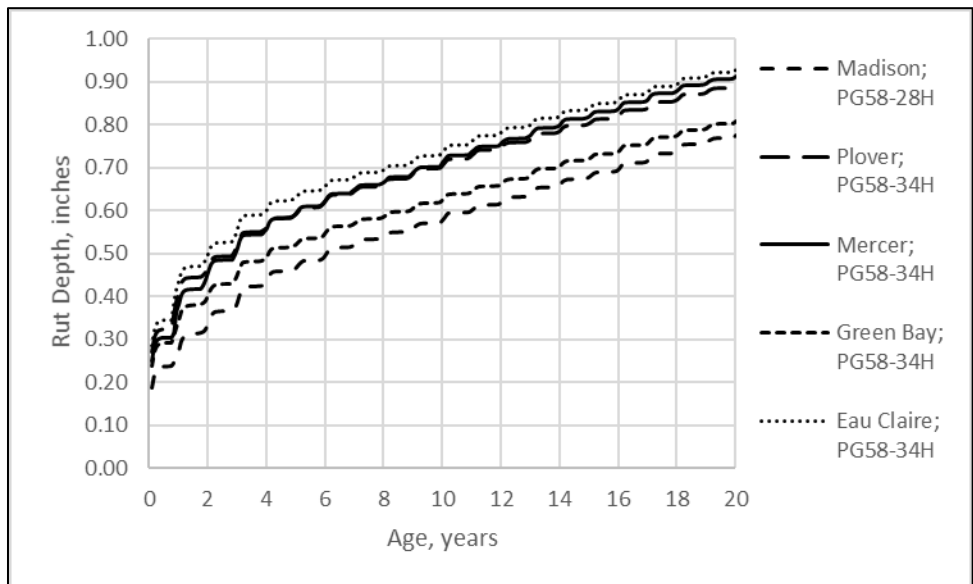
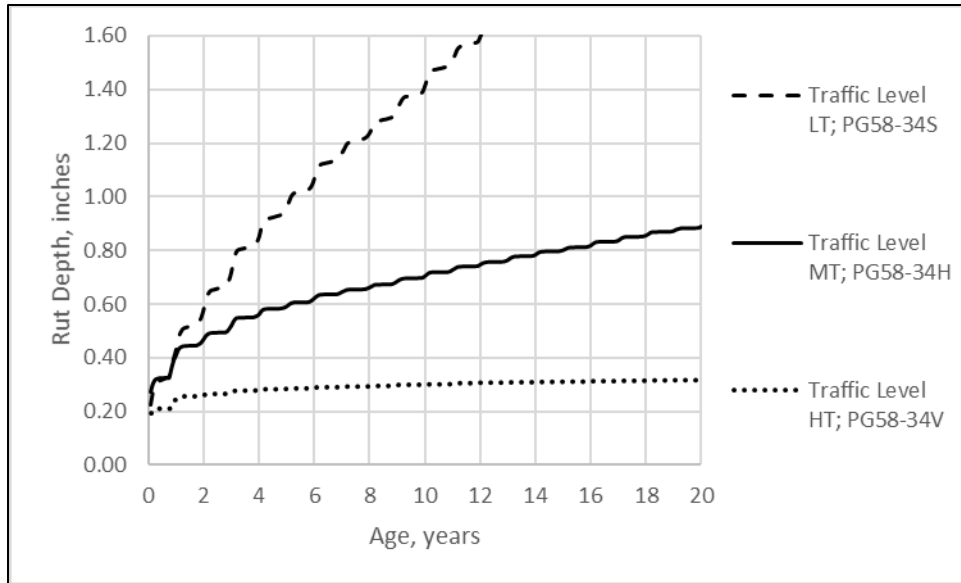
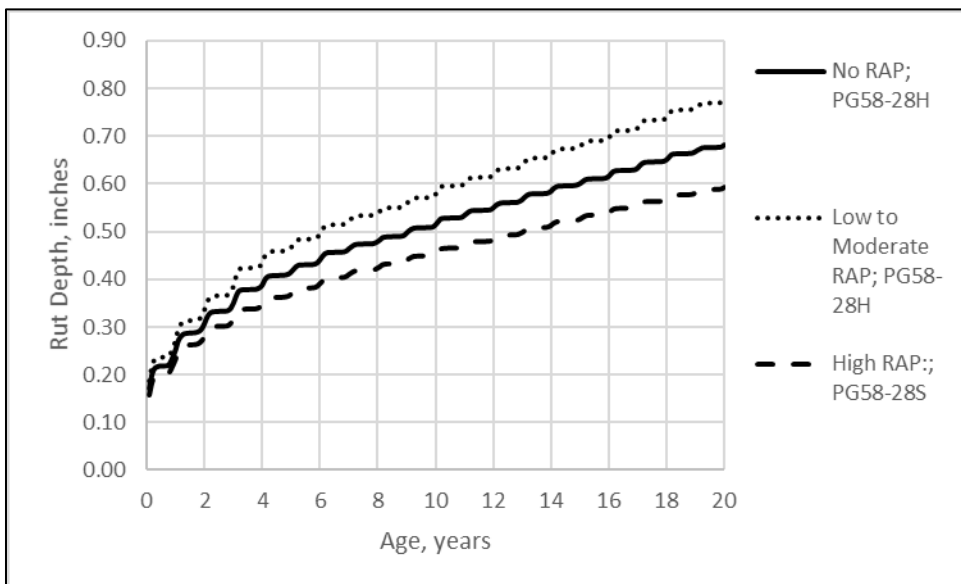


Figure 22. Predicted Rut Depths for different Climate Locations using the Traffic Level MT.



**Figure 23. Predicted Rut Depths for different Traffic Levels for the Plover Climate Location; PG58-34 Asphalt.**



**Figure 24. Predicted Rut Depths for different Amounts of RAP/RAS for the Madison Climate Location and Traffic Level MT; PG58-28 Asphalt.**

**5.2.3 Bottom-up Fatigue Cracking**

Figure 25 displays the bottom-up fatigue or alligator cracks predicted for the asphalt mixture included in the asphalt materials catalog for the five designated locations (see Table 54) for the HT truck traffic level ( $N_{Design}$  of 100 gyrations and FAA greater than 45). Figure 26 displays the bottom-up fatigue cracks for mixtures designed for the three truck traffic levels for the north Wisconsin site (Mercer). Figure 27 displays the bottom-up fatigue cracks for different amounts of RAP/RAS for the north Wisconsin location (Mercer climate location) and traffic level HT ( $N_{Design}$

of 100 gyrations and FAA greater than 45). Traffic level or  $N_{Design}$  and FAA and the amount of RAP/RAS have a significant impact on the predicted bottom-up fatigue cracks.

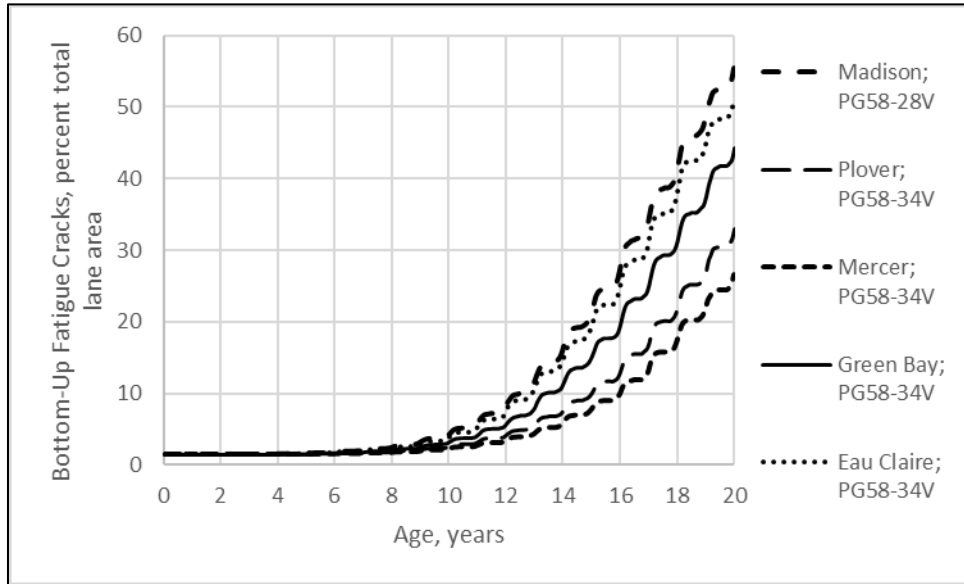


Figure 25. Predicted Bottom-Up Fatigue Cracks for different Climate Locations using the Traffic Level HT.

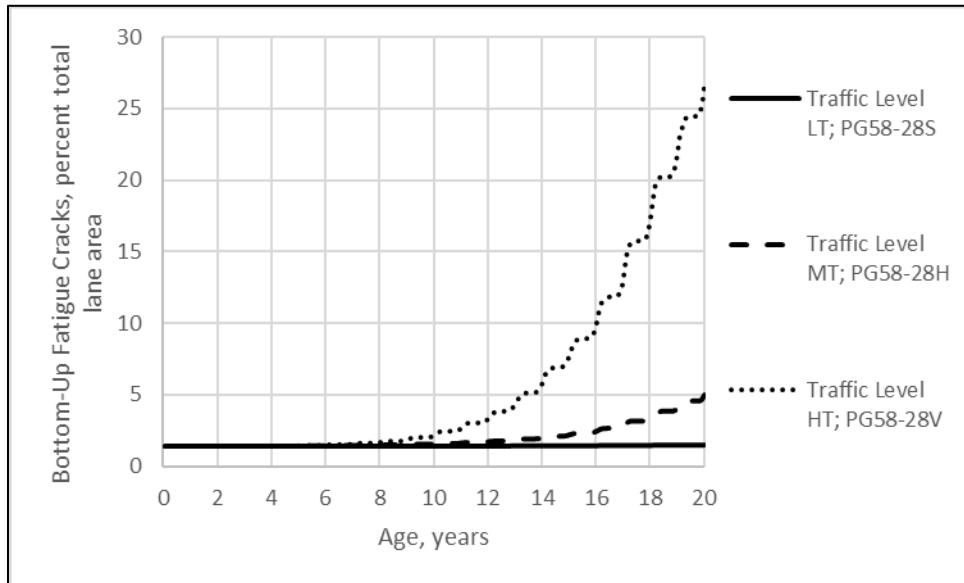


Figure 26. Predicted Bottom-Up Fatigue Cracks for different Traffic Levels for the Mercer Climate Location; PG58-34 Asphalt.

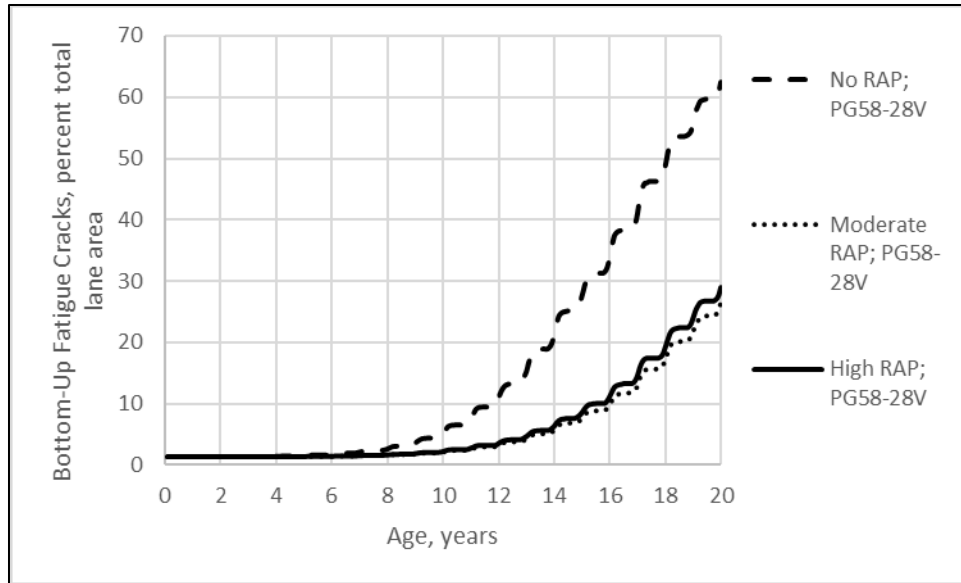


Figure 27. Predicted Bottom-Up Fatigue Cracks for different Amounts of RAP/RAS for the Mercer Climate Location and Traffic Level HT; PG58-34 Asphalt.

### 5.3 AASHTO Layer Coefficients

Two approaches were used to estimate the AASHTO asphalt structural layer coefficients: the relationship included in the 1993 AASHTO Design Guide based solely on the elastic or dynamic modulus of the asphalt mixture at the reference temperature, and varying the structural layer coefficient of the asphalt layers until the ESALs calculated from the structural number matched the accumulated ESALs to the time or age of the pavement when the distress or IRI threshold value is exceeded for the simulated pavement structure.

#### 5.3.1 Elastic Modulus Approach

The elastic modulus approach is very simplistic in that the structural layer coefficient is based on the measured elastic or dynamic modulus of the mixture measured at 68°F (20°C) and 10 Hz load frequency. Equation 14 is the relationship for calculating the asphalt structural layer coefficient used in the 1993 AASHTO Design Guide.

$a_1 = 0.1665(\ln[E]) - 1.7309$ <p>Where:</p> <p><math>a_1</math> = 1993 AASHTO asphalt structural layer coefficient.</p> <p><math>E</math> = Elastic modulus measured at 68 °F (20°C), psi.</p>	Equation 14
--	-------------

Table 56 lists the dynamic modulus and structural layer coefficient for each asphalt mixture included in the test plan. The structural layer coefficients in Table 56 are organized by increasing dynamic modulus values for the asphalt base and wearing surface mixtures. The asphalt base mixtures have a greater structural layer coefficient because they are stiffer relative to the wearing

**Expansion of AASHTOWare ME Design Inputs  
Final Report WHRP 0092-20-03**

surface mixtures. The following lists the average structural layer coefficients for the different mixture clusters and traffic level.

- Asphalt base mixtures, layer coefficient: 0.56 (independent of traffic level)
- Asphalt Wearing Surface:
  - SMA Mixtures, Traffic Level HT: 0.53
  - Traffic Level HT: 0.55
  - Traffic Level MT: 0.44
  - Traffic Level LT: 0.41

**Table 56. Asphalt structural layer coefficients derived from the elastic or dynamic modulus of the mixture (see Chapter 3)**

Layer	Mixture Identification		Dynamic Modulus, ksi	Calculated AASHTO Structural Layer Coefficient (Equation 14)
Base	0057	PG58-28S; 3 LT; 19 mm; 40 Gyrations	1,090	0.58
Base	0119	PG58-28S; 3 HT; 19 mm; 100 Gyrations	1,070	0.58
Base	1060	PG58-28H; 3 HT; 19 mm; 100 Gyrations	1,020	0.57
Base	0003	PG58-28S; 3 MT; 12.5 mm; 75 Gyrations	875	0.55
Base	1166	PG58-26S; 2 HT; 25 mm; 100 Gyrations	750	0.52
Wearing Surface	0251	PG58-28V; 4 HT; 12.5 mm; 100 Gyrations	1,030	0.57
Wearing Surface	0093	PG58-28H; 4HT; 12.5 mm; 100 Gyrations	990	0.57
Wearing Surface	0121	PG58-28V; 4 SMA; 12.5 mm; 100 Gyration	880	0.55
Wearing Surface	0165	PG58-28S; 4HT; 12.5 mm; 100 Gyrations	760	0.52
Wearing Surface	1020	PG58-34V; 4 SMA; 12.5 mm; 100 Gyration	710	0.51
Wearing Surface	0319	PG58-28H; 4 MT; 12.5 mm; 75 Gyrations	620	0.49
Wearing Surface	7130	PG58-34V; 5 MT; 9.5 mm; 75 Gyrations	480	0.45
Wearing Surface	0208	PG58-28S; 4 LT; 12.5 mm; 40 Gyrations	470	0.44
Wearing Surface	0258	PG58-28S; 4 MT; 12.5 mm; 75 Gyrations	440	0.43
Wearing Surface	0236	PG58-28S; 4 MT; 12.5 mm; 75 Gyrations	390	0.41
Wearing Surface	0127	PG58-34S; 4 MT; 12.5 mm; 75 Gyrations	370	0.40
Wearing Surface	8357	PG58-34S; 4 LT; 12.5 mm; 40 Gyrations	330	0.38

A couple of items to remember and understand prior to using the AASHTO asphalt structural layer coefficients listed in Table 56 for flexible pavement design:

- The elastic modulus values used in equation 14 were initially based on the IDT resilient modulus test. The total resilient modulus was the measured variable for a 0.1 second load duration and a 0.9 second rest period. The use of equation 14 was not calibrated globally.
- Under section 2.3.5 (page II-17) of the 1993 AASHTO Design Guide, it states: “*Caution is recommended for modulus values above 450,000 psi. Although higher modulus asphalt concretes are stiffer and more resistant to bending, they are also more susceptible to thermal and fatigue cracking.*”



### 5.3.2 Distress Prediction/Simulation Approach

This section summarizes the runs made for estimating the AASHTO asphalt structural layer coefficients from the predicted distresses using the PMED software and mixture properties measured within this study. The predicted distresses were for the five locations listed in Table 54 and the three truck traffic levels included in Table 55. IRI, bottom-up fatigue cracking, and rut depths were considered in determining the age to failure or the age at which the threshold value was exceeded and the cumulative ESALs at that age. Appendix J describes the step-by-step procedure and includes a couple of examples for deriving the structural layer coefficients.

Table 57 lists the asphalt structural layer coefficients based of the predicted distresses at a 90 and 50 percent reliability levels. The 50 percent reliability level should be used in comparing the structural layer coefficients between the two approaches. The structural layer coefficients for a 90 percent reliability level are provided for information purposes only.

**Table 57. Asphalt structural layer coefficients derived from predicted distresses using the PMED software and asphalt material property catalog (see Chapter 4)**

Asphalt Mixture Catalog/Material Library Identification	Location	Structural Number; 1993 AASHTO Design Guide, Calculated from PMED Simulations		
		90% Reliability	50% Reliability	
			Wearing Surface	Asphalt Base
LT; PG58-28; RAP	Madison	0.340	0.450	0.528
LT; PG58-28; RAP	Eau Claire	0.270	0.380	0.435
LT; PG58-28 & -34; RAP	Plover	0.305	0.430	0.469
LT; PG58-28 & -34; RAP	Mercer	0.318	0.460	0.483
LT; PG58-28 & -34; RAP	Green Bay	0.383	0.542	0.570
MT; PG58-28; RAP	Madison	0.435	0.500	0.578
MT; PG58-28; RAP	Eau Claire	0.309	0.370	0.405
MT; PG58-28 & -34; RAP	Plover	0.299	0.420	0.455
MT; PG58-28 & -34; RAP	Mercer	0.439	0.539	0.539
MT; PG58-28 & -34; RAP	Green Bay	0.426	0.545	0.550
HT; PG58-28; RAP	Madison	0.333	0.503	0.430
HT; PG58-28; RAP	Eau Claire	0.303	0.376	0.375
HT; PG58-28 & -34; RAP	Plover	0.333	0.415	0.417
HT; PG58-28 & -34; RAP	Mercer	0.326	0.405	0.400
HT; PG58-28 & -34; RAP	Green Bay	0.365	0.416	0.450

\* 50 percent reliability or the average values are suggested for use from the 1993 AASHTO Design Guide.

The following summarizes the average structural layer coefficients for the different asphalt layers derived from the predicted distress values using the PMED software:

- Asphalt Base Mixtures:
  - Traffic level HT 0.41
  - Traffic levels MT 0.51
  - Traffic level LT 0.50
- Wearing Surface Mixtures:

**Expansion of AASHTOWare ME Design Inputs  
Final Report WHRP 0092-20-03**

- Traffic level HT and SMA 0.42
- Traffic level MT 0.47
- Traffic level LT 0.45

### 5.3.3 Summary

Some important observations noted from the AASHTO asphalt structural layer coefficient calculated using the two approaches are briefly listed below:

- The structural layer coefficients determined using equation 14 (see Table 56) ranged from 0.38 to 0.58. The structural layer coefficients estimated from the distress predictions ranged from 0.37 to 0.58 (see Table 57). Although the range of values are the same, the mixtures with the higher structural layer coefficients based on the dynamic modulus (equation 14) are different from the mixtures with the higher coefficients based on predictions of distress.
  - The asphalt base exhibit the higher modulus and greater layer coefficient based on equation 14, while traffic level LT designed wearing surfaces exhibit the softer mixtures with the lower layer coefficient.
  - Conversely, the asphalt base and wearing surfaces designed for traffic level HT exhibit the lower layer coefficients based on predicted distresses, while the base and wearing surface mixtures designed for traffic levels MT and LT exhibit the higher layer coefficients.
- In estimating the structural layer coefficients from the predicted distresses, the asphalt mixtures highly susceptible to rutting, generally exhibited better resistance to fracture.
- Under section 2.1.3 (page II-9, paragraph 4) of the 1993 AASHTO Design Guide, it states: *“It is important to note that by treating design uncertainty as a separate factor, the designer should no longer use conservative estimates for all the other design input requirements. Rather than conservative values, the designer should use his best estimate of the mean or average value for each input value. The selected level of reliability and overall standard deviation will account for the combined effect of the variation of all the design variables.”*

## CHAPTER 6 CONCLUSIONS AND RECOMMENDATIONS

### 6.1 Conclusions and Observations

The following briefly lists the important findings or outcomes and observations from the laboratory testing of asphalt mixtures for use in the PMED software.

- The input level 1 measured asphalt properties were found to be consistently different from the input level 3 default properties that are included in the PMED software.
- A catalog of asphalt binders and mixtures was created for use in flexible pavement design. Table 53 in Chapter 4 included the suggested matrix for selecting a set of asphalt mixture and binder properties for use in flexible pavement design. The selection variables are dependent on the mixture property, but include: RAP/RAS content, asphalt grade, and FAA or  $N_{\text{Design}}$  used for mixture design. XML files were created that can be directly imported into the PMED software to simplify the inputs and reduce the potential for input blunders. Table 58, Table 59, and Table 60 include a listing of the XML files provided to WisDOT. Table 58 is for the XML files for the wearing surface, Table 59 is for the asphalt base mixtures, and Table 60 is for selected subgrade soils.
- Asphalt binders typically used in Wisconsin were provided from two different sources for the two high use binder grades. The binder properties were similar from the two sources when graded in accordance with AASHTO T 350. The measured properties included in the catalog for a specific grade can be used for flexible pavement design, regardless of the producer or source.
- The asphalt mixtures that exhibited poor rut depth resistance, exhibited better resistance to bottom-up fatigue cracks. The dynamic modulus between the different mixtures, however, was not significantly different.
- $N_{\text{Design}}$  and FAA were found to be related to or have a significant impact on the asphalt material properties measured for the PMED catalog. The asphalt mixtures were ranked in terms of increasing and decreasing resistance to distresses in reporting the test results. Initially some of the mixtures were believed to be outliers. However, FAA explained why some of the mixture appeared to be different. FAA was identified as the mixture component property in ranking the mixtures and in completing the clustered analysis for creating the asphalt materials catalog or library.  $N_{\text{Design}}$  was another property from the mixture design process correlated to the asphalt mixture properties. Both FAA and  $N_{\text{Design}}$  are included matrix for selecting a set of mixture properties for flexible pavement design. FAA should be used as the first selection variable.  $N_{\text{Design}}$  was included in the matrix, for the condition when FAA is unknown during the pavement design process. Other volumetric and component asphalt properties were evaluated in creating the materials catalog but were found to be insignificant or did not explain some of the differences in measured results between the asphalt mixtures.

**Table 58. Wearing surface asphalt mixtures and subgrade soil XML files created for use in design with the PMED software.**

XML File Identification	File Description	XML File Number
Surface_LT_28S_RAP	Default wearing surface mixture for low traffic in southern Wisconsin using PG58-28S with low to moderate levels of RAP/RAS.	1
Surface_LT_28H_RAP	Default wearing surface mixture for low traffic in southern Wisconsin using PG58-28H with low to moderate levels of RAP/RAS.	2
Surface_MT_28S_RAP	Default wearing surface mixture for moderate traffic in southern Wisconsin using PG58-28S with low to moderate levels of RAP/RAS.	3
Surface_MT_28H_RAP	Default wearing surface mixture for moderate traffic in southern Wisconsin using PG58-28H with low to moderate levels of RAP/RAS.	4
Surface_MT_28V_RAP	Default wearing surface mixture for moderate traffic in southern Wisconsin using PG58-28V with low to moderate levels of RAP/RAS.	5
Surface_HT_28S_RAP	Default wearing surface mixture for high traffic in southern Wisconsin using PG58-28S with low to moderate levels of RAP/RAS.	6
Surface_HT_28H_RAP	Default wearing surface mixture for moderate traffic in southern Wisconsin using PG58-28H with low to moderate levels of RAP/RAS.	7
Surface_HT_28V_RAP	Default wearing surface mixture for moderate traffic in southern Wisconsin using PG58-28V with low to moderate levels of RAP/RAS.	8
Surface_High RAP	Default wearing surface mixture with RAP contents of 50 percent.	9
Surface_MT_28H_No RAP	Default wearing surface mixture without RAP/RAS using PG58-28 designed for FAA between 43 and 45.	10
Surface_HT_28V_No RAP	Default wearing surface mixture without RAP/RAS using PG58-28 designed for FAA greater than 45.	11
Surface_MT_34H_No RAP	Default wearing surface mixture without RAP/RAS using PG58-34 designed for FAA between 43 and 45.	12
Surface_HT_34V_No RAP	Default wearing surface mixture without RAP/RAS using PG58-34 designed for FAA greater than 45.	13
Surface_HT_Mix0093	Individual asphalt wearing surface mix.	14
Surface_SMA_Mix0121	Individual asphalt wearing surface mix.	15
Surface_MT_Mix0127	Individual asphalt wearing surface mix.	16
Surface_HT_Mix0165	Individual asphalt wearing surface mix.	17
Surface_LT_Mix0208	Individual asphalt wearing surface mix.	18
Surface_MT_Mix0236	Individual asphalt wearing surface mix.	19
Surface_HT_Mix0258	Individual asphalt wearing surface mix.	20
Surface_MT_Mix0319	Individual asphalt wearing surface mix.	21
Surface_SMA_Mix1020	Individual asphalt wearing surface mix.	22
Surface_MT_Mix7132	Individual asphalt wearing surface mix.	23
Surface_LT_Mix8357	Individual asphalt wearing surface mix.	24

**Table 59. Asphalt base mixture XML files created for use in design with the PMED software.**

XML File Identification	File Description	XML File Number
Base_LT_28S_RAP	Default asphalt base mixture for low traffic using PG58-28S with low to moderate levels of RAP/RAS.	25
Base_LT_28H_RAP	Default asphalt base mixture for low traffic using PG58-28H with low to moderate levels of RAP/RAS.	26
Base_MT_28S_RAP	Default asphalt base mixture for moderate traffic using PG58-28S with low to moderate levels of RAP/RAS.	27
Base_No RAP_HT	Default asphalt base mixture without any RAP/RAS.	28
Base_High RAP_HT	Default asphalt base mixture with high amount of RAP (50 percent)	29
Base_MT_Mix0003	Individual asphalt base mix.	30
Base_LT_Mix0057	Individual asphalt base mix.	31
Base_HT_Mix0119	Individual asphalt base mix.	32
Base_HT_Mix1060	Individual asphalt base mix.	33
Base_HT_Mix1166	Individual asphalt base mix.	34

**Table 60. Subgrade soil XML files created for use in design with the PMED software.**

XML File Identification	File Description	XML File Number
A-6; Dodgeville; Optimum	Subgrade soil properties for the Dodgeville soil group in southern Wisconsin, optimum water content and maximum dry unit weight.	35
A-2-4; Chetek; Optimum	Subgrade soil properties for the Chetek soil group in central Wisconsin, optimum water content and maximum dry unit weight.	36
A-2-4; Pence; Optimum	Subgrade soil properties for the Pence soil group in northern Wisconsin, optimum water content and maximum dry unit weight.	37
A-4; Shiocton; Optimum	Subgrade soil properties for the Shiocton soil group in eastern Wisconsin, optimum water content and maximum dry unit weight.	37
A-2-4; Eleva; Optimum	Subgrade soil properties for the Eleva soil group in western Wisconsin, optimum water content and maximum dry unit weight.	38

- The simulations used to estimate the AASHTO structural layer coefficients were based on the global calibration factors. Revisions to the calibration coefficients of the distress transfer function will have an impact on the structural layer coefficients.
- The following bullets summarize the impact of selected input variables on the predicted distresses.

- The combination of climate and mixture properties have a significant impact on the predicted length of transverse cracks (see Figure 18) and bottom up fatigue (alligator) cracks (see Figure 25), but a minor impact of total rutting (see Figure 22).
- The amount of RAP/RAS has a significant impact on the predicted length of transverse cracks (see Figure 21) and a minor impact of total rutting (see Figure 24). The amount of RAP/RAS exhibited a minor impact on bottom-up fatigue cracks, but with and without RAP/RAS exhibited a significant impact on bottom-up fatigue cracks (see Figure 27).
- The combination of traffic level and mixture properties have a significant impact on the predicted asphalt layer rut depth (see Figure 22) and bottom-up fatigue cracks (see Figure 26).

## **6.2 Recommendations: Moving Forward with ME Design Implementation**

The following provides some suggestions for implementing and using the PMED software for flexible pavement design.

- The input level 1 measured asphalt properties were found to be consistently different from the input level 3 default properties that are included in the PMED software. The input level 3 properties should not be mixed with the input level 1 properties. WisDOT should use the derived asphalt properties included in the asphalt materials catalog. For mixture types not included in the current catalog, the design will need to make a decision on the closest representative mixture in the catalog.
- The PMED software includes the use of laboratory derived mixture properties that can be used for innovative and other materials. Calibration factors were derived during the global calibration process and it is assumed that the global calibration factors are applicable to all types of dense-graded asphalt mixtures and material specifications. The global calibration factors should be verified for use in Wisconsin.
- FAA and  $N_{\text{Design}}$  are included in the matrix for the design to use in selecting a set of mixture properties for flexible pavement design. FAA should be used as the first selection variable.  $N_{\text{Design}}$  was included in the matrix when FAA is unknown during the pavement design process.
- New XML files are available for use in flexible pavement design. The XML files can be directly imported into the PMED software to reduce the potential for input blunders. The new XML files were based on the asphalt binders and mixtures tested within this study. It is recommended that WisDOT review the matrix of XML files and the selection variables in terms of typical mixture design features.

**Expansion of AASHTOWare ME Design Inputs  
Final Report WHRP 0092-20-03**

- A deliverable for this project was to recommend a sampling strategy for updating the asphalt mixture library over time. The following lists some suggestions for the future to verify the catalog for the asphalt binders and mixtures.
  - Table 7 listed the asphalt binder grades included in the testing plan. The asphalt binders included in the catalog (XML files) are believed to be sufficient, unless the binder specification is changed.
  - Table 12 listed the asphalt mixtures included in the testing plan, which focused on RAP and/or RAS combined amounts of around 3 to 30 percent, because these asphalt mixtures represent the higher tonnage of mixtures placed within the past 2 years. Few asphalt mixtures have been tested with no and high amounts of RAP/RAS.
  - Only two mixtures were tested with a FAA less than 43. If WisDOT typically allows LT mixtures designed with a FAA less than 43, more of these mixtures should be tested and the average values included in the catalog.
  - High RAP mixtures (defined as more than 40 percent RAP) were included in the catalog. The properties, however, were derived from other studies and only two high RAP mixtures were tested. If WisDOT starts to allow the use of “high” RAP mixtures, the properties included in the catalog should be verified with testing additional mixtures.
  - The following identifies asphalt mixtures and mixture tests that can be considered for future testing relative to this project’s testing plan, if WisDOT plans to use a higher tonnage of these asphalt mixtures.
  - Additional asphalt mixtures and their features suggested for dynamic modulus tests are listed below. (Note: Table 12 and Table 16 identified the asphalt mixtures included in the dynamic modulus testing plan for this project.)

Asphalt Grade	N <sub>Design</sub>	Amount of RAP/RAS; %		
		High	Moderate	None
PG58-28	100	+2 Mixes		+1 Mix
	75	+2 Mixes		+1 Mix
	40			+2 Mixes
PG58-34	100	+2 Mixes	+2 Mixes	+2 Mixes
	75	+2 Mixes	+2 Mixes	+2 Mixes
	40			
PG70-22	100			
	75			

**Expansion of AASHTOWare ME Design Inputs  
Final Report WHRP 0092-20-03**

- Additional asphalt mixtures and their features suggested for IDT creep compliance and strength tests are listed below. (Note: Table 12 and Table 17 identified the asphalt mixtures included in the creep compliance and strength testing plan for this project.)

Asphalt Grade	N <sub>Design</sub>	Amount of RAP/RAS; %		
		High	Moderate	None
PG58-28	100	+2 Mixes		+1 Mix
	75	+2 Mixes		+1 Mix
	40	+1 Mix		+1 Mix
PG58-34	100	+1 Mix	+1 Mix	+1 Mix
	75	+1 Mix	+1 Mix	+1 Mix
	40			
PG70-22	100			
	75			

- Additional asphalt mixtures and their features suggested for repeated load plastic strain tests are listed below. (Note: Table 12 and Table 19 identified the asphalt mixtures included in the plastic strain testing plan for this project.)

Asphalt Grade	N <sub>Design</sub>	Amount of RAP/RAS; %		
		High	Moderate	None
PG58-28	100	+2 Mixes		+2 Mixes
	75	+2 Mixes		+2 Mixes
	40			+2 Mixes
PG58-34	100	+2 Mixes	+1 Mix	+2 Mixes
	75	+2 Mixes	+1 Mix	+2 Mixes
	40			
PG70-22	100			
	75			

- Additional asphalt mixtures and their features suggested for IDT strain at failure and flexural bending beam fatigue tests are listed below. (Note: Table 12, Table 24, and Table 25 identified the asphalt mixtures included in the fatigue strength testing plan for this project.)

Asphalt Grade	N <sub>Design</sub>	Amount of RAP/RAS; %		
		High	Moderate	None



**Expansion of AASHTOWare ME Design Inputs  
Final Report WHRP 0092-20-03**

PG58-28	100	+2 Mixes		+2 Mixes
	75	+2 Mixes	+2 Mixes	+2 Mixes
	40			+2 Mixes
PG58-34	100			
	75			
	40			
PG70-22	100			
	75			

- WisDOT is encouraged to continue to use and include FAA in their specifications, because it was found to be correlated to the material properties used to predict flexible pavement performance. All of the asphalt mixtures that had a FAA value greater than 45 ( $N_{Design}$  of 100 gyrations) were predicted to have good resistance to pavement distress based on the laboratory measured properties.
- A series of new XML files were provided to WisDOT that included files for the asphalt and soils materials library (see Table 54). XML files were prepared for the subgrade soil identified in different areas of Wisconsin which were used to illustrate the impact of the different asphalt mixtures on performance. The new XML files should be combined with the existing XML files initially prepared for implementing the PMED software. It is suggested that WisDOT consider and use the previous and new asphalt and soil XML files in future calibration efforts to verify the global calibration coefficients.
- The simulations used to estimate the AASHTO structural layer coefficients were based on the global calibration factors for version 2.6 of the AASHTOWare PMED software. The results from the simulations can be used to evaluate the application of the global calibration factors to Wisconsin.

## REFERENCES

AASHTO (2010). Guide for the Local Calibration of the Mechanistic-Empirical Pavement Design Guide, First Edition, Publication Code: LCG-1, ISBN: 978-1-56051-449-7, American Association of State Highway and Transportation Officials, Washington, DC.

Aguiar-Moya, J.P., Banerjee, A., and Prozzi, J.A. (2009). *Sensitivity analysis of the MEPDG using measured probability distributions of pavement layer thickness*. Annual Meeting of Transportation Research Board, Transportation Research Board of the National Academies, Washington, D.C.

Applied Research Associates (2004). *Development of 2002 Guide for the Design of New and Rehabilitated Pavement Structure*, NCHRP Project 1-37A, National Cooperative Highway Research Program, National Academies of Science, Washington, DC.

Ayyala, D., Chehab, G. R., and Daniel, J. S. (2010). *Sensitivity of MEPDG Level 2 and 3 Inputs using Statistical Analysis Techniques for New England States*. Annual Meetings of the Transportation Research Board, Transportation Research Board of the National Academies, Washington, D.C.

Bahia et al. (2016). *Analysis and Feasibility of Asphalt Pavement Performance-Based Specifications for WisDOT*. Wisconsin Department of Transportation, Report No. 0092-15-04.

Bahia, H., Tabatabaee, H., and Mandal, T. (2013). *Field Validation of Wisconsin Modified Binder Selection Guidelines - Phase II*. Wisconsin Department of Transportation.

Bonaquist, R. (2010). *Wisconsin Mixture Characterization Using the Asphalt Mixture Performance Tester (AMPT) on Historical Aggregate Structures*. Wisconsin Department of Transportation, Report No. WHRP 09-03.

Bonaquist, R. (2011). *Characterization of Wisconsin Mixture Low Temperature Properties for the AASHTO Mechanistic-Empirical Pavement Design Guide*. Wisconsin Department of Transportation, Report No. WHRP 11-12.

Bonaquist, R. (2011). *Effect of Recovered Binders from Recycled Shingles and Increased RAP Percentages on Resultant Binder PG*. Wisconsin Department of Transportation, Report No. WHRP 11-13.

Bonaquist, R. (2012). *Evaluation of Flow Number (Fn) as a Discriminating HMA Mixture Property*. Wisconsin Department of Transportation, Report No. WHRP 12-01.

Bonaquist, R., Cuciniello, G., Hanz, A., and Bahia, H. (2014). *Development of Guidelines and Specifications for Use of WMA Technology in Delivering HMA Products Inclusive of Non-Conventional Mixtures Such as SMA's, and Mixtures with High RAP and RAS Content*. Wisconsin Department of Transportation, Report No. WHRP 0092-12-02.

Carvalho, R., and Schwartz, C. W. (2006). *Comparisons of Flexible Pavement Designs: AASHTO Empirical Versus NCHRP Project 1-37A Mechanistic-Empirical*. Transportation Research Record: Journal of the Transportation Research Board, No. 1947, pp. 167–174, Transportation Research Board of the National Academies, Washington, D.C.

**Expansion of AASHTOWare ME Design Inputs  
Final Report WHRP 0092-20-03**

Chehab, G. R., and Daniel, J. S. (2006). *Evaluating Recycled Asphalt Pavement Mixtures with Mechanistic- Empirical Pavement Design Guide Level 3 Analysis*. Transportation Research Record: Journal of the Transportation Research Board, No. 1962, pp. 90–100, Transportation Research Board of the National Academies, Washington, D.C.

Cooper, S. B., Elseifi, M. A. and Mohammad, L. N. (2012) *Parametric Evaluation of Design Input Parameters on the Mechanistic-Empirical Pavement Design Guide Predicted Performance*. International Journal of Pavement Research and Technology, Vol. 5, No. 4, pp. 218–224.

Delgadillo, R., Motamed, A., and Bahia, H. (2007). *Field Validation of Wisconsin Modified Binder Selection Guidelines*. Wisconsin Department of Transportation.

Diefenderfer, S. D. (2010). *Analysis of the Mechanistic-Empirical Pavement Design Guide Performance Predictions: Influence of Asphalt Material Input Properties*. Virginia Department of Transportation, Report No. FHWA/VTRC 11-R3.

El-Basyouny, M. M., and Witczak, M. W. (2005). *Verification of the calibrated fatigue cracking models for the 2002 Design Guide*. Journal of the Association of Asphalt Paving Technologists, Vol. 74, pp. 653-695.

El-Basyouny, M. M., Witczak, M. W., and El-Badawy, S. (2005). *Verification for the calibrated permanent deformation models for the 2002 Design Guide*. Journal of the Association of Asphalt Paving Technologists, Vol. 74, pp. 601-652.

Graves, R. C., and Mahboub, K. C. (2006). *Pilot Study in Sampling-Based Sensitivity Analysis of NCHRP Design Guide for Flexible Pavements*. Transportation Research Record: Journal of the Transportation Research Board, No. 1947, pp. 123–135, Transportation Research Board of the National Academies, Washington, D.C.

Kim, S., Halil, C., and Kasthurirangan, G. (2007). *Effect of M-E Design Guide Inputs on Flexible Pavement Performance Predictions*. Journal of Road Materials and Pavement Design, Vol. 8, No. 3, pp. 375–397.

Lee, M. C. (2004). *Mechanistic-Empirical Pavement Design Guide: Evaluation of Flexible Pavement Inputs*. M.S. Thesis, University of Arkansas.

Mallela, J. L. Titus-Glover, H.L. Von Quintus, M.I. Darter, and H. Bahia (2008). *Implementation of the Mechanistic-Empirical Pavement Design Guide in Wisconsin*, WisDOT Project #1009-03-35, Wisconsin Department of Transportation, Madison, Wisconsin.

Rauhut, J.B.; Lytton, R.L.; and Darter, M.I. (1984). *Pavement Damage Functions for Cost Allocation, Vol. 2 – Description of Detailed Studies*. Report Number. FHWA/RD-84/019. Federal Highway Administration. Washington, DC.

Schwartz C. W., Li, R., Kim, S., Ceylan, H., Gopalakrishnan, K. (2013). *Sensitivity Evaluation of MEPDG Performance Prediction*. Research Results Digest 372, National Cooperative Highway

**Expansion of AASHTOWare ME Design Inputs  
Final Report WHRP 0092-20-03**

Research Program (NCHRP), The National Academies of Sciences, Engineering, and Medicine, Washington, D.C.

Tarefder, R. A., Sumeer, N., and Storlie, C. (2014). *Study of MEPDG Sensitivity Using Nonparametric Regression Procedures*. Journal of Computing in Civil Engineering, Vol. 28, No. 1, pp. 134–144.

Thyagarajan, S., Sivaneswaran, N., Muhunthan, B., and Petros, K. (2010). *Statistical Analysis of Critical Input Parameters in Mechanistic Empirical Pavement Design Guide*. Journal of the Association of Asphalt Paving Technologists, Vol. 79, pp. 635-662.

Titi, Hani H.; Elias, Mohammed B.; and Helwany, Sam. (2006). *Determination of Typical Resilient Modulus Values for Selected Soils in Wisconsin*. Wisconsin Highway Research Program, Wisconsin Department of Transportation, WisDOT ID No. 0092-03-11.

Titi, Hani H.; Tabatabai, Habib; Bautista, Emil; Druckrey, Andrew; Faheem, Ahmed; and Tutumluer, Erol (2012). *Base Compaction Specification Feasibility Analysis*. Wisconsin Highway Research Program, Wisconsin Department of Transportation, WisDOT ID No. 0092-11-02.

Tran, N., Robbins, M. M., Rodezno, C., and Timm, D. H. (2017). *Pavement ME Design - Impact of Local Calibration, Foundation Support, and Design and Reliability Thresholds*. National Center for Asphalt Technology (NCAT), Report No. NCAT Report 17-08.

Von Quintus, Harold L., Hyung Lee, and Ramon Bonaquist (2019). *Practitioner's Guide: Part 2—Determining Properties of Resource Responsible Asphalt Mixtures for Use in the Mechanistic Empirical Pavement Design Guide*, Unpublished Report, Federal Highway Administration, Washington, DC.

Von Quintus, Harold, Chuck Schwartz, Ramon Bonaquist, Jagannath Mallela, and Regis Carvalho. (2012). *Calibration of Rutting Models for HMA Structural and Mixture Design*, Report Number 719, National Cooperative Highway Research Program, Transportation Research Board of the National Academies, Washington, DC.

Von Quintus, Harold, Jag Mallela, and Michael I. Darter (2009). *Recommended Practice for Local Calibration of the M-E Pavement Design Guide*, NCHRP Project 1-40B Final Report, National Cooperative Highway Research Program, Transportation Research Board, Washington, DC.

Von Quintus, H.L., J.A. Scherocman, D.S. Hughes, and T.W. Kennedy. (1991). *Asphalt-Aggregate Mixture Analysis System – AAMAS*, NCHRP Report Number 338, National Cooperative Highway Research Program, Transportation Research Board, National Research Council, Washington, DC.

West, R., Rodezno, C., Leiva, F., and Taylor, A. (2018). *Regressing Air Voids for Balanced HMA Mix Design*. Wisconsin Department of Transportation, Report No. WHRP 0092-16-06.

**Expansion of AASHTOWare ME Design Inputs  
Final Report WHRP 0092-20-03**

Williams, C., Robinette, C., Bausano, J., and Breakah., T. (2007). *Testing Wisconsin Asphalt Mixtures for the AASHTO 2002 Mechanistic Design Procedure*. Wisconsin Department of Transportation, Report No. WHRP 07-06.

Yin, H., Chehab, G. R., Stoffels, S. M., Kumar, T., and Premkumar, L. (2010). *Use of Creep Compliance Interconverted from Complex Modulus for Thermal Cracking Prediction Using the M-E Pavement Design Guide*. International Journal of Pavement Engineering, Vol. 11, No. 2, pp. 95–105.

## APPENDIX A—SUMMARY OF WISCONSIN RESEARCH STUDIES FOR ASPHALT MIXTURE PROPERTIES

### A.1 Review of WISDOT Specification Changes

This section of Appendix A presents a summary of the changes made or considered for implementation in the WisDOT asphalt materials specifications since the first calibration and implementation of the PMED software in Wisconsin.

#### *2006 Specifications*

- The minimum VMA for SMA mixtures with 9.5 mm and 12.5 mm nominal maximum aggregate size was increased by 0.5 percent to 16.0 and 17.0, respectively.

#### *2010 Specifications*

- Starting 2010, the use of RAP, RAS, and Fractioned Reclaimed Asphaltic Pavement (FRAP), or their combination as well as the maximum allowable percent binder replacement without changing the asphalt binder grade was specified (see Table 1). It should be noted that the use of up to 35 percent RAP material in lower layers and up to 20 percent in upper layer were specified in earlier specifications.

**Table A61. Maximum allowable binder replacement – 2010 specification.**

<b>Recycled Materials</b>	<b>Lower Layers</b>	<b>Upper Layer</b>
RAS only	20%	15%
RAP only	35%	20%
FRAP only	35%	25%
RAS and RAP	30%	20%
RAS and FRAP	30%	25%
RAS, RAP, and FRAP	30%	25%

#### *2011 Specifications*

- The maximum allowable binder replacement from the use of recycled materials (RAS/RAP/FRAP) without changing the asphalt binder grade was increased (see Table 2).

#### *2013 Specifications*

- Warm mix asphalt (WMA) additives or processes was allowed to be used.
- As part of the QC management, the VMA control and warning limits for JMF were tightened from -1.5 and -1.2 to -0.5 and -0.2, respectively.

**Table A62. Maximum allowable binder replacement – 2011 specification.**

<b>Recycled Materials</b>	<b>Lower Layers</b>	<b>Upper Layer</b>
RAS only	25%	20%
RAP and FRAP	40%	25%
RAS, RAP, and FRAP	35%	25%

*2015 Specifications*

- The minimum VMA for E-3 mixtures (i.e.,  $1 \times 10^6 < \text{ESALs (20 years design life)} < 3 \times 10^6$ ) with 9.5 mm and 12.5 mm nominal maximum aggregate size was increased by 0.5 percent to 14.5 and 15.5, respectively. For such mixtures and nominal size of aggregate, the specified VFA range was also increased to 70 and 76 percent from 65 and 75 percent.
- As part of the QC management, the asphalt content control and warning limits for JMF were tightened from +/-0.4 and +/-0.3 to -0.3 and -0.2, respectively.

*2017 Specifications*

- The Multiple Stress Creep Recovery (MSCR) grading specification in accordance with AASHTO M332, “Standard Specification for Performance-Graded Asphalt Binder Using Multiple Stress Creep Recovery (MSCR) Test” was implemented. As such, the Standard (S), Heavy (H), Very Heavy (V), and Extremely Heavy (E) designation was added to quantify the polymer modification being made and replace the older grade bumping system.
- The mixture design requirement was restructured to account for switching from “E” mixtures to “LT”, “MT”, and “HT” mixtures. Table 3 shows the ESAL range for these mixtures. It should be noted that the mixture requirements (e.g., Va, VFA, etc.) for the “LT”, “MT”, and “HT” mixtures correspond to “E – 0.3”, “E – 3”, and “E – 10”, respectively.
- The Tensile Strength Ratio (TSR) requirement was increased by 5 percent.

**Table A63. Switching from “E” mixtures to “LT”, “MT”, and “HT” mixtures – 2017 specification.**

E Mixtures		LT, MT, and HT Mixtures		
Mixtures	ESALs $\times 10^6$ (20 years Design Life)	Mixtures	ESALs $\times 10^6$ (20 years Design Life)	Mixture Requirements
E – 0.3	ESAL < 0.3	LT	ESAL < 2	Similar to E – 0.3
E – 1	0.3 < ESAL < 1			
E – 3	1 < ESAL < 3	MT	2 < ESAL < 8	Similar to E – 3
E – 10	3 < ESAL < 10			
E – 30	10 < ESAL < 30	HT	ESAL > 8	Similar to E – 10
E – 30x	ESAL > 30			

*2018 Specifications*

- The regressed design, i.e., regress air voids from 4 percent design to 3 percent target in JMF, was implemented. Accordingly, the target JMF asphalt binder content first needs to be determined based on the mixture design data at 3.0 percent air voids and the specified design number of gyration ( $N_{\text{Design}}$ ). Additional asphalt binder is then added to achieve the regressed air void (i.e., 3 percent).
- As part of the QC management, the air voids control and warning limits for JMF were tightened from +/-1.3 and +/-1.0 to +1.3/-1.0 and +1.0/-0.7, respectively.
- As part of the QC management, the minimum required density was increased by 0.5 percent to 93 percent for upper and lower layers at all traffic levels.

*2020 Specifications*

- The ESAL range for “LT”, “MT”, and “HT” mixtures, shown in Table 3, was removed. However, Chapter 14 of the WisDOT Facilities Development Manual – 2019 specifies the traffic level for these mixtures as follows. The only difference is the maximum number of ESALs for “LT” mixtures which is specified as 1 million (it was 2 million in 2019 specification).
  - LT:  $ESAL \leq 1$  million
  - MT:  $1 \text{ million} < ESAL \leq 8$  million
  - HT:  $> 8$  million
- Table 4 shows the summary of pertinent updates were applied to 2020 specification with regard to SMA mixtures.

**Table A64. Updates in SMA mixture design – 2020 specification.**

<b>Requirement</b>	<b>Updates</b>
Percent air voids at $N_{Design}$	Increased by 0.5% to 4.5%
Maximum allowable percent binder replacement	Limited to 15%
Maximum percent passing sieve #200 in aggregate gradation	Dropped by 1% to 11% for SMA No. 4 and by 2% to 12% for SMA No. 5
SMA stabilizer	Required to add a cellulose fiber stabilizing additive
Number of gyration for $N_{ini}$ and $N_{max}$	Dropped from 8 and 160, respectively, to 7 and 100

**A.2 Review of Wisconsin Research Studies**

WisDOT has supported several research studies aiming to characterize the mechanical properties of Wisconsin asphalt mixtures and develop a library or catalog of the asphalt materials inputs that can be integrated into the WisDOT pavement design practice for using the AASHTOWare Pavement ME Design method. This section of Appendix A presents a summary of these efforts.

**A.2.1 WHRP 0092-04-07**

The WHRP 0092-04-07 project was one of the first studies that examined the typical WisDOT asphalt mixtures (Williams, 2007). In this study, dynamic modulus ( $E^*$ ) and flow number ( $F_n$ ) tests were performed to characterize the stiffness and rutting resistance of 21 field sampled asphalt mixture samples. The key factors considered in the experimental matrix were (a) the level of anticipated traffic; (b) the NMAS; and (c) mixture type (dense-graded or SMA).

Table A65 shows the HMAs evaluated in the WHRP 0092-04-07 project. This research study involved an extensive experimental matrix and it was one of the first studies that compared results from the MEPDG (PMED software) and empirical AASHTO 1972 design methods. However, providing a library of material properties for the asphalt mixtures tested was out of the scope for this study. In addition, at the time this project was being conducted, the MEPDG Version 0.8 was readily available and several national research studies with an overall objective of enhancing the characterization of asphalt materials for use in the ME design method were underway or started.



**Expansion of AASHTOWare ME Design Inputs  
Final Report WHRP 0092-20-03**

As such, the results of  $F_n$  and  $E^*$  tests presented in this study are not fully compatible with the current version of the AASHTOWare PMED software and therefore, caution should be exercised if the presented results are intended to be used. The  $F_n$  was based on unconfined tests (PMED requires confined tests) and  $E^*$  was measured over only two temperatures (PMED requires a lower cold temperature than was used).

**Table A65. Experimental matrix in WHRP 0092-04-07 project.**

Mixture type	NMAAS	Traffic Level				
		E – 0.3	E – 1	E – 3	E – 10	E – 30
Dense Graded	19.0 mm	PG 58-28 <sup>R</sup>	PG 58-28 PG 58-34	PG 58-28 <sup>R</sup> PG 58-28 <sup>R</sup> PG 58-28 <sup>R</sup>	PG n/a PG 58-34 <sup>P</sup>	PG 64-28
	12.5 mm	PG 58-28 PG 58-28 <sup>R</sup>	PG 58-28 <sup>R</sup> PG 58-28 <sup>R</sup>	PG 58-28 PG 64-22 <sup>PR</sup> PG 64-34 <sup>PR</sup>	PG 58-34 <sup>P</sup> PG 58-22 PG 64-28 <sup>PR</sup>	No mixture
SMA	25.0 mm	No mixture	No mixture	PG 58-28 <sup>R</sup>	No mixture	No mixture
	12.5 mm	No mixture	No mixture	No mixture	PG 70-22	No mixture

<sup>R</sup>: with RAP; <sup>P</sup>: Polymer modified; n/a: not specified

**A.2.2 WHRP 0092-08-06**

The dynamic  $E^*$  and  $F_n$  data for 12 asphalt mixtures representing typical and good performing WisDOT mixtures were measured using the Asphalt Mixture Performance Tester (AMPT) and associated analysis procedures in the WHRP 0092-08-06 research project (Bonaquist, 2010). As shown in Table A66, the experimental matrix involves four different sources of aggregate, two design traffic levels, and two binder grades.

The objectives of this research project were to compare the mechanical properties of these mixtures with the performance of pavements built with similar mixtures and determine the sensitivity of the AMPT tests to the key mixture design factors including design traffic level, aggregate angularity, VMA, and binder grade. Most importantly, the resulting database of  $E^*$  has served as a library of material properties for the implementation of the mechanistic approaches for pavement structural design and asphalt mixture design by WisDOT.

**Table A66. Experimental matrix in WHRP 0092-08-06 project.**

Aggregate Source	NMAAS	Traffic Level		
		E – 3	E – 10	E – 10
Cisler	12.5 mm	PG 58-28	PG 58-28	PG 70-28*
Christian/Gade	12.5 mm			
Glenmore	19.0 mm			
Wimmie	12.5 mm			

\*Modified Binder

An example of the  $E^*$  master curve for the asphalt mixtures tested in this study is shown in Figure A28. It was reported that for a given aggregate source, mixtures with different design traffic level

**Expansion of AASHTOWare ME Design Inputs  
Final Report WHRP 0092-20-03**

(i.e., E – 3 and E – 10) and binder grade (i.e., PG 58-28 and modified PG70-28) represent similar dynamic modulus master curve, while the  $E^*$  master curve differs from one aggregate source to another. On the other hand, as depicted in Figure A29, the binder grade had a significant effect on the rutting resistance of the evaluated mixtures. The flow number was increased by a factor of 6 to 20 as the binder grade was bumped from PG 58-28 to PG 70-28.

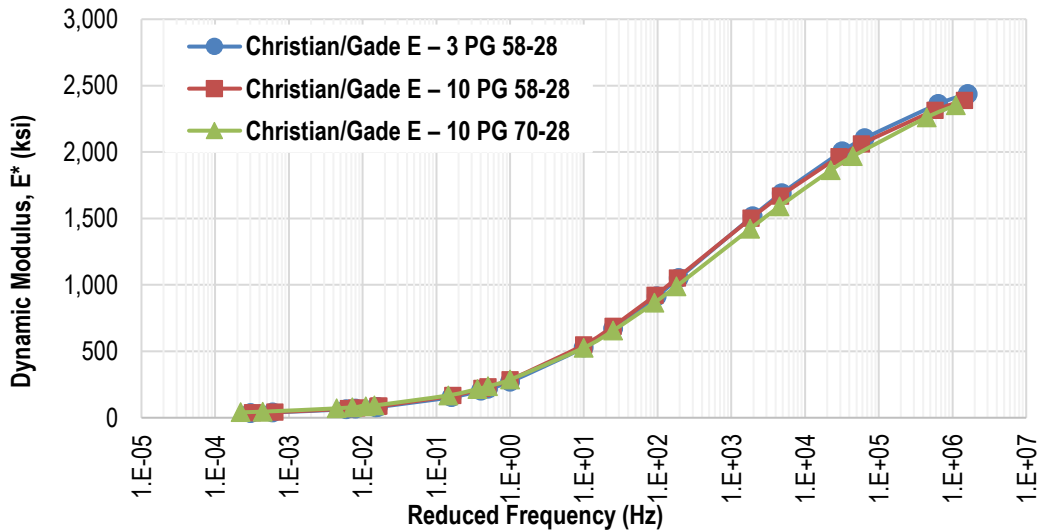


**Figure A28. Dynamic modulus master curves for the Christian/Gade mixtures in WHRP 0092-08-06 project.**

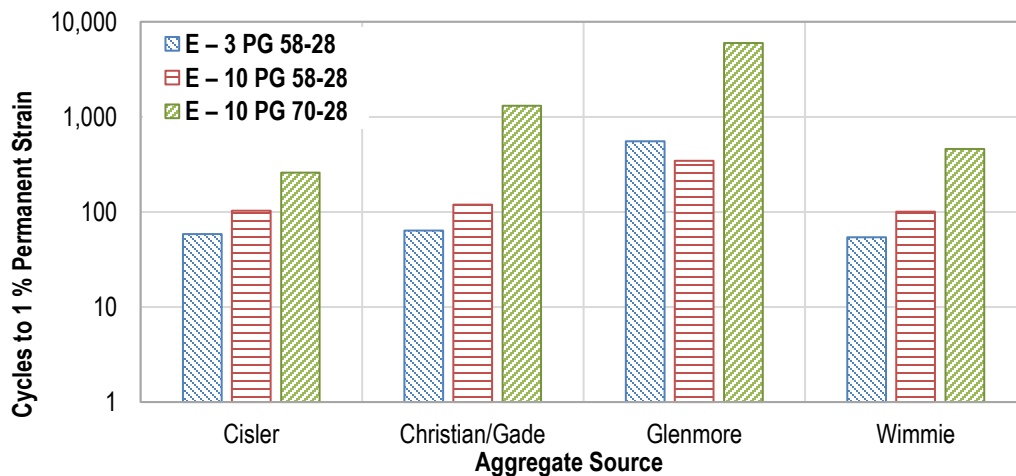


**Figure A29. Cycles to 1 percent permanent strain in the confined Flow Number tests in WHRP 0092-08-06 project.**

**A.2.3 WHRP 0092-10-06**

The WHRP 0092-10-06 reviewed the practices for using RAP/RAS in asphalt mixtures and evaluated the properties of recycled asphalt binders from Wisconsin sources (Bonaquist, 2011). To effectively use RAP/RAS in asphalt mixtures without jeopardizing acceptable performance at low temperatures, the properties of the blended binder in the mixture were evaluated by constructing blending charts for recycled materials commonly used in Wisconsin.

A recommended procedure for blending chart analysis for mixtures with multiple recycled binders was presented. This study also assessed the WisDOT 2011 standard specifications criteria for binder replacement and evaluated the potential effects of using RAP and RAS on pavement service life. The recommended binder replacement is listed in Table A67. It has been argued that these recommended criteria remove the difference between the reliability of mixtures with RAP and mixtures with RAS. It should be noted that these criteria have not been fully implemented in the current WisDOT Standard Specifications (see Table 2).

**Table A67. Recommended binder replacement criteria in WHRP 0092-10-06.**

Recycled Binder Type	Maximum Binder Replacement	
	Lower Layers	Upper Layer
RAP and FRAP	45%	20%
RAS	20%	5%
Combination of RAP and RAS	Reduce RAP binder replacement 2.25 % for each 1 % RAS binder replacement.	Reduce RAP binder replacement 4 % for each 1 % RAS binder replacement.

#### **A.2.4 WHRP 0092-10-07**

In another research study, WHRP 0092-10-07, low temperature creep compliance and tensile strength properties of 16 WisDOT mixtures, including the mixtures examined in WHRP 0092-08-06, were measured (Bonaquist, 2011). Creep compliance is an important mixture property as related to transverse cracking. An objective of these two studies (i.e., WHRP 0092-08-06 and WHRP 0092-10-07) was to establish a range of mechanical properties for representative WisDOT asphalt mixtures and provide WisDOT with a complete level 1 library of asphalt mixtures being used in the practice for the implementation of the AASHTOWare PMED method. This library is currently being used in the WisDOT PMED design practice.

Table A68 represents the experimental matrix in the WHRP 0092-10-07 project in which the mixtures were produced using four binder grades: PG58-28 without and with 25 percent RAP binder, PG58-34 without and with 25 percent RAP binder. As noted earlier, the WisDOT Standard Specifications specifies 25 percent as the maximum allowable percent binder replacement without changing the asphalt binder grade. It should be mentioned that the mixtures with RAP binder were prepared by extracting and recovering RAP binder and then replacing 25 percent of the binder in each mixture with the recovered RAP binder.

It was found that, for the mixtures evaluated in WHRP 0092-10-07 project, the low temperature creep compliance was only a function of the low temperature performance grade of the binder in the mixture meaning that it is not sensitive to the changes in aggregate source and the design traffic level. On the other hand, the tensile strength at -10°C (14°F) is not a function of these mixture design factors (i.e., binder grade, aggregate source, and design traffic level) and the average value of 430 psi was determined for the mixtures examined in this study.

**Table A68. Experimental matrix in WHRP 0092-10-07 project.**

Aggregate Source	NMAS	Traffic Level	
		E – 3	E – 10
Cisler	12.5 mm	PG 58-34	PG 58-28
Christian/Gade	12.5 mm	PG 58-28	PG 58-34
Glenmore	19.0 mm	PG 58-34	PG 58-28
Wimmie	12.5 mm	PG 58-28	PG 58-34

Note: All the mixtures were produced without and with 25 percent rap binder.

Figure A30 shows the creep compliance master curves averaged over all mixtures for each binder. As expected, the mixtures produced with PG58-34 (i.e., the softest binder) represent the highest thermal cracking resistance, while adding RAP binder made the compliance master curve flatter (i.e., increase in the induced thermal stress). The ranking based on the creep compliance test results was in agreement with the continuous binder grade results presented in Figure A30. For the mixtures tested, adding approximately 25 percent RAP binder to the PG58-34 binder resulted in the mixtures with similar compliance as mixtures with PG58-28 binder.

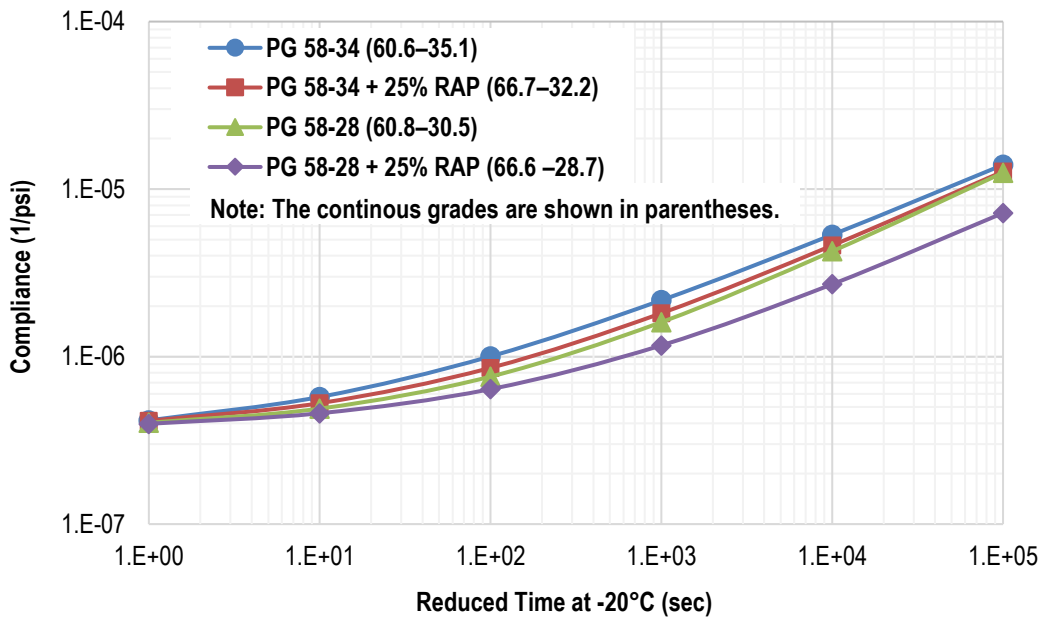


**Figure A30. Averaged creep compliance master curves in WHRP 0092-10-07 project.**

In this study, a predictive equation was developed to estimate the creep compliance of typical WisDOT mixtures. This equation, which is expressed below, is a function of the low temperature continuous grade of the asphalt binder and it estimates the compliance values at -20°C (-4°F) (i.e., reference temperature). The authors noted that this equation is applicable for the low temperature grades between -35.1°C (-31.2°F) and -28.7°C (-19.7°F) and therefore, it should be used with caution for a binder with low temperature grade outside this range.

$$D(t) = 3.729 \times 10^{-7} + 10^{-9.3552 - 0.0645 \times PG_{Low}} \left( \frac{t}{10^{0.0655(T+4)}} \right)^{0.4705}$$

Where:  $D(t)$  is the creep compliance (1/psi);  $T$  is the temperature (°F);  $PG_{Low}$  is the low temperature continuous grade of the asphalt binder (°C);  $t$  is the time.

### **A.2.5 WHRP 0092-09-01**

The use of the unconfined flow number test in the asphalt mixture design and acceptance was further evaluated in the WHRP 0092-09-01 (Bonaquist, 2012). The effect of changes in mixture composition on the flow number was investigated and flow number criteria for WisDOT asphalt mixtures were developed.

Bonaquist reported that the binder grade is a critical factor in mixture design. Hence, polymer modified binders were recommended to achieve adequate rutting resistance for the design traffic levels of E – 10 and higher. An increase in binder content, percent passing the sieve 200, VMA and air voids within the acceptable WisDOT warning limits resulted in the reduction of rutting resistance to approximately 30 percent of the design value.

Based on the findings from this study, tentative rutting resistance criteria for the flow number test were proposed. The flow number test was recommended to be conducted on the mixtures with the asphalt content corresponding to the WisDOT high production warning limit (+0.3 percent). These criteria, which are shown in Table A69, however, have not been implemented in the WisDOT Standard Specifications.

**Table A69. Recommended criteria for the Flow Number test in WHRP 0092-09-01 project.**

Design Traffic Level, MESAL	Normal Traffic Speed ( $\geq 40$ mph)		Slow Traffic Speed (20 mph)	
	2 hr. Conditioning at Compaction Temperature	4 hr. Conditioning at 135 °C	2 hr. Conditioning at Compaction Temperature	4 hr. Conditioning at 135 °C
1	5	5	10	10
3	10	15	20	30
10	20	45	40	90
30	45	135	90	270
30x	105	420	210	840

### **A.2.6 WHRP 0092-13-02**

In order to establish specification criteria applicable to modified binder being used in the production of Wisconsin asphalt mixtures, a research study entitled “Field Validation of Wisconsin Modified Binder Selection Guidelines” was carried out in two phases (Delgadillo et al., 2007; Bahia et al., 2013). Asphalt binder and mixture test results were compared to field performances between 2004 and 2012. The performance of the surveyed field sections included rutting, fatigue damage, and thermal cracking distress.

The MSCR test, the Linear Amplitude Sweep (LAS) test, and the Single Edged notched Bending procedure (BBR-SENB) test were utilized for the characterization of the asphalt binders at high, intermediate, and low service temperatures, respectively. Based on the results of laboratory testing

along with comparative studies to the measured field performance, suggestions for consideration of modifications to the current WisDOT binder selection criteria were made. Except for the MSCR criteria which were implemented in the 2017 WisDOT Standard Specifications, the other test methods and criteria have not been implemented by the state of Wisconsin.

#### **A.2.7 WHRP 0092-12-02**

To develop recommended specifications for asphalt concrete that cover all types of mixtures (i.e., HMA, WMA, SMA, mixtures with high RAP/RAS content) in WisDOT Standard Specifications, the WHRP 0092-12-02 project was performed and two specifications were developed (Bonaquist et al., 2014). One draft specification includes performance tests related to rutting resistance and thermal cracking resistance for mixture design and acceptance. The other uses a performance test for rutting resistance during design and the binder replacement criteria developed in WHRP Project 0092-10-06 to control thermal cracking. It has been mentioned that the draft specifications developed in this study need additional validation work before either specification can be considered for implementation. Accordingly, the outcome of this research study has been yet implemented in WisDOT Standard Specifications.

#### **A.2.8 WHRP 0092-14-20**

To validate the findings and recommendations of the previous research works on the proposed asphalt binder specification, laboratory test results and field survey performance data were collected and analyzed (Bahia et al., 2016). With respect to high temperature performance, an attempt was made to correlate the MSCR parameters to high temperature mixture performance using the Flow Number test.

The measured MSCR non-recoverable creep compliance ( $J_{nr}$ ) at 3.2 kPa and percent recovery (%R) in comparison with the mixture flow number at equivalent temperatures are shown in Figure A31 and Figure A32, respectively. It was concluded that “*if states wish to implement a performance based specification, it appears the  $J_{nr}$  value is the most important, and the %R is included to force the use of elastomeric modification (which may or may not directly benefit performance).*” As noted earlier, WisDOT currently uses the MSCR grading specification in accordance with “AASHTO M332 Standard Specification for Performance-Graded Asphalt Binder Using Multiple Stress Creep Recovery (MSCR) Test”. Chapter 14 of the WisDOT Facilities Development Manual – 2019 demonstrates the changes from the former grade bumping system to MSCR protocol as represented in Table A70.

#### **A.2.9 WHRP 0092-15-04**

The use of performance-related properties of asphalt mixtures as a supplement to the Superpave volumetric mixture design and the implementation of asphalt pavement performance-based specifications were evaluated in the WHRP 0092-15-04 project (Bahia et al., 2016). It was concluded that aggregate source, design traffic level, and binder grade are the key components of the mixture design, and therefore their impact on the mechanical performance of the evaluated mixtures (i.e., dynamic modulus and Flow Number) was found to be significant. It was also reported that “*A database for all  $E^*$  testing has been developed and is available to WisDOT in*

electronic format as part of this final report.” Further evaluation for the adoption and use of this database will be conducted if it becomes available to the research team.

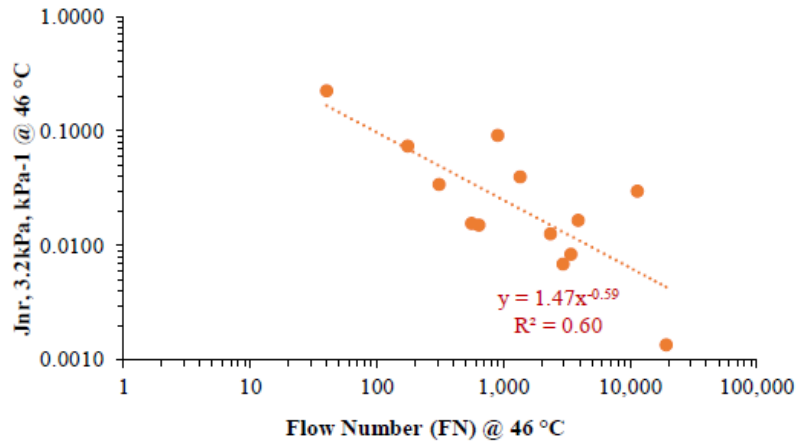


Figure A31. Flow Number in comparison with MSCR Jnr at 3.2 kPa in WHRP 0092-14-20 project (Bahia et al., 2016).

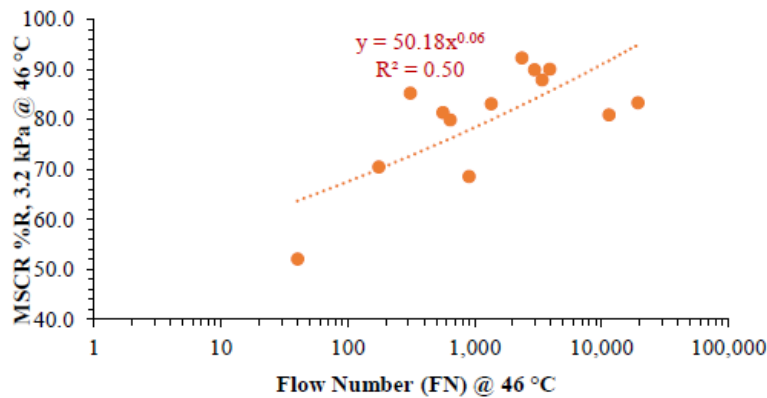


Figure A32. Flow Number in comparison with MSCR %R in WHRP 0092-14-20 project (Bahia et al., 2016).

Table A70. Suggested translation from PG to MSCR Binder grade in WisDOT Facilities Development Manual – 2019.

Previously Selected PG Grade	Suggested MSCR Binder
58-34	58-34 S
58-34 P	58-34 H
64-34 P	58-34 V
58-28	58-28 S
64-28 P	58-28 H
70-28 P	58-28 V

S: Standard Designation – ESAL ≤ 8 million.

H: Heavy Designation – 8 million < ESAL ≤ 30 million or slower moving traffic at design speeds between 15 to 45 mph.

V: Very Heavy – ESAL > 30 million ESALs or traffic moving slower than 15 mph.

E: Extremely Heavy – ESAL > 30 million and standing traffic.

### **A.2.10 WHRP 0092-16-06**

The impact of the air voids regression approach (regressed mixture design) on cracking, rutting, and moisture damage resistance of asphalt mixtures for a total of six mixes designed for low, medium, and high traffic levels with various contents of RAP and RAS was evaluated in WHRP 0092-16-06 (West et al., 2018). Mixture performance tests included the Illinois Flexibility Index Test to evaluate intermediate temperature cracking resistance, the Disc-Shaped Compacted Tension for low-temperature cracking resistance, and the Hamburg Wheel Tracking Test for rutting and moisture resistance. It was concluded that results from this project indicate that the regressed air voids approach can improve cracking resistance without compromising the deformation resistance of asphalt mixes.

### **A.3 Appendix A References**

Bahia et al. (2016). *Analysis and Feasibility of Asphalt Pavement Performance-Based Specifications for WisDOT*. Wisconsin Department of Transportation, Report No. 0092-15-04.

Bahia, H., Lyngdal, E., Varma, R., Sweirtz, D., and Teymourpour, P. (2016). *Modified Binder (PG+) Specifications and Quality Control Criteria*. Wisconsin Department of Transportation, Draft Final Report.

Bahia, H., Tabatabaee, H., and Mandal, T. (2013). *Field Validation of Wisconsin Modified Binder Selection Guidelines - Phase II*. Wisconsin Department of Transportation.

Bonaquist, R. (2010). *Wisconsin Mixture Characterization Using the Asphalt Mixture Performance Tester (AMPT) on Historical Aggregate Structures*. Wisconsin Department of Transportation, Report No. WHRP 09-03.

Bonaquist, R. (2011). *Characterization of Wisconsin Mixture Low Temperature Properties for the AASHTO Mechanistic-Empirical Pavement Design Guide*. Wisconsin Department of Transportation, Report No. WHRP 11-12.

Bonaquist, R. (2011). *Effect of Recovered Binders from Recycled Shingles and Increased RAP Percentages on Resultant Binder PG*. Wisconsin Department of Transportation, Report No. WHRP 11-13.

Bonaquist, R. (2012). *Evaluation of Flow Number (Fn) as a Discriminating HMA Mixture Property*. Wisconsin Department of Transportation, Report No. WHRP 12-01.

Bonaquist, R., Cuciniello, G., Hanz, A., and Bahia, H. (2014). *Development of Guidelines and Specifications for Use of WMA Technology in Delivering HMA Products Inclusive of Non-Conventional Mixtures Such as SMA's, and Mixtures with High RAP and RAS Content*. Wisconsin Department of Transportation, Report No. WHRP 0092-12-02.

Delgadillo, R., Motamed, A., and Bahia, H. (2007). *Field Validation of Wisconsin Modified Binder Selection Guidelines*. Wisconsin Department of Transportation.

West, R., Rodezno, C., Leiva, F., and Taylor, A. (2018). *Regressing Air Voids for Balanced HMA Mix Design*. Wisconsin Department of Transportation, Report No. WHRP 0092-16-06.



**Expansion of AASHTOWare ME Design Inputs  
Final Report WHRP 0092-20-03**

Williams, C., Robinette, C., Bausano, J., and Breakah., T. (2007). *Testing Wisconsin Asphalt Mixtures for the AASHTO 2002 Mechanistic Design Procedure*. Wisconsin Department of Transportation, Report No. WHRP 07-06.

## APPENDIX B—SUMMARY OF ASPHALT MIXTURE LIBRARIES: OTHER STATE DOTS

Appendix B provides a summary of the previous and ongoing efforts of select SHAs for developing a catalog of asphalt material design inputs for the implementation of the ME design method using the PMED software. The focus was primarily given to mid-western states, as well as the states in the Wet-Freeze climatic zone defined by the LTPP program.

### B.1 Agency Libraries for Asphalt Mixtures

SHAs who have their own Mechanistic-Empirical (ME) based design method (e.g., Illinois, Minnesota, Kentucky, California, and Texas) were not considered in this literature review. Some of the SHAs that have their own ME-based design method, however, are now even sponsoring implementation/calibration projects regarding the use of the PMED software (e.g., Illinois, Kentucky, and Texas). In addition, it should be noted that several SHAs (e.g., Nebraska, Georgia, etc.) are in the process of updating and/or developing their PMED materials library. Some of these are included in the summaries that follow.

#### *B.1.1 Pennsylvania Department of Transportation (PENNDOT)*

The Pennsylvania Department of Transportation (PENNDOT) made a decision to look into implementing the PMED software back in 2012 and adopted the PMED software in 2019. As part of PENNDOT's implementation process, different studies were sponsored to develop input libraries to assist PENNDOT staff and consultants in using the software, as well as in standardizing some of the inputs. Most of the initial effort was focused on creating the traffic and materials libraries.

Regarding the materials libraries, asphalt mixtures, Portland cement concrete (PCC) mixtures, aggregate base, and soils were tested to create the materials library across the materials and mixtures typically used or encountered in Pennsylvania. The asphalt mixture library currently includes 25 asphalt mixtures ranging from dense-graded neat asphalt base mixtures to SMA surface mixtures. The asphalt binders typically used across Pennsylvania were also tested and included in the asphalt materials library. Table B71 includes the asphalt mixtures organized by selected mixture factors that PENNDOT considers in selecting a specific asphalt mixture for a design project (Brink, et al., 2020).

The asphalt mixture tests that PENNDOT sponsored included: dynamic modulus in accordance with AASHTO T342, repeated load plastic deformation in accordance with a modified version of AASHTO T378 (or the NCHRP Report 917 procedure), indirect tensile creep compliance and indirect tensile strength in accordance with AASHTO T322, and the indirect tensile strength/failure tensile strain in accordance with a modified version of ASTM D6931 for estimating the fatigue strength. The individual dynamic modulus data are included for all of the asphalt mixtures, but the other asphalt mixture properties (fatigue strength coefficients, plastic deformation coefficients, and creep-compliance) are clustered for similar mixtures, as shown by Figure B33 through Figure B35. Other agencies have implemented this clustering process for both

**Expansion of AASHTOWare ME Design Inputs  
Final Report WHRP 0092-20-03**

their traffic and materials libraries. The clustering of asphalt mixtures with similar properties was investigated or used in evaluating the WisDOT asphalt material test results.

**Table B71. PENNDOT's Asphalt Mixture Library.**

Nominal Maximum Aggregate Size	ESAL Range	NDesign, Number of Gyration	Binder Type/Layer Type						
			PG 64-22			PG 76-22		PG 58-28	
			Wearing Surface	Binder Layer	Base Layer	Wearing Surface	Binder Layer	Binder Layer	
9.5 mm	< 0.3M	50							
		75							
		100							
	0.3M to 3M	50							
		65	Mix 9, WMA						
		75	Mix 1, HMA; Mix 8, HMA; Mix 19, HMA						
		100							
	3M to 30M	50							
		75							
		100	Mix 10, WMA			Mix 20, HMA; Mix 21, WMA; Mix 22, WMA; Mix 23, WMA; Mix 24, SMA			
	> 30M	50							
		75							
		100				Mix 25, SMA			
	12.5 mm	< 0.3M	50						
			75						
100									
0.3M to 3M		50							
		75							
		100							
3M to 30M		50							
		75							
		100				Mix 2, HMA; Mix 5, HMA			
> 30M		50							
		75							
		100							

**Table B71. PENNDOT's Asphalt Mixture Library (continued).**

Nominal Maximum Aggregate Size	ESAL Range	NDesign, Number of Gyration	Binder Type/Layer Type					
			PG 64-22			PG 76-22		PG 58-28
			Wearing Surface	Binder Layer	Base Layer	Wearing Surface	Binder Layer	Binder Layer
19 mm	< 0.3M	50		Mix 13, HMA				
		75						
		100						
	0.3M to 3M	50						
		75		Mix 3, HMA; Mix 14, HMA; Mix 18, WMA				
		100						
	3M to 30M	50						
		75						
		100					Mix 4, HMA; Mix 15, HMA	
	> 30M	50						
		75						
		100						
25 mm	< 0.3M	50			Mix 17, HMA			
		75						
		100						
	0.3M to 3M	50						
		75			Mix 6, WMA; Mix 12, HMA			Mix 16, HMA
		100			Mix 7, HMA; Mix 11, HMA			
	3M to 30M	50						
		75						
		100						
	> 30M	50						
		75						
		100						
NOTE: The shaded cells in this table represent the combination of asphalt mixture designation factors that are typically not used in Pennsylvania.								

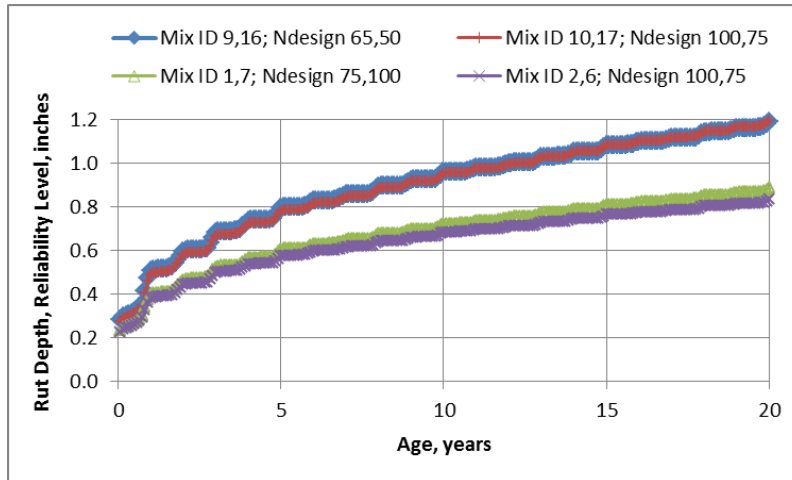


Figure B33. Clustering of the PENNDOT asphalt mixtures that result in similar rut depth predictions.

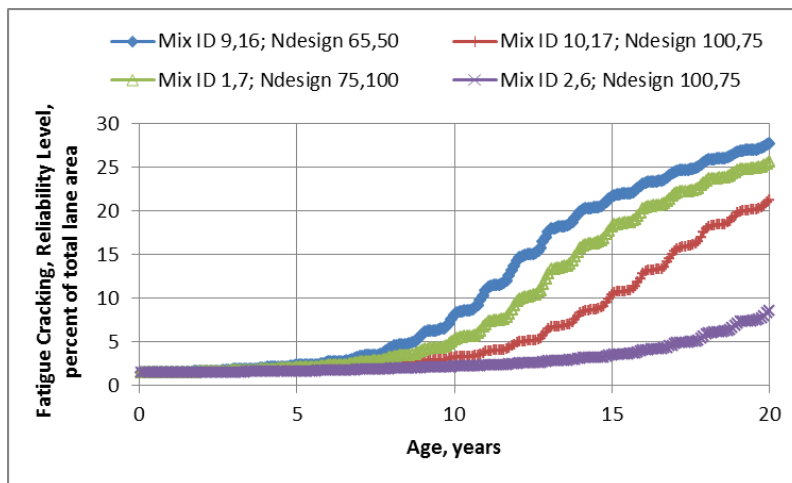


Figure B34. Clustering of the PENNDOT asphalt mixtures that result in similar bottom-up alligator cracking predictions.

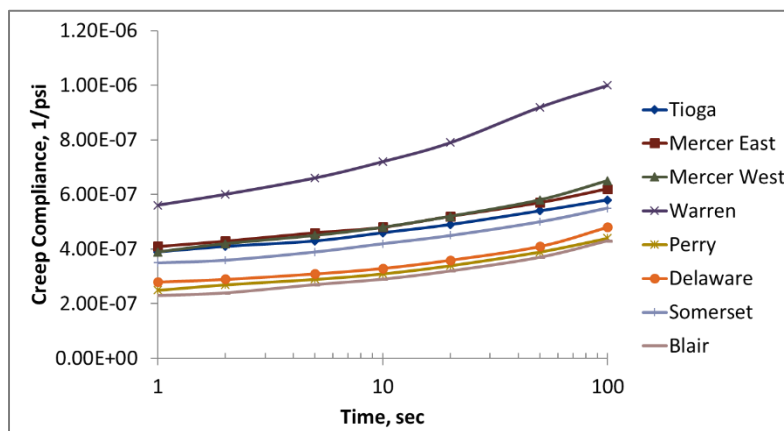


Figure B35. Clustering of the PENNDOT asphalt mixtures that result in similar transverse cracking predictions.

### ***B.1.2 Federal Highway Administration (FHWA)***

The Federal Highway Administration (FHWA) sponsored a study in 2017 to develop a Practitioners Guide for deriving the properties of non-typical asphalt mixtures for use in the PMED software. The non-typical asphalt mixtures were defined as Resource Responsible Asphalt Mixtures (R<sup>2</sup>AMs). The Practitioners Guide was grouped into two parts: one for conducting the tests and the other for interpreting the results from the tests to derive the performance property inputs to the PMED software (Bonaquist, 2019; Von Quintus, et al., 2019).

The tests included in the Practitioners Guide included: dynamic modulus in accordance with AASHTO T 342, repeated load plastic deformation in accordance with a modified version of AASHTO T 378 (or the NCHRP Report 917 procedure), fatigue strength in accordance with AASHTO T 321, and indirect tensile creep compliance and indirect tensile strength in accordance with AASHTO T 322.

A total of 9 R<sup>2</sup>AMs were tested, and typical mixture properties that represent the laboratory-derived coefficients for fatigue strength, plastic strain, and creep compliance were provided or included in the report. Some of the results from the fatigue strength and creep compliance tests were found to be significantly different than for typical dense-graded neat asphalt mixtures. Figure B36 graphically shows some of the differences in the fatigue strength coefficients. These results were used in providing a recommendation to WisDOT in the use of R<sup>2</sup>AMs in Wisconsin.

### ***B.1.3 Nebraska Department of Roads (NDOR)***

The Nebraska Department of Roads (NDOR) is in the process of implementing and calibrating the PMED software and is planning to use the software for pavement design in 2021. As part of NDOR's calibration process, input libraries are being developed similar to PENNDOT. The difference between the PENNDOT and NDOR implementation is NDOR conducted forensic investigations of the sites included within the calibration, while PENNDOT did not sponsor any forensic investigations.

Multiple asphalt mixtures were sampled by NDOR and tested to create input libraries to assist NDOR staff in using the software, as well as in standardizing some of the inputs. The asphalt mixture library include 15 asphalt mixtures ranging from dense-graded neat asphalt base mixtures with high percentages of RAP to dense-graded polymer modified asphalt (PMA) surface mixtures with high RAP contents (ARA, 2021). The asphalt mixture tests that NDOR sponsored includes: dynamic modulus in accordance with AASHTO T342, repeated load plastic deformation in accordance with a modified version of AASHTO T378 (or the NCHRP Report 917 procedure), indirect tensile creep compliance and indirect tensile strength in accordance with AASHTO T322, and the indirect tensile strength/failure tensile strain in accordance with a modified version of ASTM D6931 for estimating the fatigue strength.

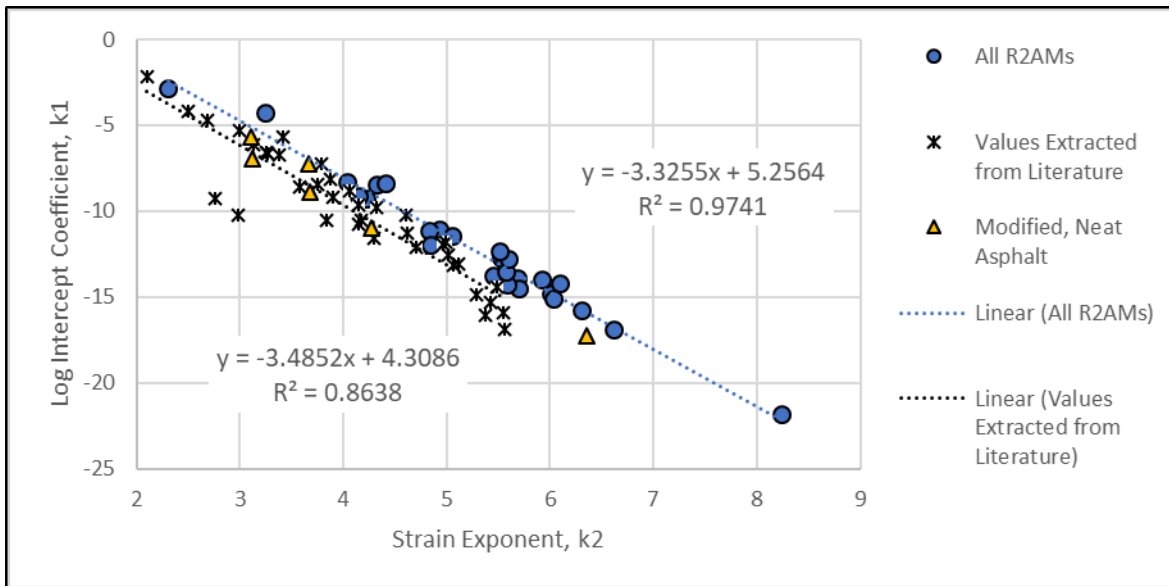


**Figure B36. Comparison of the strain exponent and intercept for the R<sup>2</sup>AMs and neat, virgin asphalt mixtures.**

#### ***B.1.4 Michigan Department of Transportation (MDOT)***

As part of the Michigan Department of Transportation (MDOT) plans for implementation of the AASHTOWare PMED software, a comprehensive research project namely “Preparation for Implementation of the Mechanistic-Empirical Pavement Design Guide in Michigan” was completed in 2013. This research study had three distinct parts: (1) characterization of asphalt mixtures for the PMED in Michigan, (2) evaluation of the PMED for pavement rehabilitation design in Michigan, and (3) calibration and validation of the PMED performance models for Michigan conditions.

In order to address the need for generating a catalog or library of the PMED inputs for typical asphalt mixtures produced in the state of Michigan, Part 1 of this research involved laboratory characterization of commonly-used asphalt mixtures and binders by MDOT (Kutay and Jamrah, 2013). The experimental program included 64 unique asphalt mixtures and 44 unique binders and the following laboratory tests:

- Asphalt mixture dynamic modulus ( $E^*$ ) master curve
- Asphalt binder complex shear modulus ( $G^*$ ) master curve
- Asphalt mixture indirect tensile strength ( $IDT$ ) at  $-10^{\circ}\text{C}$  ( $14^{\circ}\text{F}$ )
- Asphalt mixture creep compliance ( $D(t)$ ) master curve

In addition to the laboratory testing tasks, the modified Witczak equation, as well as the ANNACAP software for prediction of  $E^*$ , were evaluated for the MDOT mixtures. The calibrated Witczak model performed well in comparison with the measured data of MDOT mixtures, while the predicted  $E^*$  using the ANNACAP software did not. As such, a new ANN-based model was developed. This study resulted in the development of a software package, called DYNAMOD, which serves as the level 1 database of the typical MDOT asphalt mixture. In accordance with the

definition of the hierarchal input levels, the use of the DYNAMOND software is input level 2. The software also generates input files that can be imported directly into the PMED software (Michigan Department of Transportation, 2017).

### ***B.1.5 Missouri Department of Transportation (MoDOT)***

The Missouri Department of Transportation (MoDOT) began implementation of the PMED software in 2004 by preparing a Road Map (Mallela et al., 2009). The objective of this Road Map was to identify the steps and activities needed to locally calibrate the distress prediction models. Another objective of the Road Map was to streamline a design process for MoDOT and its consultants using the PMED software. The broad scope of work for this project included:

1. Developing default data libraries for PMED software inputs of relevance to Missouri.
2. Verifying, validating, and if needed recalibrating relevant performance prediction models for use in Missouri.
3. Developing recommendations for MEPDG implementation in Missouri.

The MoDOT objectives for developing and performing the laboratory testing program in support of the PMED software were reported as follows:

- Develop a set of default material property values that can be used in the flexible pavement design process for the level 1 inputs for asphalt mixtures.
- Determine the effect of air voids on the dynamic modulus, permanent deformation coefficients, and indirect tensile strength and failure strain over a range of mixtures used in Missouri.
- Confirm the dynamic modulus regression equation included in the PMED software for conventional and specialty (polymer modified asphalt or SMA) mixtures.
- Provide asphalt material property data to improve on the local calibration process and reduce the standard error of the predicted distresses.

To achieve these objectives, the following laboratory tests were performed to determine the required inputs for typical MoDOT mixtures.

- Asphalt mixture dynamic modulus ( $E^*$ ) master curve
- Compressive repeated load permanent deformation (RLPD)
- Indirect tensile strength ( $IDT$ ), failure strain, and creep compliance ( $D(t)$ )

Nine different mixture types and three air void levels (4, 6.5, and 9) were included in the laboratory test program for the  $E^*$  and RLPD experimental plan. The IDT creep compliance and strength test plan included six different mixtures. It was reported that the Witczak  $E^*$  prediction equation provides reasonable estimates for the asphalt mixes included in the test plan. However, there was a significant difference between the measured (input level 1) and predicted (input level 3) of  $D(t)$  master curves for MoDOT mixtures.

It should be noted that MoDOT sponsored a second PMED local calibration which is ongoing. This second calibration effort focused on pavement rehabilitation models. In addition, the



materials database library is being updated with contemporary pavement materials properties, including reclaimed materials or R<sup>2</sup>Ms.

### ***B.1.6 Indiana Department of Transportation (INDOT)***

Starting in 2004, the Indiana Department of Transportation (INDOT) moved toward the implementation of the PMED software and it was implemented as a primary pavement design tool in 2009 (Nantung et al. 2005). The INDOT plan was to generate a database for dynamic modulus, creep compliance, and indirect tensile strength of common Indiana asphalt mixtures. The representative samples from the asphalt contractors were collected to determine these input parameters.

According to the Indiana Design Manual 2013, the PMED method shall be used for the design of each pavement structure (Indiana Department of Transportation, 2013). This manual also mentions that the INDOT's Division of Pavement maintains input files associated with material properties that are available to an INDOT designer as well as a pavement designer outside of INDOT on the INDOT's Office of Pavement Engineering website. The INDOT database of asphalt materials consists of a hybrid level 1 and level 3 design inputs for the common INDOT mixtures which provide the following input data:

- Asphalt mixture dynamic modulus ( $E^*$ ) master curve
- Superpave asphalt binder test data (complex shear modulus ( $G^*$ ) and phase angle ( $\delta$ ))
- Asphalt mixture general inputs (aggregate gradation, effective binder content, air voids, etc.)

Input level 3 default asphalt properties are used for the fatigue strength coefficients, plastic strain coefficients, and IDT creep compliance and strength values.

### ***B.1.7 Ohio Department of Transportation (ODOT)***

The Ohio Department of Transportation (ODOT) began evaluating the feasibility of using the PMED software in a project called "Guidelines for Implementing NCHRP 1-37A ME Design Procedures in Ohio." The objective of the project was to develop guidelines for implementing the PMED software by accomplishing the following tasks (Mallela et al. 2009):

- Assess the ODOT's needs in terms of new and rehabilitation designs, laboratory and field testing equipment, and traffic data collection and processing.
- Default values (means and ranges) for those inputs that have adequate data from previous research applicable to Ohio conditions.
- Identify the gap for local calibration using a more extensive database assembled from projects located throughout the state

At the time this study was being conducted, several publications had explored various aspects of using the PMED software in Ohio. These studies collectively provided information that was key to the smooth and successful development of PMED input libraries. This information was used to build a library of level 2 and level 3 asphalt mixture inputs. This library consisted of predictive equations for  $E^*$  and Poisson's Ratio as well as measured Superpave binder test data (complex

shear modulus ( $G^*$ ) and phase angle ( $\delta$ )). It was reported that the available data were tested on temperature ranges outside the ranges required for  $D(t)$  and  $IDT$ , and therefore the default Level 3 values were adopted.

### ***B.1.8 Virginia Department of Transportation (VDOT)***

The Virginia Department of Transportation (VDOT) currently uses the PMED software for projects consisting of new construction, new alignment, pavement widening (lane addition) and reconstruction on Interstates and primary arterials. One of the first VDOT research studies on the transition to ME pavement design methods with the emphasis on the influence of asphalt material input properties was completed in 2006. A catalog (level 1 and level 3) of asphalt mixture properties including dynamic modulus, creep compliance, and indirect tensile strength, along with the associated asphalt binder properties was compiled. Loose samples for 11 mixes (3 surface, 4 intermediate, and 4 base mixes) were collected from different plants across the state of Virginia (Flintsch et al., 2006).

Based on the results of this laboratory study using the limited number of mixtures and only one binder grade (only PG 64-22), it was concluded that “*VDOT’s Materials Division should consider implementing the ME pavement design method using Level 3 asphalt material inputs. However, local calibration of the predictive models and further evaluation using additional mixtures and binders may significantly impact (or reverse) this recommendation.*” As such, it was recommended that the level 1 asphalt mixture and binder test data need to be collected to populate a more comprehensive catalog of asphalt mixture properties and validate the pavement performance prediction trends seen from the level 3 analysis (Diefenderfer, 2010).

### ***B.1.9 Kansas Department of Transportation (KDOT)***

The Kansas Department of Transportation (KDOT) started evaluating the PMED software in the early 2000s. The first research study sponsored by KDOT involved two parts for flexible and rigid pavements. The objectives of the project with respect to flexible pavement design were (Romanoschi and Bethu, 2009):

- Assist the implementation of the ME design guide in Kansas by building a library of material and traffic inputs.
- Build a database of dynamic modulus and creep compliance and tensile strength at low temperature for the asphalt mixes typically used in Kansas.
- Evaluate the prediction models incorporated in the PMED software.

The dynamic modulus, creep compliance, and tensile strength were measured on eight asphalt mixtures that were representative of those produced in Kansas. The volumetric properties of these mixes as well as the Superpave asphalt binder test data were also measured. It was recommended that the database of the asphalt binder measurements must be constantly updated for new binders. It was also recommended that the dynamic modulus test for the Kansas mixes be continued.

Another recommendation made regarding the dynamic modulus test results was that the Witczak predictive model needs to be used with caution for Kansas mixtures. The Witczak predictive equation must be modified to better reflect the dynamic moduli predictions for the Kansas mixes,

after conducting a more extensive modulus testing program. In addition, specific relationships to predict the tensile strength and creep compliance from mix and binder properties should be developed for the Kansas mixes.

#### ***B.1.10 Utah Department of Transportation (UDOT)***

UDOT has already adopted the PMED software and has been using the software for a couple of years (Darter, et al., 2005). UDOT just completed an updated local calibration because a high percentage of the asphalt mixtures placed in Utah are PMA mixtures, many full-depth PMA mixtures. As part of UDOT's recalibration process, a decision was made to expand their asphalt mixture library to include more PMA mixtures.

UDOT is currently testing an additional 12 asphalt mixtures that were sampled in 2019. The asphalt mixture tests that UDOT sponsored include: dynamic modulus in accordance with AASHTO T342, repeated load plastic deformation in accordance with a modified version of AASHTO T378 (or the NCHRP Report 917 procedure), indirect tensile creep compliance and indirect tensile strength in accordance with AASHTO T322, and the IDT strength/failure tensile strain in accordance with a modified version of ASTM D6931 for estimating the fatigue strength. The previous materials library results along with the current testing program will be used to create clustered input properties for use in design, similar to the process used by PENNDOT.

#### ***B.1.11 Mississippi Department of Transportation (MDOT)***

MDOT has sponsored multiple projects in preparing to implement the PMED software. The more recent project includes a field investigation of all sites to be included in MDOT's local calibration. The asphalt mixture tests included in the field investigation and those performed on mixtures sampled during construction are: dynamic modulus in accordance with AASHTO T342, repeated load plastic deformation in accordance with a modified version of AASHTO T378 (or the NCHRP Report 917 procedure), indirect tensile creep compliance and indirect tensile strength in accordance with AASHTO T322, and the indirect tensile strength/failure tensile strain in accordance with a modified version of ASTM D6931 for estimating the fatigue strength. The total number of asphalt mixtures tested will exceed 25, but the tests results will be combined into clusters that result in similar laboratory-derived asphalt mixture properties by distress type (Von Quintus, et al., 2015).

## **B.2 Summary**

Many SHAs have developed material libraries or catalogs for the implementation of the PMED software in the past decade. The asphalt material libraries consist of input level 1 laboratory-derived properties and input level 2 predicted properties for agency-specific asphalt mixtures. A review of selected SHAs PMED design practice revealed that dynamic modulus has been considered as the cornerstone for developing the asphalt material libraries. Creep compliance and indirect tensile strength tests are the next common tests among the reviewed material libraries. The reason why SHAs focused more on using the dynamic modulus test is related to the assumption included in the NCHRP 1-37A project report.

**Expansion of AASHTOWare ME Design Inputs  
Final Report WHRP 0092-20-03**

The assumption from NCHRP project 1-37A to develop the PMED rudimentary software was the dynamic modulus measured on different asphalt mixtures adequately accounted for differences between the plastic deformation and fatigue strength differences between asphalt mixtures. Thus, one set of plastic strain and fatigue strength coefficients was assumed to be applicable for all asphalt mixtures which was used in the global calibration.

That assumption was initially used by many agencies, but has been found to be incorrect. So, most agencies are now moving towards actually measuring the fatigue strength and plastic strain coefficients in the laboratory, as well as dynamic modulus. Most, if not all, of the reviewed research studies are now sponsoring projects to determine the laboratory-derived mixture k-values measured for the rutting and fatigue cracking using repeated load plastic strain test and bending beam test or the indirect tensile strength/failure strain test, respectively.

The asphalt mixture tests being used by multiple agencies are listed below.

- Dynamic modulus in accordance with AASHTO T 342.
- Repeated load plastic deformation in accordance with a modified version of AASHTO T 378 (or the NCHRP Report 917 procedure [Von Quintus, et al., 2013]).
- Fatigue strength in accordance with AASHTO T 321. This test method is time-consuming and expensive. As such, some agencies are using the IDT strength/failure tensile strain in accordance with a modified version of ASTM D6931 for estimating the fatigue strength.
- IDT creep compliance and strength in accordance with AASHTO T 322.

The laboratory-derived properties that are asphalt mixture type specific have explained some of the residual error between the predicted and measured distresses. Another important finding from the review of previous calibration and material studies is the importance of field investigations for the test sections to derive the local calibration values.

### **B.3 Appendix B References**

ARA (2021). *Nebraska DOT User Guide for AASHTOWare Pavement ME Design*, Nebraska Department of Transportation, Lincoln, Nebraska.

Bonaquist, Ramon (2019). *Practitioner's Guide: Part 1—Performance Testing of Resource Responsible Asphalt Mixtures to Support Mechanistic Empirical Pavement Design*, Draft Final Report, Federal Highway Administration, Washington, DC.

Brink, Wouter, Paul Wilke, Michael Darter, and Harold L. Von Quintus (2020). *PennDOT Pavement ME Design User Input Guide*, Contract #E02978, Task Order #2.1, Pennsylvania Department of Transportation, Harrisburg, Pennsylvania.

Darter, Michael I., Leslie Titus-Glover, and Harold L. Von Quintus (2005). *Implementation of the Mechanistic Empirical Pavement Design Guide in Utah*, Volume I – Summary Report, Utah Department of Transportation, Salt Lake City, Utah.

**Expansion of AASHTOWare ME Design Inputs  
Final Report WHRP 0092-20-03**

Diefenderfer, S. D. (2010). *Analysis of the Mechanistic-Empirical Pavement Design Guide Performance Predictions: Influence of Asphalt Material Input Properties*. Virginia Department of Transportation, Report No. FHWA/VTTC 11-R3.

Flintsch, G. W. Loulizi, A., Diefenderfer, S. D., Galal, K. A., and Diefenderfer, B. K. (2006). *Asphalt Materials Characterization in Support of Implementation of the Proposed Mechanistic-Empirical Pavement Design Guide*. Virginia Department of Transportation, Report No. VTTC 07-CR10.

Graves, R. C., and Mahboub, K. C. (2006). *Pilot Study in Sampling-Based Sensitivity Analysis of NCHRP Design Guide for Flexible Pavements*. Transportation Research Record: Journal of the Transportation Research Board, No. 1947, pp. 123–135, Transportation Research Board of the National Academies, Washington, D.C.

Indiana Department of Transportation. (2013). *Indiana Design Manual*. Indiana Department of Transportation.

Kutay, M.E. and Jamrah, A. (2013). *Preparation for Implementation of the Mechanistic-Empirical Pavement Design Guide in Michigan: Part 1-HMA Mixture Characterization*. Michigan Department of Transportation, Report No. RC-1593.

Mallela et al. (2009). *Guidelines for Implementing NCHRP 1-37A M-E Design Procedures in Ohio: Volume 1 – Summary of Findings, Implementation Plan, and Next Steps*. Ohio Department of Transportation, Report No. FHWA/OH-2009/9A.

Mallela et al. (2009). *Implementing the AASHTO Mechanistic-Empirical Pavement Design Guide in Missouri*. Missouri Department of Transportation, Report No. RI04-002.

Michigan Department of Transportation. (2017). *Michigan DOT User Guide for Mechanistic-Empirical Pavement Design Interim Edition*. Michigan Department of Transportation.

Nantung et al. (2005). *Implementation Initiatives of the Mechanistic–Empirical Pavement Design Guides in Indiana*. Transportation Research Record: Journal of the Transportation Research Board, No. 1919, pp. 142–151, Transportation Research Board of the National Academies, Washington, D.C.

Romanoschi, S. A. and Bethu, S. (2009). *Implementation of the 2002 AASHTO Design Guide for Pavement Structures in KDOT Part-II: Asphalt Concrete Pavements*. Report No. Kansas Department of Transportation, K-TRAN: KSU-04-4 Part 2.

Von Quintus, H., Mallela, J., Bonaquist, R., Schwartz, C., and Carvalo, R. (2013). *Calibration of Rutting Models for Structural and Mix Design*, NCHRP Report 719, National Cooperative Highway Research Program, Transportation Research Board, Washington, DC.

**Expansion of AASHTOWare ME Design Inputs  
Final Report WHRP 0092-20-03**

Von Quintus, Harold L., Chetana Rao, and Biplab Bhattacharya (2015). Implementation and Preliminary Local Calibration of Pavement ME Design in Mississippi, Volume I, Report Number FHWA/MS-DOT-RD-013-170, Research Division, Mississippi Department of Transportation.

Von Quintus, Harold L., Hyung Lee, and Ramon Bonaquist (2019). *Practitioner's Guide: Part 2—Determining Properties of Resource Responsible Asphalt Mixtures for Use in the Mechanistic Empirical Pavement Design Guide*, Draft Final Report, Federal Highway Administration, Washington, DC.

Yin, H., Chehab, G. R., Stoffels, S. M., Kumar, T., and Premkumar, L. (2010). *Use of Creep Compliance Interconverted from Complex Modulus for Thermal Cracking Prediction Using the M-E Pavement Design Guide*. International Journal of Pavement Engineering, Vol. 11, No. 2, pp. 95–105.

### APPENDIX C—ASPHALT BINDER TEST DATA

Appendix C includes the asphalt binder test data for the 12 binders included in the binder test plan.

#### C.1 AASHTO T 315 Test Data

The following is a tabular summary of the binder test data measured in accordance with AASHTO T 315 to provide the inputs required by the PMED software for input level 1.

Sample Identification	Binder Grade	Test Temperature (°C [°F])	Dynamic Shear Modulus, G* (Pa)	Phase Angle, $\delta$ (°)
AC2111	58-28S	10 [50]	8,986,000	56.0
		22 [71.6]	1,262,000	64.0
		34 [93.2]	149,200	72.0
		46 [114.8]	19,500	78.5
		58 [136.4]	3,450	83.7
AC2112	58-28S	10 [50]	8,535,000	56.1
		22 [71.6]	1,013,000	66.5
		34 [93.2]	117,700	73.7
		46 [114.8]	16,100	79.7
		58 [136.4]	2,910	84.4
AC2113	58-28H	10 [50]	4,615,000	64.3
		22 [71.6]	1,074,000	62.5
		34 [93.2]	156,000	66.0
		46 [114.8]	25,740	67.1
		58 [136.4]	6,350	67.6
AC2128	58-28V	10 [50]	9,866,000	53.56
		22 [71.6]	1,295,000	60.56
		34 [93.2]	187,300	64.08
		46 [114.8]	31,000	64.5
		58 [136.4]	8,110	64.1
AC2115	58-34S	10 [50]	3,199,000	57.2
		22 [71.6]	394,200	65.1
		34 [93.2]	65,500	67.3
		46 [114.8]	11,600	70.4
		58 [136.4]	2,840	73.6
AC2116	58-34H	10 [50]	3,321,000	57.2
		22 [71.6]	416,500	64.2
		34 [93.2]	71,020	65.0
		46 [114.8]	13,420	65.2
		58 [136.4]	3,740	65.8

Expansion of AASHTOWare ME Design Inputs  
Final Report WHP 0092-20-03

Sample Identification	Binder Grade	Test Temperature (°C [°F])	Dynamic Shear Modulus, G* (Pa)	Phase Angle, $\delta$ (°)
AC2117	58-34V	10 [50]	2,657,000	61.8
		22 [71.6]	430,300	63.4
		34 [93.2]	78,190	62.9
		46 [114.8]	16,200	61.0
		58 [136.4]	4,900	60.0
AC2118	58-28H	10 [50]	10,280,000	53.4
		22 [71.6]	1,192,000	61.0
		34 [93.2]	192,800	64.6
		46 [114.8]	37,300	65.8
		58 [136.4]	8,870	68.8
AC2119	58-28V	10 [50]	10,330,000	53.5
		22 [71.6]	1,330,000	58.9
		34 [93.2]	207,400	62.3
		46 [114.8]	43,100	62.2
		58 [136.4]	11,200	62.8
AC2121	58-34S	10 [50]	4,085,000	56.6
		22 [71.6]	434,200	65.1
		34 [93.2]	84,600	68.1
		46 [114.8]	17,400	71.8
		58 [136.4]	3,920	76.6
AC2122	58-34H	10 [50]	3,946,000	55.8
		22 [71.6]	449,800	63.4
		34 [93.2]	92,400	63.6
		46 [114.8]	21,000	63.3
		58 [136.4]	5,850	64.7
AC2125	58-34V	10 [50]	3,309,000	59.5
		22 [71.6]	530,000	62.2
		34 [93.2]	103,000	62.0
		46 [114.8]	22,800	61.7
		58 [136.4]	6,450	62.9



## C.2 AASHTO M 332 Data

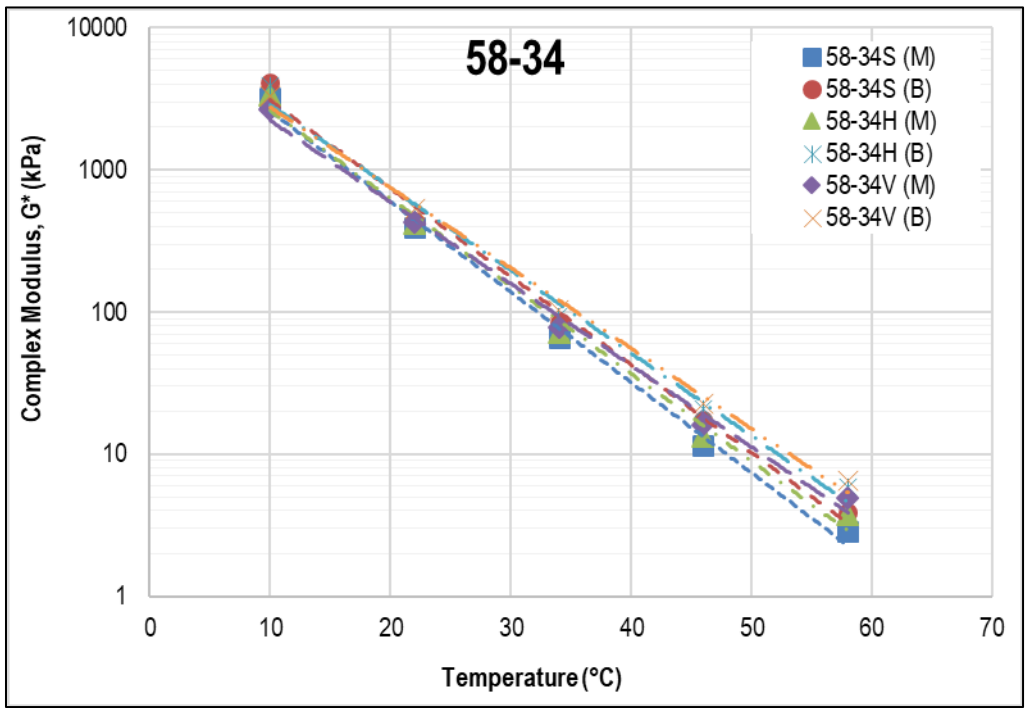
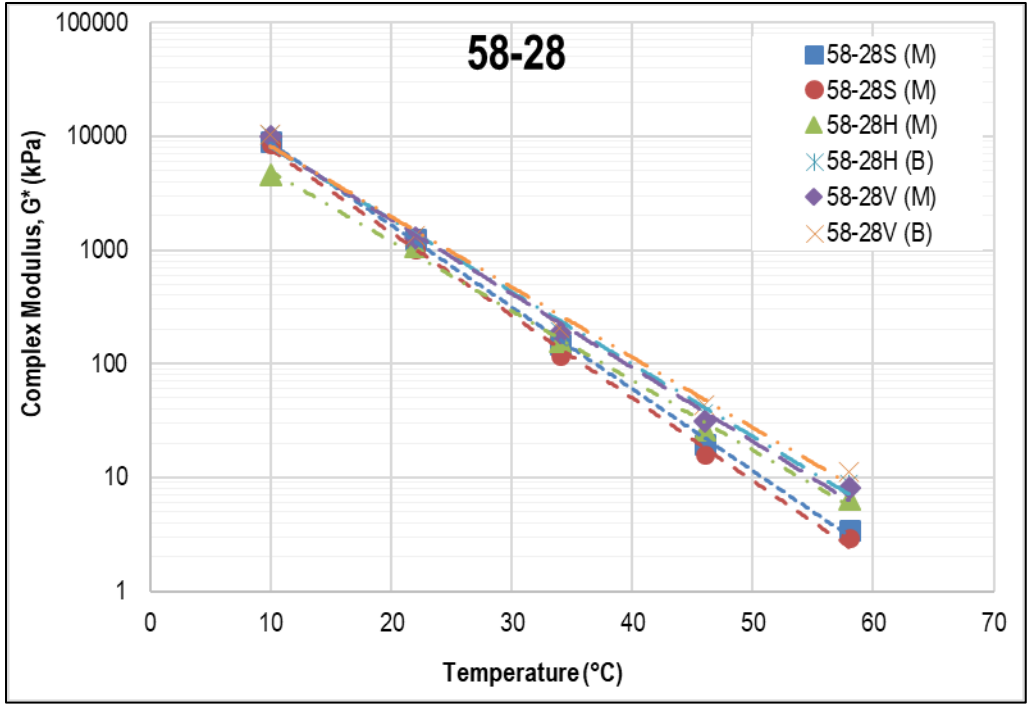
The following is a tabular summary of the binder test data measured in accordance with AASHTO M 332.

Sample ID	Binder Grade	Test Temperature (°C)	Percent Recovery (%)		R <sub>diff</sub> (%)	Jnr (kPa <sup>-1</sup> )		Jnr <sub>diff</sub> (%)
			R <sub>0.1</sub>	R <sub>3.2</sub>		Jnr <sub>0.1</sub>	Jnr <sub>3.2</sub>	
AC2111	58-28S	58	3.71	0.45	87.93	2.58	2.84	9.93
AC2112	58-28S	58	5.77	-0.05	100.85	3.00	3.42	14.04
AC2113	58-28H	58	55.87	44.81	19.79	0.42	0.54	27.44
AC2128	58-28V	58	70.22	63.32	9.82	0.20	0.25	23.79
AC2115	58-34S	58	24.06	8.98	62.66	1.98	2.67	34.92
AC2116	58-34H	58	54.54	41.34	24.21	0.71	0.94	32.48
AC2117	58-34V	58	78.49	72.10	8.14	0.21	0.27	29.01
AC2118	58-28H	58	54.79	41.18	24.84	0.32	0.43	36.81
AC2119	58-28V	58	71.21	62.03	12.89	0.14	0.19	35.52
AC2121	58-34S	58	15.41	3.26	78.88	1.73	2.24	29.50
AC2122	58-34H	58	62.94	46.94	25.42	0.37	0.56	53.42
AC2125	58-34V	58	69.80	57.10	18.20	0.25	0.37	49.72

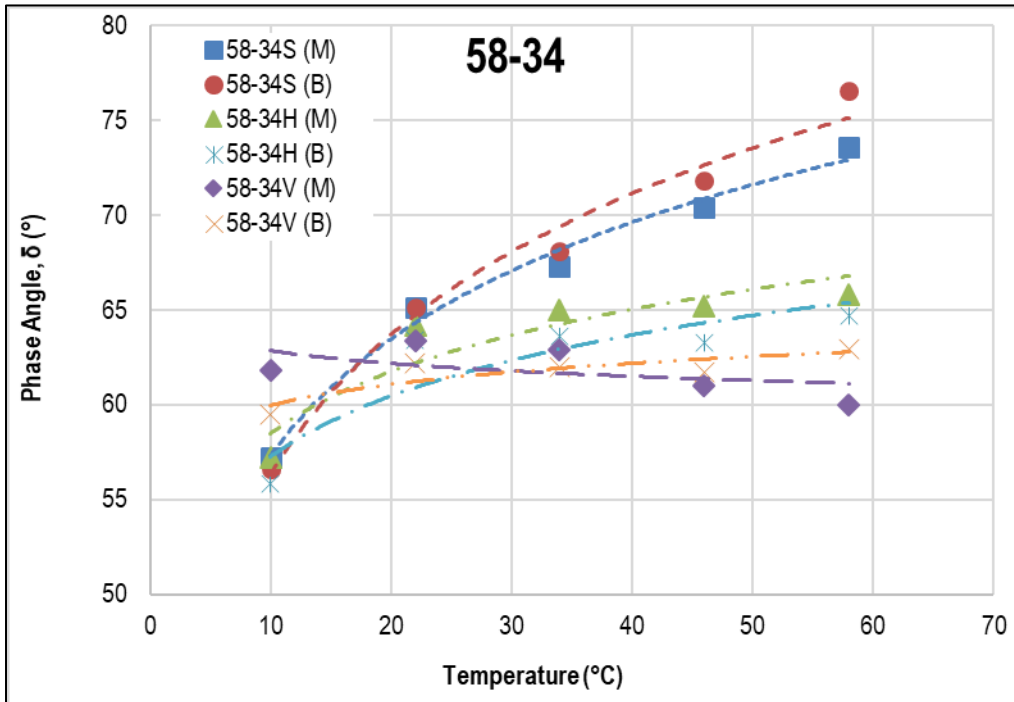
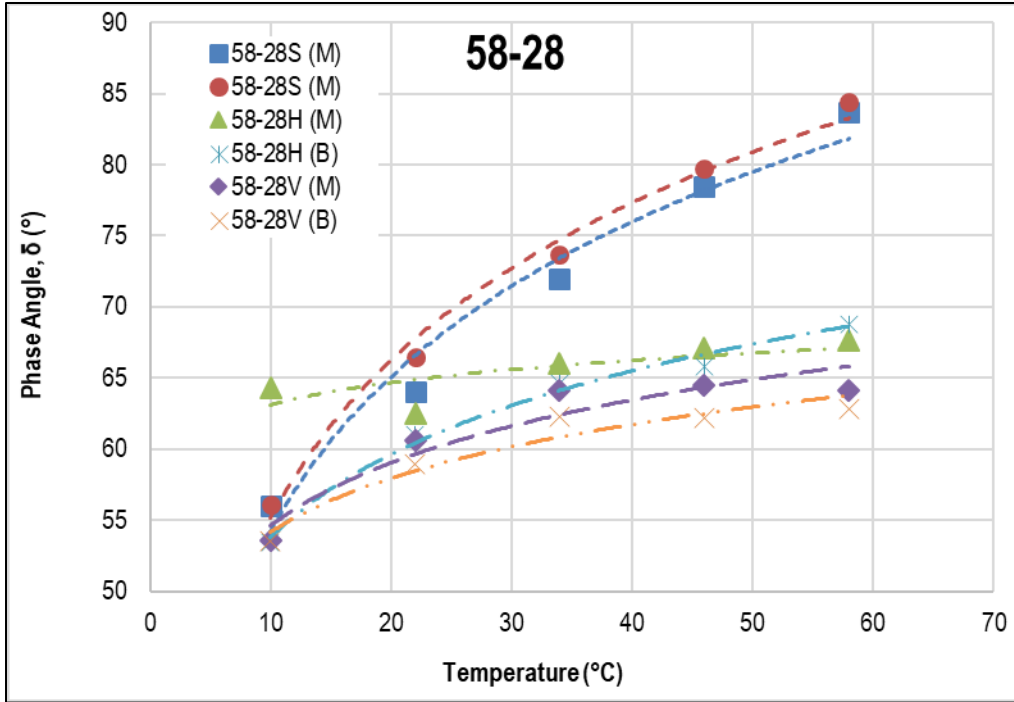
## C.3 Graphical Presentation and Comparison of Asphalt Binder Test Data

The following is a graphical summary and comparison of the binder test data. Three sets of graphs are provided for the two binder grades (PG58-28 and PG58-34). The first set of graphs display the complex modulus versus temperature, the second set of graphs display phase angle versus temperature, and the third set of graphs display phase angle versus complex modulus.

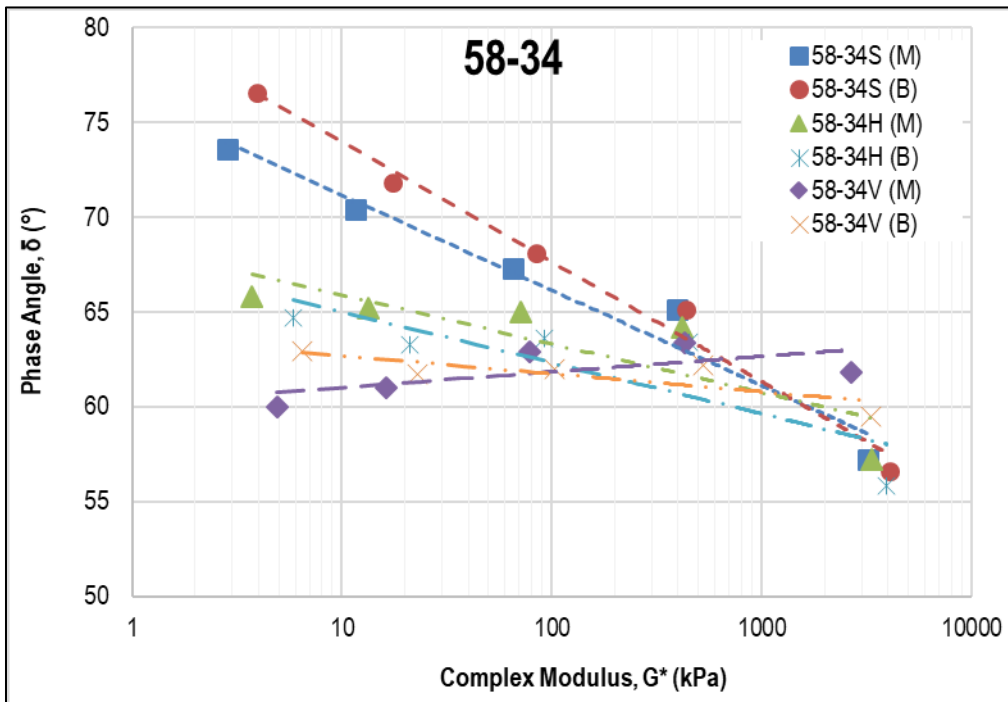
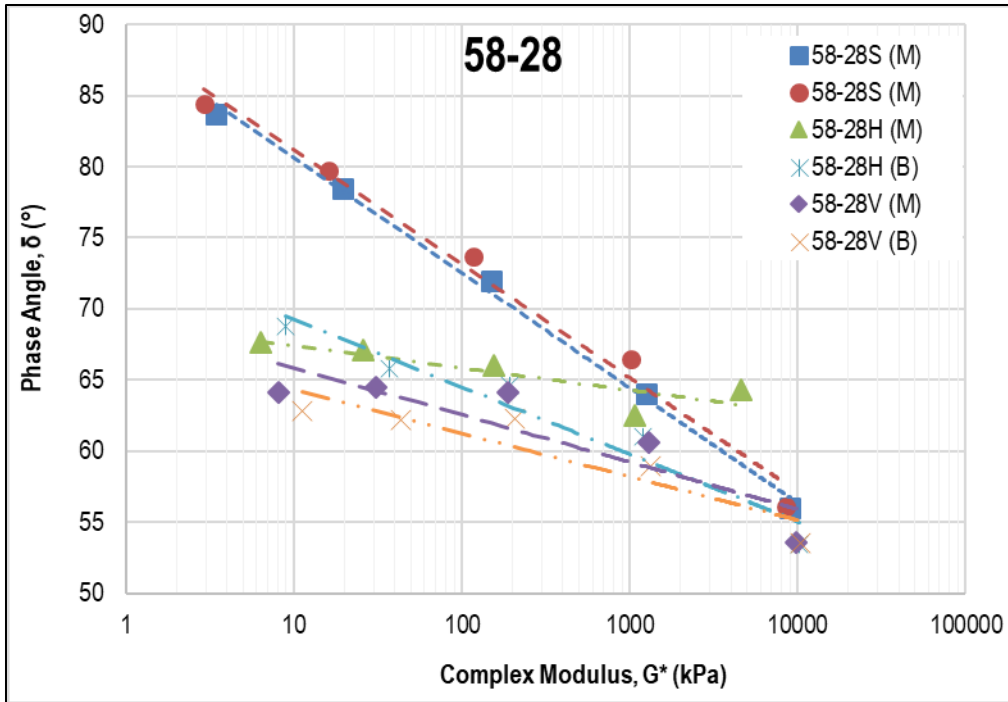
Expansion of AASHTOWare ME Design Inputs  
 Final Report WHRP 0092-20-03



Expansion of AASHTOWare ME Design Inputs  
 Final Report WHRP 0092-20-03



Expansion of AASHTOWare ME Design Inputs  
 Final Report WHRP 0092-20-03



**APPENDIX D—ASPHALT MIXTURE DESIGN DATA**

Appendix D includes a tabulation of information and data extracted from the asphalt mixture design reports for all of the dense-graded asphalt mixtures. The information and data are summarized for the different layers: asphalt base and wearing surface mixtures.

**D.1 Asphalt Base Mixtures with PG58-28 Binders**

<b>Mix Number</b>		<b>0003</b>	<b>0057</b>	<b>0119</b>	<b>1060</b>	<b>1166</b>
Main Project Number		0250-11-11	0250-11-11	1020-03-76	1030-20-84	1166-00-79
Asphalt Binder		PG58-28S	PG58-28S	PG58-28S	PG58-28H	PG58-28S
Mix Traffic Level		3 MT	3 LT	3 HT	3 HT	2 HT
NMAS		12.5 mm	19 mm	19 mm	19 mm	25 mm
Percentage Aggregate Blend, %	RAP	32.0	21.0	20.0	10.0	10.0
	RAS	---	3.0	---	4.0	2.0
	1.5" Chip	---	---	---	---	28.0
	7/8" Chip	---	26.0	---	15.0	---
	3/4" Chip	17.5	---	18.0	---	---
	5/8" Chip	7.0	---	---	---	---
	3/8" Chip	---	7.0	20.0	17.0	26.0
	Manufactured. Sand	19.3	10.0	35.0	44.0	29.0
	Natural Sand/Wash Gravel	24.0	32.5	7.0	10.0	5.0
	Dust	0.2	0.5	---	---	---
Gradation, Sieve Size, percent passing	19 mm	99.1	99.0	97.9	96.7	88.7
	12.5 mm	90.2	90.1	82.3	86.7	77.5
	9.5 mm	80.6	82.0	70.5	83.9	73.2
	#4	63.2	59.5	57.4	68.0	53.8
	#16	30.5	29.4	20.1	28.8	32.3
	#30	26.1	20.9	19.9	16.4	21.1
	#50	11.6	14.5	11.7	7.0	10.4
	#200	4.2	4.1	3.1	3.9	3.0
Additive	Type	---	---	---	---	Evotherm
	Amount, %	---	---	---	---	0.35
N-Design, number of gyrations		75	40	100	100	100
Design Air Voids, %		4.00	4.01	3.98	4.00	4.03
Asphalt Content, total by wt., %		4.7	4.5	4.5	5.2	5.3
Asphalt Specific Gravity		1.031	1.030	1.034	1.017	1.035
Dust to Asphalt Ratio		1.04	0.97	0.75	0.91	0.60
VMA, %		13.4	14.2	13.8	14.0	15.5
VFA, %		70.3	71.7	71.0	71.5	74.1
Specific Gravity	Aggregate, Bulk	2.655	2.742	2.723	2.702	2.672
	Aggregate, Effective	2.705	2.761	2.753	2.784	2.694
	Mix, Bulk	2.413	2.464	2.459	2.451	2.383
	Mix, Maximum	2.513	2.567	2.561	2.553	2.483

## D.2 Wearing Surface Mixtures with PG58-28 Binders

Mix Number		0093	0165	0208	0236	0251
Main Project Number		1110-13-71	1111-03-72	6923-01-70	1560-04-70	1370-15-71
Asphalt Binder		PG58-28H	PG58-28S	PG58-28S	PG58-28S	PG58-28V
Mix Traffic Level		4 HT	4 HT	4 LT	4 MT	4 HT
NMAS		12.5 mm	12.5 mm	12.5 mm	12.5 mm	12.5 mm
Percentage Aggregate Blend, %	RAP	25.0	9.0	20.0	20.0	9.0
	RAS	---	4.0	---	---	3.4
	7/8" Chip	---	---	---	---	---
	3/4" Chip	---	---	---	21.0	---
	5/8" Chip	9.0	13.0	37.0	---	7.0
	1/2" Chip	---	---	---	---	---
	3/8" Chip	8.0	20.0	---	11.0	21.0
	Manufactured Sand	47.0	45.0	43.0	23.0	46.0
	Natural Sand/Wash Gravel	10.5	8.5	---	25.0	13.1
	Dust	0.5	0.5	---	---	0.5
Lime	---	---	---	---	---	
Gradation, Sieve Size, percent passing	19 mm	100	100	100	100	100
	12.5 mm	96.2	97.0	93.0	91.9	99.1
	9.5 mm	89.1	87.8	82.3	82.8	89.6
	#4	78.0	65.9	63.1	66.8	66.5
	#16	40.4	34.7	42.6	39.4	34.9
	#30	28.4	24.2	32.1	27.9	20.9
	#50	15.5	14.3	17.0	16.0	10.8
Additive	Type	---	Evotherm	Evotherm	---	---
	Amount, %	---	0.40	0.35	---	---
N-Design, number of gyrations		100	100	40	75	100
Design Air Voids, %		4.02	3.99	4.01	3.99	4.00
Asphalt Content, total by wt., %		5.4	5.0	5.0	5.2	5.2
Asphalt Specific Gravity		1.030	1.030	1.035	1.034	1.032
Dust to Asphalt Ratio		0.70	0.97	1.02	0.82	1.13
VMA, %		15.5	14.6	14.8	15.8	14.6
VFA, %		74.1	72.6	72.8	74.7	72.7
Specific Gravity	Aggregate, Bulk	2.727	2.675	2.693	2.764	2.701
	Aggregate, Effective	2.769	2.709	2.722	2.782	2.754
	Mix, Bulk	2.436	2.405	2.416	2.455	2.433
	Mix, Maximum	2.538	2.505	2.517	2.557	2.534

**Expansion of AASHTOWare ME Design Inputs  
Final Report WHRP 0092-20-03**

<b>Mix Number</b>		<b>0088*</b>	<b>0258</b>	<b>0319</b>	<b>0121</b>
Main Project Number		1071-02-71	7550-00-62	1053-10-62	1016-05-75
Asphalt Binder		PG58-28S	PG58-28S	PG58-28H	PG58-28V
Mix Traffic Level		4 LT	4 MT	4 MT	4 SMA
NMAS		12.5 mm	12.5 mm	12.5 mm	12.5 mm
Percentage Aggregate Blend, %	RAP	21.0	20.0	23.0	---
	RAS	---	---	---	3.0
	7/8" Chip	---	---	---	---
	3/4" Chip	28.0	---	---	34.0
	5/8" Chip	---	25.0	12.0	---
	1/2" Chip	---	---	15.0	16.0
	3/8" Chip	---	---	---	19.0
	Manufactured Sand	28.0	40.0	22.0	18.0
	Natural Sand/Wash Gravel	23.0	15.0	27.5	---
	Dust	---	---	0.5	---
	Lime	---	---	---	10.0
Gradation, Sieve Size, percent passing	19 mm	100	99.6	100	100
	12.5 mm	90.3	95.0	97.4	91.2
	9.5 mm	81.6	88.4	89.0	78.2
	#4	67.8	74.5	67.1	34.7
	#16	41.0	39.2	42.3	19.0
	#30	30.3	27.3	32.7	15.7
	#50	17.4	17.1	15.0	12.9
	#200	4.1	4.7	4.5	8.3
Additive	Type	---	---	---	---
	Amount, %	---	---	---	---
N-Design, number of gyrations		40	75	75	100
Design Air Voids, %		4.03	4.02	4.01	3.6
Asphalt Content, total by wt., %		6.0	5.4	5.2	6.1
Asphalt Specific Gravity		1.028	1.028	1.036	1.034
Dust to Asphalt Ratio		0.84	1.00	NA	1.38
VMA, %		15.2	14.8	14.8	17.8
VFA, %		73.4	72.9	72.8	74.6
Specific Gravity	Aggregate, Bulk	2.638	2.652	2.687	2.652
	Aggregate, Effective	2.726	2.707	2.731	2.666
	Mix, Bulk	2.380	2.388	2.416	2.322
	Mix, Maximum	2.480	2.488	2.517	2.432

\* Mixture design information was provided, but this wearing surface mixture was excluded from the test plan.

### D.3 Wearing Surface Mixtures with PG58-34 Binders

Mix Number		0127	7130	8357	1020
Main Project Number		7510-02-60	7130-08-70	0250-11-11	1016-05-75
Asphalt Binder		PG58-34S	PG58-34V	PG58-34S	PG58-34V
Mix Traffic Level		4 MT	5 HT	4 LT	4 SMA
NMAS		12.5 mm	9.5 mm	12.5 mm	12.5 mm
Percentage Aggregate Blend, %	RAP	18.0	22.0	20.0	---
	RAS	---	---	---	3.0
	7/8" Chip	---	---	---	---
	3/4" Chip	---	---	22.0	34.0
	5/8" or 1/2" Chip	30.0	25.0	---	---
	3/8" Chip	15.0	---	33.0	16.0
	Manufactured Sand	32.0	38.0	25.0	19.0
	Natural Sand	5.0	15.0	---	18.0
	Dust	---	---	---	---
Lime	---	---	---	10.0	
Gradation, Sieve Size, percent passing	19 mm	100	100	100	100
	12.5 mm	92.1	99.6	93.9	91.2
	9.5 mm	77.2	95.9	84.4	78.2
	#4	63.6	73.2	64.8	34.7
	#16	41.3	37.1	43.5	19.0
	#30	28.0	23.4	33.2	15.7
	#50	14.6	11.9	16.9	12.9
#200	3.3	3.1	4.7	8.3	
Additive	Type	---	---	---	---
	Amount, %	---	---	---	---
N-Design, number of gyrations		75	75	40	100
Design Air Voids, %		3.95	3.99	4.00	3.6
Asphalt Content, total by wt., %		5.2	6.1	5.3	6.1
Asphalt Specific Gravity		1.023	1.023	1.023	1.034
Dust to Asphalt Ratio		0.66	0.61	0.99	1.38
VMA, %		15.3	15.9	15.2	17.8
VFA, %		74.2	75.0	73.7	74.6
Specific Gravity	Aggregate, Bulk	2.637	2.633	2.627	2.652
	Aggregate, Effective	2.657	2.701	2.659	2.666
	Mix, Bulk	2.356	2.357	2.353	2.322
	Mix, Maximum	2.453	2.455	2.451	2.432



## APPENDIX E—DYNAMIC MODULUS TEST DATA

Appendix E includes the dynamic modulus test data for all of the asphalt mixtures measured in accordance with AASHTO T 342. A tabular summary of the test data, as well as the dynamic modulus master curves are included in this appendix. The regression equations embedded in the PMED software to calculate the dynamic modulus for input level 3 are explained and described in the NCHRP 1-37A final report (2004).

### E.1 Dynamic Modulus Tabular Summary of Test Data

Asphalt Base Mixture #0003; PG58-28S, 3 MT; Dynamic Modulus, psi

Mix Number	Temp, °F	Frequency					
		0.1	0.5	1	5	10	25
3	14	2,151,909	2,446,636	2,551,662	2,748,526	2,815,311	2,889,477
3	40	947,314	1,348,770	1,526,575	1,921,005	2,075,560	2,261,138
3	70	174,784	317,717	405,906	680,579	827,394	1,042,113
3	100	37,319	60,274	76,052	136,120	176,599	248,946
3	130	16,739	21,389	24,392	35,392	42,804	56,515

Asphalt Base Mixture #0057; PG58-28S, 3 LT; Dynamic Modulus, psi

Mix Number	Temp, °F	Frequency					
		0.1	0.5	1	5	10	25
57	14	2,335,767	2,579,999	2,664,619	2,820,012	2,871,792	2,928,740
57	40	1,183,865	1,591,360	1,761,738	2,121,904	2,257,189	2,415,759
57	70	249,118	438,749	549,689	873,605	1,036,301	1,264,081
57	100	50,760	83,829	106,387	190,450	245,488	341,006
57	130	21,095	27,538	31,730	47,177	57,609	76,872

Asphalt Base Mixture #0119; PG58-28S, 3 HT; Dynamic Modulus, psi

Mix Number	Temp, °F	Frequency					
		0.1	0.5	1	5	10	25
119	14	2,267,016	2,536,570	2,631,213	2,806,645	2,865,566	2,930,632
119	40	1,120,759	1,528,490	1,702,437	2,076,408	2,218,973	2,387,472
119	70	251,996	436,194	544,194	861,654	1,022,448	1,249,091
119	100	59,335	95,075	119,083	207,112	264,013	361,979
119	130	26,756	34,512	39,512	57,707	69,837	91,985

**Expansion of AASHTOWare ME Design Inputs  
Final Report WHRP 0092-20-03**

**Asphalt Base Mixture #1060; PG58-28H, 3 HT; Dynamic Modulus, psi**

Mix Number	Temp, °F	Frequency					
		0.1	0.5	1	5	10	25
1060	14	2,104,467	2,369,871	2,467,694	2,658,024	2,725,361	2,802,382
1060	40	1,060,079	1,412,772	1,565,809	1,905,057	2,039,569	2,203,610
1060	70	269,458	442,722	539,772	815,935	953,558	1,147,499
1060	100	63,051	103,005	128,746	218,029	272,810	363,697
1060	130	24,016	33,176	38,999	59,704	73,129	96,989

**Asphalt Base Mixture #1166; PG58-28S, 2 HT; Dynamic Modulus, psi**

Mix Number	Temp, °F	Frequency					
		0.1	0.5	1	5	10	25
1166	14	1,821,492	2,143,756	2,265,211	2,504,121	2,589,054	2,686,135
1166	40	746,949	1,087,674	1,246,876	1,620,686	1,775,791	1,969,303
1166	70	155,099	269,178	339,026	558,592	678,412	857,742
1166	100	39,902	61,891	76,451	129,658	164,365	225,220
1166	130	18,966	24,196	27,493	39,189	46,823	6,0573

**Asphalt Wearing Surface Mixture #0093; PG58-28H, 4 HT; Dynamic Modulus, psi**

Mix Number	Temp, °F	Frequency					
		0.1	0.5	1	5	10	25
93	14	2,151,443	2,426,111	2,524,578	2,710,645	2,774,394	2,845,707
93	40	1,036,517	1,420,755	1,587,514	1,953,165	2,095,561	2,266,401
93	70	232,333	399,933	498,071	787,911	936,075	1,146,997
93	100	53,877	86,894	108,903	188,910	240,292	328,508
93	130	23,262	30,494	35,134	51,910	63,021	83,199

**Asphalt Wearing Surface Mixture #0165; PG58-28S, 4 HT; Dynamic Modulus, psi**

Mix Number	Temp, °F	Frequency					
		0.1	0.5	1	5	10	25
165	14	1,822,203	2,103,227	2,210,813	2,427,547	2,506,949	2,599,847
165	40	821,185	1,135,832	1,278,119	1,607,011	1,743,013	1,913,665
165	70	177,429	306,656	381,517	603,030	717,855	884,571
165	100	33,589	59,170	76,184	137,313	176,050	241,947
165	130	10,207	15,301	18,639	30,939	39,175	54,174

**Expansion of AASHTOWare ME Design Inputs  
Final Report WHRP 0092-20-03**

Asphalt Wearing Surface Mixture #0208; PG58-28S, 4 LT; Dynamic Modulus, psi

Mix Number	Temp, °F	Frequency					
		0.1	0.5	1	5	10	25
208	14	1,684,493	2,052,397	2,191,772	2,465,126	2,561,552	2,670,907
208	40	526,124	854,721	1,019,202	1,425,528	1,600,450	1,822,337
208	70	69,415	135,931	181,545	344,236	443,343	602,911
208	100	14,846	23,426	29,454	53,549	70,818	103,671
208	130	7,243	8,987	10,107	14,199	16,967	22,137

Asphalt Wearing Surface Mixture #0236; PG58-28S, 4 MT; Dynamic Modulus, psi

Mix Number	Temp, °F	Frequency					
		0.1	0.5	1	5	10	25
236	14	1,530,291	1,924,219	2,076,285	2,377,142	2,483,599	2,604,158
236	40	431,088	727,805	884,170	1,288,267	1,468,618	1,701,693
236	70	64,272	117,272	153,957	288,887	374,269	516,336
236	100	19,411	27,279	32,609	53,182	67,608	94,859
236	130	11,952	13,806	14,969	19,078	21,764	26,650

Asphalt Wearing Surface Mixture #0251; PG58-28V, 4 HT; Dynamic Modulus, psi

Mix Number	Temp, °F	Frequency					
		0.1	0.5	1	5	10	25
251	14	2,109,743	2,342,928	2,430,132	2,603,033	2,665,606	2,738,403
251	40	1,128,676	1,446,239	1,582,210	1,883,098	2,003,092	2,150,698
251	70	314,360	491,681	58,6556	846,274	972,107	1,147,165
251	100	70,999	116,295	144,473	237,960	292,984	381,623
251	130	23,142	33,400	39,851	62,347	76,605	101,416

Asphalt Wearing Surface Mixture #0258; PG58-28S, 4 MT; Dynamic Modulus, psi

Mix Number	Temp, °F	Frequency					
		0.1	0.5	1	5	10	25
258	14	1,318,999	1,718,072	1,880,171	2,215,456	2,339,183	2,482,908
258	40	407,315	677,513	821,496	1,201,198	1,374,814	1,603,511
258	70	80,337	142,253	183,620	329,631	418,826	563,858
258	100	26,606	38,581	46,616	76,993	97,735	135,843
258	130	15,702	18,940	20,978	28,221	32,973	41,612

**Expansion of AASHTOWare ME Design Inputs  
Final Report WHRP 0092-20-03**

Asphalt Wearing Surface Mixture #0319; PG58-28H, 4 MT; Dynamic Modulus, psi

Mix Number	Temp, °F	Frequency					
		0.1	0.5	1	5	10	25
319	14	1,736,941	2,059,716	2,182,990	2,428,588	2,517,051	2,619,047
319	40	670,430	991,258	1,143,696	1,508,086	1,662,050	1,856,562
319	70	125,701	222,496	282,688	475,740	583,299	746,951
319	100	29,592	46,602	57,952	99,926	127,673	176,929
319	130	13,367	17,204	19,624	28,228	33,864	44,057

Asphalt Wearing Surface Mixture #0121; PG58-28V, 4 SMA; Dynamic Modulus, psi

Mix Number	Temp, °F	Frequency					
		0.1	0.5	1	5	10	25
1020	14	1,771,987	2,142,267	2,278,499	2,537,351	2,625,509	2,723,084
1020	40	659,483	1,034,235	1,215,055	1,642,528	1,818,056	2,033,181
1020	70	126,751	232,144	301,446	534,829	668,703	873,718
1020	100	37,240	56,094	69,112	119,585	154,482	218,494
1020	130	21,066	25,637	28,595	39,453	46,792	60,432

Asphalt Wearing Surface Mixture #0127; PG58-34S, 4 MT; Dynamic Modulus, psi

Mix Number	Temp, °F	Frequency					
		0.1	0.5	1	5	10	25
127	14	1,426,553	1,834,479	1,994,592	2,314,751	2,428,890	2,558,525
127	40	383,721	663,017	814,124	1,214,207	1,396,380	1,634,436
127	70	59,815	108,003	141,634	267,169	347,877	483,921
127	100	19,550	27,042	32,110	51,668	65,402	91,418
127	130	12,511	14,346	15,497	19,570	22,234	27,080

Asphalt Wearing Surface Mixture #7130; PG58-34V, 5 HT; Dynamic Modulus, psi

Mix Number	Temp, °F	Frequency					
		0.1	0.5	1	5	10	25
7130	14	1,533,165	1,914,686	2,063,427	2,361,390	2,468,355	2,590,752
7130	40	488,309	788,751	943,048	1,335,083	1,508,370	1,731,839
7130	70	87,306	154,725	199,471	355,687	449,981	601,774
7130	100	26,825	38,506	46,316	75,756	95,822	132,677
7130	130	15,730	18,655	20,483	26,922	31,112	38,686

**Expansion of AASHTOWare ME Design Inputs  
Final Report WHRP 0092-20-03**

Asphalt Wearing Surface Mixture #8357; PG58-34S, 4 LT; Dynamic Modulus, psi

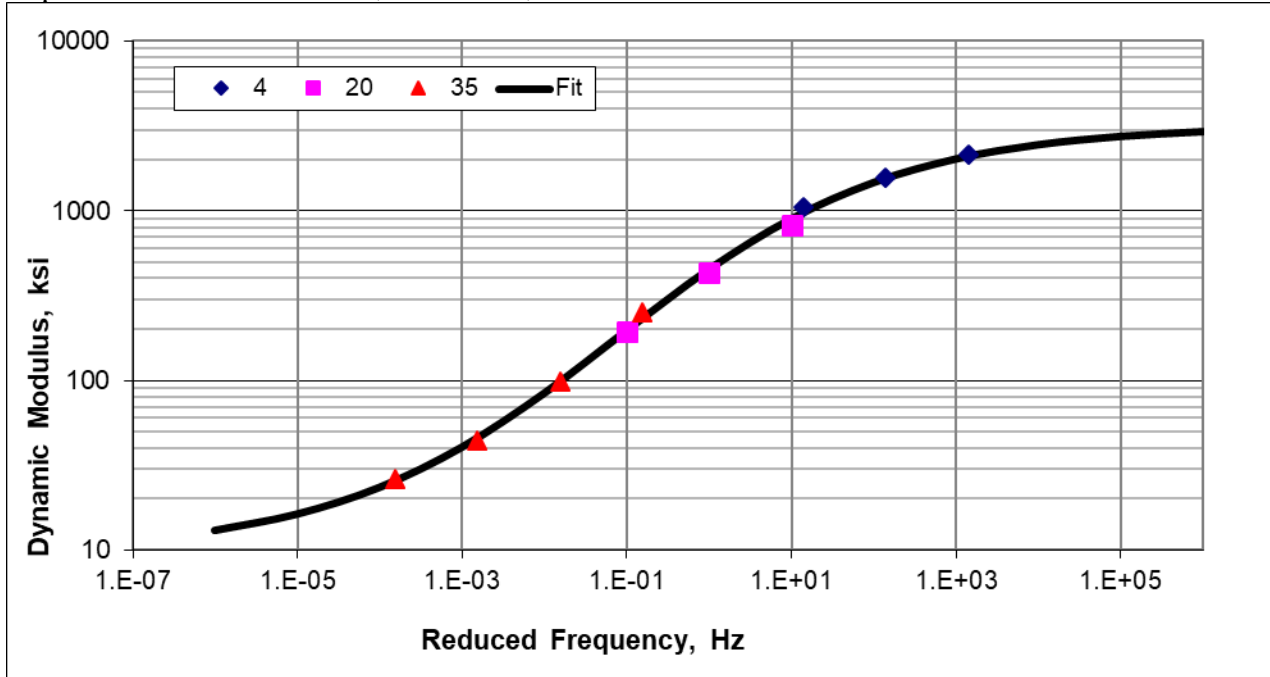
Mix Number	Temp, °F	Frequency					
		0.1	0.5	1	5	10	25
8357	14	1,310,427	1,705,031	1,865,058	2,196,016	2,318,253	2,460,420
8357	40	348,421	596,060	731,116	1,095,731	1,266,089	1,493,689
8357	70	55,047	98,751	128,739	238,935	309,174	427,489
8357	100	17,071	24,088	28,783	46,621	58,956	82,026
8357	130	10,292	12,041	13,127	16,925	19,383	23,817

Asphalt Wearing Surface Mixture #1020; PG58-34V, 4 SMA; Dynamic Modulus, psi

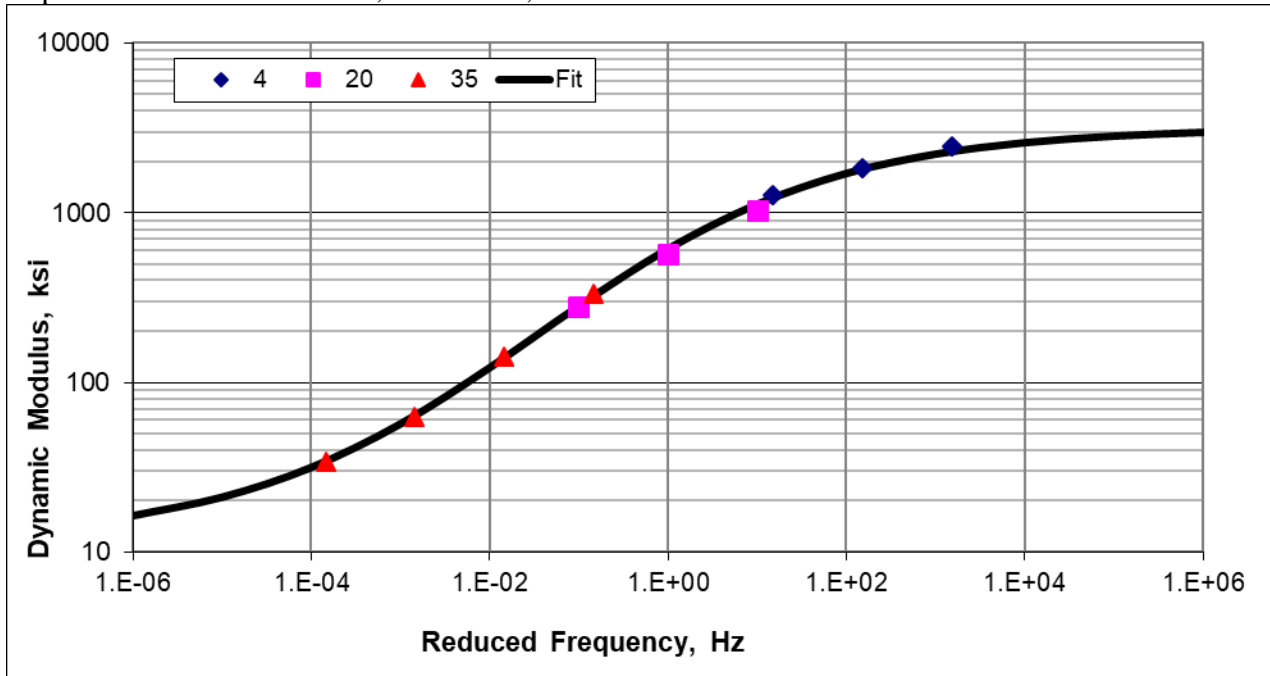
Mix Number	Temp, °F	Frequency					
		0.1	0.5	1	5	10	25
121	14	2,068,884	2,361,234	2,465,345	2,660,162	2,726,091	2,799,162
121	40	918,372	1,312,825	1,487,340	1,873,448	2,024,202	2,204,691
121	70	174,442	319,699	409,238	686,765	834,092	1,048,197
121	100	37,332	61,513	78,268	142,404	185,675	262,827
121	130	16,379	21,318	24,545	36,524	44,690	59,915

## E.2 Dynamic Modulus Master Curves

Asphalt Base Mixture #0003; PG58-28S, 3 MT

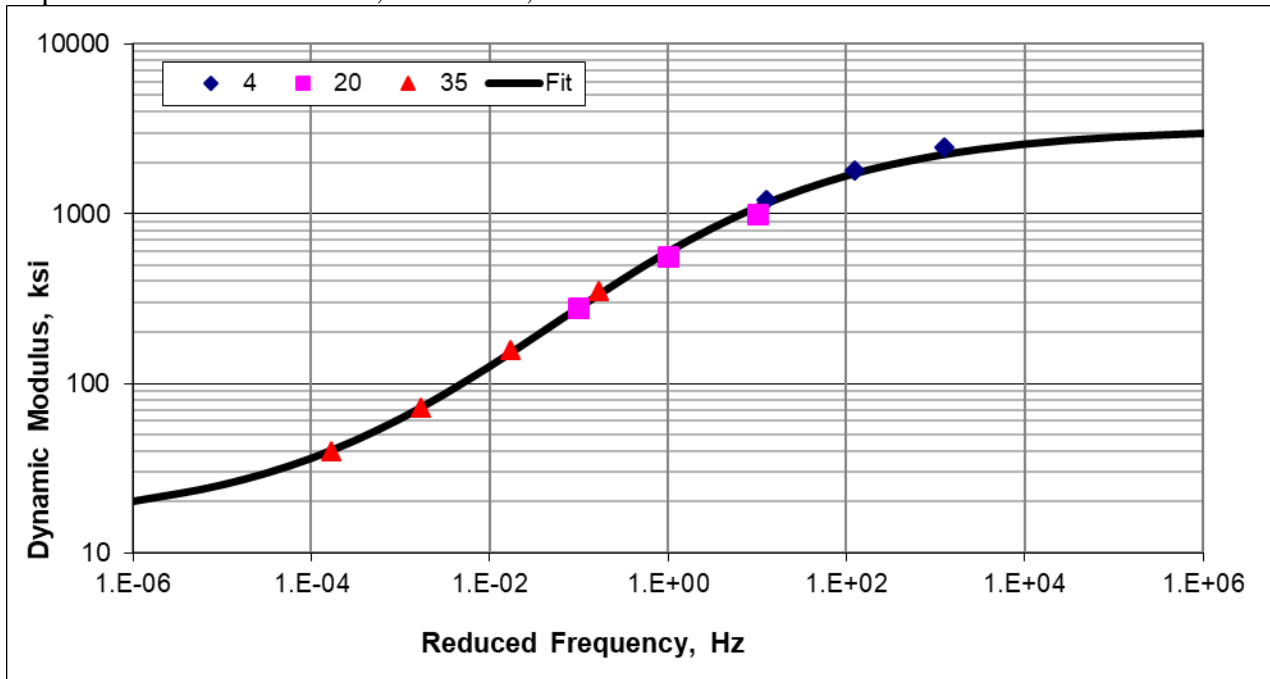


Asphalt Base Mixture #0057; PG58-28S, 3 LT

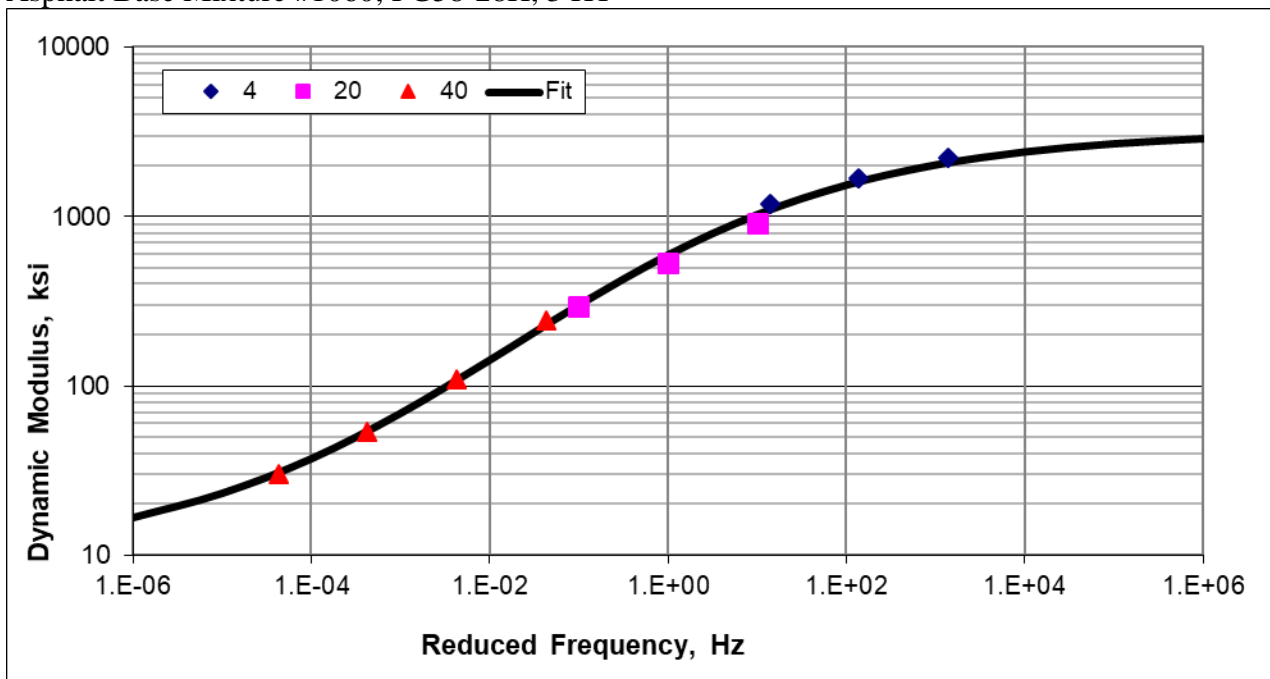


Expansion of AASHTOWare ME Design Inputs  
Final Report WHRP 0092-20-03

Asphalt Base Mixture #0119; PG58-28S, 3 HT

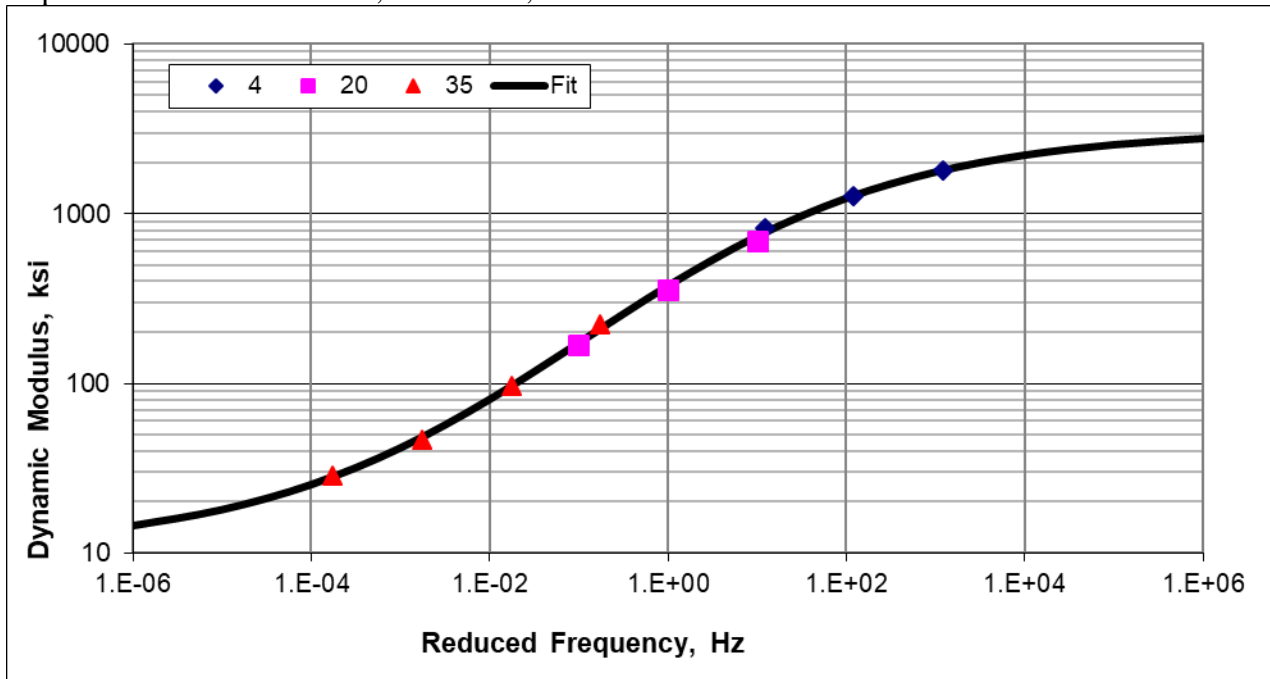


Asphalt Base Mixture #1060; PG58-28H, 3 HT

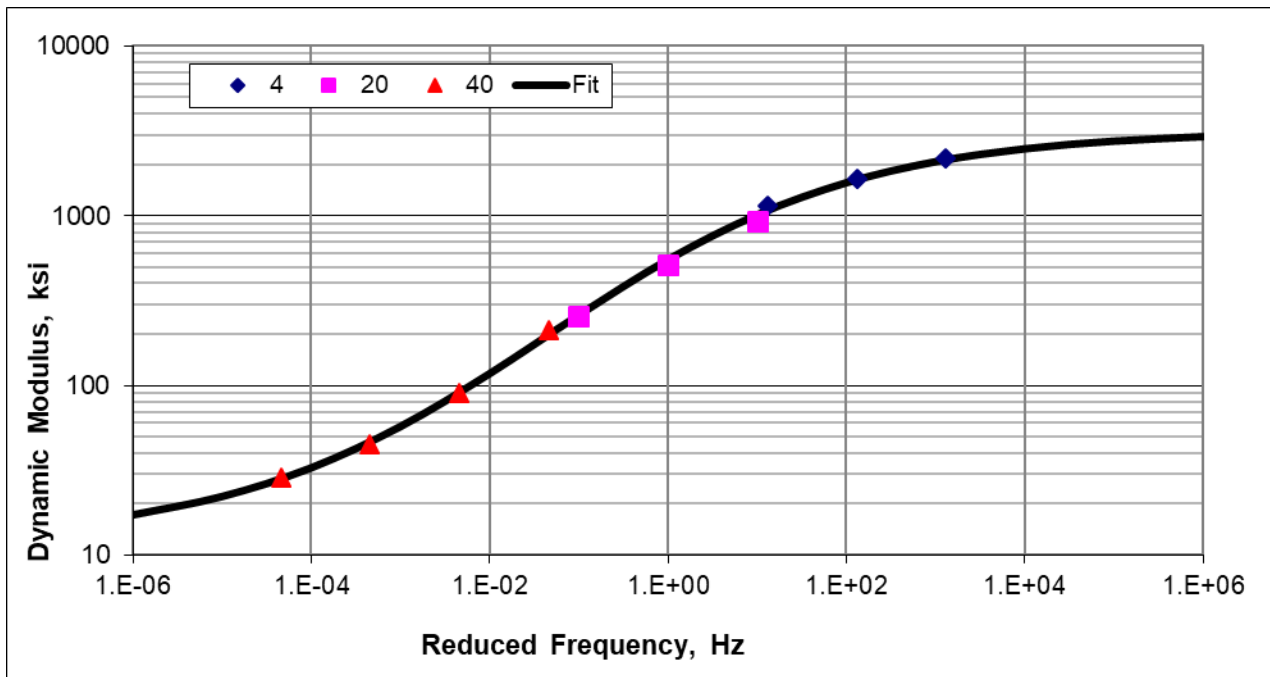


Expansion of AASHTOWare ME Design Inputs  
Final Report WHRP 0092-20-03

Asphalt Base Mixture #1166; PG58-28S, 2 HT



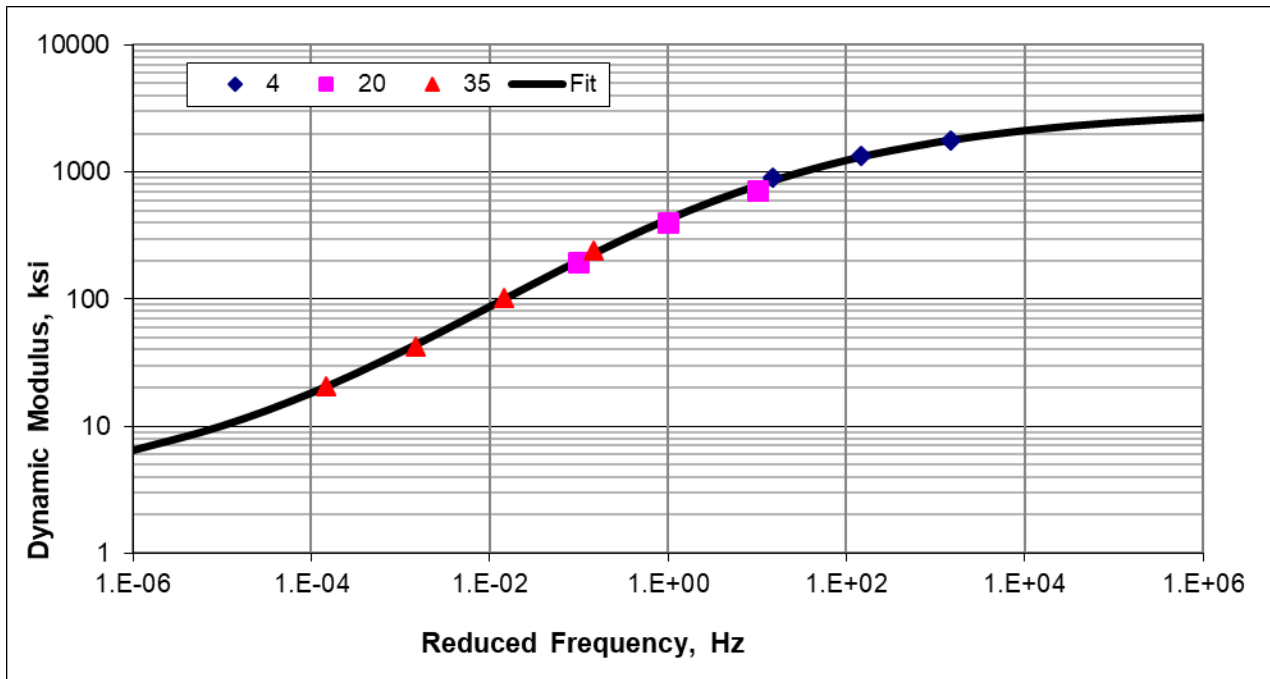
Asphalt Wearing Surface Mixture #0093; PG58-28H, 4 HT



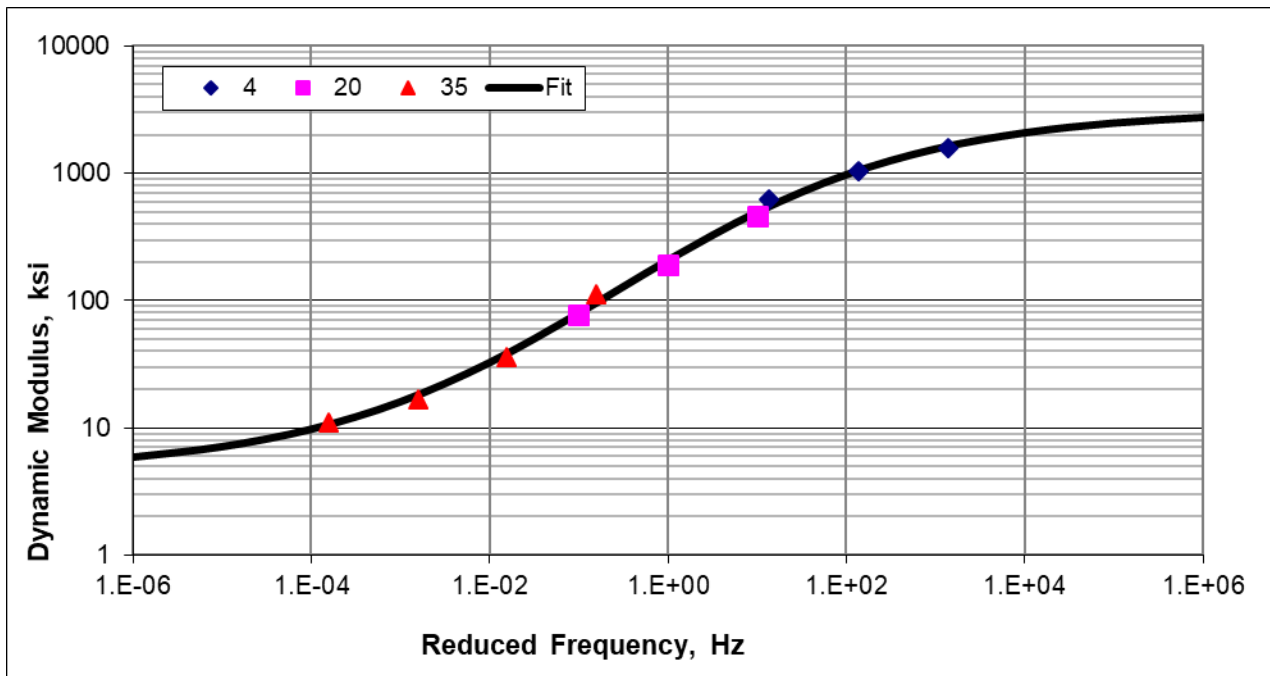


Expansion of AASHTOWare ME Design Inputs  
Final Report WHRP 0092-20-03

Asphalt Wearing Surface Mixture #0165; PG58-28S, 4 HT

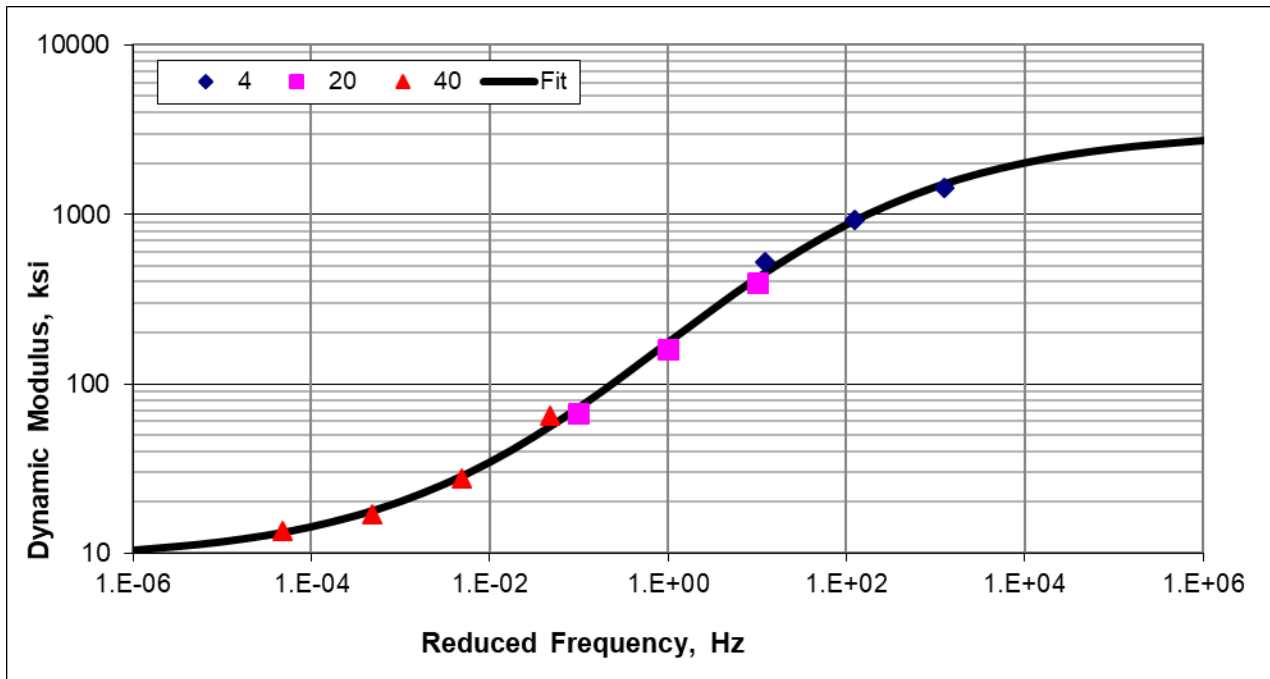


Asphalt Wearing Surface Mixture #0208; PG58-28S, 4 LT

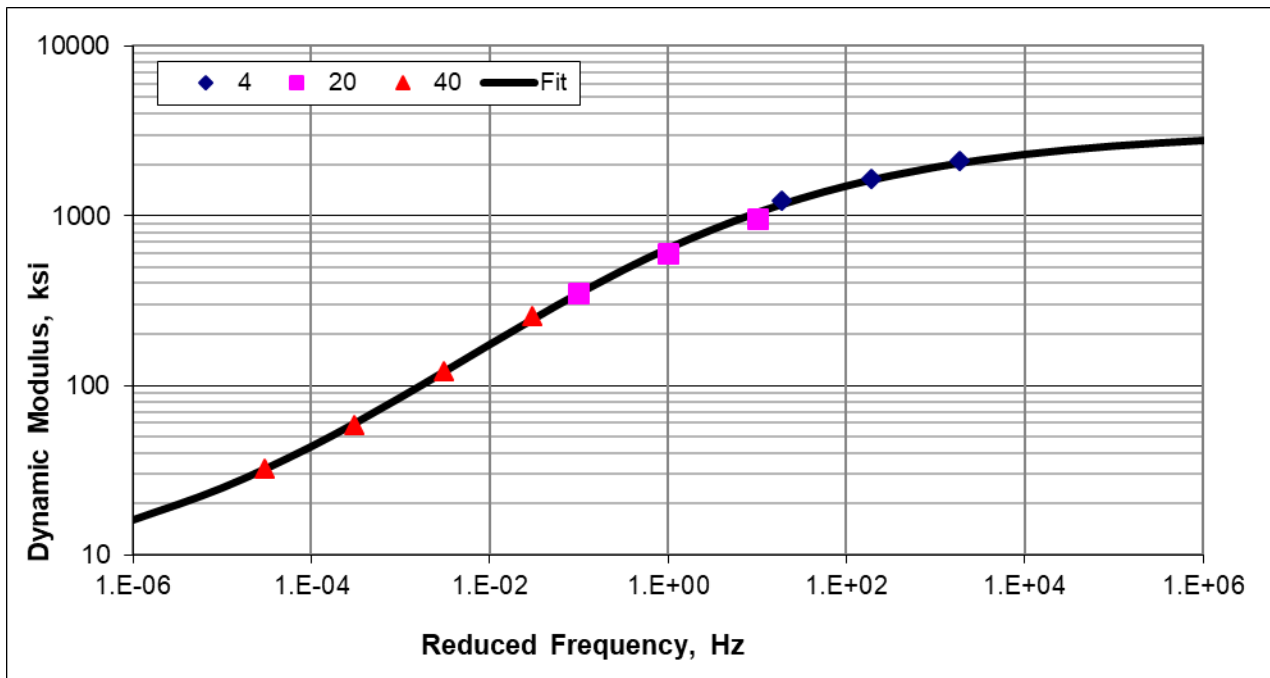


Expansion of AASHTOWare ME Design Inputs  
Final Report WHRP 0092-20-03

Asphalt Wearing Surface Mixture #0236; PG58-28S, 4 MT

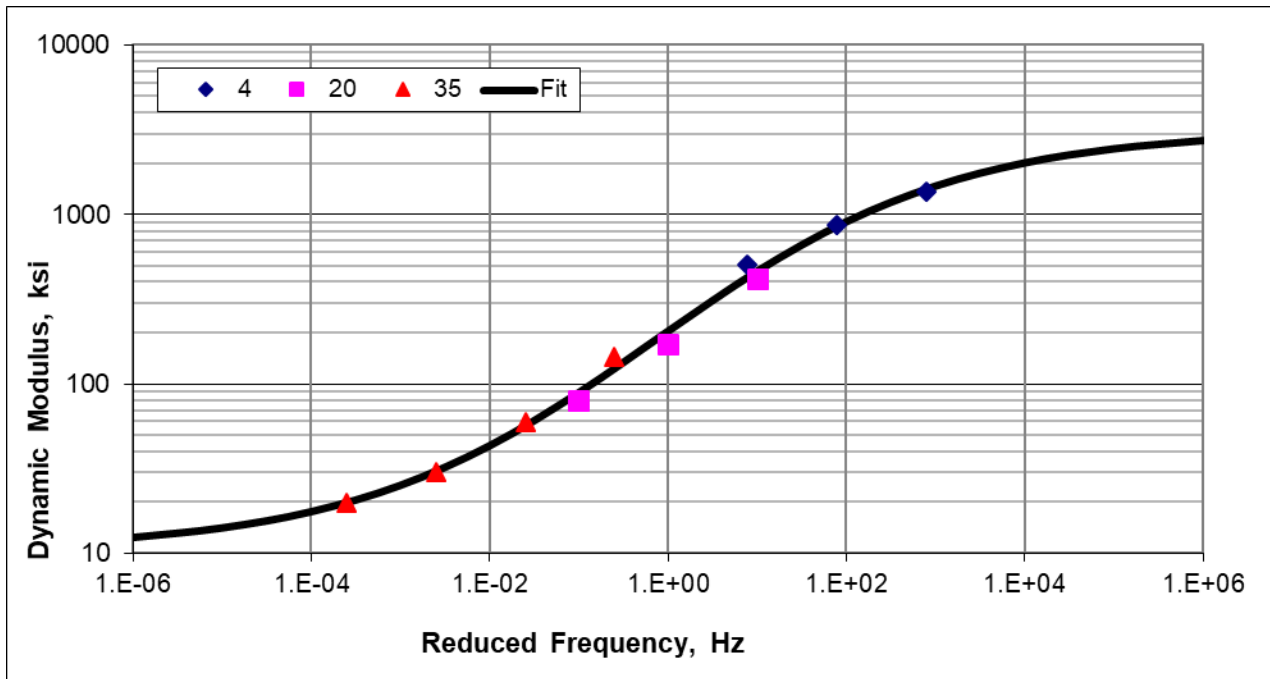


Asphalt Wearing Surface Mixture #0251; PG58-28V, 4 HT

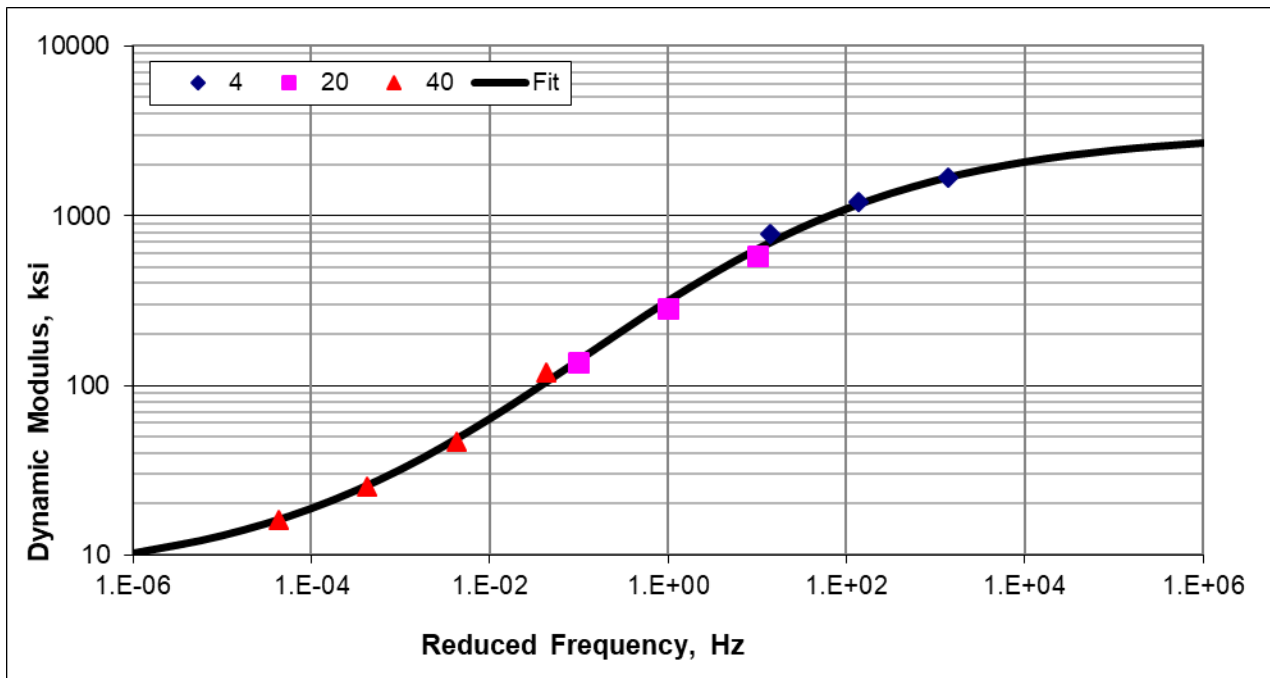


Expansion of AASHTOWare ME Design Inputs  
Final Report WHRP 0092-20-03

Asphalt Wearing Surface Mixture #0258; PG58-28S, 4 MT

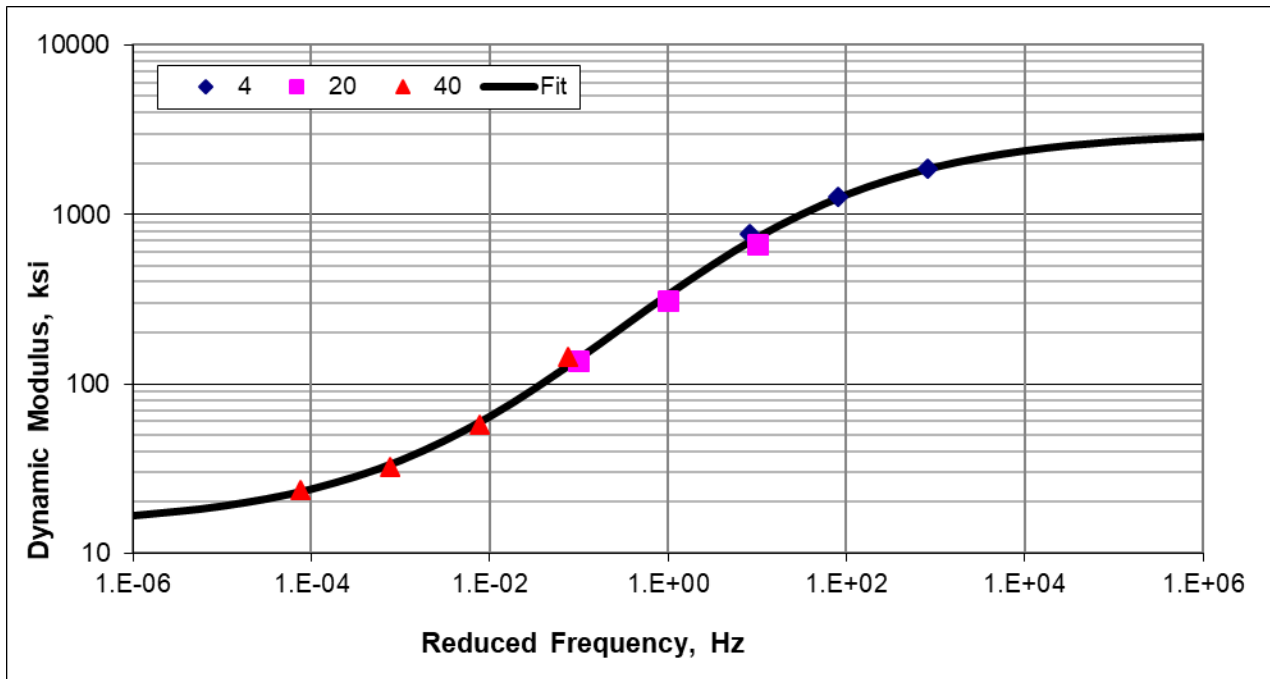


Asphalt Wearing Surface Mixture #0319; PG58-28H, 4 MT

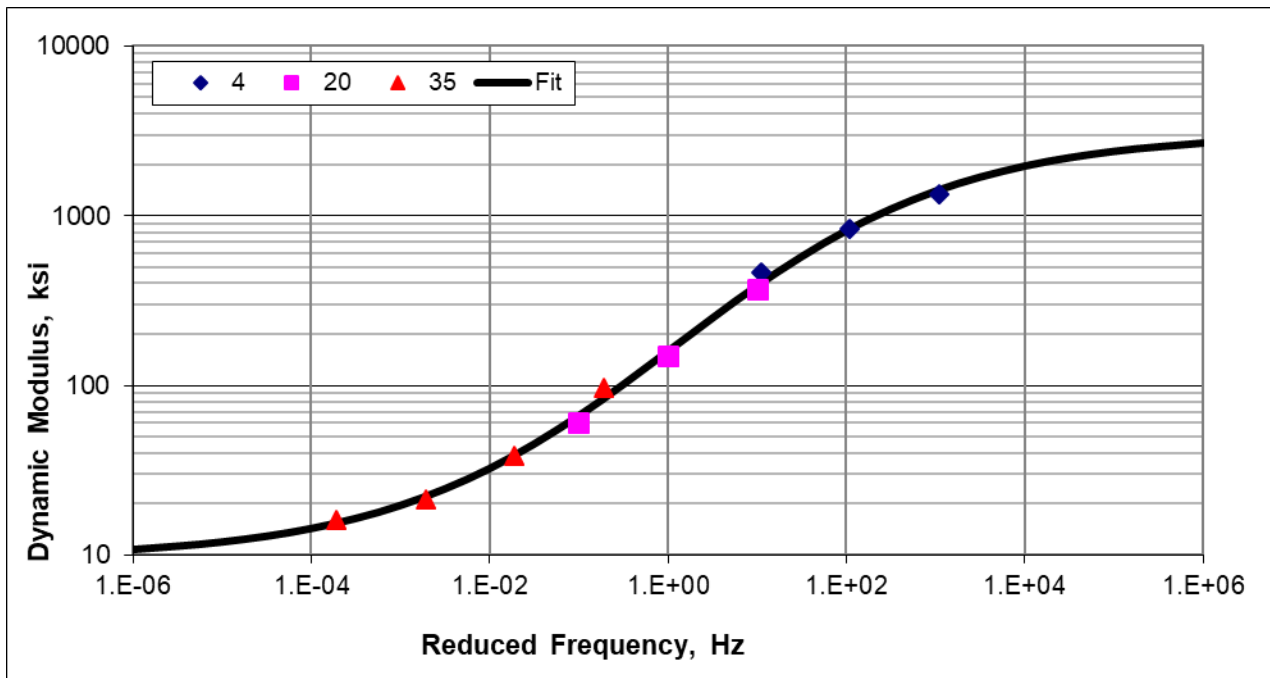


Expansion of AASHTOWare ME Design Inputs  
Final Report WHRP 0092-20-03

Asphalt Wearing Surface Mixture #0121; PG58-28V, 4 SMA

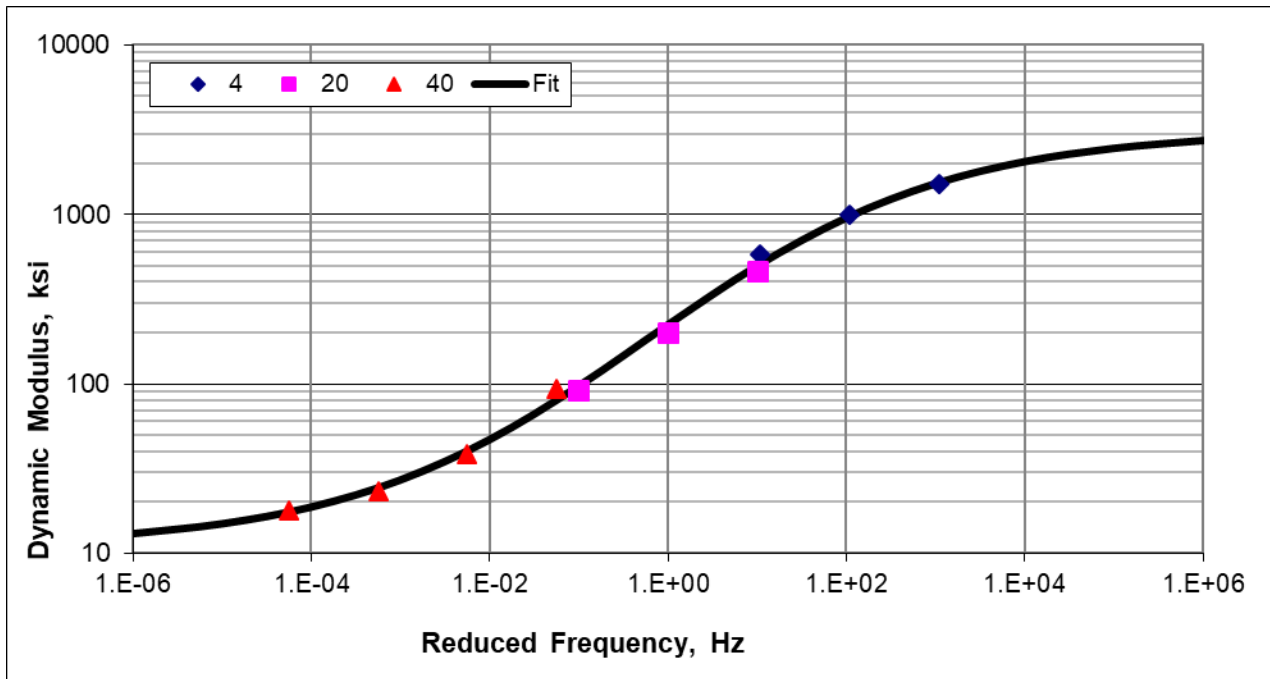


Asphalt Wearing Surface Mixture #0127; PG58-34S, 4 MT

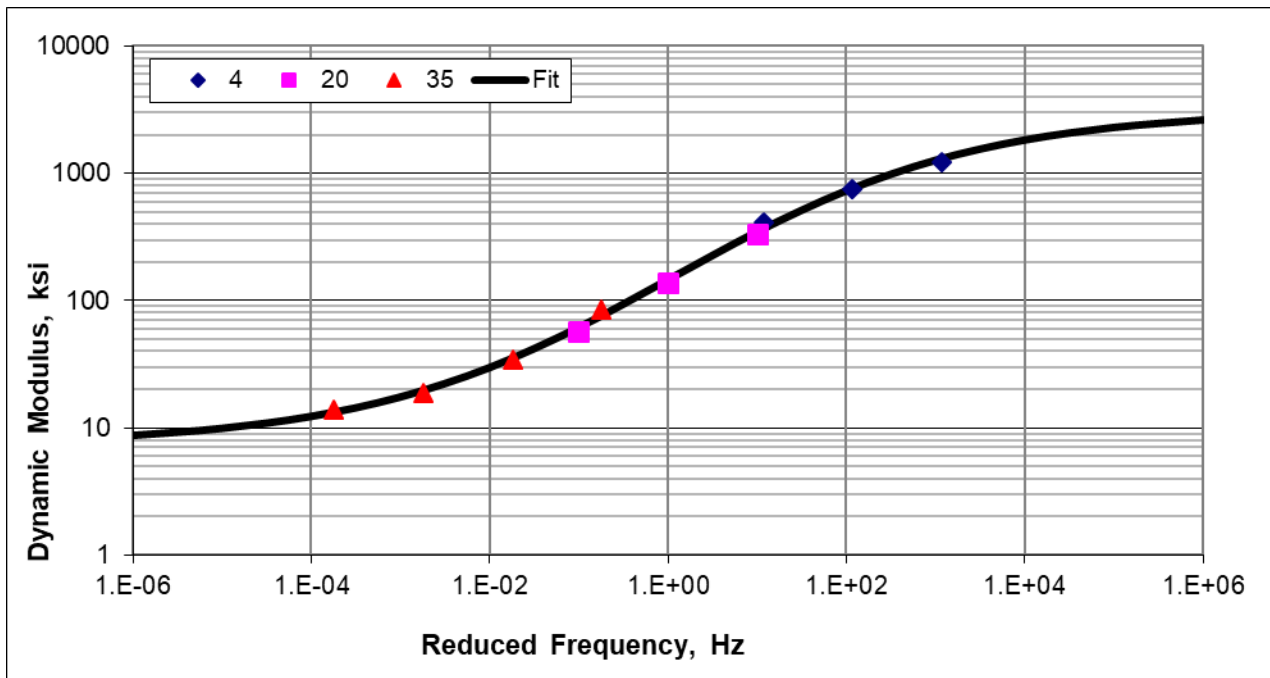


Expansion of AASHTOWare ME Design Inputs  
Final Report WHRP 0092-20-03

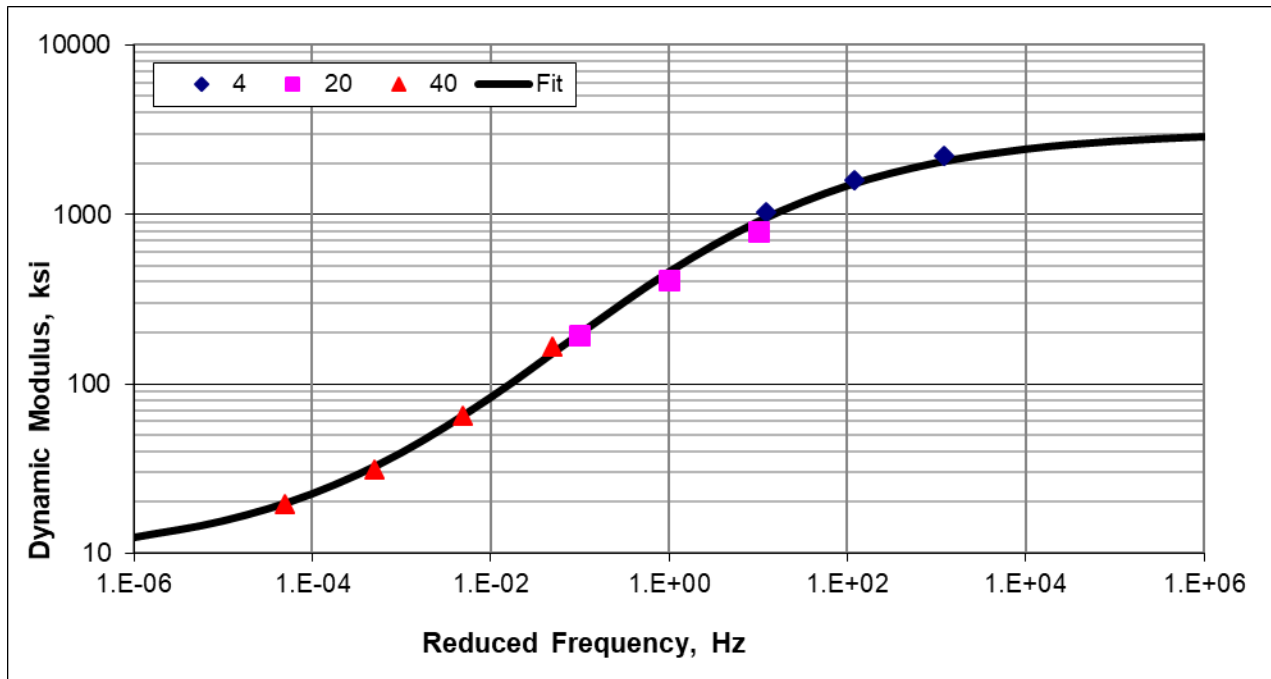
Asphalt Wearing Surface Mixture #7130; PG58-34V, 5 HT



Asphalt Wearing Surface Mixture #8357; PG58-34S, 4 LT



Wearing Surface Mixture #1020; PG58-34V, 4 SMA



### E.3 Appendix E References

Applied Research Associates, Inc (2004). *Guide for Mechanistic-Empirical Design of New and Rehabilitated Pavement Structures: Part 1-Introduction and Part 2-Design Inputs*, Final Report, NCHRP Project 1- 37A, National Cooperative Highway Research Program, Transportation Research Board, National Research Council, Washington, DC.

## APPENDIX F—IDT CREEP COMPLIANCE AND STRENGTH TEST DATA

Appendix F includes the indirect tensile creep compliance and strength test data for the asphalt mixtures measured in accordance with AASHTO T 322. A tabular summary of the test data, as well as the creep compliance master curves are included in this appendix. The regression equations embedded in the PMED software to calculate the IDT creep compliance and strength for input level 3 are explained and described in the NCHRP 1-37A final report (2004).

### F.1 Indirect Tensile Creep Compliance Tabular Summary of Test Data

Asphalt Wearing Surface Mixture #0093; IDT Strength – 512 psi.  
 PG58-28H, 4 HT; Creep Compliance, 1/psi

Loading Time, Sec.	Test Temperature		
	Minus 4°F	14°F	32°F
1	2.85E-07	3.70E-07	6.00E-07
2	3.00E-07	4.05E-07	7.00E-07
5	3.15E-07	4.95E-07	9.30E-07
10	3.37E-07	5.28E-07	1.14E-06
13	3.43E-07	5.49E-07	1.25E-06
16	3.47E-07	5.67E-07	1.29E-06
20	3.54E-07	5.88E-07	1.36E-06
25	3.63E-07	6.13E-07	1.46E-06
32	3.7E-07	6.45E-07	1.56E-06
40	3.82E-07	6.81E-07	1.71E-06
50	3.9E-07	7.2E-07	1.84E-06
63	4.07E-07	7.63E-07	2.01E-06
79	4.24E-07	8.05E-07	2.17E-06
100	4.41E-07	8.39E-07	2.28E-06

Asphalt Wearing Surface Mixture #0121; IDT Strength – 448 psi.  
 PG58-28V, 4 SMA; Creep Compliance, 1/psi

Loading Time, Sec.	Test Temperature		
	Minus 4°F	14°F	32°F
1	3.00E-07	4.30E-07	6.50E-07
2	3.15E-07	4.80E-07	7.50E-07
5	3.35E-07	5.40E-07	1.02E-06
10	3.54E-07	6.1E-07	1.31E-06
13	3.64E-07	6.41E-07	1.41E-06
16	3.71E-07	6.66E-07	1.48E-06
20	3.8E-07	6.98E-07	1.57E-06
25	3.91E-07	7.32E-07	1.69E-06
32	4.02E-07	7.74E-07	1.83E-06
40	4.14E-07	8.19E-07	1.97E-06
50	4.26E-07	8.72E-07	2.15E-06
63	4.4E-07	9.26E-07	2.35E-06
79	4.55E-07	9.89E-07	2.56E-06

**Expansion of AASHTOWare ME Design Inputs  
Final Report WHRP 0092-20-03**

100	4.63E-07	1.05E-06	2.8E-06
-----	----------	----------	---------

Asphalt Wearing Surface Mixture #0127; IDT Strength – 417 psi.  
PG58-34S, 4 MT; Creep Compliance, 1/psi

Loading Time, Sec.	Test Temperature		
	Minus 4°F	14°F	32°F
1	2.90E-07	6.00E-07	1.60E-06
2	3.30E-07	7.20E-07	2.05E-06
5	4.10E-07	9.50E-07	3.00E-06
10	5.33E-07	1.14E-06	4.06E-06
13	5.56E-07	1.22E-06	4.61E-06
16	5.73E-07	1.29E-06	4.68E-06
20	5.93E-07	1.36E-06	5.2E-06
25	6.18E-07	1.45E-06	5.8E-06
32	6.47E-07	1.54E-06	6.33E-06
40	6.8E-07	1.66E-06	6.91E-06
50	7.13E-07	1.78E-06	7.63E-06
63	7.55E-07	1.92E-06	8.66E-06
79	7.96E-07	2.1E-06	9.54E-06
100	8.3E-07	2.24E-06	1.06E-05

Asphalt Wearing Surface Mixture #0165; IDT Strength – 430 psi.  
PG58-28S, 4 HT; Creep Compliance, 1/psi

Loading Time, Sec.	Test Temperature		
	Minus 4°F	14°F	32°F
1	3.10E-07	4.60E-07	8.00E-07
2	3.35E-07	5.20E-07	9.50E-07
5	3.73E-07	6.22E-07	1.20E-06
10	4.07E-07	7E-07	1.48E-06
13	4.18E-07	7.35E-07	1.58E-06
16	4.25E-07	7.62E-07	1.69E-06
20	4.36E-07	7.97E-07	1.8E-06
25	4.48E-07	8.37E-07	1.94E-06
32	4.62E-07	8.86E-07	2.11E-06
40	4.73E-07	9.37E-07	2.29E-06
50	4.87E-07	9.93E-07	2.47E-06
63	5.01E-07	1.05E-06	2.69E-06
79	5.16E-07	1.13E-06	2.96E-06
100	5.23E-07	1.19E-06	3.15E-06



**Expansion of AASHTOWare ME Design Inputs  
Final Report WHRP 0092-20-03**

Asphalt Wearing Surface Mixture #0208; IDT Strength – 358 psi.  
PG58-28S, 4 LT; Creep Compliance, 1/psi

Loading Time, Sec.	Test Temperature		
	Minus 4°F	14°F	32°F
1	3.05E-07	5.00E-07	1.15E-06
2	3.35E-07	6.00E-07	1.50E-06
5	3.75E-07	7.30E-07	2.15E-06
10	4.05E-07	8.65E-07	2.83E-06
13	4.19E-07	9.26E-07	3.07E-06
16	4.32E-07	9.59E-07	3.3E-06
20	4.45E-07	1.02E-06	3.61E-06
25	4.61E-07	1.09E-06	3.91E-06
32	4.8E-07	1.16E-06	4.34E-06
40	5E-07	1.22E-06	4.74E-06
50	5.2E-07	1.31E-06	5.25E-06
63	5.45E-07	1.42E-06	5.79E-06
79	5.74E-07	1.53E-06	6.54E-06
100	5.96E-07	1.65E-06	7.32E-06

Asphalt Wearing Surface Mixture #0236; IDT Strength – 481 psi.  
PG58-28SH, 4 MT; Creep Compliance, 1/psi

Loading Time, Sec.	Test Temperature		
	Minus 4°F	14°F	32°F
1	3.20E-07	5.50E-07	1.50E-06
2	3.55E-07	6.80E-07	2.00E-06
5	3.98E-07	8.90E-07	2.95E-06
10	4.36E-07	1.09E-06	3.99E-06
13	4.52E-07	1.17E-06	4.46E-06
16	4.64E-07	1.23E-06	4.77E-06
20	4.82E-07	1.31E-06	5.21E-06
25	5E-07	1.39E-06	5.64E-06
32	5.23E-07	1.49E-06	6.25E-06
40	5.47E-07	1.62E-06	6.88E-06
50	5.72E-07	1.76E-06	7.51E-06
63	6.01E-07	1.92E-06	8.32E-06
79	6.33E-07	2.11E-06	9.25E-06
100	6.57E-07	2.31E-06	1.01E-05

**Expansion of AASHTOWare ME Design Inputs**  
**Final Report WHRP 0092-20-03**

Asphalt Wearing Surface Mixture #0258; IDT Strength – 457 psi.  
 PG58-28S, 4 MT; Creep Compliance, 1/psi

Loading Time, Sec.	Test Temperature		
	Minus 4°F	14°F	32°F
1	3.15E-07	6.00E-07	1.30E-06
2	3.50E-07	7.00E-07	1.65E-06
5	4.10E-07	9.00E-07	2.38E-06
10	4.63E-07	1.09E-06	3.07E-06
13	4.83E-07	1.15E-06	3.34E-06
16	4.97E-07	1.22E-06	3.6E-06
20	5.17E-07	1.3E-06	3.92E-06
25	5.35E-07	1.37E-06	4.31E-06
32	5.61E-07	1.48E-06	4.65E-06
40	5.85E-07	1.58E-06	5.13E-06
50	6.09E-07	1.67E-06	5.64E-06
63	6.37E-07	1.81E-06	6.24E-06
79	6.68E-07	1.94E-06	6.87E-06
100	6.85E-07	2.02E-06	7.49E-06

Asphalt Wearing Surface Mixture #0319; IDT Strength – 465 psi.  
 PG58-28H, 4 MT; Creep Compliance, 1/psi

Loading Time, Sec.	Test Temperature		
	Minus 4°F	14°F	32°F
1	3.10E-07	4.63E-07	8.85E-07
2	3.33E-07	5.20E-07	1.05E-06
5	3.60E-07	6.15E-07	1.40E-06
10	3.9E-07	6.96E-07	1.71E-06
13	3.99E-07	7.29E-07	1.85E-06
16	4.07E-07	7.6E-07	1.95E-06
20	4.19E-07	7.92E-07	2.09E-06
25	4.28E-07	8.32E-07	2.25E-06
32	4.41E-07	8.8E-07	2.47E-06
40	4.57E-07	9.23E-07	2.68E-06
50	4.72E-07	9.71E-07	2.94E-06
63	4.9E-07	1.03E-06	3.18E-06
79	5.07E-07	1.08E-06	3.49E-06
100	5.19E-07	1.11E-06	3.72E-06

**Expansion of AASHTOWare ME Design Inputs**  
**Final Report WHP 0092-20-03**

Asphalt Wearing Surface Mixture #1020; IDT Strength – 378 psi.  
 PG58-34V, 4 SMA; Creep Compliance, 1/psi

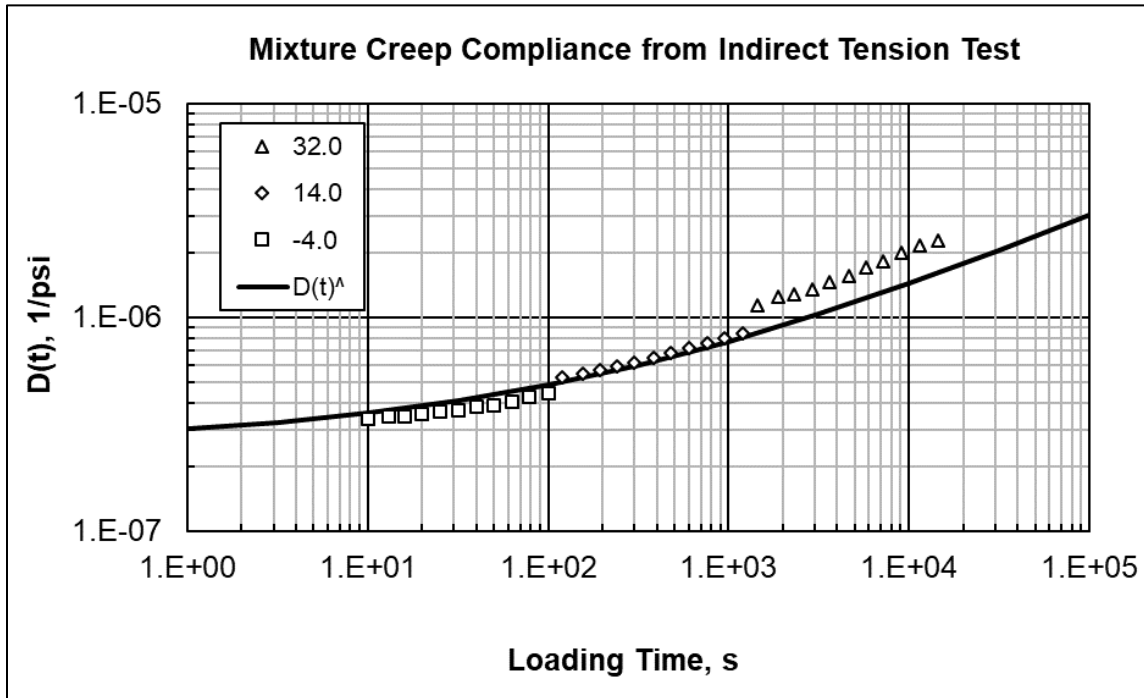
Loading Time, Sec.	Test Temperature		
	Minus 4°F	14°F	32°F
1	3.10E-07	4.80E-07	1.20E-06
2	3.40E-07	5.80E-07	1.52E-06
5	4.00E-07	7.50E-07	2.08E-06
10	4.46E-07	9.19E-07	2.68E-06
13	4.6E-07	9.8E-07	2.9E-06
16	4.76E-07	1.03E-06	3.14E-06
20	4.9E-07	1.1E-06	3.38E-06
25	5.08E-07	1.17E-06	3.66E-06
32	5.32E-07	1.26E-06	4.09E-06
40	5.52E-07	1.35E-06	4.47E-06
50	5.75E-07	1.45E-06	4.95E-06
63	5.98E-07	1.58E-06	5.35E-06
79	6.22E-07	1.71E-06	5.98E-06
100	6.33E-07	1.84E-06	6.44E-06

Asphalt Wearing Surface Mixture #8357; IDT Strength – 398 psi.  
 PG58-34S, 4 LT; Creep Compliance, 1/psi

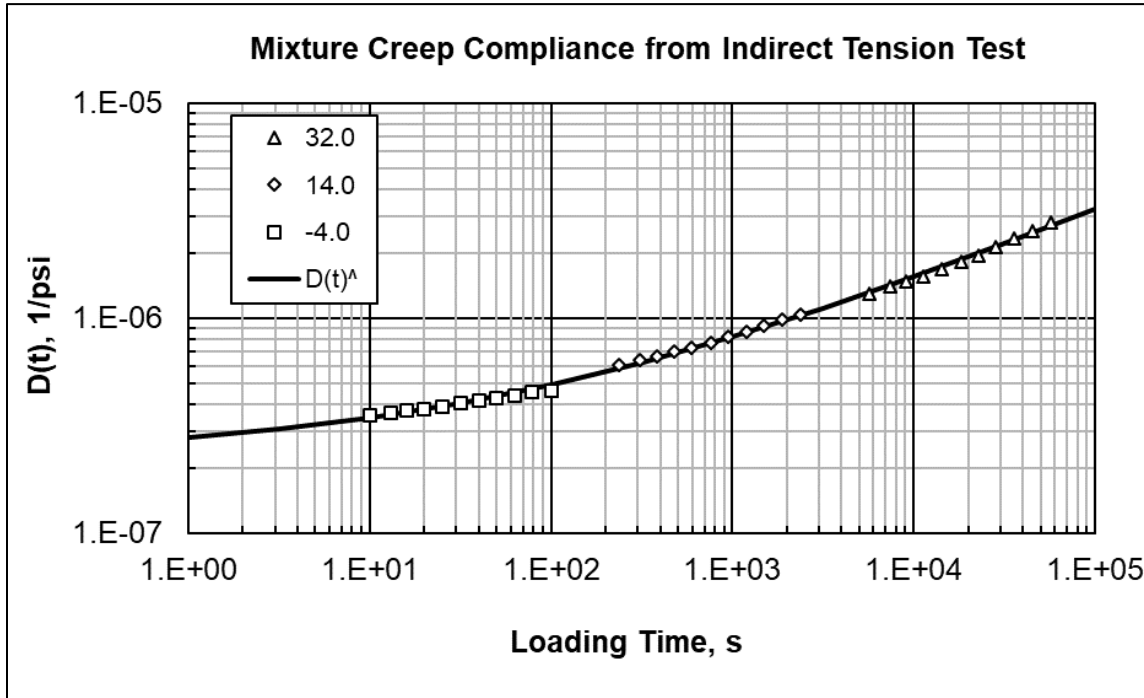
Loading Time, Sec.	Test Temperature		
	Minus 4°F	14°F	32°F
1	3.75E-07	7.00E-07	1.75E-06
2	4.15E-07	8.30E-07	2.40E-06
5	4.78E-07	1.10E-06	3.60E-06
10	5.28E-07	1.3E-06	4.89E-06
13	5.5E-07	1.4E-06	5.57E-06
16	5.7E-07	1.48E-06	6.02E-06
20	5.92E-07	1.59E-06	6.64E-06
25	6.16E-07	1.7E-06	7.21E-06
32	6.47E-07	1.86E-06	8.22E-06
40	6.77E-07	2.01E-06	8.81E-06
50	7.11E-07	2.19E-06	9.76E-06
63	7.51E-07	2.4E-06	1.06E-05
79	8.04E-07	2.68E-06	1.22E-05
100	8.51E-07	2.98E-06	1.38E-05

## F.2 Indirect Tensile Creep Compliance Master Curves

Asphalt Wearing Surface Mixture #0093; IDT Strength – 512 psi.  
PG58-28H, 4 HT

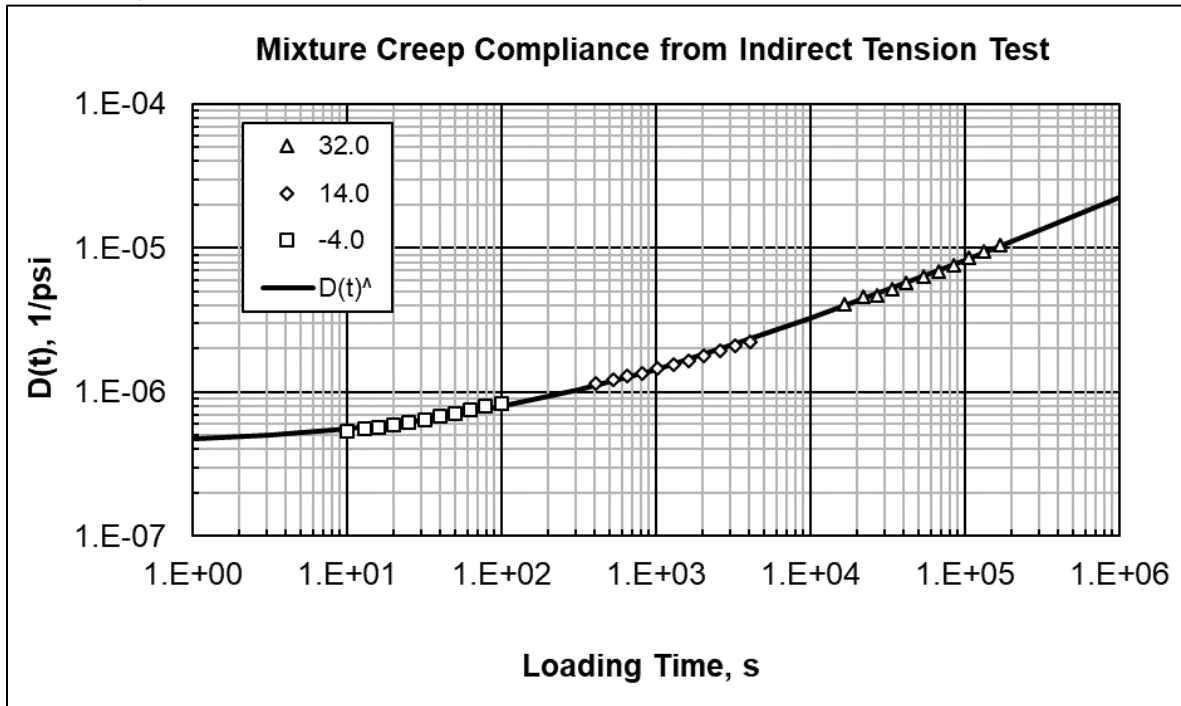


Asphalt Wearing Surface Mixture #0121; IDT Strength – 448 psi.  
PG58-28V, 4 SMA

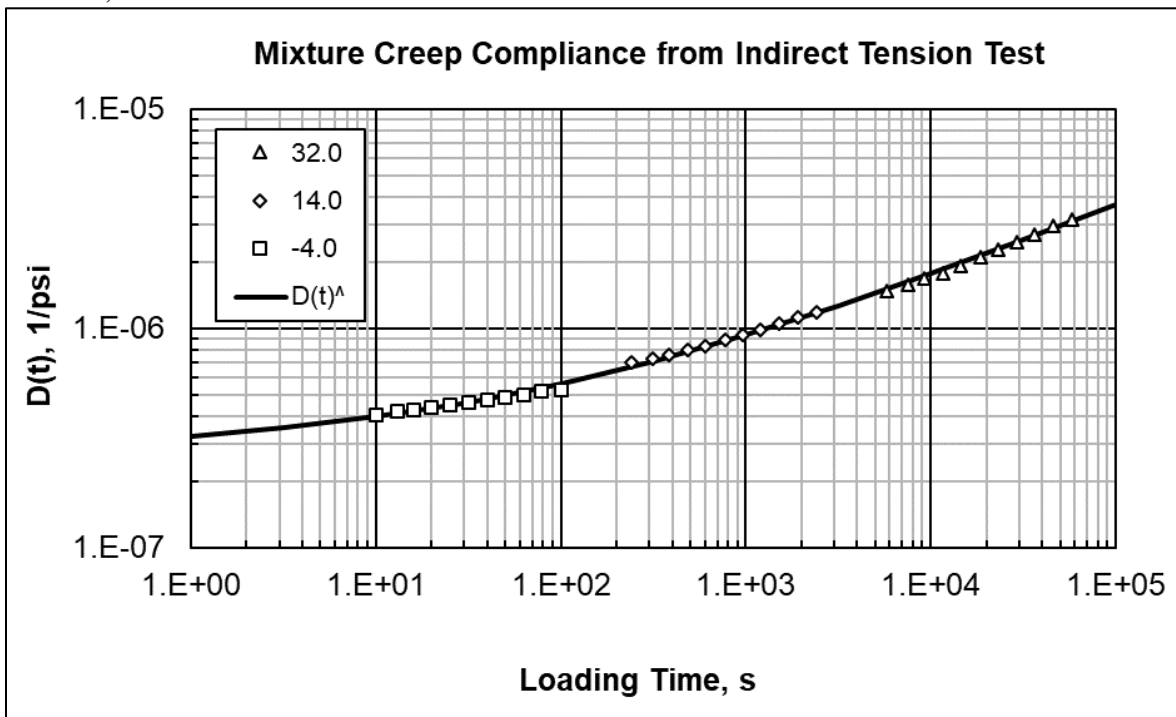


Expansion of AASHTOWare ME Design Inputs  
Final Report WHRP 0092-20-03

Asphalt Wearing Surface Mixture #0127; IDT Strength – 417 psi.  
PG58-34S, 4 MT

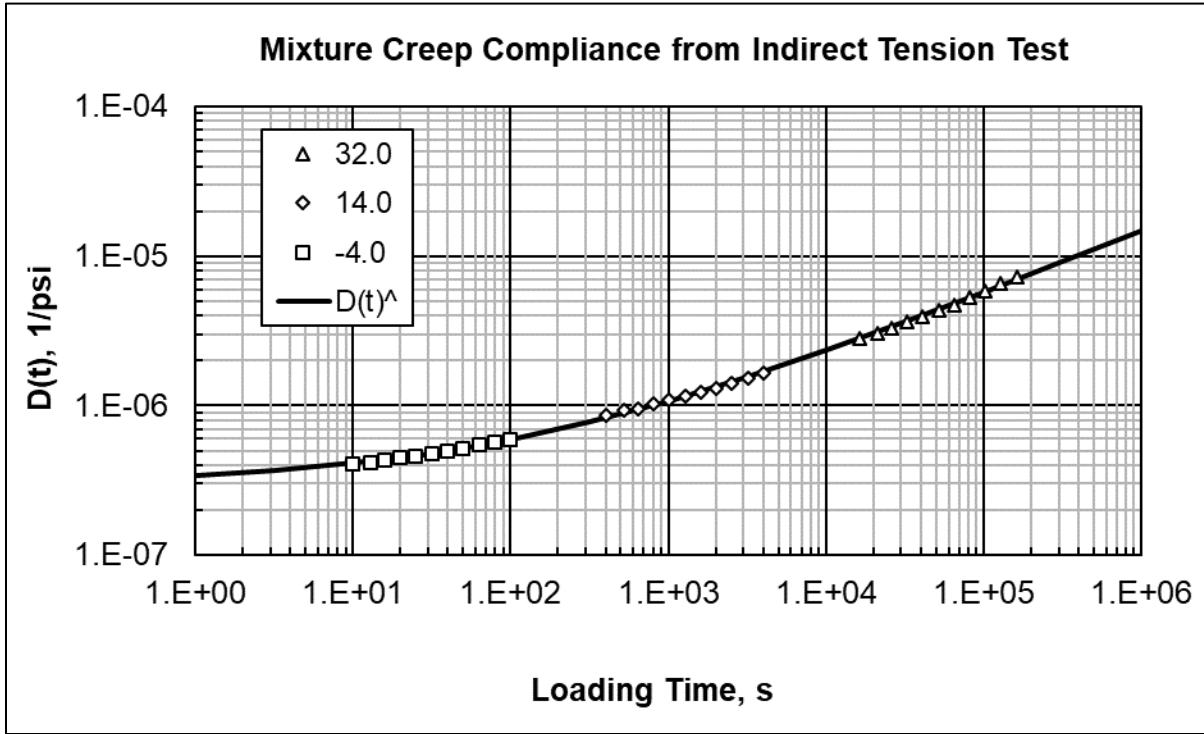


Asphalt Wearing Surface Mixture #0165; IDT Strength – 430 psi.  
PG58-28S, 4 HT

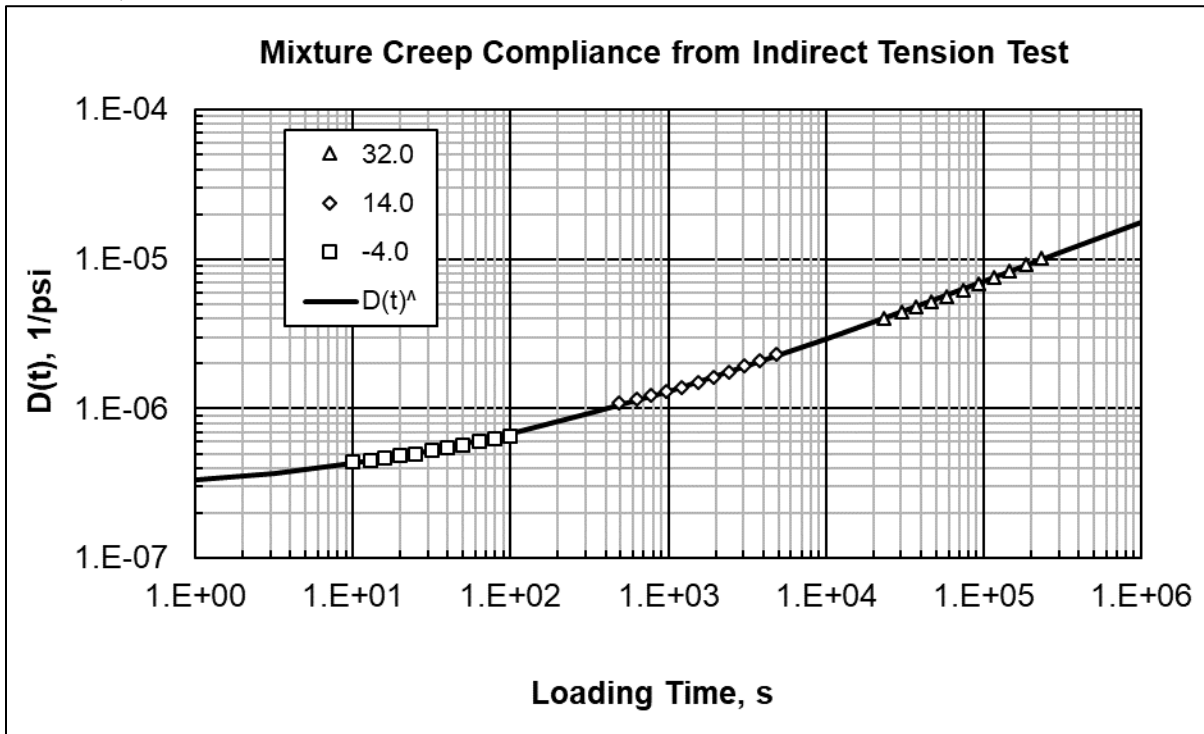


Expansion of AASHTOWare ME Design Inputs  
Final Report WHRP 0092-20-03

Asphalt Wearing Surface Mixture #0208; IDT Strength – 358 psi.  
PG58-28S, 4 LT

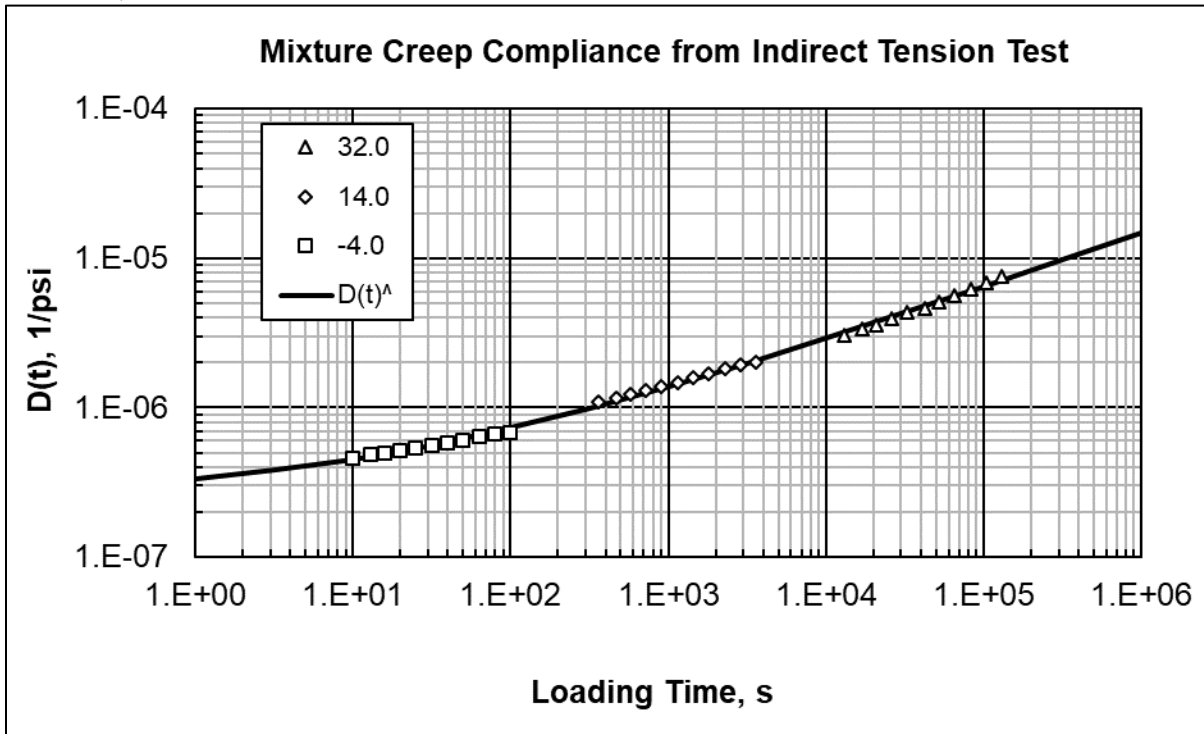


Asphalt Wearing Surface Mixture #0236; IDT Strength – 481 psi.  
PG58-28S, 4 MT

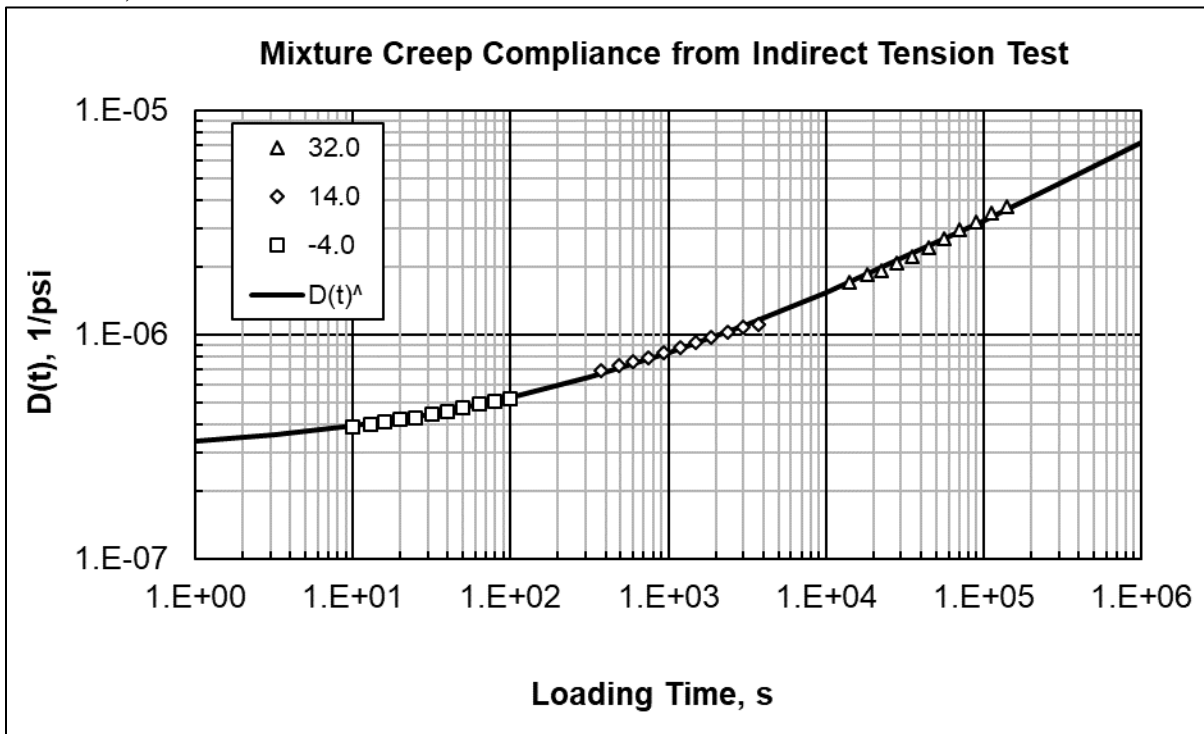


Expansion of AASHTOWare ME Design Inputs  
Final Report WHRP 0092-20-03

Asphalt Wearing Surface Mixture #0258; IDT Strength – 457 psi.  
PG58-28S, 4 MT

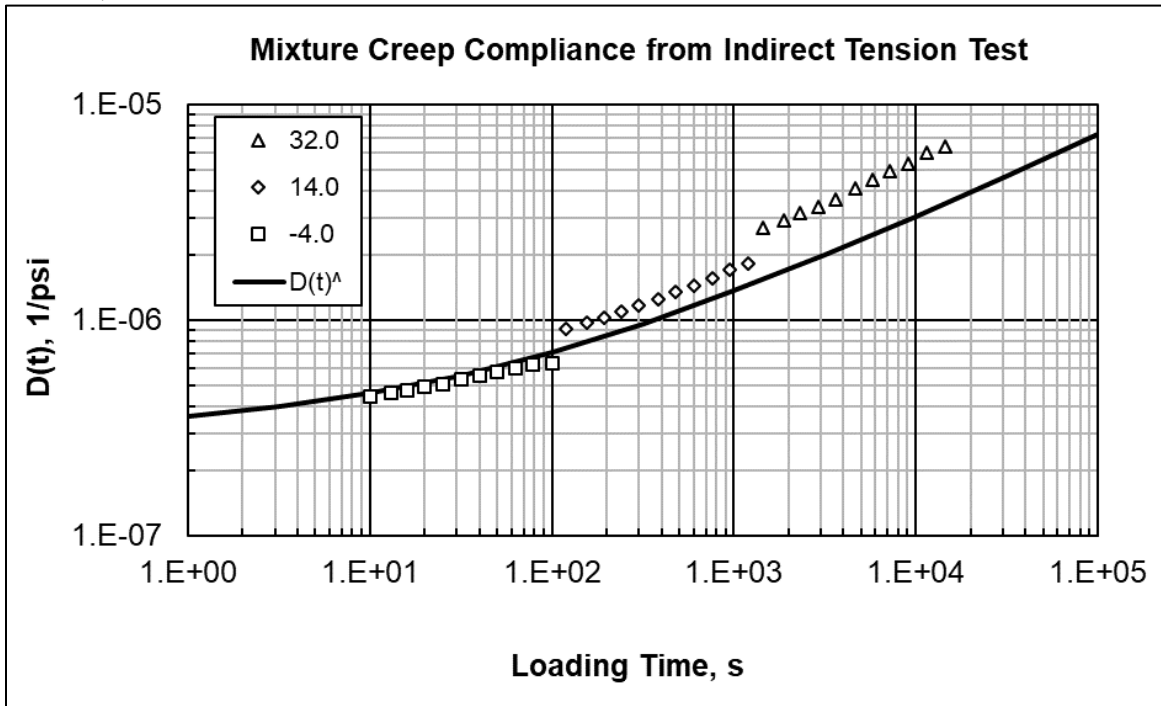


Asphalt Wearing Surface Mixture #0319; IDT Strength – 465 psi.  
PG58-28H, 4 MT

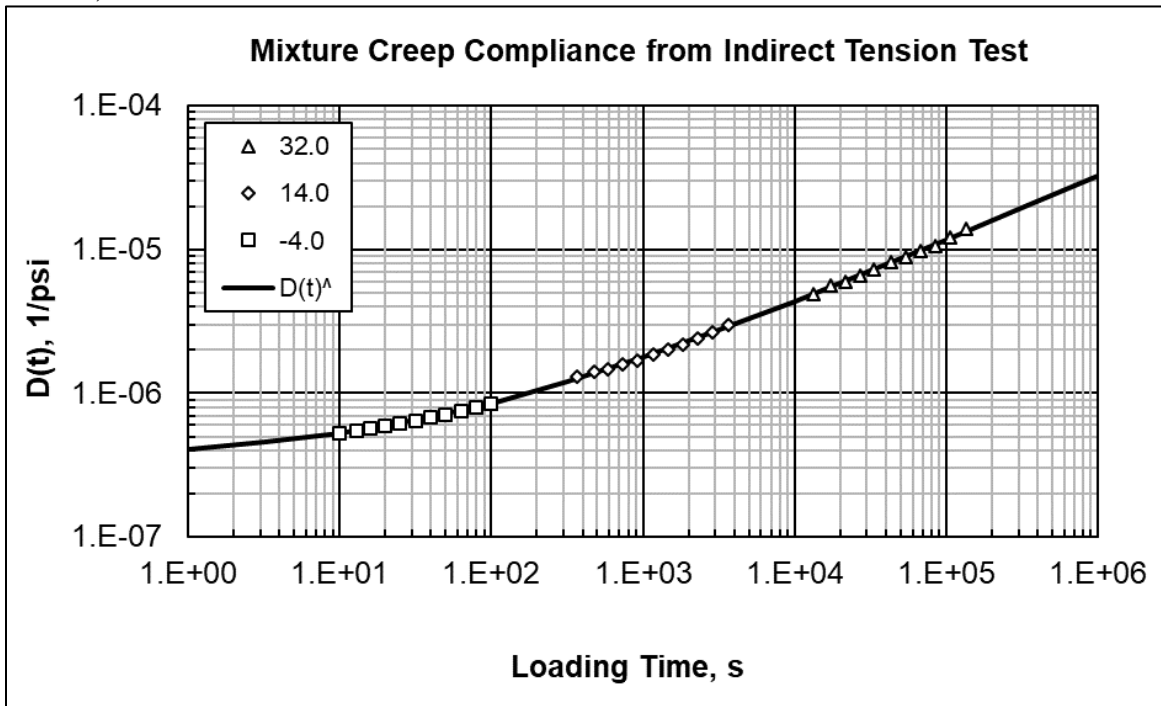


Expansion of AASHTOWare ME Design Inputs  
 Final Report WHRP 0092-20-03

Asphalt Wearing Surface Mixture #1020; IDT Strength – 378 psi.  
 PG58-34V, 4 SMA



Asphalt Wearing Surface Mixture #8357; IDT Strength – 398 psi.  
 PG58-34S, 4 LT





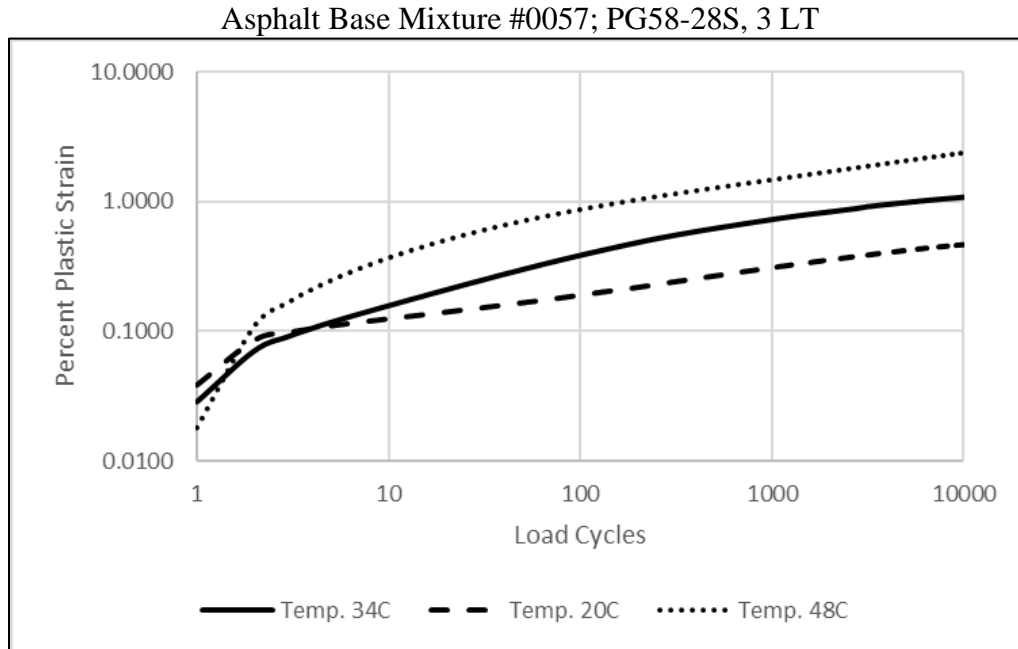
### **E.3 Appendix F References**

Applied Research Associates, Inc (2004). *Guide for Mechanistic-Empirical Design of New and Rehabilitated Pavement Structures: Part 1-Introduction and Part 2-Design Inputs*, Final Report, NCHRP Project 1- 37A, National Cooperative Highway Research Program, Transportation Research Board, National Research Council, Washington, DC.

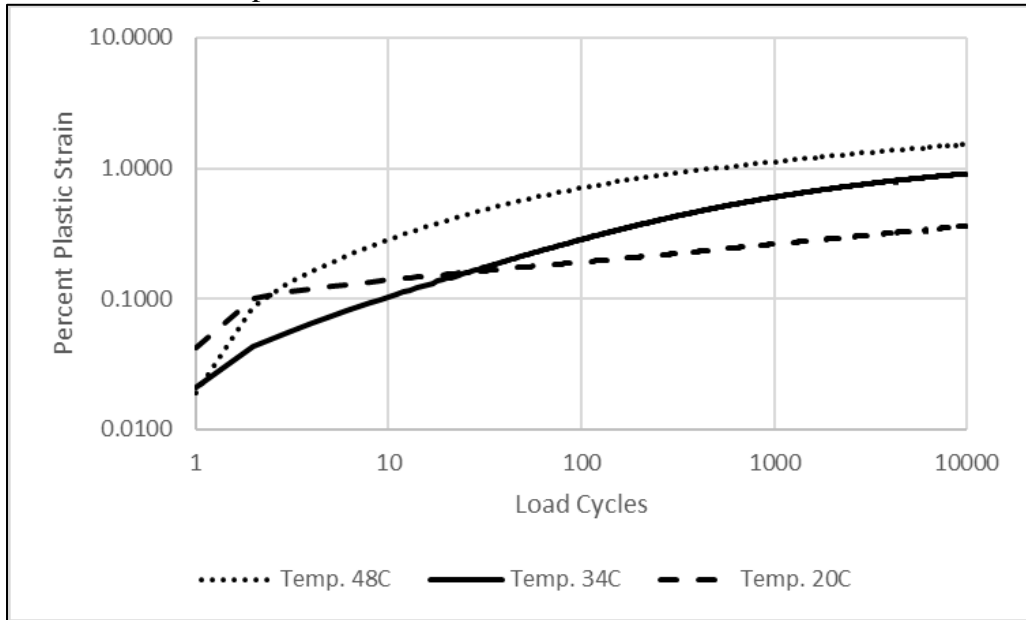
## APPENDIX G—REPEATED LOAD PLASTIC STRAIN TEST DATA

Appendix G includes the repeated load plastic strain test data for the asphalt mixtures measured in accordance with the procedure included in NCHRP Report 719 (Von Quintus, 2012). The procedure used to analyze the repeated load plastic strain test data and derive the plastic strain coefficients (the k-values of the rut depth transfer function) is also summarized in this appendix.

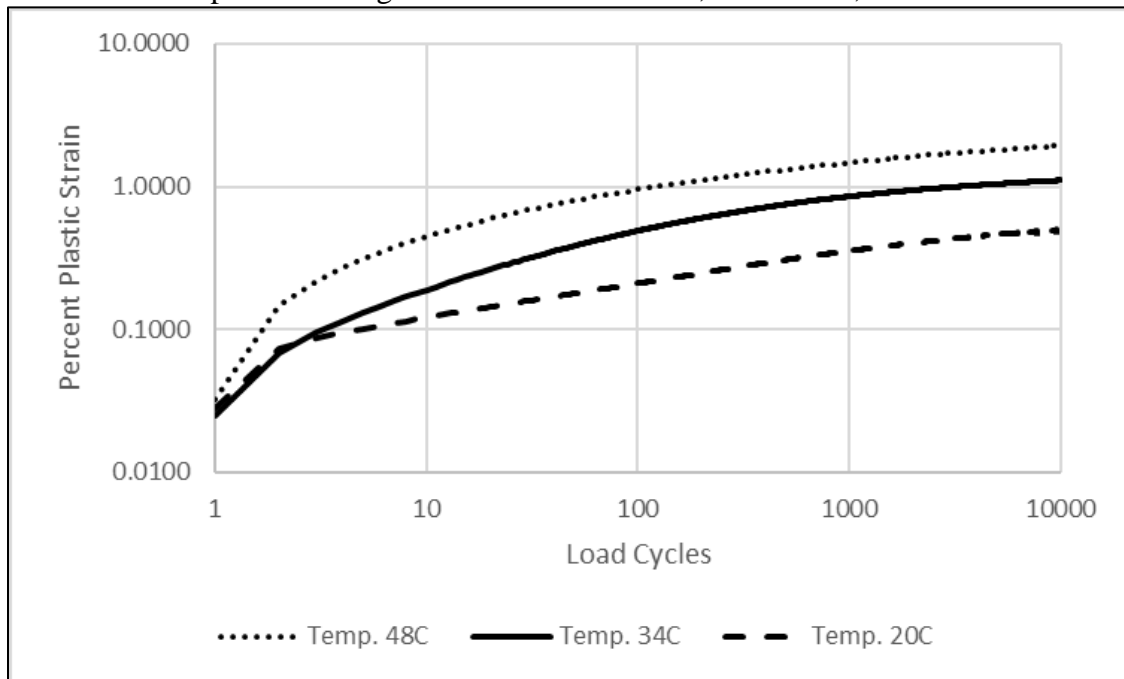
### G.1 Graphical Presentation of Repeated Load Plastic Strain Test Data



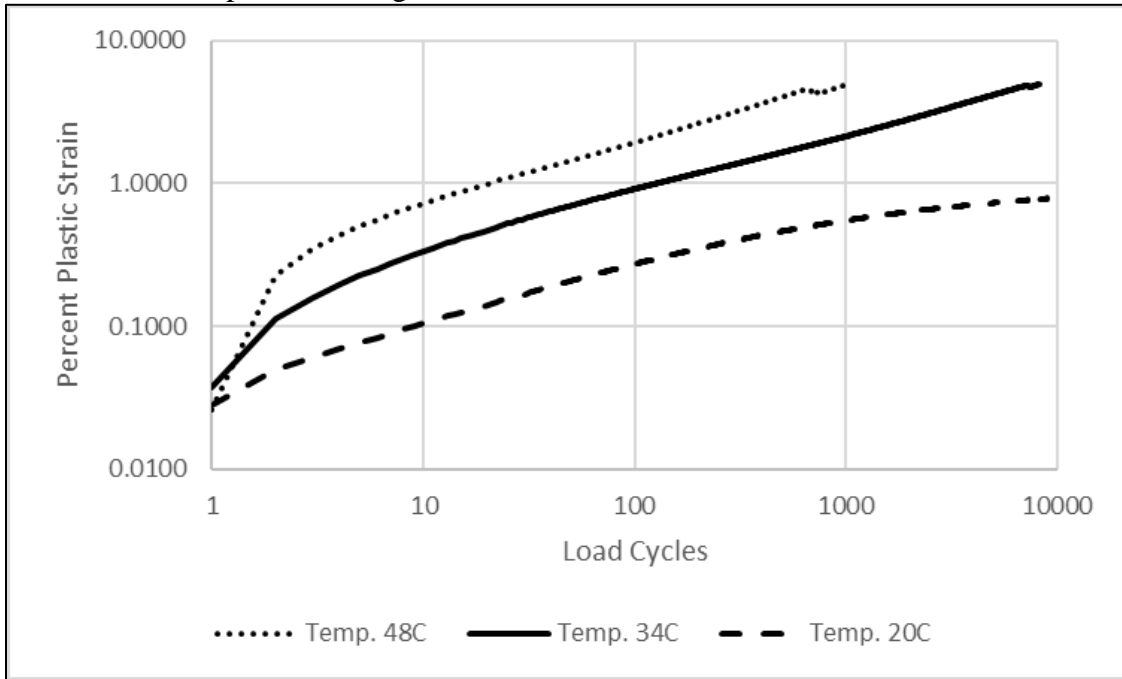
Asphalt Base Mixture #1060; PG58-28H, 3 HT



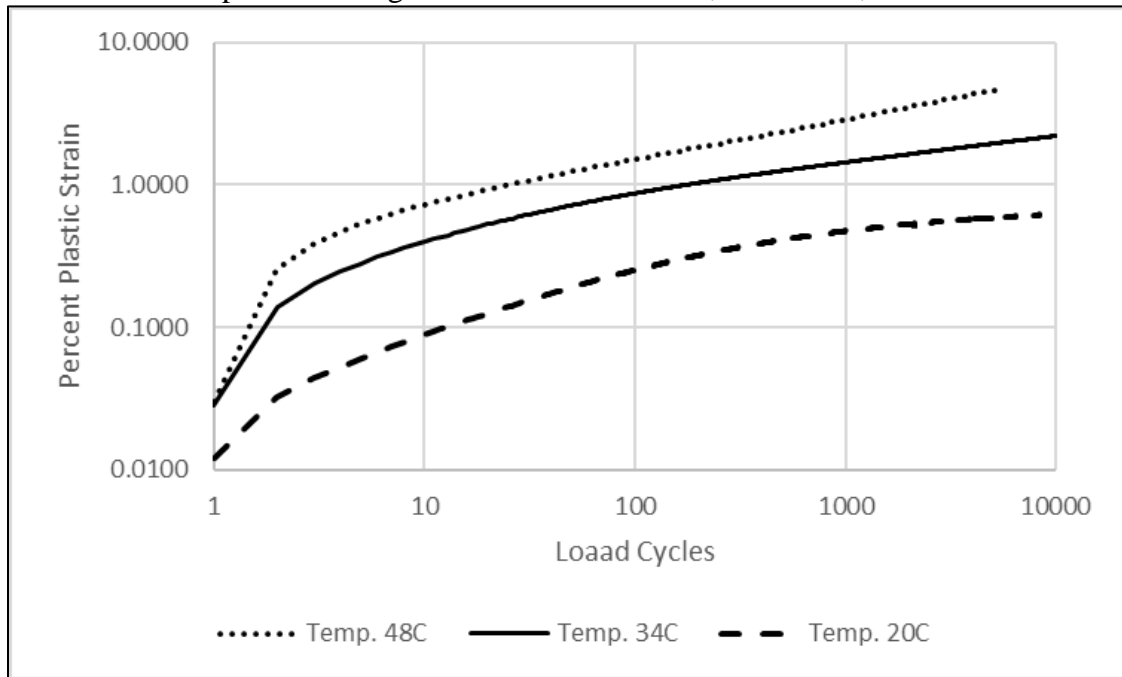
Asphalt Wearing Surface Mixture #0121; PG58-28V, 4 SMA



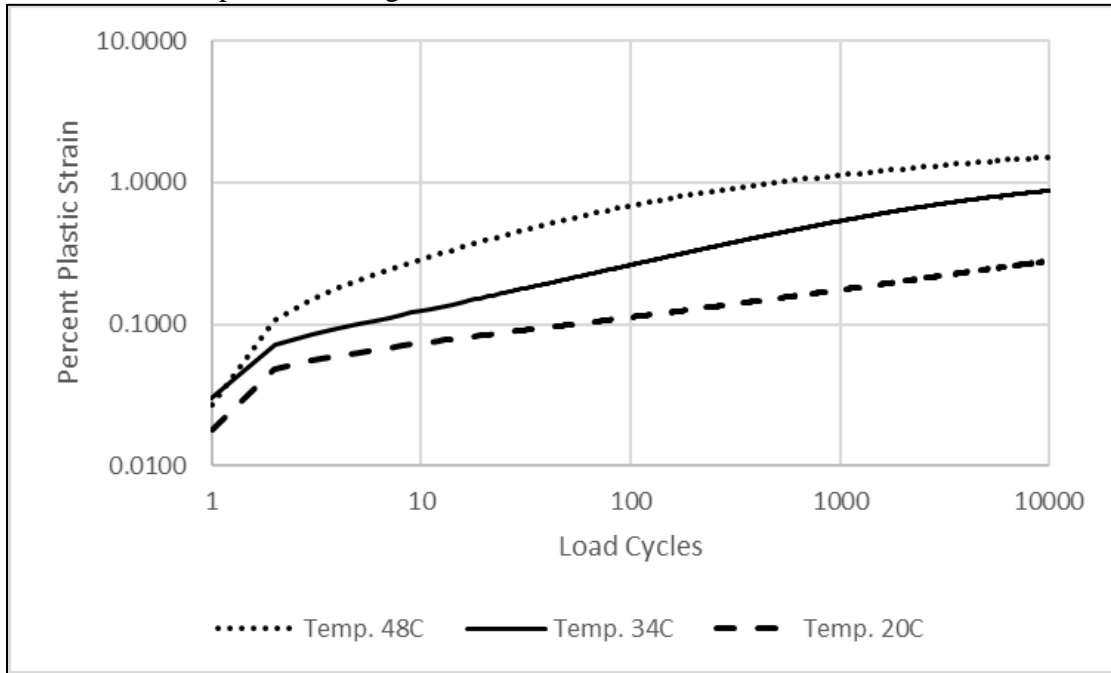
Asphalt Wearing Surface Mixture #0208; PG58-28S, 4 LT



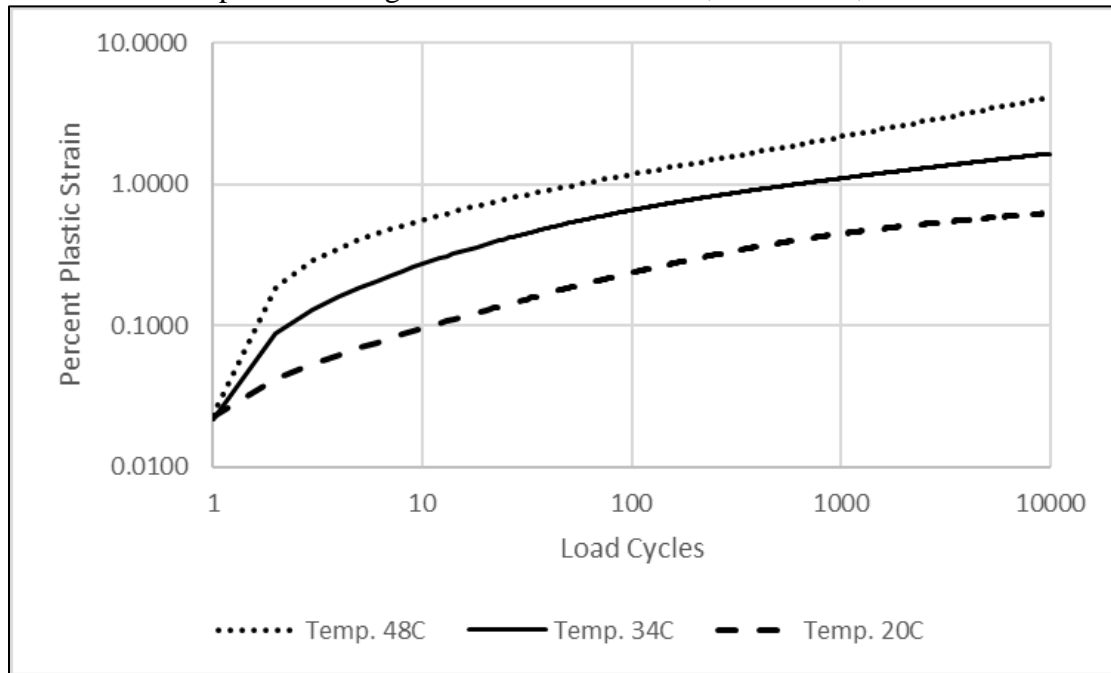
Asphalt Wearing Surface Mixture #0236; PG58-28S, 4 MT



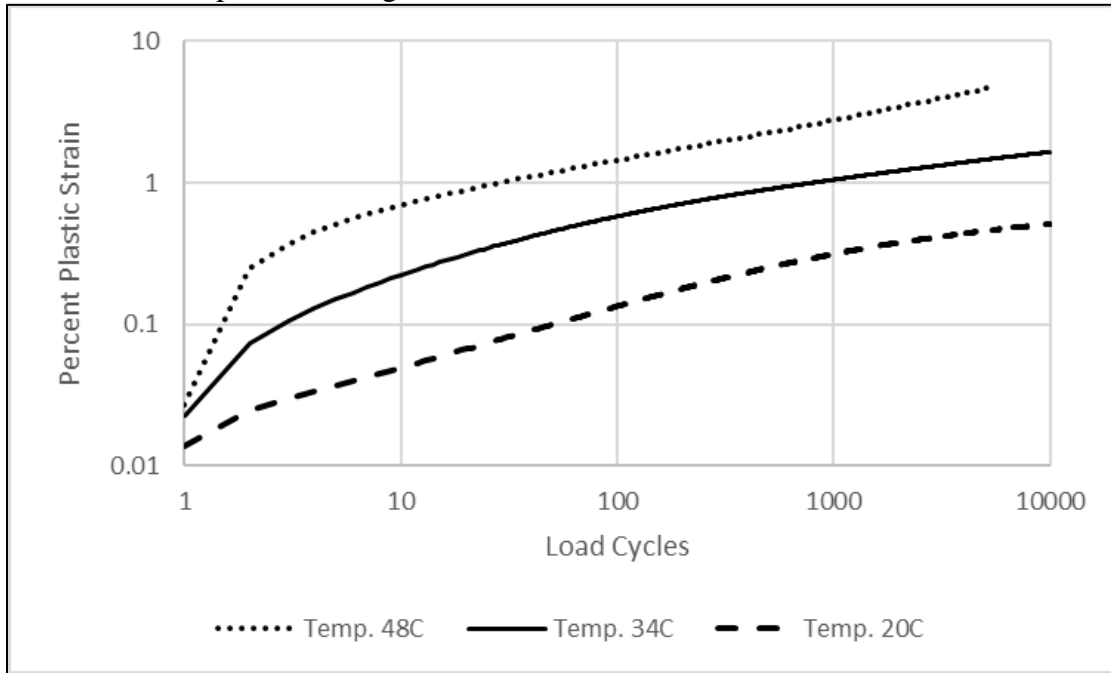
Asphalt Wearing Surface Mixture #0251; PG58-28V, 4 HT



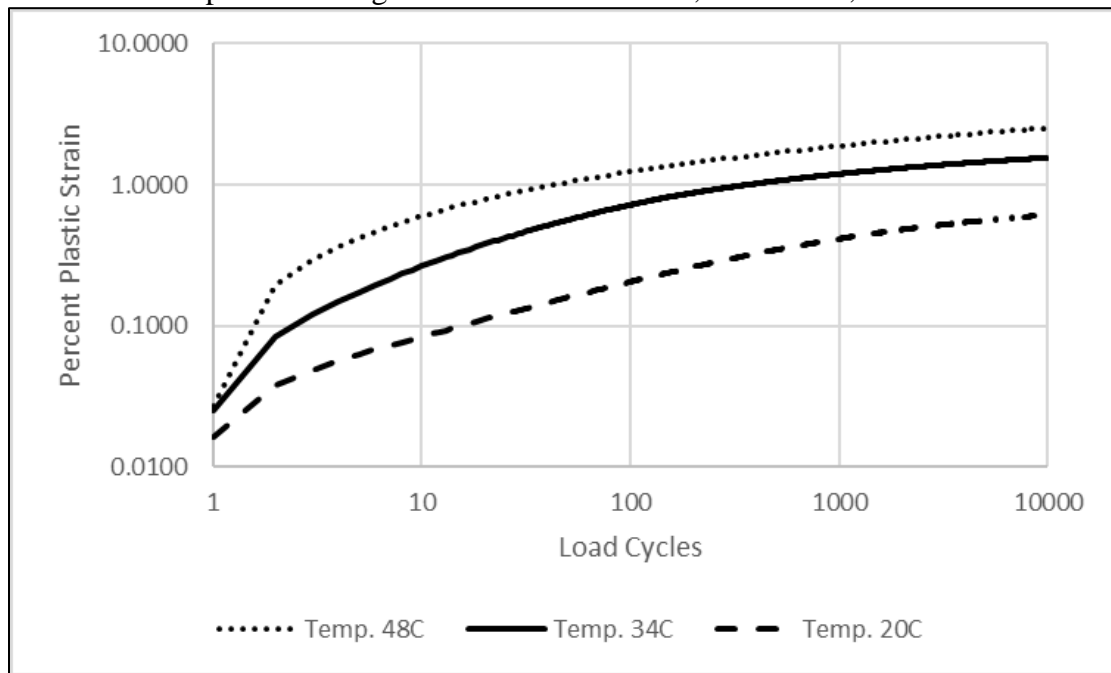
Asphalt Wearing Surface Mixture #0258; PG58-28S, 4 MT



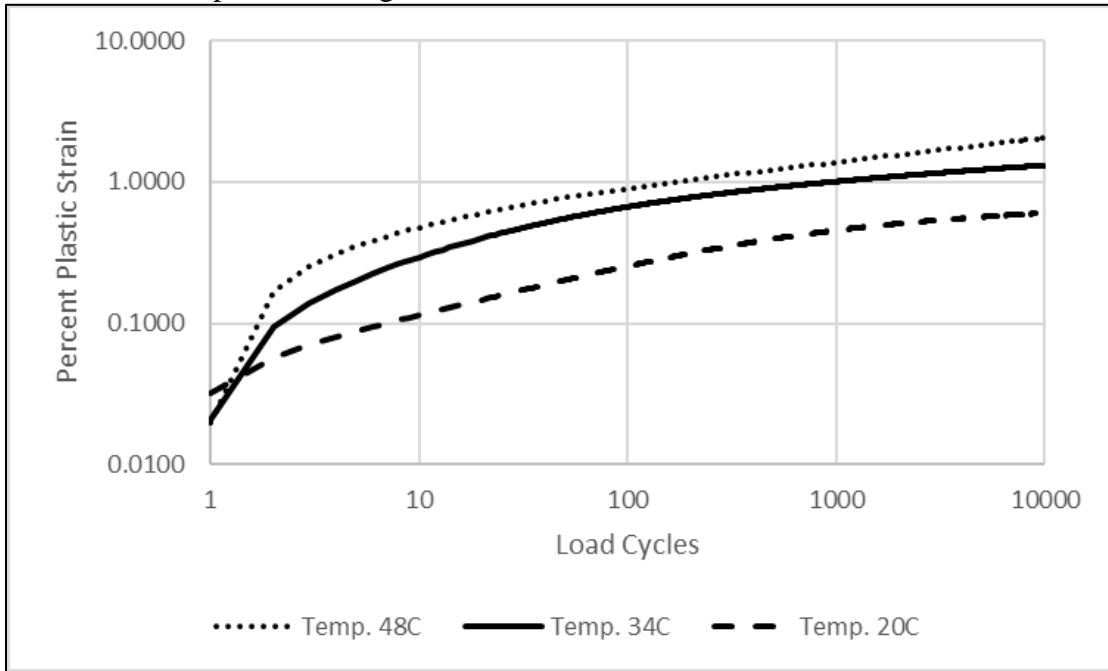
Asphalt Wearing Surface Mixture #0319; PG58-28H, 4 MT



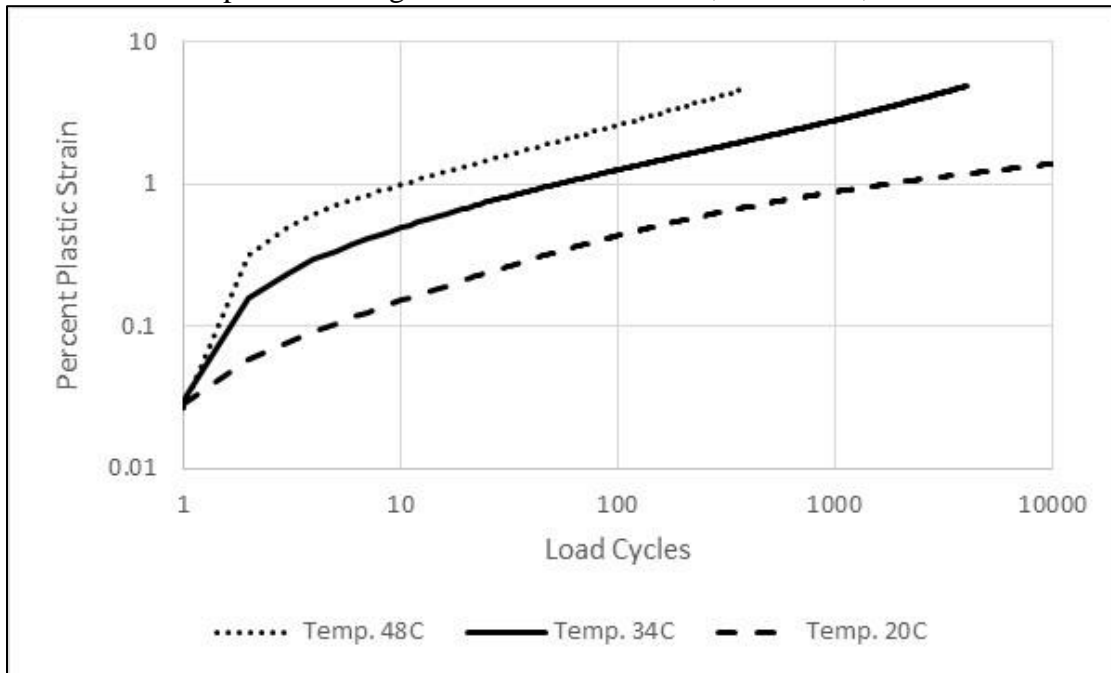
Asphalt Wearing Surface Mixture #1020; PG58-34V, 4 SMA



Asphalt Wearing Surface Mixture #7130; PG58-34V, 5 MT



Asphalt Wearing Surface Mixture #8357; PG58-34S, 4 LT



## G.2 Procedure to Derive the Plastic Strain k-Coefficients

The rut depth transfer function is shown in equation G.1. The k-coefficients in equation G.1 are derived from laboratory repeated load plastic strain test tests, which are explained below.

$$\varepsilon_p = \varepsilon_r 10^{k_{1r}\beta_{1r}} N^{k_{3r}\beta_{3r}} T^{k_{2r}\beta_{2r}} \quad \text{Equation G.1}$$

Where:

$\varepsilon_p$  = Accumulated axial plastic strain in the test specimen, in/in.

$\varepsilon_r$  = Resilient or elastic strain in the test specimen, in/in.

N = Number of load cycles.

T = Test temperature, °F.

$k_{1r}, k_{2r}, k_{3r}$  = Laboratory-derived, plastic strain coefficients using linear regression techniques.

$\beta_{1r}, \beta_{2r}, \beta_{3r}$  = Calibration coefficients; the  $\beta$ -values are not a part of the measured or laboratory-derived analyses. They are the parameters to remove any bias between the measured and predicted rut depths.

- $k_{1r}$  is the intercept. The lower the intercept, the lower the predicted rut depth.
- $k_{3r}$  is the number of load cycles exponent or slope within the secondary zone, and assumed to be independent of temperature. The lower the slope, the lower the growth rate of the predicted rut depth and the lower the predicted rut depth.
- $k_{2r}$  is the temperature exponent and assumed to be independent of time. The lower the temperature exponent, the less sensitive plastic strains are to temperature and the lower the predicted rut depth.

The procedure to derive the asphalt rut depth k-coefficients is summarized in this section of Appendix G and is grouped into three analyses or interpretation of the laboratory test results, which are listed below.

1. Classification of accumulative plastic strain responses.
2. Determining the slope and intercept form the steady state region of individual test specimens.
3. Combining test results for similar responses to derive the plastic strain coefficients.

### G.2.1 Definition/Classification of the Accumulated Plastic Strain Responses

The results from the repeated load plastic strain (see section G.1) typically go through three zones or regions, which were described in Chapter 3. The overall repeated load plastic strain accumulations, however, are classified into 3 response patterns as defined and explained below, which can include two or three of the three regions (see Figure G37, Figure G38, and Figure G39):



- 1) The log of the plastic strain continually increases linearly with the log of the number of load cycles beyond the primary zone or region, defined as the steady-state or secondary stage – Pattern A. In other words, there is no tertiary flow, as illustrated in Figure G37.
- 2) The log of the plastic strain increases at an increasing rate beyond the steady-state zone, defined as tertiary flow or the tertiary zone – Pattern B. This accumulated plastic strain response is illustrated in Figure G38.
- 3) The log of the plastic strain increases with the log of the number of load cycles but at a decreasing rate beyond the steady-state region, defined as the follow-on or second primary zone – Pattern C. This accumulated plastic strain response is illustrated in Figure G39.

Each test specimens should be classified into one of the different accumulated plastic strain response patterns. The accumulated plastic strain response pattern of each test specimen is determined by first determining if tertiary flow occurred during the test (Pattern B). This can be done using the flow number algorithm from AASHTO T 378. If tertiary flow was not exhibited or found, the test specimen accumulated plastic strain response is evaluated for the occurrence of a second primary stage or plastic strain hardening (Pattern C). This is done by determining the incremental slope with the number of load cycles. When the slope starts to decrease with the number of loading cycles is the start of the second primary stage or region.

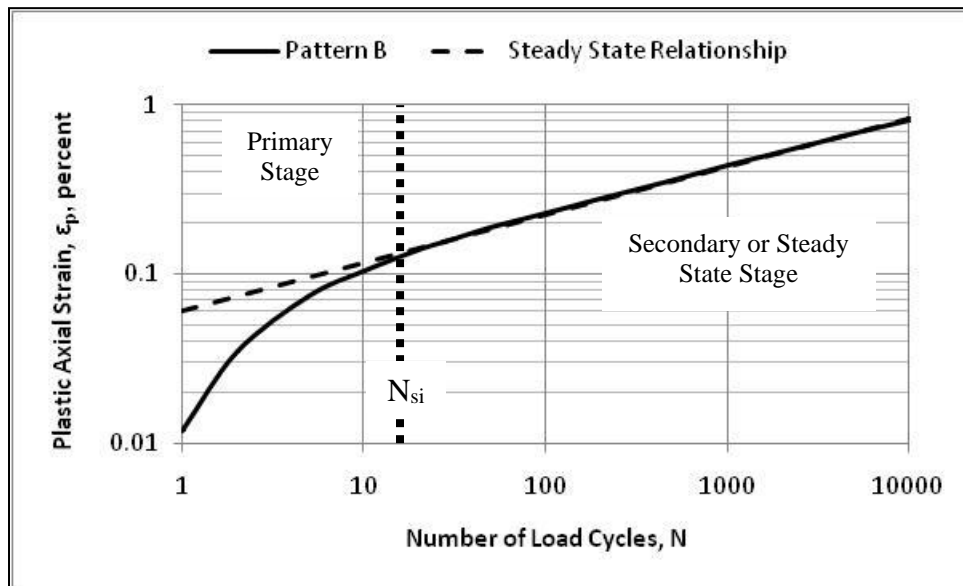


Figure G37. Pattern A typical plastic strain curve for an asphalt mixture in logarithmic scale.

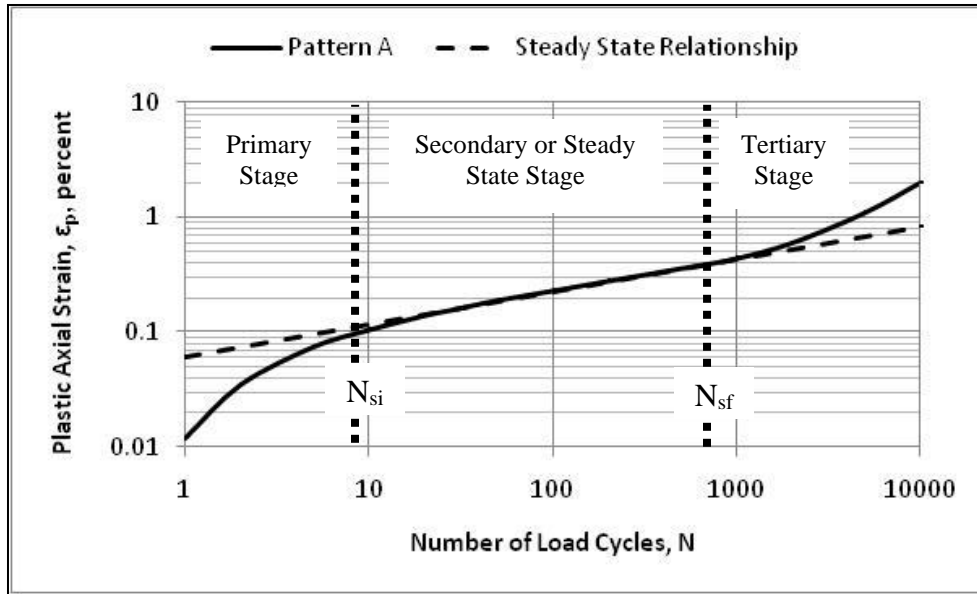


Figure G38. Pattern B typical plastic strain curve for an asphalt mixture in logarithmic scale.

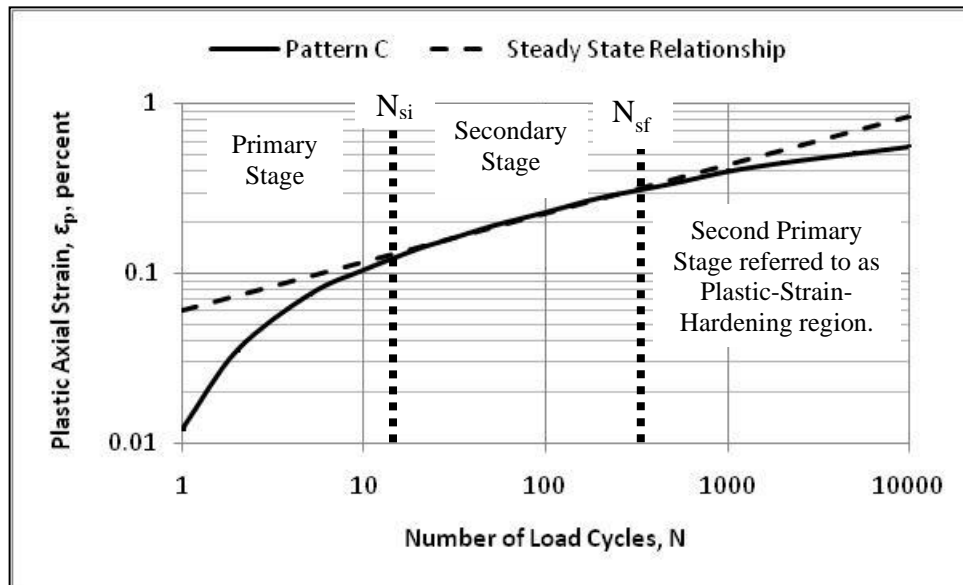


Figure G39. Pattern C typical plastic strain curve for an asphalt mixture in logarithmic scale.

### G.2.2 Determine Plastic Strain Coefficients for Individual Test Specimens

The primary analysis of repeated load plastic strain test data is the determination of the slope,  $b$ , and log-intercept,  $a$ , of the secondary zone of the plastic strain curve (see Figure G37, Figure G38, and Figure G39). The intercept and slope for each test specimen are obtained by fitting the data within the secondary or steady state zone of the plastic strain curve to the simplified equation G.2

using linear regression techniques. The following provides some guidance on determining the slope and intercept of individual test specimens.

$$\log(\varepsilon_p) = \log(a) + b * \log(N)$$

Equation G.2

Where:

$\varepsilon_p$  = Plastic axial strain

N = Number of load cycles

a = Intercept from the secondary or steady state zone

b = Slope for the secondary or steady state zone

The following lists the steps to determine the slope and intercept for each individual test specimen and how they should be combined to determine the slope and intercept for the same test temperatures.

1. For test specimens that exhibit tertiary flow (Pattern B, Figure G38), exclude the data within the tertiary flow zone. Inspect the testing equipment to ensure that the membrane is sealing properly, there are no leaks in the membrane, and the specimen is properly vented. The following are some options to consider in interpreting the test data.
  - a. If tertiary flow was exhibited on specimens within each test temperature, simply exclude the plastic strains measured within the tertiary flow zone and derive the intercept and slope in accordance with #d below, except the upper number of load cycles is the point where tertiary flow occurs. However, tertiary flow occurring within each test temperature is an indication that the mixture is susceptible to lateral distortion and excessive rut depths. The lower number of load cycles is where the steady state zone starts (typically from 100 to 1,000 load cycles).
  - b. If tertiary flow was exhibited at one or both of the lower test temperatures, eliminate that portion of the plastic strain curve and derive the slope and intercept in accordance with #d 3 below, except that the upper number of load cycles is the point at which tertiary flow occurred.
  - c. If tertiary flow occurs only on the specimens tested at the high test temperature and continues to occur on additional specimens after ensuring there are no membrane leaks and the specimen is properly vented, then decrease the testing temperature by 5 °C (9 °F). If tertiary flow continues to be observed at the revised high test temperature, eliminate that portion of the plastic strain curve and derive the slope and intercept in accordance with #d below, except the upper number of load cycles is the point at which tertiary flow occurs.
  - d. Calculate the slope and intercept in the steady state region; between the number of load cycles where the steady state region starts and ends.
2. For test specimens that do not exhibit tertiary flow (Pattern A, Figure G37), fit the data from 1,000 to 10,000 load cycles to equation G.2 using linear regression. The 1,000 load

cycle First take the base 10 logarithm of the number of load cycles and the base 10 logarithm of the plastic strain. Then use linear regression to determine the slope and intercept of the secondary zone of plastic strain curve. Eliminating the first 1,000 load cycles is to exclude the primary zone from the regression analysis.

3. For test specimens that exhibit a second primary zone (Pattern C, Figure G39), fit the data within the steady state region to equation G.2 using linear regression. For test specimens that do not exhibit a clear steady state region, fit the data between load cycle 1,000 to cycle 10,000 to determine the slope and intercept.

### ***G.2.3 Combine Results to Derive the Plastic Strain k-Coefficients***

The MEPDG assumes the number of load cycles exponent,  $b$  or  $k_{3r}$ , is independent of temperature. This assumption, however, is not applicable to all asphalt mixtures over the entire temperature range between the winter and summer months. The assumption was evaluated within NCHRP project 9-30A by comparing the results between input levels 1, 2, and 3 for plastic strain coefficients (Von Quintus, et al., 2013). The results suggested the error from this assumption was nil compared to the errors associated with other parameters, especially the rut depth measurement error in comparing the predicted and measured rut depths.

The following lists the steps to determine the plastic strain coefficients in equation G.1 for specific dense-graded asphalt mixtures; the data from all test temperatures combined.

1. For equations G.1 and G.2,  $k_{3r}$  is equal to  $b$  and  $k_{1r}$  is defined by the intercept and resilient strain for a specific test temperature, as shown in equation G.3.
2. The resilient or elastic axial strain for each test temperature for the repeated load permanent deformation test is required to derive the intercept and temperature exponent. The resilient strain is measured and recorded as part of the repeated load plastic strain test.

$$k_{1r} = \text{Log}(a_{(T)}) - \text{Log}(\epsilon_r) - k_{2r} \text{Log}(T) \quad \text{Equation G.3}$$

Where:

$a_{(T)}$  = Intercept from the secondary zone of the plastic strain versus load cycles relationship on a logarithmic scale for a specific test temperature.

3. Determine the average  $k_{3r}$ , slope or number of load cycles exponent from the secondary zone, in accordance with the following rules.
  - a. If the slope does not consistently change with temperature (consistently and statistically increase or decrease with test temperature), average the slopes or  $b$  values from all tests.
  - b. If the slope consistently increases or decreases with temperature but the increase or decrease is statistically indifferent, average the slopes or  $b$  values from all tests.
  - c. If the slope is statistically indifferent between the two higher test temperatures but these two are different from the slope measured at the low test temperature, average

the slopes or b values from the two higher test temperatures and ignore the results from the low test temperature.

- d. If the slope consistently increases or decreases with test temperature and there is a statistical difference between all three test temperatures, determine the representative slope at the equivalent annual temperature for rut depth. The equivalent annual temperature can be calculated by equation G.4) by interpolating between the three test temperatures.

$$T_{RD\ Equiv} = 0.6651(T_{LTPPBind}) - 3.4427 \quad \text{Equation G.4}$$

Where:

$$\begin{aligned} T_{RD\ Equiv} &= \text{Equivalent annual temperature for the rut depth predictions, } ^\circ\text{C} \\ T_{LTPPBind} &= \text{LTPPBind temperature at the 50 percent reliability level, } ^\circ\text{C} \end{aligned}$$

- e. If the average slope or b value is less than 0.16, simply set the slope to 0.16. The reason for not using b values less than 0.16 is that the slope derived from the field rut depth time history data collected within NCHRP project 9-30A (NCHRP Report #719) was always greater than an average value of 0.22 (Von Quintus, et al., 2012). As such 0.16 times the field adjustment or calibration factor of 1.36 equals 0.22. The field adjustment factor is assumed to be mixture independent.
4. Determine the temperature exponent,  $k_{2r}$ , and intercept,  $k_{1r}$ , for all test temperatures using linear regression analyses for equation G.2.

### **G.3 Appendix G References**

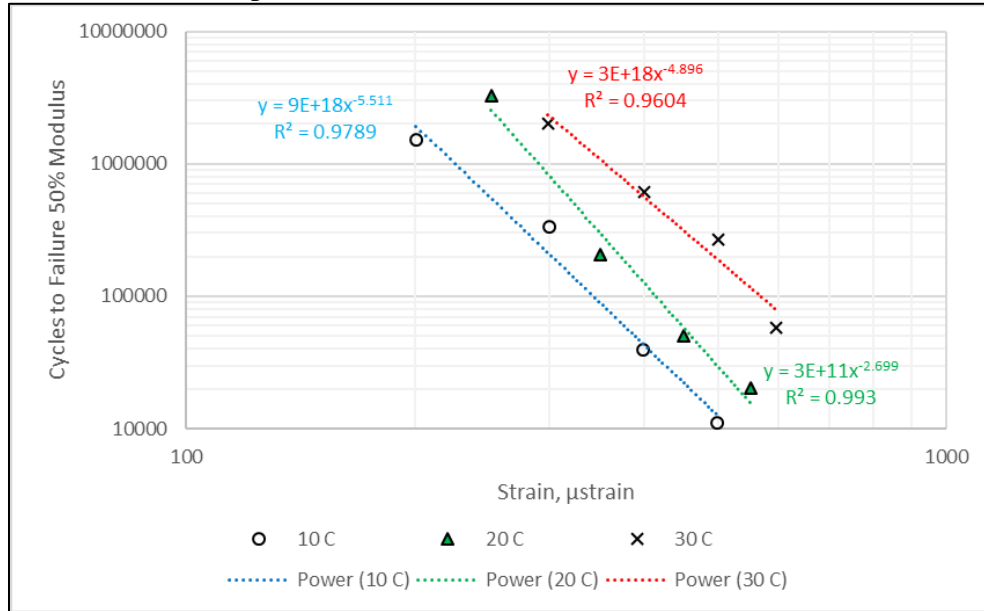
Von Quintus, Harold, Chuck Schwartz, Ramon Bonaquist, Jagannath Mallela, and Regis Carvalho, *Calibration of Rutting Models for HMA Structural and Mixture Design*, Report Number 719, National Cooperative Highway Research Program, Transportation Research Board of the National Academies, Washington, DC, April 2012.

## APPENDIX H—BENDING BEAM FATIGUE STRENGTH TEST DATA

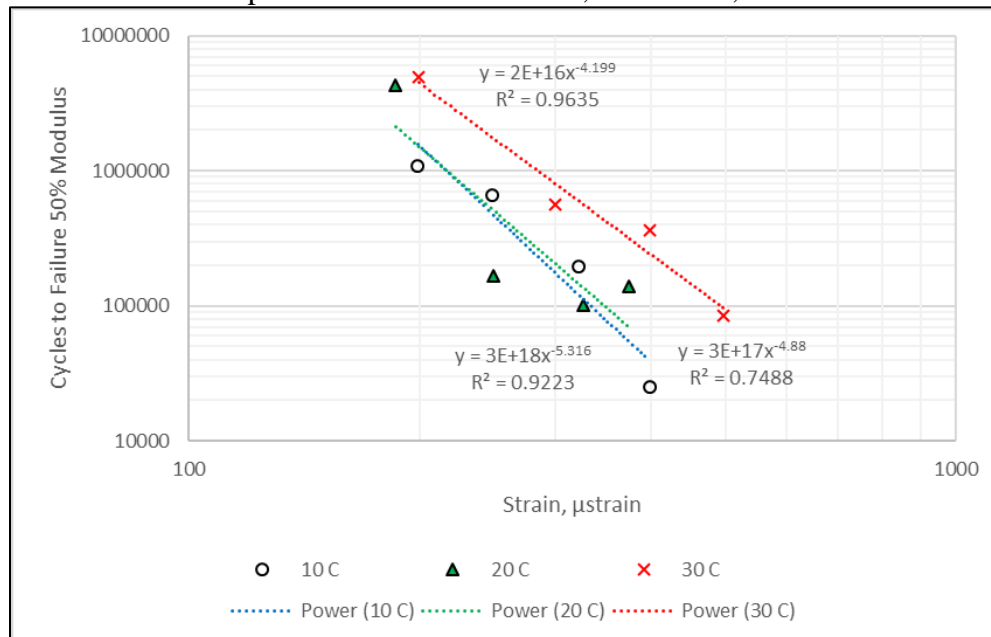
Appendix H includes the repeated load flexural bending beam fatigue strength test data for the asphalt mixtures measured in accordance with the AASHTO T 322. The procedure used to analyze the bending beam fatigue strength test data is also summarized in this appendix.

### H.1 Graphical Presentation of Bending Beam Fatigue Strength Test Data

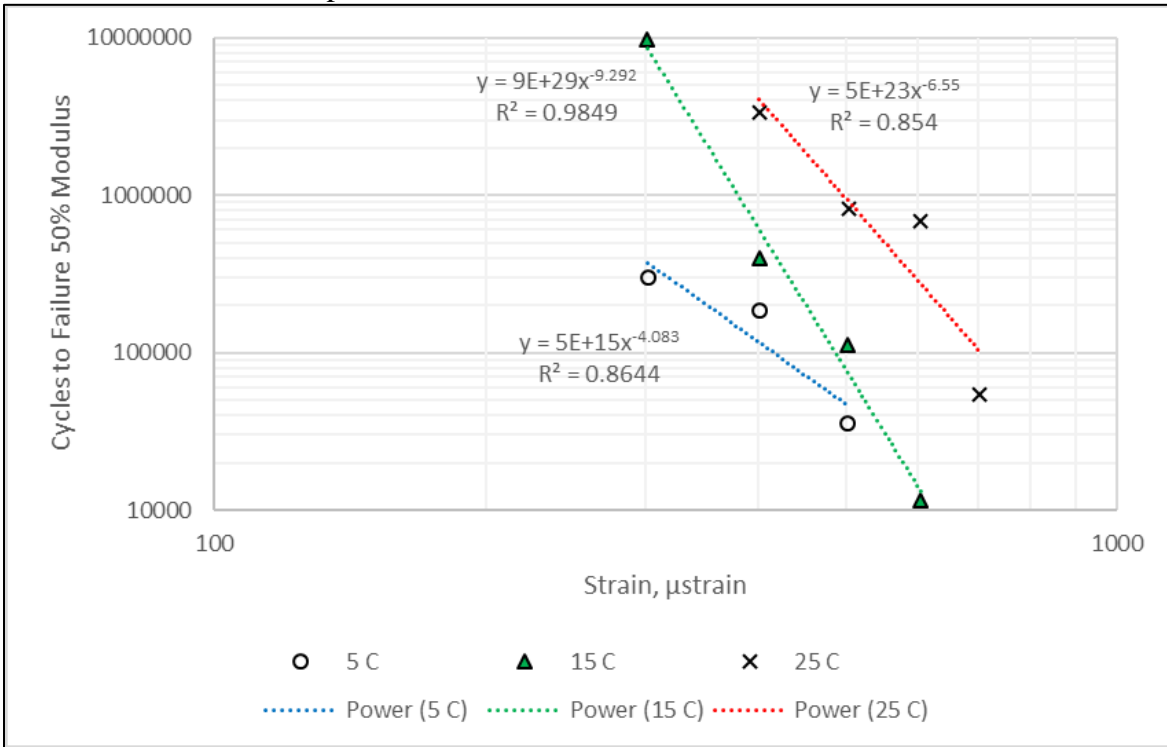
Asphalt Base Mixture #0057; PG58-28, 3LT



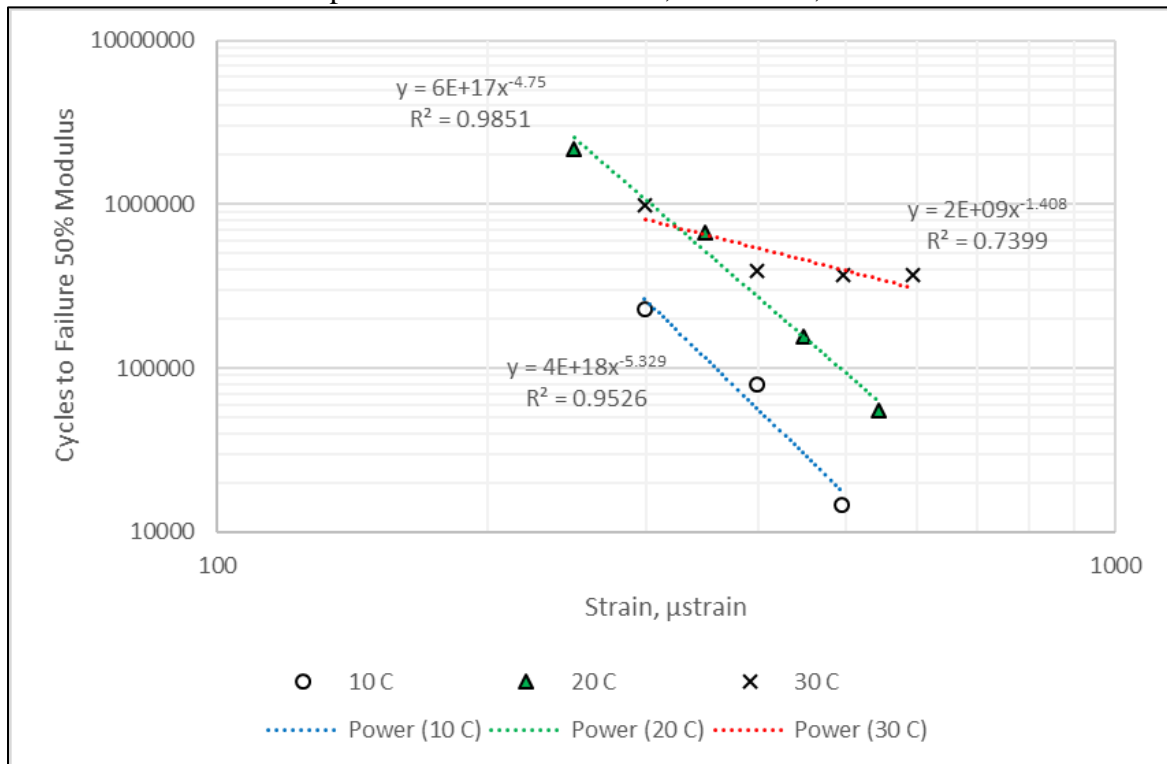
Asphalt Base Mixture #0119; PG58-28S, 3HT



Asphalt Base Mixture #1060; PG58-28H, 3HT



Asphalt Base Mixture #1166; PG58-28S, 2HT



## H.2 Procedure to Derive the Fatigue Strength k-Coefficients

Analysis of the flexural fatigue data collected in accordance with AASHTO T 321 to determine the fatigue life of the beam test specimen is straightforward and summarized in this section of Appendix H.

### H.2.1 Definition of Fatigue Life or Strength

The traditional definition of the fatigue life or strength of an individual beam specimen is the number of cycles required to reduce the flexural stiffness of the specimen to 50 percent of the initial flexural stiffness. The initial flexural stiffness is defined as the flexural stiffness at 50 cycles. The traditional definition of fatigue life for an individual beam specimen was applied in estimating the fatigue strength coefficients derived for the current and earlier versions of the Pavement ME Design software.

### H.2.2 Determine Fatigue Life of Individual Beam Specimens for Same Test Temperature

Multiple beam specimens are tested in accordance with AASHTO T 321 at different tensile strains for three test temperatures. The test temperatures are typically 10, 20, and 30 °C. The outcome from the flexural beam tests is a tabulation of tensile strain, temperature, and fatigue life or number of load cycles to the traditional definition of fatigue failure.

The analysis of flexural fatigue data from multiple beam specimens is to develop a relationship by performing a regression of the logarithm of the fatigue life versus the logarithm of the flexural strain. Equation H.1 is the relationship between tensile strain and fatigue strength for individual test temperatures. The fitting of data for the same test temperature to equation H.1 is easily performed using the regression function in Excel, as explained below (see Appendix H.1):

1. For each beam tested, first take the base 10 logarithm of the average tensile strain during the test, and the base 10 logarithm of the fatigue life.
2. Use the linear regression function in Excel to determine the slope,  $k_2$ , and the intercept,  $k_1$ , of the basic relationship between the applied tensile strain and number of load cycles to failure, as defined by multiple beams tested to failure using the traditional or current definition of fatigue life.
3. An important point to recognize in comparing the results between different test temperatures is the flexural, bending beam tests are highly variable. The test results need to be carefully reviewed prior to deriving the fatigue k-coefficients. Outliers need to be identified within and between the test temperatures.

$$N_f = k_1 \left( \frac{1}{\varepsilon_t} \right)^{k_2} \quad \text{Equation H.1}$$

Where:

$N_f$  = Number of cycles to failure

$\varepsilon_t$  = Tensile strain,  $\mu$ strain

$k_1, k_2$  = Regression fitting coefficients



### H.2.3 Determine Fatigue Strength K-Coefficients for Combined Test Temperatures

The fatigue life or allowable number of load cycles equation included in the Pavement ME Design software is shown in equation H.2. The allowable number of load cycles is used in the incremental damage analysis. Equation H.2 includes an adjustment factor, C, between the volumetric difference between test specimens, as well as combining the results using different test temperatures or flexural stiffness. The equation for the C adjustment factor is shown in equation H.3.

$$N_f = k_{1f} C \left(\frac{1}{\varepsilon_t}\right)^{k_{2f}} \left(\frac{1}{E}\right)^{k_{3f}} \quad \text{Equation H.2}$$

Where:

$N_f$  = Allowable number of load cycles.

$\varepsilon_t$  = Tensile strain, in/in.

$E$  = Asphalt dynamic modulus, psi.

$C$  = Mixture volumetric property factor; defined by equation H.3.

$k_{1f}, k_{2f}, k_{3f}$  = Laboratory-derived fatigue strength coefficients.

$$C = 10^{(VFA-0.69)} \quad \text{Equation H.3}$$

Where:

$VFA$  = Voids filled with asphalt expressed as a decimal.

The analysis of flexural fatigue data from the three test temperatures is to derive the fatigue strength k-coefficients in equation H.2. The steps included in this process are listed and explained below:

1. The fatigue strength k-coefficient in equation H.2 (intercept  $k_{1f}$ , strain exponent  $k_{2f}$ , and modulus exponent  $k_{3f}$ ) are determined using a linear regression analysis of equation H.2 on a logarithmic basis. The volumetric adjustment factor, however, is initially excluded because there should be no bias in the volumetric properties (asphalt content and air voids) between all beam specimens. If there is a consistent difference or bias in the air voids or asphalt content between the different beams tested at different strain levels and temperatures, the volumetric C factor may need to be included as an independent parameter in the regression analyses. Including the volumetric C factor in the initial analyses will complicate the interpretation of the test data.
2. The dynamic modulus noted in equation H.2 is measured in accordance with AASHTO T 342, while the fatigue strength coefficients are determined from AASHTO T 321. The asphalt modulus measured from the bending beam (flexural) fatigue test and the dynamic modulus (uniaxial or unconfined compression) measured for the MEPDG are not the same. Thus, this difference or discrepancy needs to be taken into account in determining the  $k_{3f}$  exponent for the Pavement ME Design software, as included in equation H.4. A default value for the flexural to dynamic modulus ratio is 1.08.

$$k_{3f}(MEPDG) = k_{3f}(Beam) \frac{\text{Log}(E_{flexural})}{\text{Log}(E_{Dynamic}^*)} \quad \text{Equation H.4}$$

3. The intercept ( $k_{1f}$ ) in equation H.2 needs to account for the average volumetric properties for all of the test specimens. Equation H.5 is used to determine the intercept,  $k_{1f}$ , value based on the average volumetric properties, if excluded from the initial analysis of the beam fatigue strength test results.

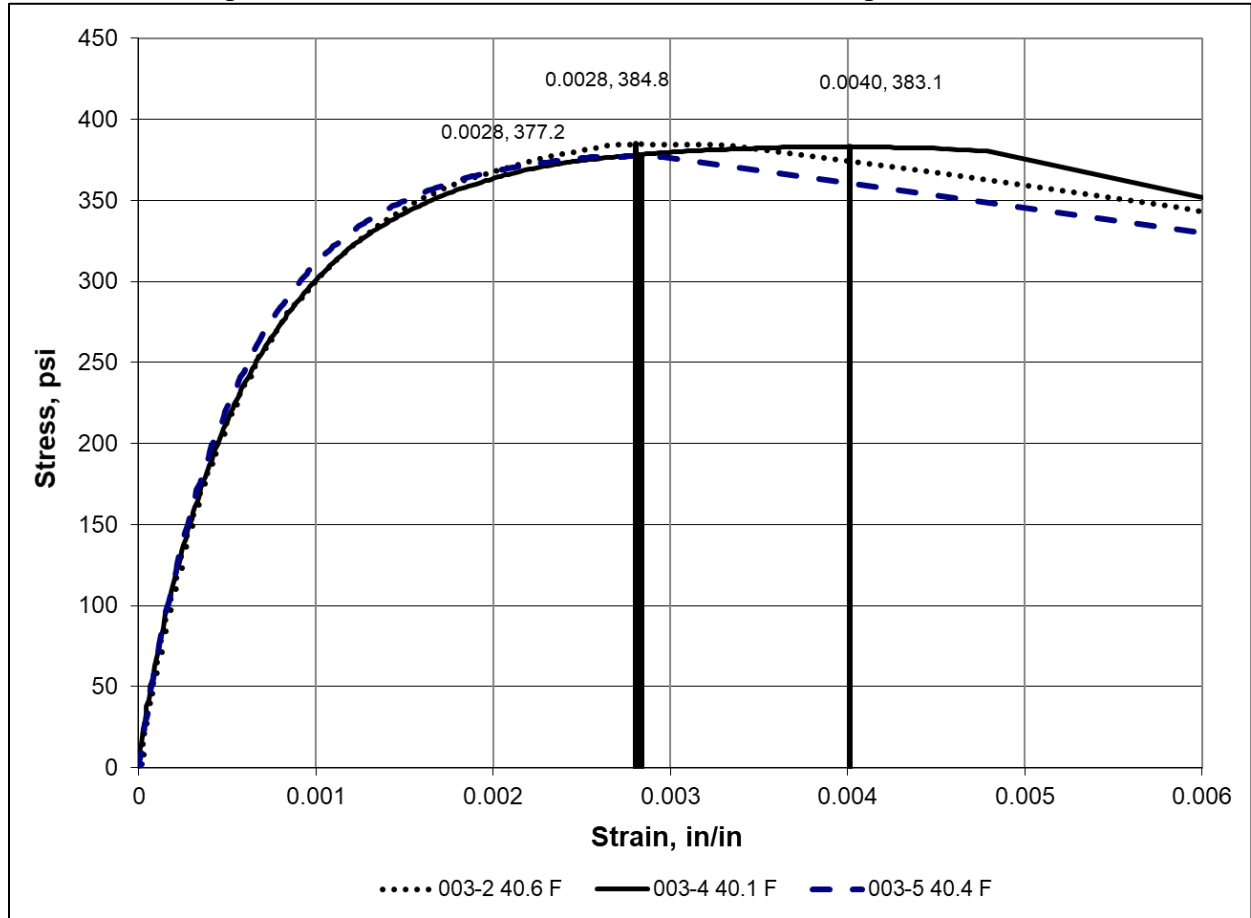
$$k_{1f}(MEPDG) = \frac{k_{1f}(Beam)}{c} \quad \text{Equation H.5}$$

### APPENDIX I—TENSILE STRAIN AT FAILURE TEST DATA

Appendix I includes the indirect tensile strain at failure test data measured in accordance with NCHRP Report 338. The procedure used to analyze the indirect tensile strain at failure test data to estimate the fatigue strength coefficients is also summarized in this appendix.

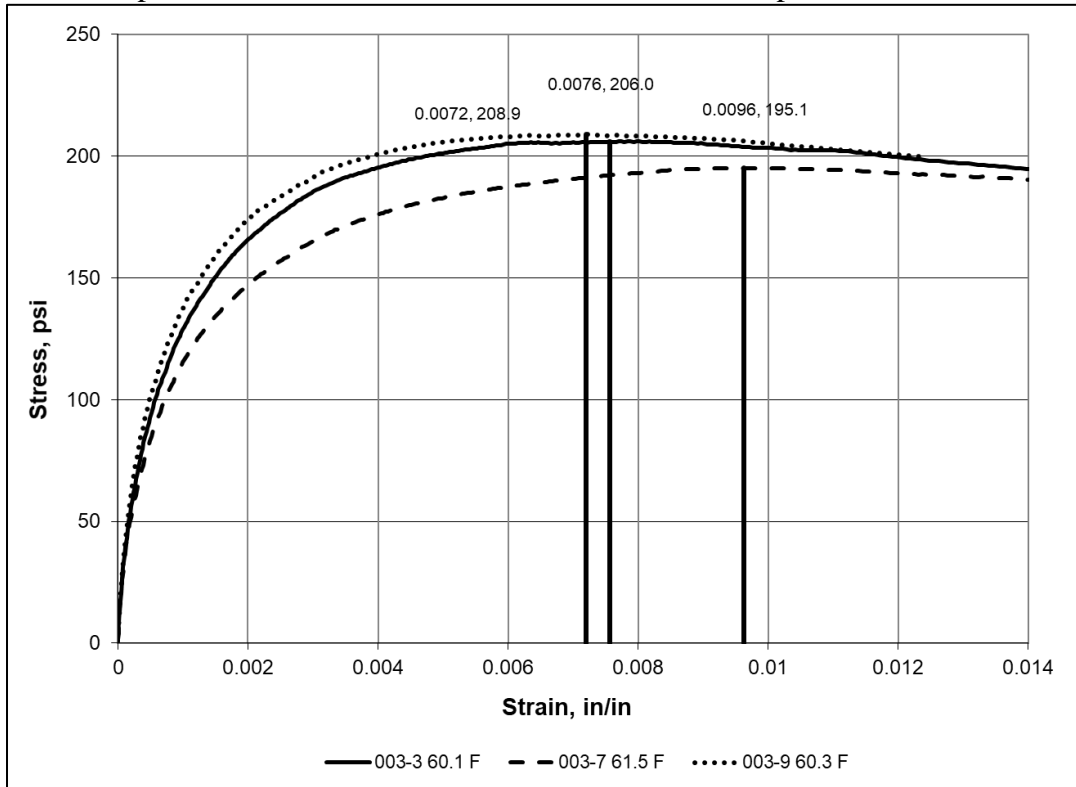
#### I.1 Graphical Presentation of Indirect Tensile Failure Strain Test Data

Asphalt Base Mixture #0003; PG58-28S, 3MT; Temperature – 40 °F

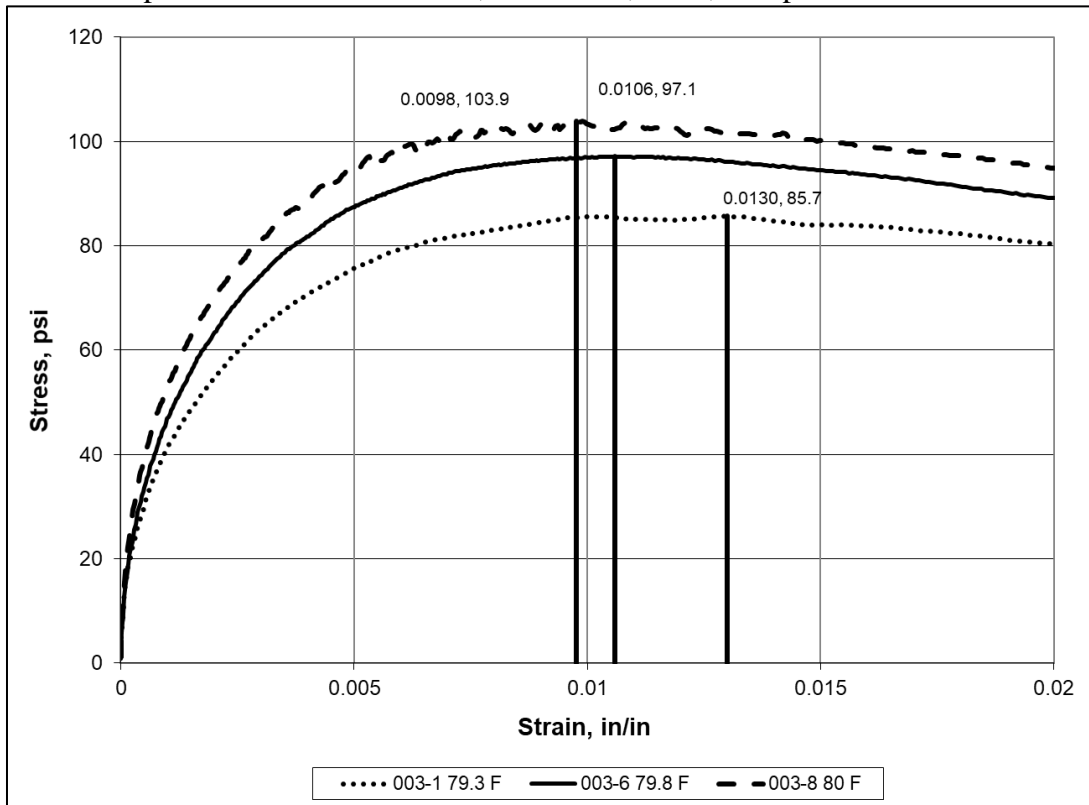


Expansion of AASHTOWare ME Design Inputs  
 Final Report WHRP 0092-20-03

Asphalt Base Mixture #0003; PG58-28S, 3MT; Temperature – 60 °F:

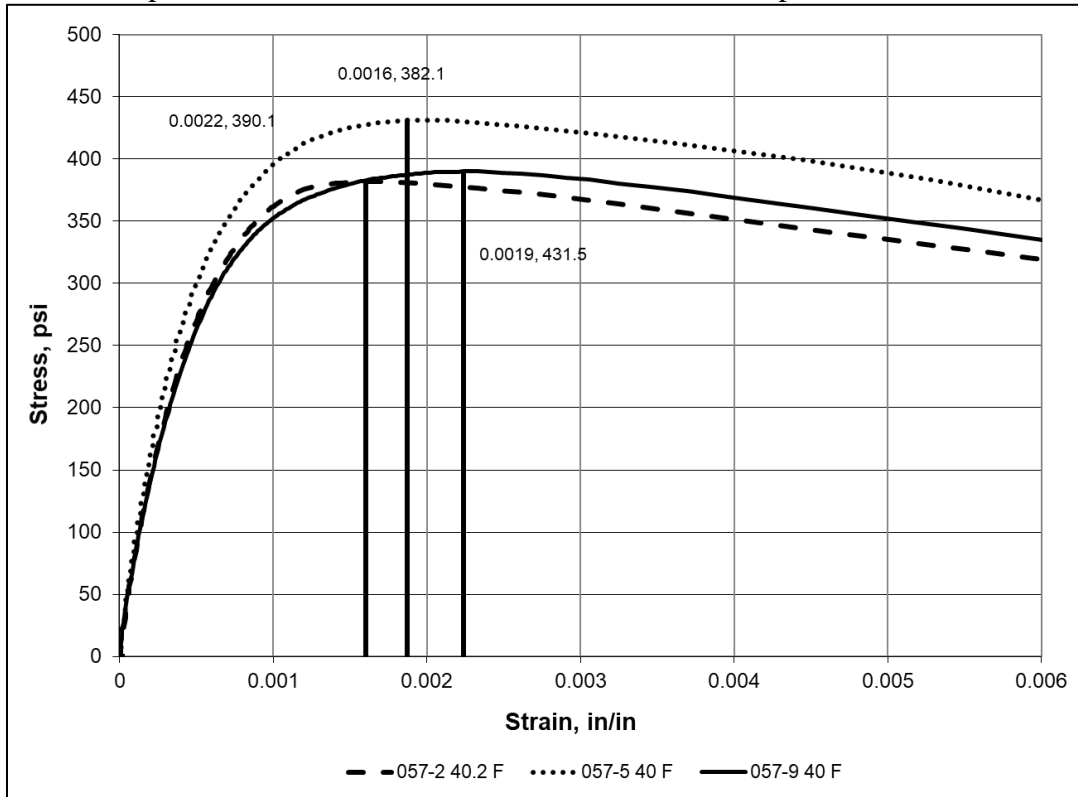


Asphalt Base Mixture #0003; PG58-28S, 3MT; Temperature – 80 °F:

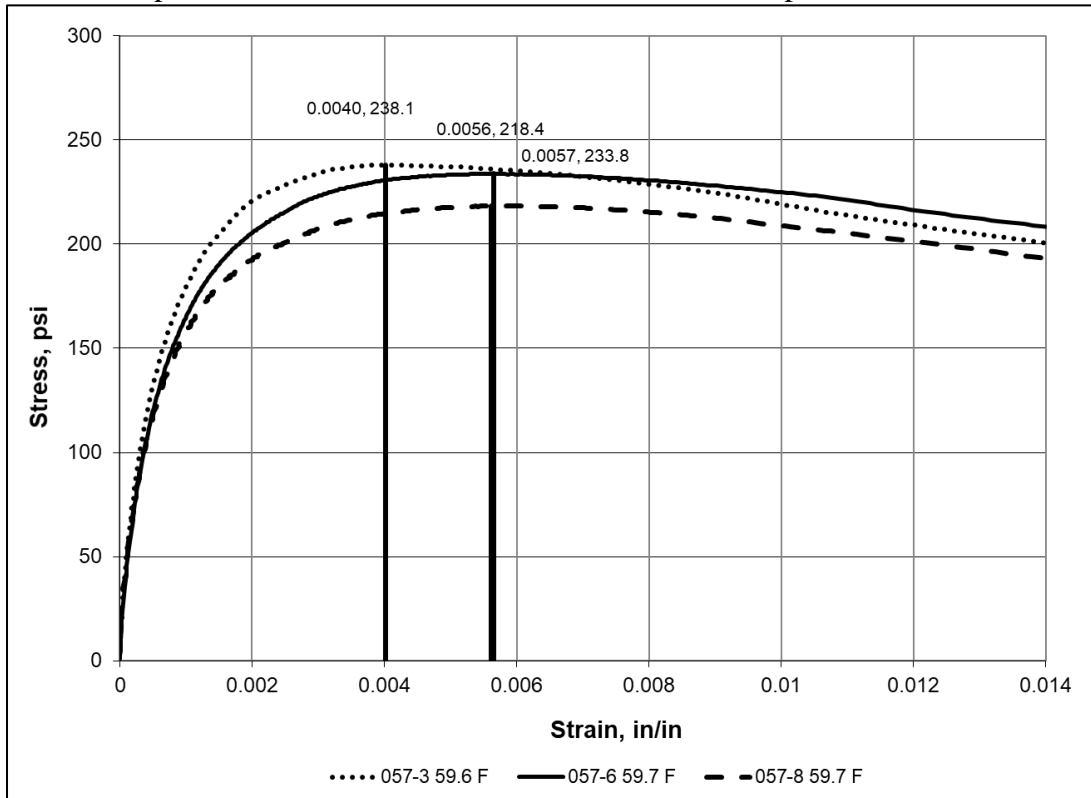


**Expansion of AASHTOWare ME Design Inputs  
Final Report WHRP 0092-20-03**

Asphalt Base Mixture #0057; PG58-28S, 3LT; Temperature – 40 °F

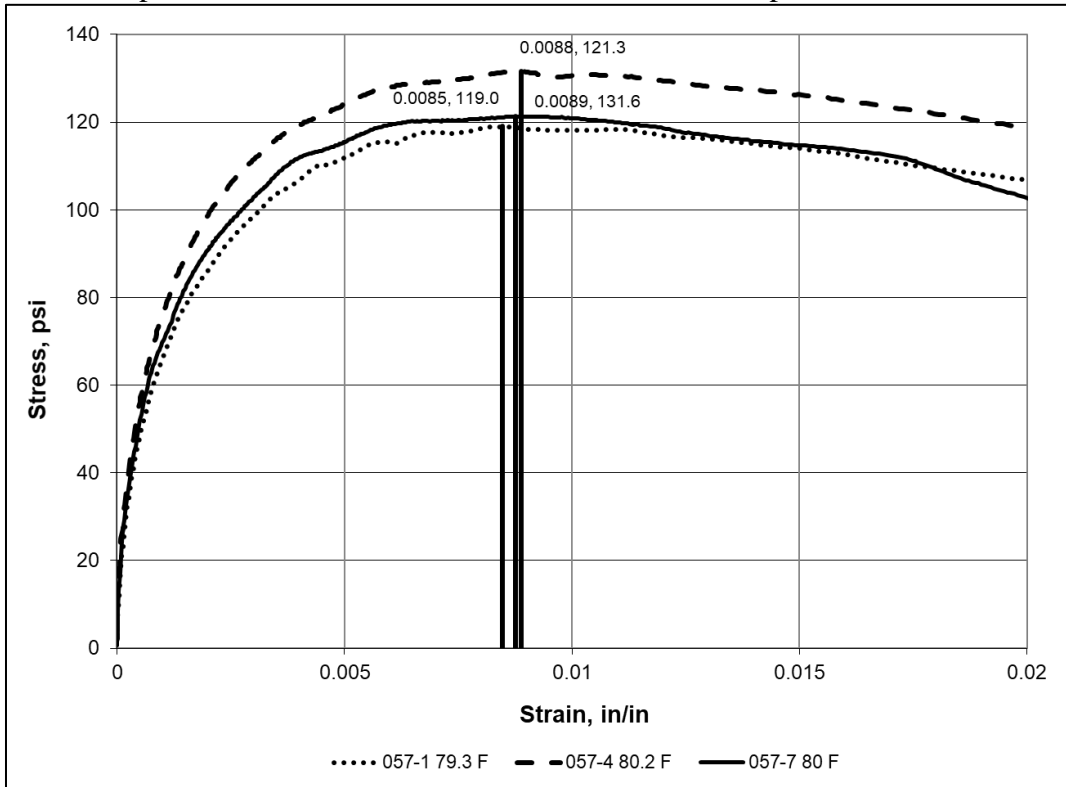


Asphalt Base Mixture #0057; PG58-28S, 3LT; Temperature – 60 °F

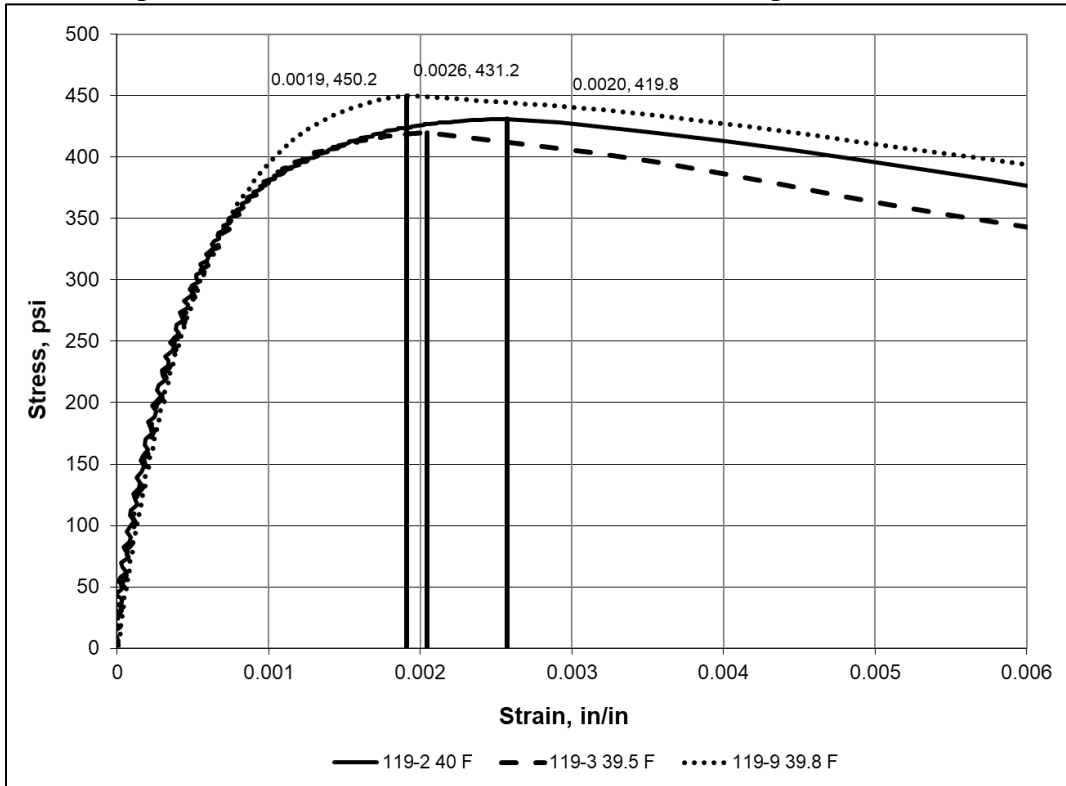


**Expansion of AASHTOWare ME Design Inputs  
Final Report WHRP 0092-20-03**

Asphalt Base Mixture #0057; PG58-28S, 3LT; Temperature – 80 °F

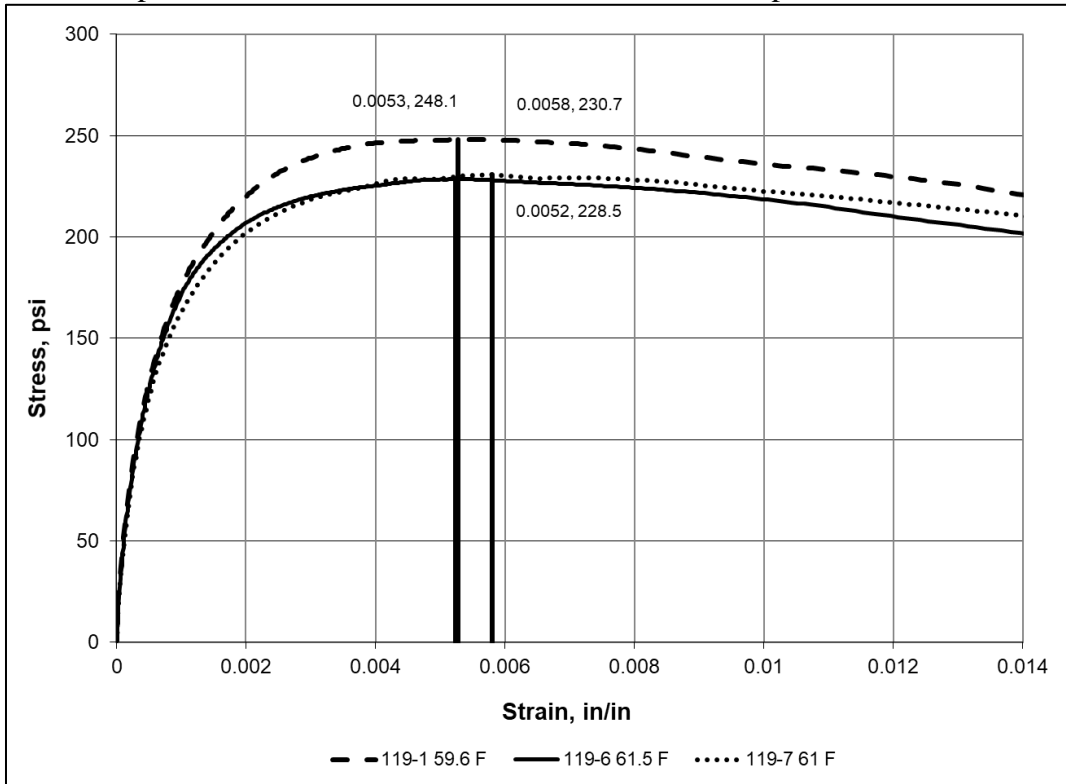


Asphalt Base Mixture #0119; PG58-28S, 3HT; Temperature – 40 °F

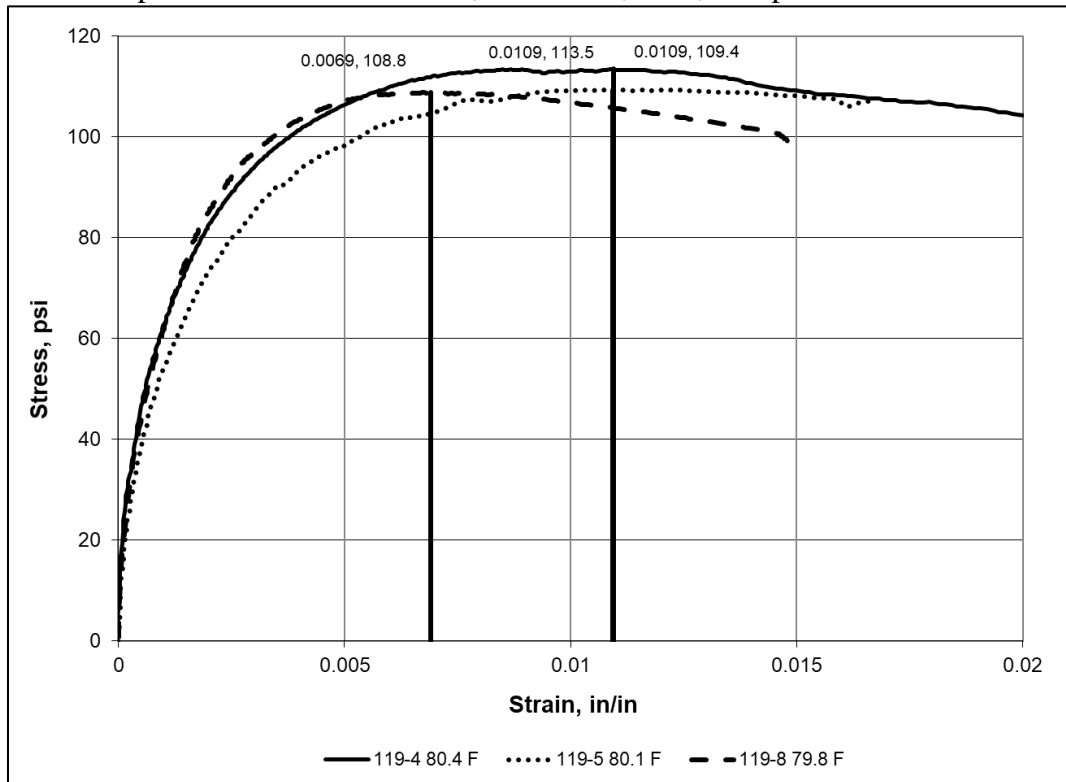


**Expansion of AASHTOWare ME Design Inputs  
Final Report WHRP 0092-20-03**

Asphalt Base Mixture #0119; PG58-28S, 3HT; Temperature – 60 °F

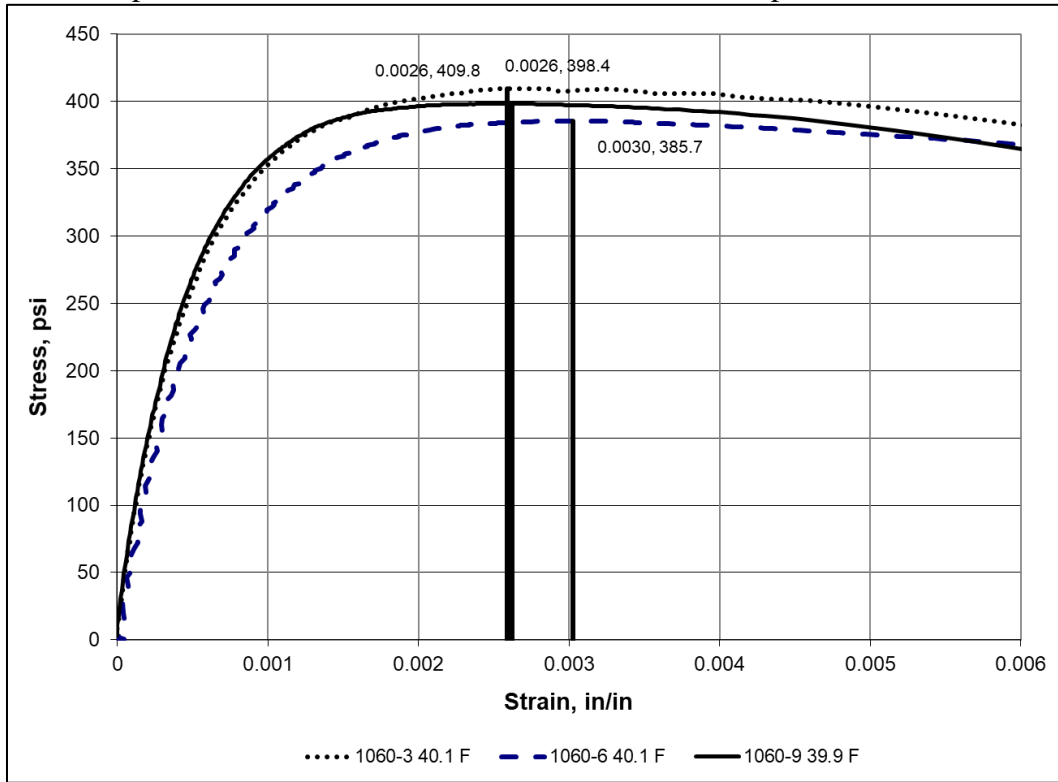


Asphalt Base Mixture #0119; PG58-28S, 3HT; Temperature – 80 °F

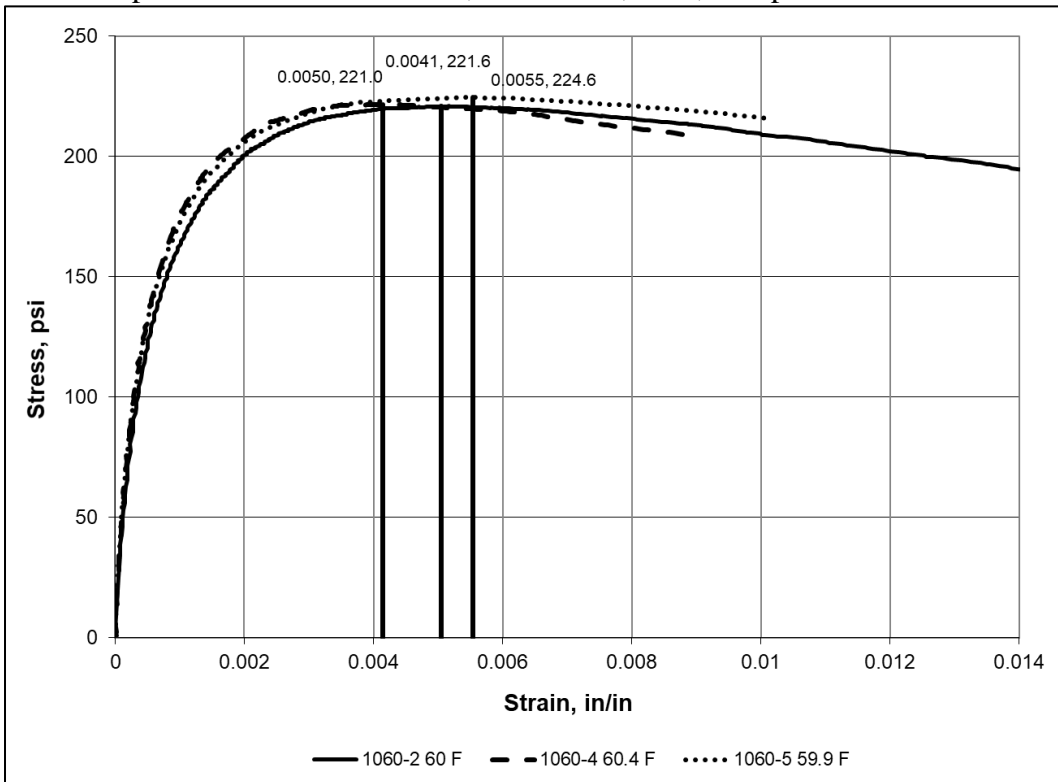


**Expansion of AASHTOWare ME Design Inputs**  
**Final Report WHRP 0092-20-03**

Asphalt Base Mixture #1060; PG58-28H, 3HT; Temperature – 40 °F



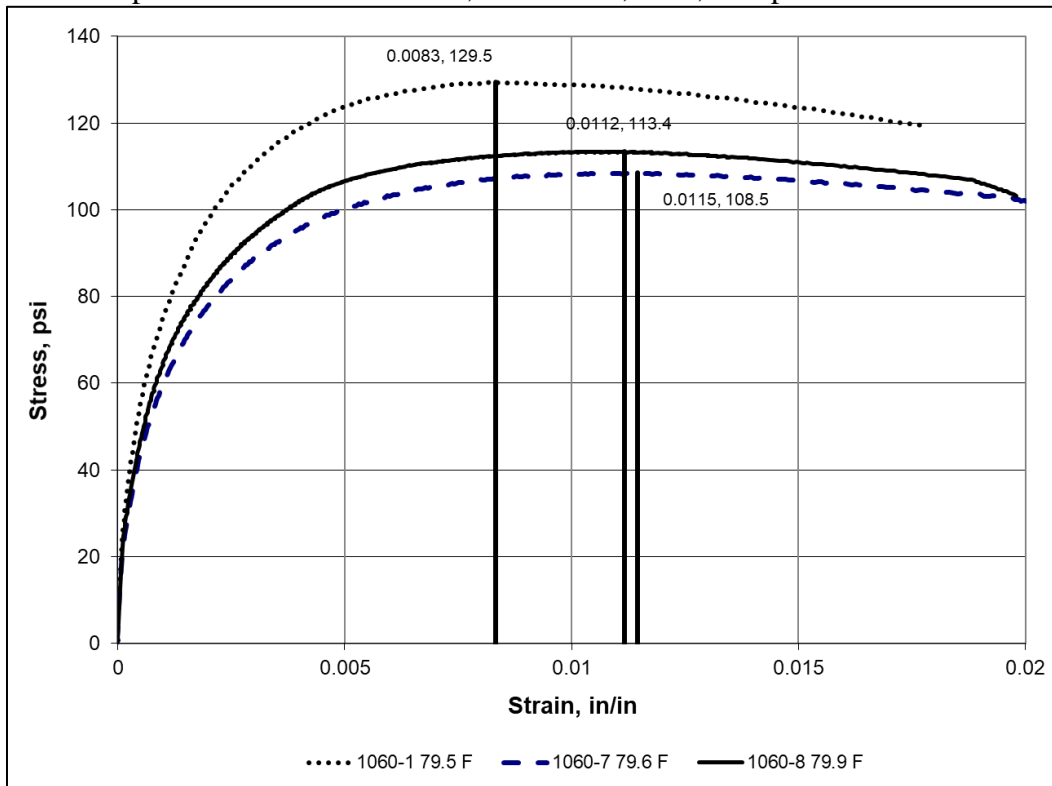
Asphalt Base Mixture #1060; PG58-28H, 3HT; Temperature – 60 °F



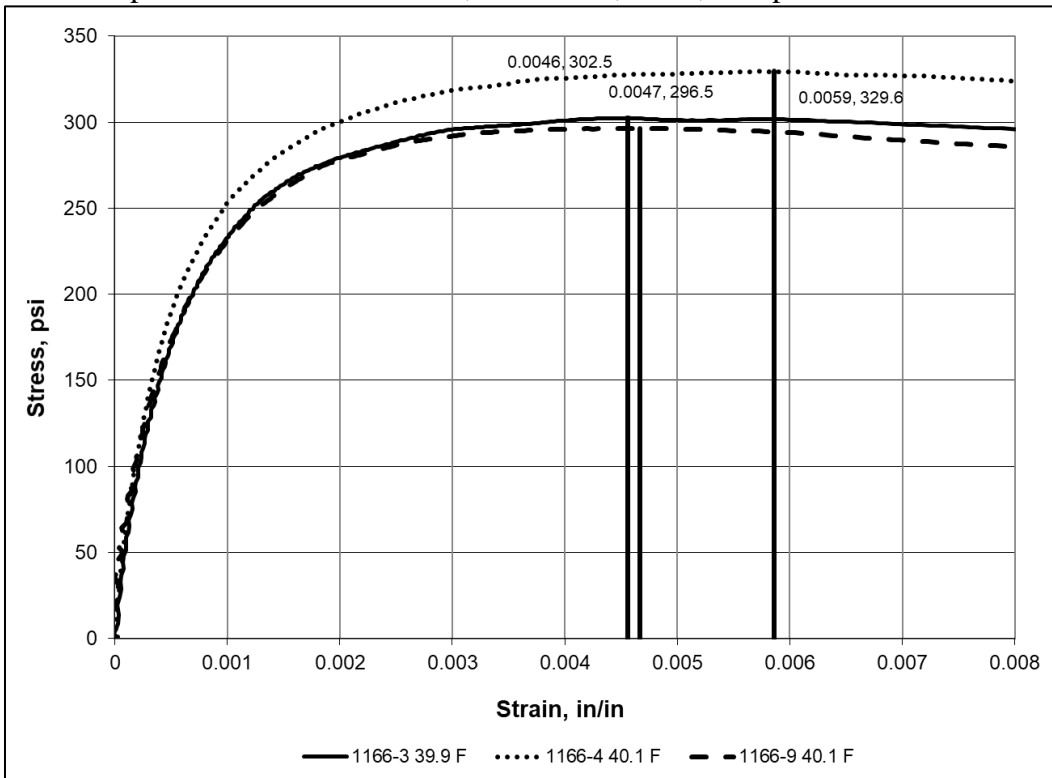


**Expansion of AASHTOWare ME Design Inputs**  
**Final Report WHRP 0092-20-03**

Asphalt Base Mixture #1060; PG58-28H, 3HT; Temperature – 80 °F

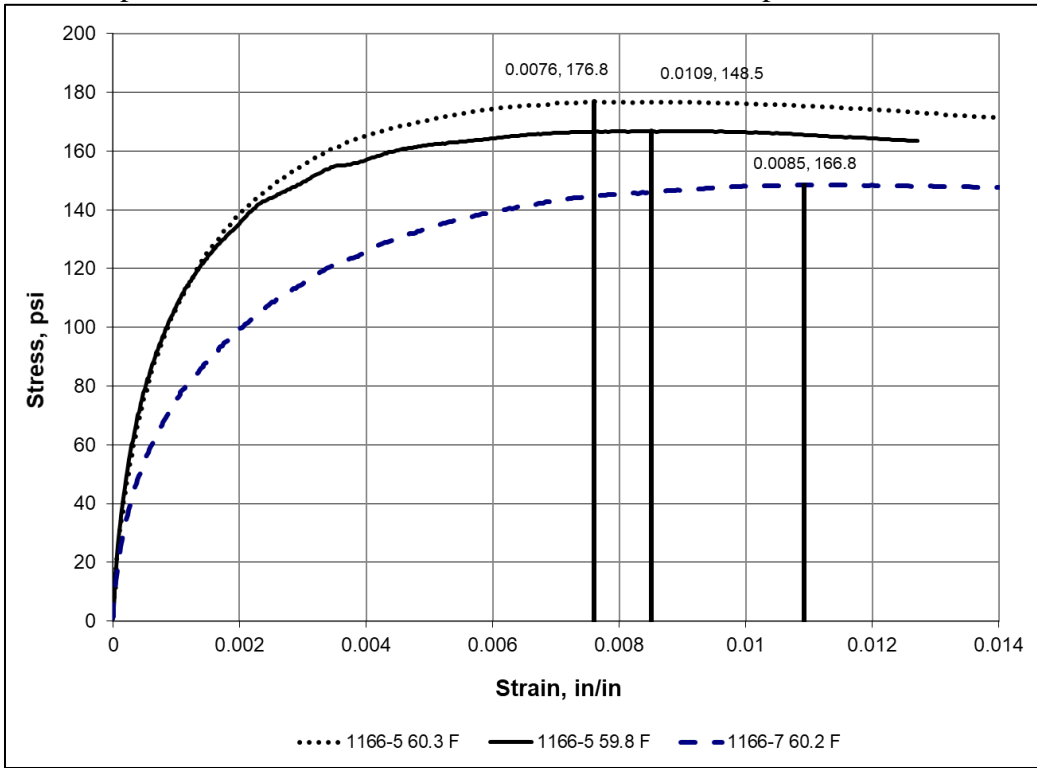


Asphalt Base Mixture #1166; PG58-28S, 2 HT; Temperature – 40 °F

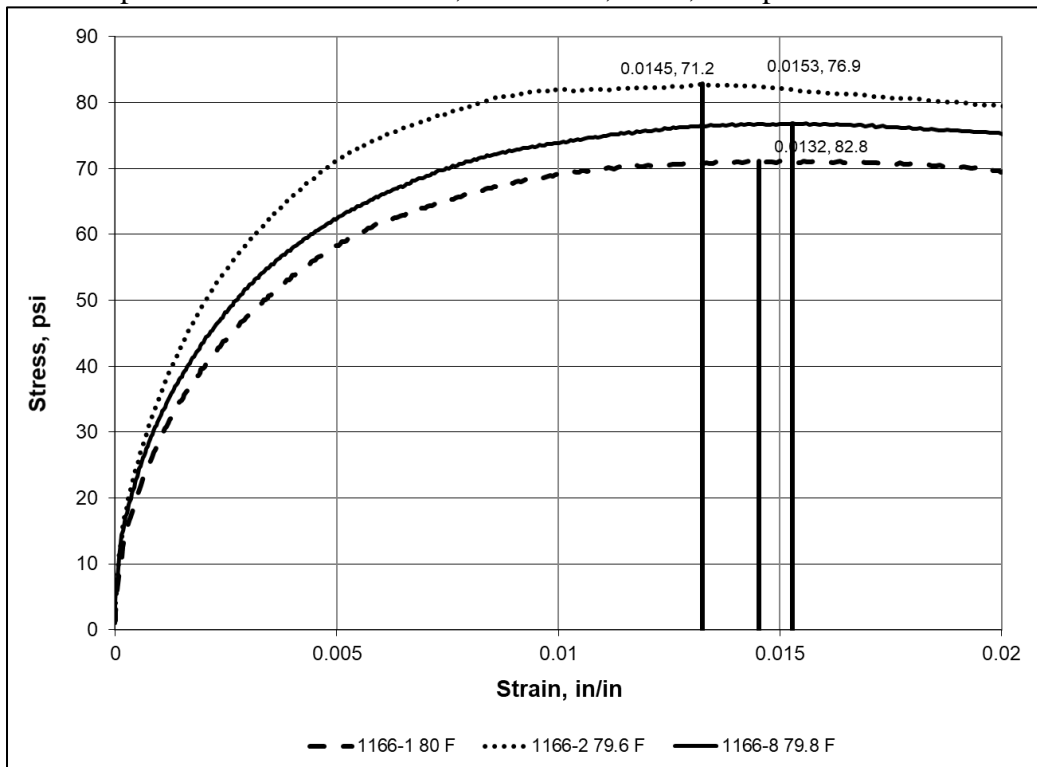


**Expansion of AASHTOWare ME Design Inputs**  
**Final Report WHRP 0092-20-03**

Asphalt Base Mixture #1166; PG58-28S, 2 HT; Temperature – 60 °F

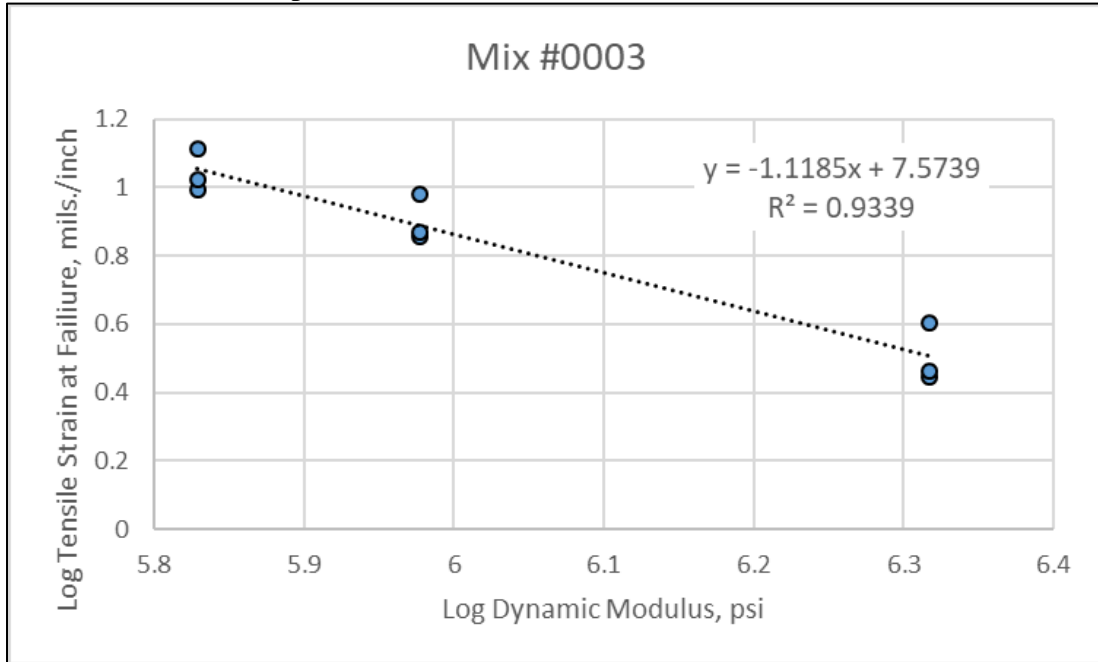


Asphalt Base Mixture #1166; PG58-28S, 2 HT; Temperature – 80 °F

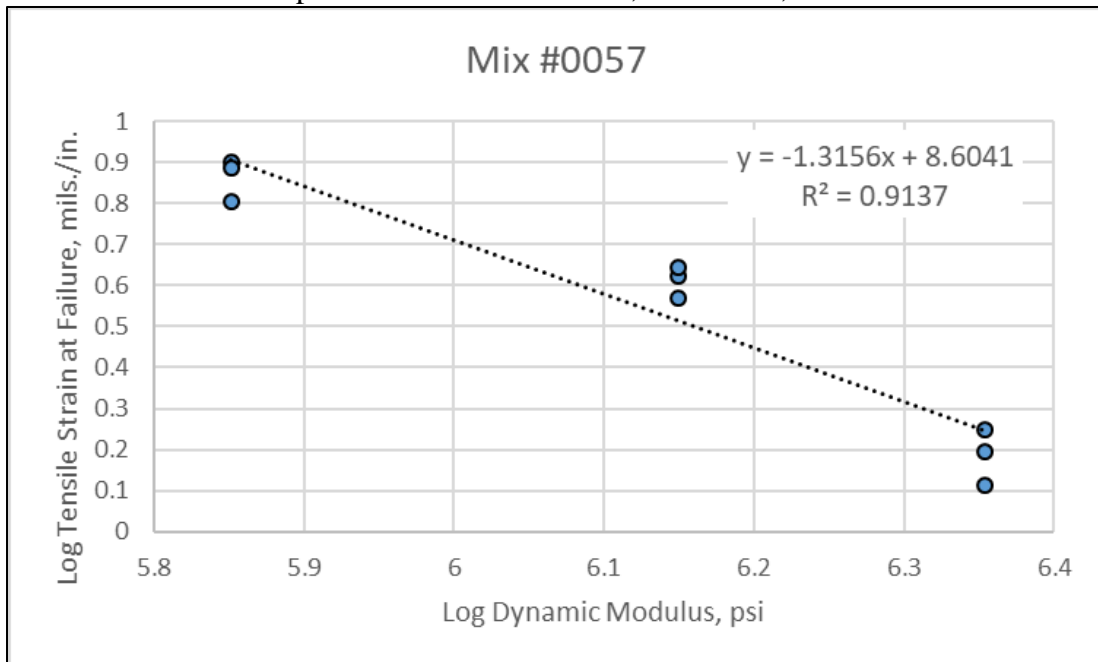


## I.2 Relationship between Dynamic Modulus and Tensile Failure Strain

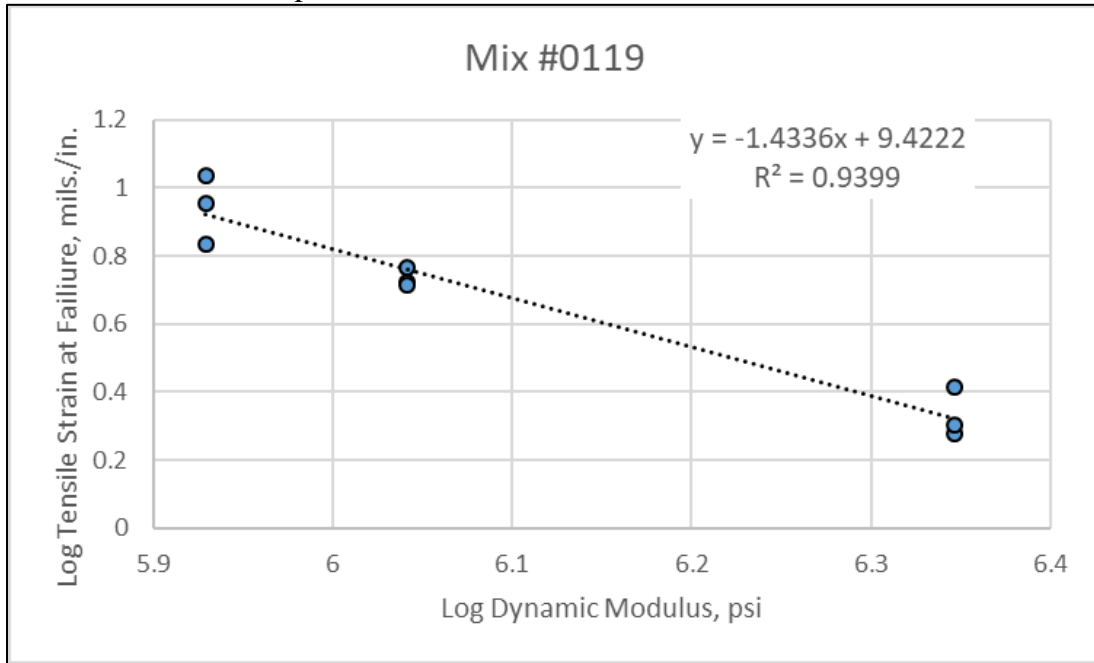
Asphalt Base Mixture #0003; PG58-28S, 3MT



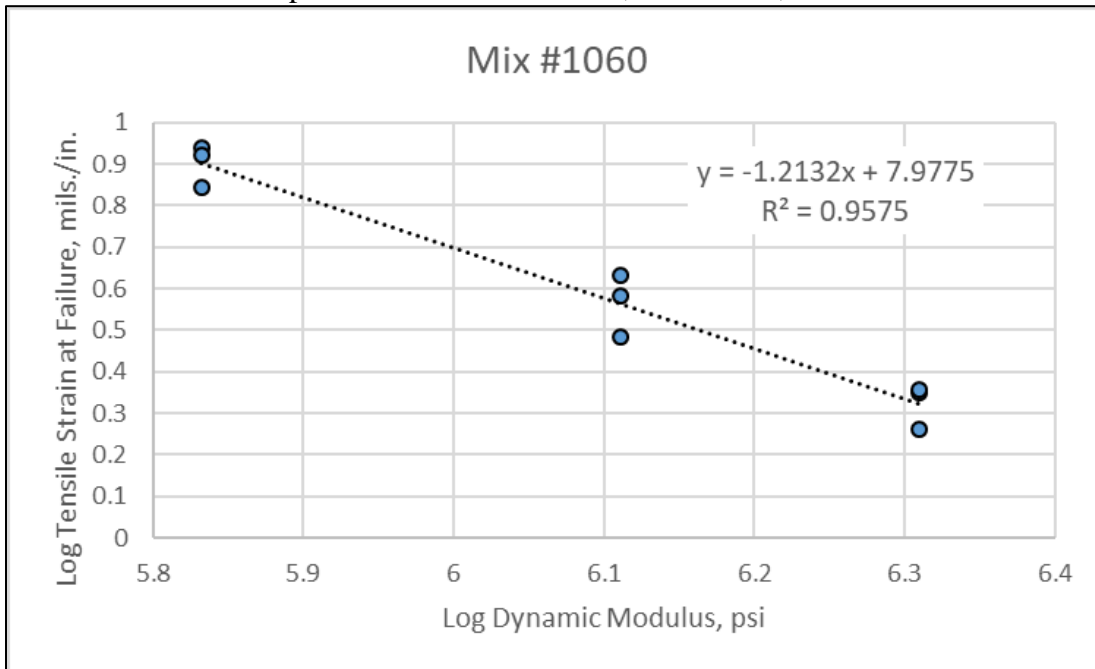
Asphalt Base Mixture #0057; PG58-28S, 3LT



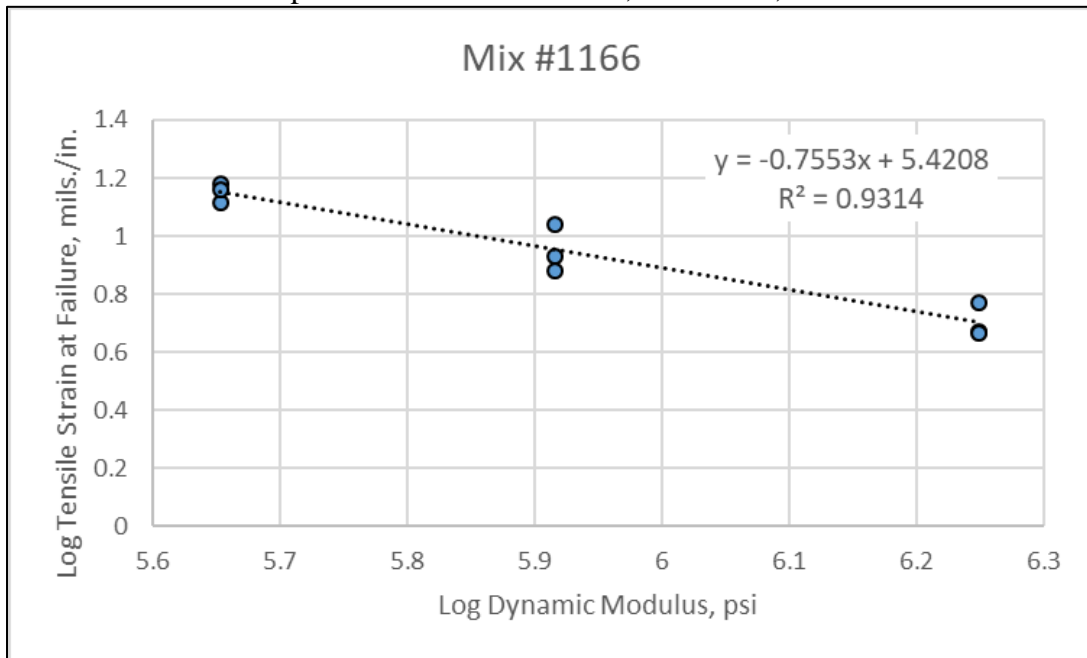
Asphalt Base Mixture #0119; PG58-28S, 3HT



Asphalt Base Mixture #1060; PG58-28H, 3 HT



Asphalt Base Mixture #1166; PG58-28S, 2HT



### I.3 Procedure to Estimate the Fatigue Strength k-Values

#### I.3.1 Summary of Test Procedure

The IDT strength test is performed in accordance with a modification of AASHTO T 322-07 (2011) and ASTM D6931. First of all, extensometers are attached to both cut faces of the core to record the horizontal and vertical deformations of the cores during the strength test, as designated in AASHTO T 322 (see Figure I40). Secondly, the loading rate is 2 inches/minute to account for the higher test temperatures, as designated by ASTM D6931.

[Note: The IDT failure strain test was used and suggested as part of the Asphalt Aggregate Mixture Analysis System (AAMAS) and FHWA Cost Allocation study (Von Quintus, et al., 1991; and Rauhut, et al., 1984). The initial test procedure used LVDTs external to the test specimen. Latter versions of this test now use the specimen mounted LVDTs as described in AASHTO T 322.]

Dimensions of height and diameter are measured for each test specimen or core. The load and horizontal and vertical deformations located on both faces of the sample are recorded versus time at a sampling or data acquisition rate of about 200 Hz. Figure I14 is a graphical illustration of the measured horizontal deformation or strain versus the applied load or stress.

A minimum of three test specimens are tested at each test temperature because the indirect tensile strain can be highly variable. The three test temperatures are: 40, 60, and 80 °F. These three temperatures are applicable to most dense-graded asphalt mixtures. The higher temperature depends on the asphalt grade. A higher test temperature range (40, 70 and 100 °F) can be used for stiff mixtures, while a lower temperature range (40, 55, and 70 °F) can be used for soft mixtures.

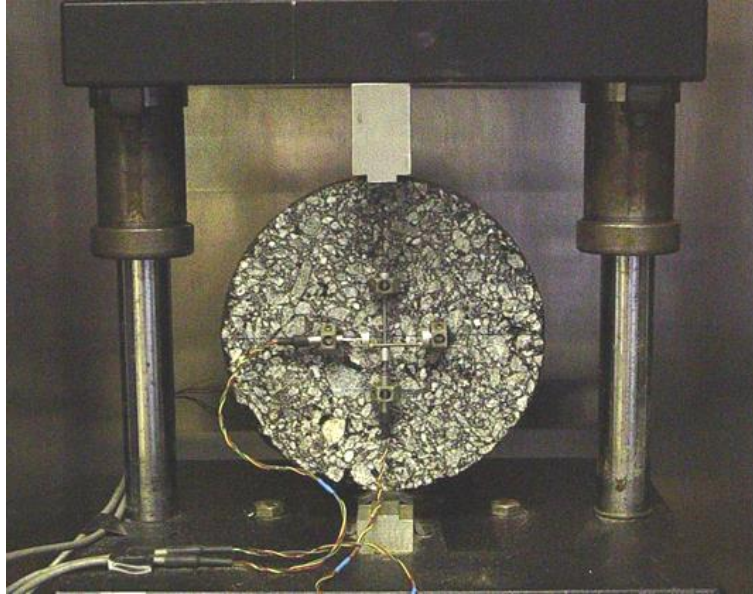


Figure I40. LVDTs Attached to the IDT Test Specimen for Measuring Horizontal and Vertical Displacements in the Center of the Specimen.

### ***1.3.2 Failure Strain Definition for Fatigue Strength Estimate***

The failure strain for an individual IDT test specimen is determined when the IDT specimen starts to exhibit cracks along the edge of the loading platens, which is difficult to identify by the data acquisition system. The failure tensile strain has been defined as the tensile strain at peak load, which is easy to determine from a data acquisition standpoint, but the IDT specimen is in a damaged condition at peak load. In other words, the IDT specimen can still sustain higher loads, but the test specimen is exhibiting damage outside the measurement zone when the LVDTs are attached to both sides of the specimen faces. The damaged area can have an impact on the test outcome, which can be highly dependent on localized surface conditions.

This physical condition to define the failure tensile strain is difficult to determine, especially at the higher test temperatures. Figure I41 displays the stress-strain plot of the IDT specimen for 40 F, while Figure I42 displays the stress-strain plot at 80 F for the same asphalt mixture. The maximum tensile strain can be highly variable between the individual test specimens for the higher temperatures.

To minimize the end effects caused by localized cracking around the loading platens, 99 percent of the peak load or stress is determined to define the tensile strain at failure in mils per inch (see Figure I41 and Figure I42). The three lines in Figures I41 and Figure I42 represent the horizontal tensile strain from the LVDTs attached to each side of the test specimen along the diametric axis and the average of both sides.

[Note: The value of 99 percent of peak load to determine the failure strain was suggested in the AAMAS procedure by painting the surface of the specimen and observing the cracking that occurred around the loading platen and the measured deformation and loads (Von Quintus, et al., 1991). This earlier procedure used LVDTs located along the horizontal axis of the specimen. The

**Expansion of AASHTOWare ME Design Inputs**  
**Final Report WHP 0092-20-03**

current procedure (AASHTO T 322) has the LVDTs attached to the specimen face (see Figure I40). The LVDTs being attached to the specimen faces measure deformations in a localized area which exclude the area around the loading platens. However, the failure strain definition is still based on using 99 percent of the peak load or stress (see Figure I41 and Figure I42).

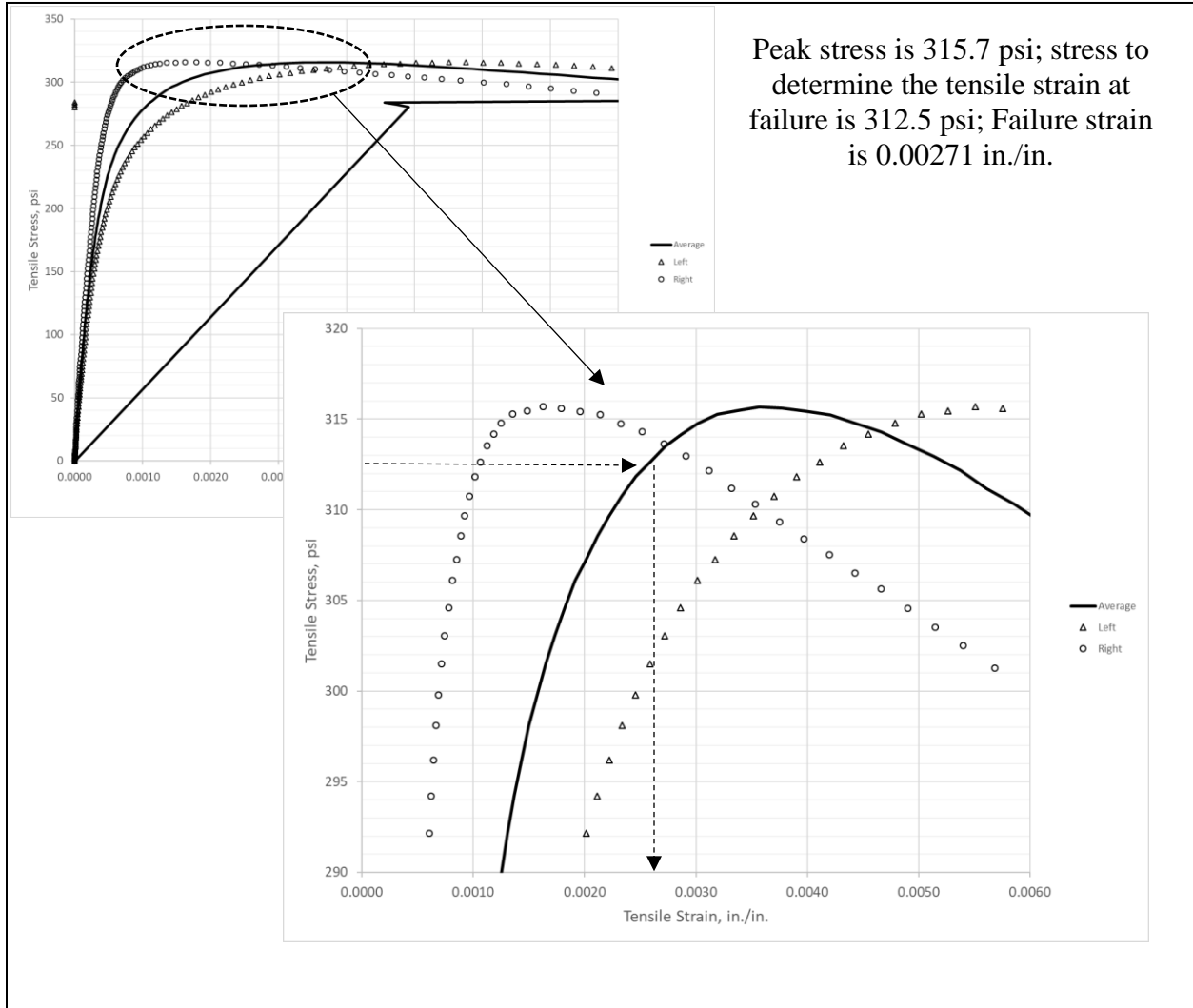


Figure I41. Test Results from the IDT Strength Test at the Low Test Temperature (40 °F).

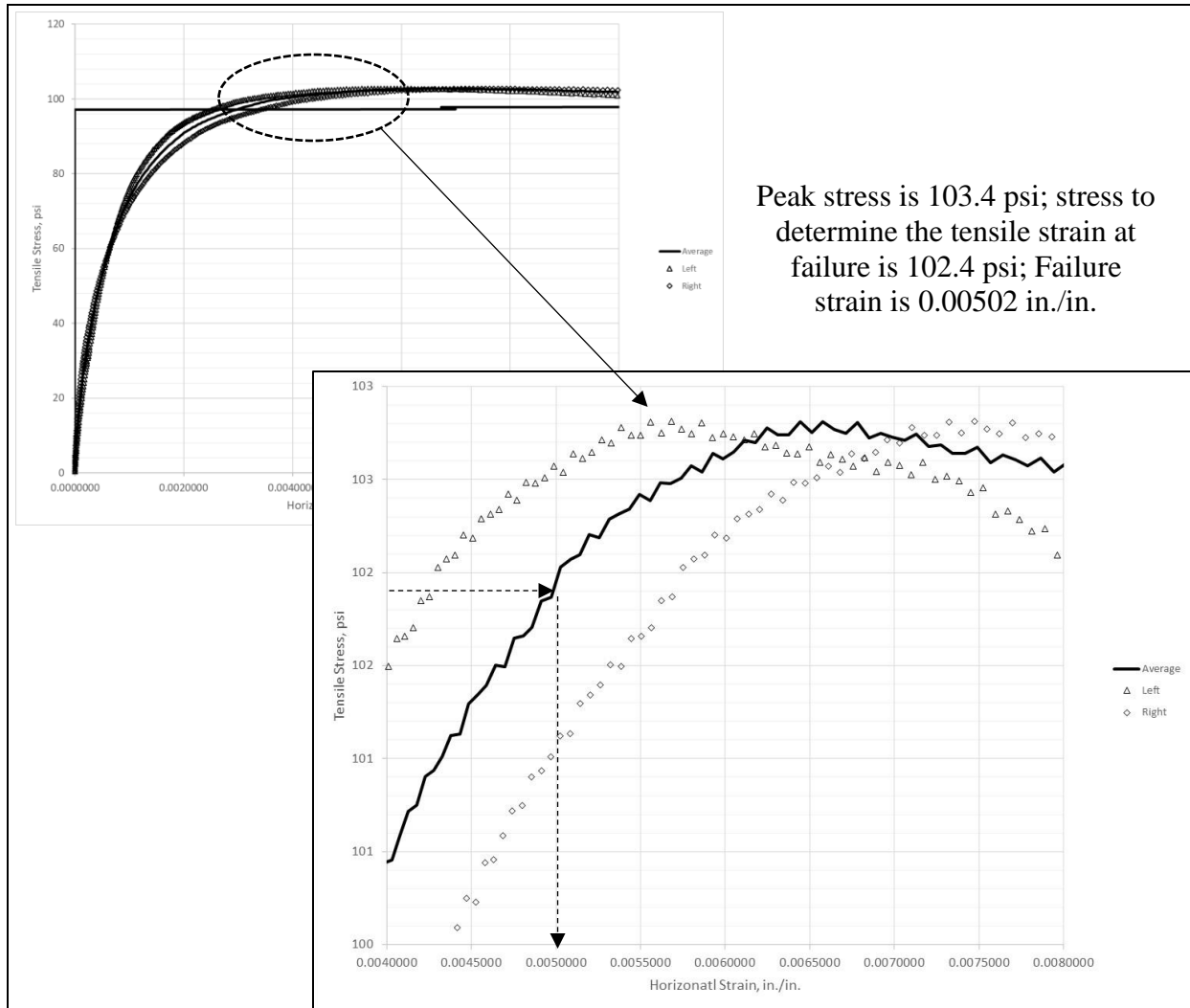


Figure I42. Test Results from the IDT Strength Test at the High Test Temperature (80 °F).

### 1.3.3 Analysis of the IDT Failure Strain Data

The outcome from the IDT strength-failure strain test is the dynamic modulus at the test temperature for 10 Hz (AASHTO T 342, see Appendix D) and tensile strain at failure. The dynamic modulus – tensile failure strain relationship represented by equation I1 is similar to the flexural bending beam and IDT fatigue strength relationship for the tensile strain value for one load cycle to cause failure (the intercept value) on a log-log basis, as represented by equation I2 for the bending beam test.

The IDT repeated load fatigue test exhibits the same relationship to the bending beam fatigue test, except the magnitudes of the coefficients are different (Rauhut, et al., 1984). The following lists the steps for determining the slope and intercept of the modulus-tensile failure strain relationship from all test temperatures.



$$\text{Log}\epsilon_f = b - m(\text{Log}E_{Uniaxial}^*) \quad \text{Equation I.1}$$

Where:

$\epsilon_f$  = Tensile failure strain, mils/inch.

$E_{Uniaxial}^*$  = Dynamic modulus at 10 Hz from uniaxial cylindrical specimen, psi.

m, b = Regression fitting coefficients; m is the slope and b is the intercept.

$$\text{Log}\epsilon_t = \frac{\text{Log}(k_{1f})}{k_{2f}} - \frac{k_{3f}}{k_{2f}} (\text{Log}E_{Flexural}) \quad \text{Equation I.2}$$

1. Measure the dynamic modulus of the mixture at three different temperatures for 10 Hz using the indirect tensile test. The three temperatures are 40, 60, and 80 °F. Additional temperatures and loading frequencies can be used in the test program to create a dynamic modulus master curve in accordance with AASHTO T 342.
2. Measure the tensile strain at failure using the IDT strength-failure strain test in accordance with the procedure included in NCHRP Report 338 (Von Quintus, et al., 1991) at three test temperatures of 40, 60, and 80 °F using a constant loading ram rate of 2 inches per minute. The tensile strain at failure is determined at 99 percent of the peak or maximum load resisted by the specimen.
3. Prepare a plot of the log dynamic modulus in psi versus the log tensile strain at failure in mils/inch (see section I.2). Use the excel regression tool and determine “m” or slope of the measured relationship and “b” or intercept of the measured relationship in accordance with equation I.1. The intercept “b” and slope “m” are an estimate of the fatigue strength coefficients from the bending beam flexural fatigue test outcomes. The equation fits the data well in most cases, and is similar to the mathematical relationship from the beam fatigue strength tests, excluding the volumetric property factor or adjustment for the flexural strain to cause failure at the first load cycle.

#### ***1.3.4 Determine the Fatigue Strength k-Coefficients***

The fatigue strength model coefficients are determined from the flexural beam fatigue test, AASHTO T 321, as described in Appendix H. This section of Appendix I describes the procedure for determining the fatigue strength coefficients or laboratory-derived k-values from the IDT strength-failure strain testing. Use of the IDT strength test to estimate the fatigue strength parameters dates back to the AAMAS procedure, as previously mentioned (Von Quintus, et al., 1991).

1. Equation I.2 is the relationship between the intercept term for different flexural modulus values from the beam fatigue test (N=1). Equation I.3 is the relationship between the strain exponent,  $k_{2f}$ , and the modulus exponent,  $k_{3f}$ . The mathematical parameters in equation I.3 are assumed to be proportional to the parameters in equation I.4, regarding the flexural beam fatigue strength test and the IDT strength test outcomes, excluding the volumetric property factor in determining the strain exponent,  $k_{2f}$ .

$k_{2f} = \left(\frac{-k_{3f}}{m}\right) \left(\frac{\text{Log}(E_{\text{Flexural}})}{\text{Log}(E_{\text{Uniaxial}}^*)}\right)$	Equation I.3
$k_{2f} = \frac{\text{Log}(k_{1f})}{\text{Log}\left(\frac{b}{1000}\right)}$	Equation I.4

2. The term  $\text{Log}(E_{\text{Flexural}})/\text{Log}(E_{\text{Uniaxial}}^*)$  is temperature dependent, but the MEPDG assumes it, as well as the  $k_{2f}$  coefficient, to be temperature independent. The flexural modulus is not measured for IDT strength testing, while  $E_{\text{Uniaxial}}^*$  is measured on different test specimens. From different studies regarding a comparison of the flexural and dynamic uniaxial and confined (triaxial) based modulus values and other test methods, an average logarithmic modulus ratio of 1.08 is assumed for all test temperatures and dense-graded mixtures, if not measured.
  
3. The assumption that the failure strains from the flexural beam and IDT test are directly proportional for all mixtures is questionable but believed to be reasonable for a surrogate test. For the flexural beam fatigue and IDT strength outcomes, the intercept and tensile strain exponent are related, because of the mathematical analysis or interpretation of the test data, as well as the intercept and modulus exponent. Equation I.5 is the relationship or correspondence between the intercept,  $k_{1f}$ , and tensile strain exponent,  $k_{2f}$ , derived for many dense-graded asphalt mixtures, while equation I.6 is the correspondence between the intercept,  $k_{1f}$ , and modulus exponent,  $k_{3f}$ .

$\text{Log}(k_{1f}) = 3.4852(k_{2f}) + 4.3086$	Equation I.5
$\text{Log}(k_{1f}) = 7.218(k_{3f}) - 15.693$	Equation I.6

4. The modulus exponent and tensile strain exponent are calculated from the IDT strength test outcomes of “b” and “m.” As stated previously, the tensile strain intercept (flexural fatigue testing) and failure strain intercept (IDT fatigue testing) for different modulus values are not the same but proportional. A constant coefficient is used to convert the indirect tensile to flexural bending beam results. Equation I.7 estimates the modulus exponent, while equation I.8 estimates the tensile strain exponent from the IDT strength-failure strain test.

$k_{3f} = \frac{15.693}{1.08\left(\frac{\text{Log}(b/1000)}{m}\right) + 7.218}$	Equation I.7
$k_{2f} = \frac{k_{3f}}{m} (1.08) F_{\text{IDT-Flex}}$	Equation I.8
Where: $F_{\text{IDT-Flex}} =$ The test factor translating the IDT response to the flexural beam response. The value included in the conversion is 1.55.	

5. The intercept is directly related to the “b” coefficient from the IDT strength test. Equation I.9 estimates the intercept based on IDT tests and is used to adjust the intercept to a standard volumetric property with the volumetric factor,  $C$  (see Appendix G). For simplicity, the

**Expansion of AASHTOWare ME Design Inputs  
Final Report WHRP 0092-20-03**

$k_{1f}$  intercept in mils per inch is equal to the “b” value from the IDT strength-failure strain data in mils per inch. The  $k_{1f}(Specimen_{IDT})$  intercept in mils per inch represents the average VFA for the test specimens included for a specific mixture or set of cores.

$$k_{1f}\left(\frac{\text{mils}}{\text{inch}}\right) = \frac{k_{1f}(Specimen_{IDT})}{c} = \frac{b}{c} \quad \text{Equation I.9}$$

#### **I.4 Appendix I References**

Rauhut, J.B.; Lytton, R.L.; and Darter, M.I., *Pavement Damage Functions for Cost Allocation, Vol. 2 – Description of Detailed Studies*. Report Number. FHWA/RD-84/019. Federal Highway Administration. Washington, DC, 1984.

Von Quintus, Harold L., J. Brent Rauhut, and Thomas W. Kennedy, *Comparisons of Asphalt Concrete Stiffness as Measured by Various Testing Techniques*, Proceedings, Journal of the Association of Asphalt Paving Technologists, Vol. 51, 1982.

Von Quintus, H.L., J.A. Scherocman, D.S. Hughes, and T.W. Kennedy, “Asphalt-Aggregate Mixture Analysis System – AAMAS,” NCHRP Report Number 338, National Cooperative Highway Research Program, Transportation Research Board, National Research Council, March 1991.

## APPENDIX J—PROCEDURE TO DERIVE THE AASHTO ASPHALT STRUCTURAL LAYER COEFFICIENT

Appendix J includes the procedure for deriving or calculating the asphalt structural layer coefficient from the distress or performance predictions using the PMED software. A couple of examples are included in this appendix to demonstrate the process and structural layer coefficients included in Table 57 of Chapter 5.

### J.1 Procedure to Derive Structural Layer Coefficients

The procedure used to determine/estimate the asphalt structural layer coefficients is outlined in the following steps.

1. Establish the flexible pavement structure (layer thicknesses and properties) for the specific location or climate (see Table 54 in Chapter 5) and traffic level (see Table 55 in Chapter 5). A conventional flexible pavement was used in determining the structural layer coefficient consisting of a 2-inch asphalt wearing surface, as asphalt base layer, and a crushed aggregate base. The layer thicknesses used were explained in Chapter 5.
2. Predict the distresses of the flexible pavement using the PMED software and determine the earliest age or time at which a load-related threshold value is exceeded for one of the distresses or performance measures (IRI, alligator fatigue cracking, and total rut depth). Adjust the asphalt base layer thickness so that the design life of the flexible pavement is around 20 years using a 50 percent reliability level.
3. Extract the 20-year ESALs calculated by the PMED software from an intermediate file and determine the cumulative ESALs to the time when the threshold value is exceeded.
4. Determine the soil support value for the designated location.
5. Calculate the structural number needed for the ESALs defined in step #3 from the predicted distresses and performance measure using the asphalt pavement design equation included in the WisDOT design program.
6. Reduce or increase the asphalt base or wearing surface thickness by 1 inch, and repeat steps 2 through 5 for the revised asphalt layer thicknesses. The structural layer coefficient for the asphalt layer which remained unchanged between the two runs will be the same for both runs; the difference between the two simulations is a result of the change in the asphalt layer thickness (asphalt base or wearing surface).
7. Calculate the structural layer coefficient for the asphalt base layer and wearing surface using an assumed structural layer coefficient for the crushed aggregate.

The WisPave design program uses the AASHTO 1972 Asphalt Pavement Design Equation, which is listed below:

$$\text{Log}(ESALs) = 9.36\text{Log}(SN + 1) - 0.2 + \frac{\text{Log}\left(\frac{4.2 - P_t}{4.1 - 1.5}\right)}{0.4 + \frac{1094}{(SN + 1)^{5.19}}} + \text{Log}\left(\frac{1}{R}\right) + 0.372(S - 3.0)$$

Where:

**Expansion of AASHTOWare ME Design Inputs  
Final Report WHRP 0092-20-03**

ESALs	Cumulative equivalent single axle loads to the age or time at which failure is designated for within the design life of the flexible pavement structure.
SN	Structural number.
P <sub>t</sub>	Terminal serviceability index; WisDOT uses 2.5.
R	Regional factor; WisDOT uses 3.0
S	Soil support value

Using the WisDOT assumed values listed above, the asphalt pavement design equation reduces to:

$$\text{Log}(ESALs) = 9.36\text{Log}(SN + 1) - 0.6771 - \frac{0.2009}{0.4 + \frac{1094}{(SN + 1)^{5.19}}} + 0.372(S - 3.0)$$

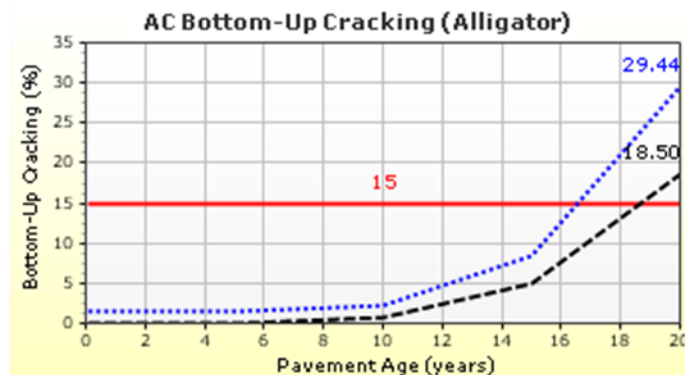
**J.2 Selected Examples**

The following sections in this appendix are a description for some examples to determine the structural layer coefficients for the site specific inputs and assumptions defined in Chapter 5.

**J.2.1 Example 1 – Madison Climate, High Traffic (HT)**

Location/Climate:	Madison (see Table 54 in Chapter 5)
Soil Type:	Dodgeville, A-6 (see Table 54 in Chapter 5)
Soil Support Value:	3.9
Traffic Level:	HT (see Table 55 in Chapter 5)
Normalized Axle Load Distribution:	Heavy (see Table 55 in Chapter 5)
Thickness of Aggregate Base	12 inches

Thickness of Wearing Surface	2.0 inches (PG58-28V, RAP/RAS)
Thickness of Asphalt Base	10.5 inches (PG58-28V, RAP/RAS)
Performance Measure Controlling Design:	Fatigue Cracking
Cumulative Number of Trucks, 20-year design:	37,547,700
Cumulative ESALs, 20-year design:	43,740,000
Age when fatigue cracks exceed threshold value:	19.0 years (see chart below)

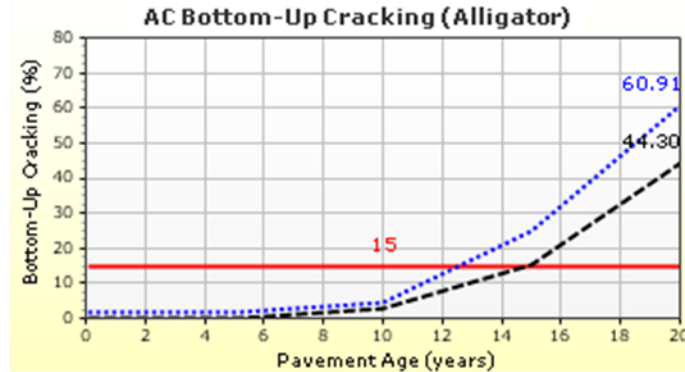


Cumulative Number of Trucks, 19.0 years:	35,253,900
Cumulative ESALs, 19.0 years:	41,068,000

**Expansion of AASHTOWare ME Design Inputs**  
**Final Report WHRP 0092-20-03**

Structural number from the asphalt pavement design equation: 6.96  
 Required structural number for the asphalt layers: 5.52

Thickness of Wearing Surface 1.5 inches (PG58-28V, RAP/RAS)  
 Thickness of Asphalt Base 10.5 inches (PG58-28V, RAP/RAS)  
 Performance Measure Controlling Design: Fatigue Cracking  
 Cumulative Number of Trucks, 20-year design: 37,547,700  
 Cumulative ESALs, 20-year design: 43,740,000  
 Age when fatigue cracks exceed threshold value: 14.9 years (see chart below)



Cumulative Number of Trucks at 14.9 years: 26,344,300  
 Cumulative ESALs at 14.9 years: 30,689,000  
 Structural number from the asphalt pavement design equation: 6.71  
 Required structural number for the asphalt layers: 5.27

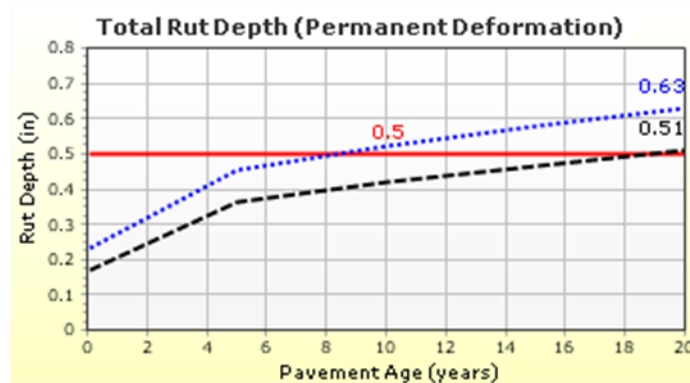
Structural Layer Coefficient, Wearing Surface Mixture: 0.503  
 Structural Layer Coefficient, Asphalt Base Mixture: 0.430

**J.2.2 Example 2 –Green Bay Climate, Moderate Traffic (MT)**

Location/Climate: Green Bay (see Table 54 in Chapter 5)  
 Soil Type: Shiocton, A-4 (see Table 54 in Chapter 5)  
 Soil Support Value: 4.1  
 Traffic Level: MT (see Table 55 in Chapter 5)  
 Normalized Axle Load Distribution: Typical (see Table 55 in Chapter 5)  
 Thickness of Aggregate Base 10 inches

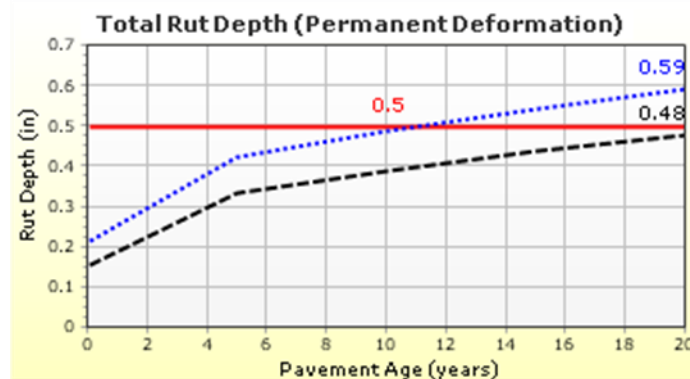
Thickness of Wearing Surface 2.0 inches (PG58-28H, RAP/RAS)  
 Thickness of Asphalt Base 5.0 inches (PG58-28S, RAP/RAS)  
 Performance Measure Controlling Design: Rutting  
 Cumulative Number of Trucks, 20-year design: 7,510,000  
 Cumulative ESALs, 20-year design: 8,510,000  
 Age when rut depth exceeds threshold value: 18.2 years (see chart below)

**Expansion of AASHTOWare ME Design Inputs**  
**Final Report WHRP 0092-20-03**



Cumulative Number of Trucks at 18.2 years: 6,675,800  
 Cumulative ESALs, 18.2 years: 7,565,000  
 Structural number from the asphalt pavement design equation: 5.43  
 Required structural number for the asphalt layers: 4.23

Thickness of Wearing Surface 2.0 inches (PG58-28H, RAP/RAS)  
 Thickness of Asphalt Base 6.0 inches (PG58-28S, RAP/RAS)  
 Performance Measure Controlling Design: Rutting  
 Cumulative Number of Trucks, 20-year design: 7,510,000  
 Cumulative ESALs, 20-year design: 8,510,000  
 Age when rut depth exceeds threshold value: years (see chart below)



Cumulative Number of Trucks at 20.8 years: 8,100,000  
 Cumulative ESALs at 20.8 years: 9,179,000  
 Structural number from the asphalt pavement design equation: 5.59  
 Required structural number for the asphalt layers: 4.39

Structural Layer Coefficient, Wearing Surface Mixture: 0.545  
 Structural Layer Coefficient, Asphalt Base Mixture: 0.550

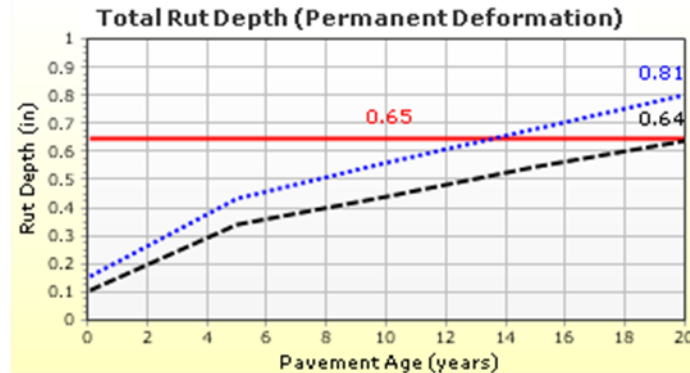
**J.2.3 Example 3 –Mercer Climate, Moderate Traffic (LT)**

Location/Climate: Mercer (see Table 54 in Chapter 5)  
 Soil Type: Pence, A-2-4 (see Table 54 in Chapter 5)  
 Soil Support Value: 5.0

**Expansion of AASHTOWare ME Design Inputs**  
**Final Report WHRP 0092-20-03**

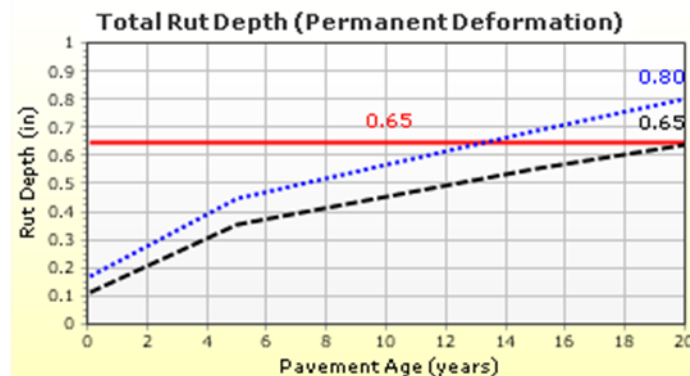
Traffic Level: LT (see Table 55 in Chapter 5)  
 Normalized Axle Load Distribution: Light (see Table 55 in Chapter 5)  
 Thickness of Aggregate Base 8 inches

Thickness of Wearing Surface 1.5 inches (PG58-28S, RAP/RAS)  
 Thickness of Asphalt Base: 4.0 inches (PG58-28S, RAP/RAS)  
 Performance Measure Controlling Design: Rutting  
 Cumulative Number of Trucks, 20-year design: 1,877,000  
 Cumulative ESALs, 20-year design: 970,000  
 Age when rut depth exceeds threshold value: 20.5 years (see chart below)



Cumulative Number of Trucks, 20.5 years: 1,950,000  
 Cumulative ESALs, 20.5 years: 1,008,000  
 Structural number from the asphalt pavement design equation: 3.58  
 Required structural number for the asphalt layers: 2.62

Thickness of Wearing Surface 1.5 inches (PG58-28S, RAP/RAS)  
 Thickness of Asphalt Base: 3.0 inches (PG58-28S, RAP/RAS)  
 Performance Measure Controlling Design: Rutting  
 Cumulative Number of Trucks, 20-year design: 1,877,000  
 Cumulative ESALs, 20-year design: 970,000  
 Age when rut depth exceeds threshold value: 20.0 years (see chart below)



Cumulative Number of Trucks at 20.0 years: 1,877,000  
 Cumulative ESALs at 20.0 years: 970,000  
 Structural number from the asphalt pavement design equation: 3.56



**Expansion of AASHTOWare ME Design Inputs**  
**Final Report WHRP 0092-20-03**

Required structural number for the asphalt layers:	2.60
Structural Layer Coefficient, Wearing Surface Mixture:	0.460
Structural Layer Coefficient, Asphalt Base Mixture:	0.483